TECHNICAL REPORTS SERIES NO. 398 (REV. 1)

Absorbed Dose Determination in External Beam Radiotherapy

An International Code of Practice for Dosimetry Based on Standards of Absorbed Dose To Water

Endorsed by the European Society for Radiotherapy and Oncology

IAEA
International Atomic Energy Agency

IAEA SAFETY STANDARDS AND RELATED PUBLICATIONS

IAEA SAFETY STANDARDS

Under the terms of Article III of its Statute, the IAEA is authorized to establish or adopt standards of safety for protection of health and minimization of danger to life and property, and to provide for the application of these standards.

The publications by means of which the IAEA establishes standards are issued in the **IAEA Safety Standards Series**. This series covers nuclear safety, radiation safety, transport safety and waste safety. The publication categories in the series are **Safety Fundamentals**, **Safety Requirements** and **Safety Guides**.

Information on the IAEA's safety standards programme is available on the IAEA Internet site

https://www.iaea.org/resources/safety-standards

The site provides the texts in English of published and draft safety standards. The texts of safety standards issued in Arabic, Chinese, French, Russian and Spanish, the IAEA Safety Glossary and a status report for safety standards under development are also available. For further information, please contact the IAEA at: Vienna International Centre, PO Box 100, 1400 Vienna, Austria.

All users of IAEA safety standards are invited to inform the IAEA of experience in their use (e.g. as a basis for national regulations, for safety reviews and for training courses) for the purpose of ensuring that they continue to meet users' needs. Information may be provided via the IAEA Internet site or by post, as above, or by email to Official.Mail@iaea.org.

RELATED PUBLICATIONS

The IAEA provides for the application of the standards and, under the terms of Articles III and VIII.C of its Statute, makes available and fosters the exchange of information relating to peaceful nuclear activities and serves as an intermediary among its Member States for this purpose.

Reports on safety in nuclear activities are issued as **Safety Reports**, which provide practical examples and detailed methods that can be used in support of the safety standards.

Other safety related IAEA publications are issued as **Emergency Preparedness and Response** publications, **Radiological Assessment Reports**, the International Nuclear Safety Group's **INSAG Reports**, **Technical Reports** and **TECDOCs**. The IAEA also issues reports on radiological accidents, training manuals and practical manuals, and other special safety related publications.

Security related publications are issued in the **IAEA Nuclear Security Series**.

The **IAEA Nuclear Energy Series** comprises informational publications to encourage and assist research on, and the development and practical application of, nuclear energy for peaceful purposes. It includes reports and guides on the status of and advances in technology, and on experience, good practices and practical examples in the areas of nuclear power, the nuclear fuel cycle, radioactive waste management and decommissioning.

ABSORBED DOSE DETERMINATION IN EXTERNAL BEAM RADIOTHERAPY

The following States are Members of the International Atomic Energy Agency:

AFGHANISTAN
ALBANIA
ALGERIA
ANGOLA
ANTIGUA AND BARBUDA
ARGENTINA
ARMENIA
AUSTRALIA
AUSTRIA
AZERBAIJAN
BAHAMAS
BAHRAIN
BANGLADESH
BARBADOS
BELARUS
BELGIUM
BELIZE
BENIN
BOLIVIA, PLURINATIONAL STATE OF
BOSNIA AND HERZEGOVINA
BOTSWANA
BRAZIL
BRUNEI DARUSSALAM
BULGARIA
BURKINA FASO
BURUNDI
CABO VERDE
CAMBODIA
CAMEROON
CANADA
CENTRAL AFRICAN REPUBLIC
CHAD
CHILE
CHINA
COLOMBIA
COMOROS
CONGO
COSTA RICA
CÔTE D'IVOIRE
CROATIA
CUBA
CYPRUS
CZECH REPUBLIC
DEMOCRATIC REPUBLIC OF THE CONGO
DENMARK
DJIBOUTI
DOMINICA
DOMINICAN REPUBLIC
ECUADOR
EGYPT
EL SALVADOR
ERITREA
ESTONIA
ESWATINI
ETHIOPIA
FIJI
FINLAND
FRANCE
GABON
GAMBIA
GEORGIA
GERMANY
GHANA
GREECE
GRENADA
GUATEMALA
GUINEA
GUYANA
HAITI
HOLY SEE
HONDURAS
HUNGARY
ICELAND
INDIA
INDONESIA
IRAN, ISLAMIC REPUBLIC OF
IRAQ
IRELAND
ISRAEL
ITALY
JAMAICA
JAPAN
JORDAN
KAZAKHSTAN
KENYA
KOREA, REPUBLIC OF
KUWAIT
KYRGYZSTAN
LAO PEOPLE'S DEMOCRATIC REPUBLIC
LATVIA
LEBANON
LESOTHO
LIBERIA
LIBYA
LIECHTENSTEIN
LITHUANIA
LUXEMBOURG
MADAGASCAR
MALAWI
MALAYSIA
MALI
MALTA
MARSHALL ISLANDS
MAURITANIA
MAURITIUS
MEXICO
MONACO
MONGOLIA
MONTENEGRO
MOROCCO
MOZAMBIQUE
MYANMAR
NAMIBIA
NEPAL
NETHERLANDS
NEW ZEALAND
NICARAGUA
NIGER
NIGERIA
NORTH MACEDONIA
NORWAY
OMAN
PAKISTAN
PALAU
PANAMA
PAPUA NEW GUINEA
PARAGUAY
PERU
PHILIPPINES
POLAND
PORTUGAL
QATAR
REPUBLIC OF MOLDOVA
ROMANIA
RUSSIAN FEDERATION
RWANDA
SAINT KITTS AND NEVIS
SAINT LUCIA
SAINT VINCENT AND THE GRENADINES
SAMOA
SAN MARINO
SAUDI ARABIA
SENEGAL
SERBIA
SEYCHELLES
SIERRA LEONE
SINGAPORE
SLOVAKIA
SLOVENIA
SOUTH AFRICA
SPAIN
SRI LANKA
SUDAN
SWEDEN
SWITZERLAND
SYRIAN ARAB REPUBLIC
TAJIKISTAN
THAILAND
TOGO
TONGA
TRINIDAD AND TOBAGO
TUNISIA
TÜRKİYE
TURKMENISTAN
UGANDA
UKRAINE
UNITED ARAB EMIRATES
UNITED KINGDOM OF GREAT BRITAIN AND NORTHERN IRELAND
UNITED REPUBLIC OF TANZANIA
UNITED STATES OF AMERICA
URUGUAY
UZBEKISTAN
VANUATU
VENEZUELA, BOLIVARIAN REPUBLIC OF
VIET NAM
YEMEN
ZAMBIA
ZIMBABWE

The Agency's Statute was approved on 23 October 1956 by the Conference on the Statute of the IAEA held at United Nations Headquarters, New York; it entered into force on 29 July 1957. The Headquarters of the Agency are situated in Vienna. Its principal objective is "to accelerate and enlarge the contribution of atomic energy to peace, health and prosperity throughout the world".

TECHNICAL REPORTS SERIES No. 398 (Rev. 1)

ABSORBED DOSE DETERMINATION IN EXTERNAL BEAM RADIOTHERAPY

AN INTERNATIONAL CODE OF PRACTICE FOR DOSIMETRY BASED ON STANDARDS OF ABSORBED DOSE TO WATER

INTERNATIONAL ATOMIC ENERGY AGENCY
VIENNA, 2024

COPYRIGHT NOTICE

Marketing and Sales Unit, Publishing Section
International Atomic Energy Agency
Vienna International Centre
PO Box 100
1400 Vienna, Austria
fax: +43 1 26007 22529
tel.: +43 1 2600 22417
email: sales.publications@iaea.org
www.iaea.org/publications

Printed by the IAEA in Austria
February 2024
STI/DOC/010/398
https://doi.org/10.61092/iaea.ve7q-y94k

IAEA Library Cataloguing in Publication Data

Names: International Atomic Energy Agency.
Title: Absorbed dose determination in external beam radiotherapy : An international code of practice for dosimetry based on standards of absorbed dose to water / International Atomic Energy Agency.
Description: Vienna : International Atomic Energy Agency, 2024. | Series: Technical reports series (International Atomic Energy Agency), ISSN 0074–1914 ; no. 398 (Rev.1) | Includes bibliographical references.
Identifiers: IAEAL 23-01610 | ISBN 978–92–0–146022–6 (paperback : alk. paper) | ISBN 978–92–0–146122–3 (pdf) | ISBN 978–92–0–146222–0 (epub)
Subjects: LCSH: Low-level radiation — Dose-response relationship. | Radiation dosimetry. | Radiotherapy.
Classification: UDC 615.849 | STI/DOC/010/398

FOREWORD

Following the 1996 recommendations of the IAEA standing Scientific Committee of the IAEA/WHO Network of Secondary Standards Dosimetry Laboratories, a coordinated research project was undertaken in 1997–1999 with the task of producing a new international code of practice using standards based on absorbed dose to water. In 2000, the IAEA published Absorbed Dose Determination in External Beam Radiotherapy: An International Code of Practice for Dosimetry Based on Standards of Absorbed Dose to Water (IAEA Technical Reports Series No. 398 (TRS-398)). At that time, most primary standards dosimetry laboratories were prepared or planning to provide calibrations in terms of absorbed dose to water at the reference radiation qualities recommended in TRS-398.

Since its publication, TRS-398 has contributed to the transition from calibrations based on primary standards of air kerma to calibrations based on absorbed dose to water. The absorbed dose to water relates directly to the quantity of interest in radiotherapy treatments. Furthermore, standards based on absorbed dose to water provide a more robust system of primary standards than air kerma based standards, allow the use of a simple formalism and offer the possibility of reducing the uncertainty in the dosimetry of radiotherapy beams. Today, absorbed dose to water is used as the basis for reference dosimetry in external beam radiotherapy by most hospitals worldwide, and a coherent dosimetry system based on standards of absorbed dose to water is available for practically all radiotherapy beams.

Advances since the 2000s include the publication of new key data for measurement standards in the dosimetry of ionizing radiation, the development of new radiation detectors that are now commercially available and the introduction of new radiotherapy technologies implementing megavoltage photon beams, protons and heavier ions. To account for these advances, in 2014 the Scientific Committee of the IAEA/WHO Network of Secondary Standards Dosimetry Laboratories recommended an update of TRS-398.

This publication addresses the need for a systematic and internationally unified approach to the calibration of ionization chambers in terms of absorbed dose to water and to the use of these detectors in the determination of absorbed dose to water for the radiation beams used in radiotherapy — namely low, medium and high energy photon beams, electron beams, proton beams and heavier ion beams. It is addressed to users provided with calibrations in terms of absorbed dose to water traceable to a primary standards dosimetry laboratory.

The IAEA wishes to express its gratitude to all those who contributed to the drafting and review of this publication; in particular, P. Andreo (Sweden), D. Burns (France), R.-P. Kapsch (Germany), M. McEwen (Canada) and

S. Vatnitsky (Russian Federation). This international code of practice has been endorsed by the European Society for Radiotherapy and Oncology (ESTRO).

The IAEA officers responsible for this publication were M. Carrara and K. Christaki of the Division of Human Health.

ACKNOWLEDGMENTS

The IAEA acknowledges T. Ackerly (Australia), D. Butler (Australia), A. Fukumura (Japan), G. Hartmann (Germany), A. Nisbet (United Kingdom), H. Nyström (Sweden), M. Pimpinella (Italy) and J. Seuntjens (Canada) for their comments and suggestions.

CONTENTS

1. INTRODUCTION

1.1. BACKGROUND

In Ref. [1], the International Commission on Radiation Units and Measurements (ICRU)[1] concluded that "although it is too early to generalize, the available evidence for certain types of tumour points to the need for an accuracy of ±5% in the delivery of an absorbed dose to a target volume if the eradication of the primary tumour is sought". The report continues: "Some clinicians have requested even closer limits such as ±2%, but at the present time [in 1976] it is virtually impossible to achieve such a standard". These statements were given in a context where uncertainties were estimated at the 95% confidence level and have been interpreted to correspond to approximately two standard deviations ($k = 2$). Thus, the requirement for an accuracy of 5% in the delivery of absorbed dose would correspond to a combined uncertainty of 2.5% at the level of one standard deviation ($k = 1$). When the first edition of this international code of practice[2] was published, in 2000, it was considered that such an accuracy requirement was too strict and the combined uncertainty should be increased to approximately one standard deviation of 5%. No definitive recommendations in this respect were available at the time.[3] A later review of radiobiological and clinical data by Wambersie [6] proposed 3.5% for the combined standard uncertainty of the dose delivery at the specification point, acknowledging that in many cases larger uncertainties were acceptable. These limits are consistent with the analysis given in Ref. [7], which, referring solely to the dosimetry component of a radiotherapy treatment, considers an uncertainty close to 3% ($k = 1$) to be the current acceptable accuracy requirement for the difference between the prescribed dose and the dose delivered to the patient at the specification point under optimal conditions. In addition to the clinical requirement, the uncertainty in the dose delivered, which starts with the uncertainty of the beam calibration, is the main concern from the dosimetry point of view.

---

[1] A list of the abbreviations used in the text is given at the end of the publication.

[2] INTERNATIONAL ATOMIC ENERGY AGENCY, Absorbed Dose Determination in External Beam Radiotherapy: An International Code of Practice for Dosimetry Based on Standards of Absorbed Dose to Water, Technical Reports Series No. 398, IAEA, Vienna (2000).

[3] Several studies have concluded that for certain types of tumour, the combined standard uncertainty in dose delivery should be smaller than ~3.5% [2–4], "even if in many cases larger values are acceptable and in some special cases even smaller values should be aimed at" [3]. It has also been stated that when taking into account the uncertainties in dose calculation algorithms, a more appropriate limit for the combined standard uncertainty of the dose delivered to the target volume would be ~5% [4, 5].

In 1987 the IAEA published an international code of practice entitled Absorbed Dose Determination in Photon and Electron Beams [8], recommending procedures to obtain the absorbed dose in water from measurements made with an ionization chamber in external beam radiotherapy. The second edition of the code of practice [9] was published in 1997, with updated dosimetry of photon beams, mainly kilovoltage X rays. The code of practice entitled 'Use of Plane Parallel Ionization Chambers in High Energy Electron and Photon Beams' [10] was published in 1997 to further update Ref. [8] with respect to plane parallel ionization chambers.

Other publications aimed at further improving the traceability, accuracy and consistency of radiation measurements have since been disseminated by the IAEA. Reference [11] was published in 2009 to support secondary standards dosimetry laboratories with the calibration of reference dosimeters for external beam radiotherapy. Furthermore, Ref. [12] was published in 2017 to provide guidance on the dosimetry of small static photon fields used in new techniques and technologies that have indirect traceability to reference dosimetry of conventional radiotherapy.

The estimation of uncertainties given in Refs [9, 10] showed that the largest contribution to the uncertainty during beam calibration arises from the different physical quantities involved and the large number of steps performed, yielding standard uncertainties of up to 4%. Even for lower uncertainty estimates [13, 14], the contribution from the first steps in the radiotherapy dosimetry chain still do not comply with the demand to minimize the final uncertainty in patient dose delivery.

The various steps between the calibration of ionization chambers and the determination of absorbed dose to water, D_w, at hospitals using dosimetry protocols based on the coefficient[4] $N_{D,air}$ (or N_{gas}) (see definitions in Section 1.4.4) introduce undesirable uncertainties into the determination of D_w. Many quantities are involved in the dosimetric chain, which starts with a calibration coefficient in terms of air kerma, N_K, measured in air using a ^{60}Co beam and ends with the absorbed dose to water, D_w, measured in water in clinical beams. Uncertainties in the chain arise mainly from conversions performed by the user at the hospital, for instance the well known factors k_m (correction factor for the lack of air equivalence of the chamber material) and k_{att} (correction factor for the attenuation and scatter of photons in the chamber material), which are used in most air kerma based codes of practice and dosimetry protocols [9, 16–26]. Uncertainties associated with the conversion of N_K to $N_{D,air}$ (or N_{gas}) mean that

[4] The standard ISO 31-0 [15] provides guidelines with regard to the use of the term 'coefficient', which should be used for a multiplier possessing dimensions, and 'factor', which should be reserved for a dimensionless multiplier.

in practice the starting point of the calibration of clinical beams already involves considerable uncertainty [13].

Reich [27] proposed the calibration of therapy level dosimeters in terms of absorbed dose to water, stressing the advantages of using the same quantity and experimental conditions as the user. The current status of the development of primary standards of absorbed dose to water for high energy photons and electrons, as well as the improvements in the radiation dosimetry concepts and data available, have made it possible to reduce the uncertainty in the calibration of radiation beams. The development of standards of absorbed dose to water at primary standards dosimetry laboratories (PSDLs) has been a major goal of the Consultative Committee on Ionizing Radiation (Comité Consultatif des Rayonnements Ionisants (CCRI)) [28]. Measurements of absorbed dose to graphite using graphite calorimeters were developed first, and they continue to be used in many laboratories. Comparisons of determinations of absorbed dose to graphite were satisfactory, and consequently the development of standards of absorbed dose to water was undertaken in some laboratories. Procedures to determine absorbed dose to water using measurements of appropriate base or derived quantities have considerably improved and expanded at PSDLs in the last two decades. Well established procedures used for such measurements are ionometry, chemical dosimetry, and water and graphite calorimetry. Although only the water calorimeter allows the direct determination of the absorbed dose to water in a water phantom, the required conversion and perturbation factors for the other procedures are now well known at many laboratories. These developments lend support to calibration coefficients being provided in terms of absorbed dose to water, $N_{D,w}$, for use in radiotherapy beams. PSDLs provide $N_{D,w}$ calibrations at ^{60}Co gamma ray beams, and some laboratories have extended these calibration procedures to high energy photon and electron beams and to medium energy kilovoltage X ray beams; others are developing the necessary techniques for such modalities.

At secondary standards dosimetry laboratories (SSDLs), calibration coefficients from a PSDL or from the International Bureau of Weights and Measures (Bureau International des Poids et Mesures (BIPM)) are transferred to hospital users. For ^{60}Co gamma ray beams, most SSDLs can provide users with a calibration coefficient in terms of absorbed dose to water, as all SSDLs have such beams. However, in general it is not feasible for SSDLs to supply experimentally determined calibration coefficients at high energy photon and electron beams.

A major advance in radiotherapy over the past decade has been the increasing use of proton and heavier ion irradiation facilities for radiotherapy.[5] Practical dosimetry in these fields is also based on the use of ionization chambers that are provided with calibrations in terms of absorbed dose to water. Therefore, the dosimetry procedures developed for high energy photons and electrons can also be applicable to protons and heavier ions. At the other end of the range of available teletherapy beams are kilovoltage X ray beams, and for these the use of standards of absorbed dose to water was introduced in Ref. [9]. However, for kilovoltage X rays there are currently few laboratories providing $N_{D,w}$ calibrations because most PSDLs have not yet established primary standards of absorbed dose to water for such radiation qualities. Nevertheless $N_{D,w}$ calibrations in kilovoltage X ray beams may be provided by PSDLs and SSDLs on the basis of their standards of air kerma and one of the current dosimetry protocols for X ray beams. Thus, a coherent dosimetry system based on standards of absorbed dose to water is now possible for practically all radiotherapy beams (see Fig. 1).[6]

1.1.1. ICRU Key data for radiation dosimetry

The development of Ref. [32] on key data for measurement standards in radiation dosimetry followed a specific request by CCRI, established by the International Committee for Weights and Measures (Comité International des Poids et Mesures (CIPM)), which supervises the work of BIPM. The materials considered in Ref. [32] are air, graphite and water.

---

[5] It was recommended by the IAEA and the ICRU [29, 30] to call any nucleus with an atomic number Z equal to or smaller than that of neon ($Z = 10$) a 'light ion', and using the term 'heavy ions' for heavier nuclei. This international code of practice provides recommendations for reference and relative dosimetry for protons (Section 10) and for ions heavier than protons — light ions (Section 11).

[6] For neutron therapy beams, the reference material to which the absorbed dose relates is the ICRU soft tissue [31]. This International Code of Practice is based on the absorbed dose to water. Owing to the strong dependence of neutron interaction coefficients on neutron energy and material composition, there is no straightforward procedure to derive the absorbed dose to soft tissue from the absorbed dose to water. Moreover, neutron dosimetry is traditionally performed with tissue equivalent ionization chambers, flushed with a tissue equivalent gas to determine the absorbed dose in a homogeneous medium. Although it is possible to express the resulting formalism [31] in terms of k_{Q,Q_o} (factor to correct for the difference between the response of an ionization chamber to the reference beam quality Q_o used for calibrating the chamber in the standards laboratory and its response to the actual user beam quality Q), for most ionization chamber types there is a lack of data on the physical parameters that apply to the measurement of absorbed dose to water in a neutron beam. Therefore, the dosimetry of radiotherapy neutron beams is not dealt with in this international code of practice.

The new key data include values of fundamental quantities for the determination of stopping powers for light and heavy charged particles. Reference [32] provides recommendations for the mean excitation energies (I) of air (85.7 eV), graphite (81 eV) and water (78 eV) and for the graphite mass density to use when evaluating the density effect (2.265 g/cm^3) in the mass electronic stopping power, S_{el}/ρ. These quantities yield new values of S_{el}/ρ for electrons and positrons, protons and light ions (alpha particles and carbon ions) and, indirectly, also change the average energy required to produce an ion pair for protons and carbon ions, W_{air}. The recommended W_{air} values are 33.97 eV for electrons (which is constant above ~10 keV) and 34.44 eV for protons; for carbon ions, the value is subject to the same increase as for protons (0.6%, assuming negligible perturbation correction factors for the ionization chambers used in its determination), that is, W_{air} = 34.71 eV. Other key data, such as the heat defect of liquid water, the radiation chemical yield for the Fricke dosimeter and the correction to account for the charge of the initial electrons set in motion by low energy photons, have been reviewed.

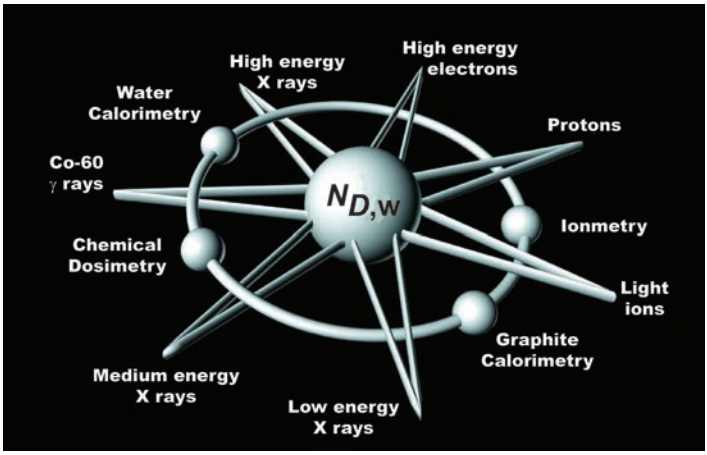

FIG. 1. Coherent dosimetry system based on standards of absorbed dose to water. Primary standards based on water calorimetry, graphite calorimetry, chemical dosimetry and ionometry allow the calibration of ionization chambers in terms of absorbed dose to water, $N_{D,w}$. *A single international code of practice provides the methodology for the determination of absorbed dose to water in low, medium and high energy and* ^{60}*Co photon beams, electron beams, proton beams and light ion beams used for external beam radiotherapy.*

The state of the art and current trends in photon cross-sections and mass energy absorption coefficients, μ_{en}/ρ, and ratios are analysed in detail, but no specific data have been recommended because of the following issues:

(a) *Cross-sections for the photoelectric effect.* Accurate synchrotron radiation measurements of μ_{en}/ρ for air at low energies made at Physikalisch-Technische Bundesanstalt (PTB) (3–10 keV [33] and 3–60 keV [34]) have questioned the adequacy of the photoelectric cross-sections in current use. The authors found better agreement with the old compilation by Hubbell [35], which was based on renormalized subshell cross-sections determined by Scofield [36], than with the values in the National Institute of Standards and Technology (NIST) database of mass attenuation and energy absorption coefficients [37], which is based on the widely used XCOM computer code [38] and the work of Seltzer [39] on the calculation of mass energy transfer coefficients (μ_{tr}/ρ) and mass energy absorption coefficients (μ_{en}/ρ), or in the Lawrence Livermore National Laboratory (LLNL) Evaluated Photon Data Library (EPDL) [40] — all of which were based on unrenormalized Scofield values. On the other hand, Ref. [32] stated that the measurements in air made by Kato et al. [41] agree better with the NIST values than with the renormalized cross-sections. Considering, however, the μ/μ_{en} ratios of experimental and theoretical datasets, Kato et al. [41] concluded that their results were consistent with those of Büermann et al. [33].

(b) *Cross-sections for the Compton effect*. Electron binding effects play a significant role at low photon energies but the implementation of the necessary corrections yields differences in the incoherent scattering cross-sections. A common approach in different datasets and Monte Carlo codes is to use an incoherent scattering function that corrects the Klein–Nishina expression as a multiplication factor. A more elaborate approach is used for the NIST XCOM and LLNL EPDL cross-sections, on the basis of the theory of Waller and Hartree [42] and accounting for binding effects using incoherent scattering function values from Hubbell et al. [43, 44]. This approach does not account for Doppler broadening — that is, the energy of photons scattered through a given angle has a unique value (called the Compton line), obtained from the Compton kinematics expressions, rather than a distribution of energies. The PENELOPE Monte Carlo system [45, 46] uses instead the relativistic impulse approximation as formulated by Ribberfors [47], which provides more realistic cross-sections and accounts for both Doppler broadening in the energy distributions of the scattered photons and binding effects.

The impact of the new data on measurement standards, and therefore on ionization chamber calibrations by standards laboratories, varies depending on

the radiation modality and type of standard used. The changes are up to ~1% for air kerma standards for kilovoltage X ray and ^{60}Co beams (also for some brachytherapy sources; e.g. ^{192}Ir). A similar change could have been expected for the ionometric absorbed dose to water BIPM standard for ^{60}Co, but the implementation of the new data is assessed in the context of known changes to other correction factors, resulting in a practically negligible change. For graphite calorimetry standards there are only small changes, mostly associated with one of the transfer methods used for converting dose in graphite to dose in water, which depends on the particular standard used at each laboratory. No changes occur for water calorimetry.

This international code of practice is based on the stopping power data tables for charged particles in Ref. [32] for graphite, water and air, whereas data from Refs [48–51] are used for other materials. For photons, the adopted cross-sections and μ_{en}/ρ values are those in the 2014 version of the PENELOPE Monte Carlo system [45, 46]. PENELOPE includes a renormalized photoelectric cross-section database for all materials, which was produced by Sabbatucci and Salvat [52] using the same theory as Scofield did [36]; the dense energy grid of this database allows an accurate description of the variation of the cross-section near absorption edges.

The resulting dosimetric data (e.g. the factors that correct for the difference between the response of an ionization chamber in the reference beam quality used for calibrating the chamber and its response in the user beam quality — i.e. the k_Q values) given in this publication do not differ substantially from those included in the first edition of this international code of practice, being generally within the uncertainties stated in the earlier report, but the present update is necessary to maintain consistency with the data used for measurement standards and to incorporate data for new ionization chambers made available since the publication of the first edition.

1.2. OBJECTIVE

1.2.1. Motivation for updating the international code of practice for dosimetry based on standards of absorbed dose to water

The first edition of this international code of practice was written in the mid-1990s. Since then, a number of developments in radiotherapy and radiation dosimetry have taken place, such as the following examples:

(a) New technologies for radiotherapy have been implemented in the field, mostly related to megavoltage photon beams, as well as proton and

heavier ion beams, whose reference dosimetry requires guidance and data for end users.

(b) New detectors have become commercially available that require data for their clinical application.

(c) The ICRU published a report on key data for measurement standards in radiation dosimetry [32], which reviewed the quantities and correction factors that play a fundamental role in dosimetry, estimated the uncertainties of key data and analysed the implications of using the data in Ref. [32] on measurements and calculations. These data were endorsed by CCRI [53] and then implemented in standards laboratories for the calibration of ionization chambers. The impact of the new data on measurement standards, and therefore on ionization chamber calibrations by standards laboratories, varies depending on the radiation modality and type of standard used.

(d) Monte Carlo simulation of radiation transport has become a widely used technique for the accurate calculation of dosimetric quantities for all beam types, superseding many of the approximations used to determine the data in the previous edition of this international code of practice. The cross-sections and coefficients in the most commonly used Monte Carlo systems have been updated following Ref. [32]. Comprehensive sets of dosimetric quantities have been calculated that reflect the impact of the new key data on the reference dosimetry of high energy radiotherapy beams.

(e) For the dosimetry of kilovoltage X rays, the predictions in the first edition of this international code of practice regarding the availability of absorbed dose to water calibrations ($N_{D,w}$) have not been realized; in addition, no specific data were recommended. Given that changes in cross-sections and coefficients for the photoelectric effect have resulted in a major change in key data, new data consistent with Ref. [32] have become available [54] for this type of beam and their insertion in an updated international code of practice is deemed necessary.

(f) The first edition of this international code of practice included recommendations for the dosimetry of radiotherapy beams in non-standard conditions, that is for beams that are not 10 cm × 10 cm. Recent developments, particularly for the dosimetry of small megavoltage photon beams (see Ref. [12]), need to be considered in a general international code of practice.

(g) The feedback received from users after years of application of the first edition of this international code of practice in clinical practice needs to be taken into account.

1.2.2. Advantages of an international code of practice based on standards of absorbed dose to water

The absorbed dose to water is of main interest in radiotherapy because it relates closely to the biological effects of radiation. The advantages of calibrations in terms of absorbed dose to water and dosimetry procedures using the associated calibration coefficients have been presented by several authors [55–57] and are described in detail in Ref. [58]. A summary of the most relevant aspects is given in the following.

1.2.2.1. Reduced uncertainty

The drive towards an improved basis for dosimetry in radiotherapy has motivated PSDLs to devote much effort to developing primary standards of absorbed dose to water for the various beam modalities. The rationale for changing the basis of calibrations from air kerma to absorbed dose to water was the expectation that the calibration of ionization chambers in terms of absorbed dose to water would considerably reduce the uncertainty in determining the absorbed dose to water in radiotherapy beams. Measurements based on calibration in air in terms of air kerma require chamber dependent conversion factors to determine the absorbed dose to water. These conversion factors do not account for differences between individual chambers of a particular type, which have been found to be significant for some chamber models. In contrast, calibrations in terms of absorbed dose to water can be performed under similar conditions to those of subsequent measurements in the user beam, so that the response of each individual chamber is taken into account. Figure 2 shows chamber to chamber variations demonstrated for a given chamber type by the lack of constancy in the $N_{D,w}/N_K$ ratio for ^{60}Co, for a large number of cylindrical ionization chambers commonly used in radiotherapy dosimetry. For a given chamber type, chamber to chamber differences of up to 0.8% have also been reported by BIPM [59]. The elimination of the uncertainty component associated with the assumption that all chambers of a given type are identical is the main reason for favouring direct calibration of ionization chambers in terms of absorbed dose to water.

In principle, primary standards of absorbed dose to water can operate in both ^{60}Co beams and accelerator beams. Thus, for high energy linac photon and electron radiation, an experimental determination of the energy dependence of ionization chambers becomes available, resulting in reduced uncertainty owing to the effect of beam quality. Similar conclusions can be drawn for therapeutic proton and light ion beams, although primary standards of absorbed dose to water are not yet widely available for these radiation qualities.

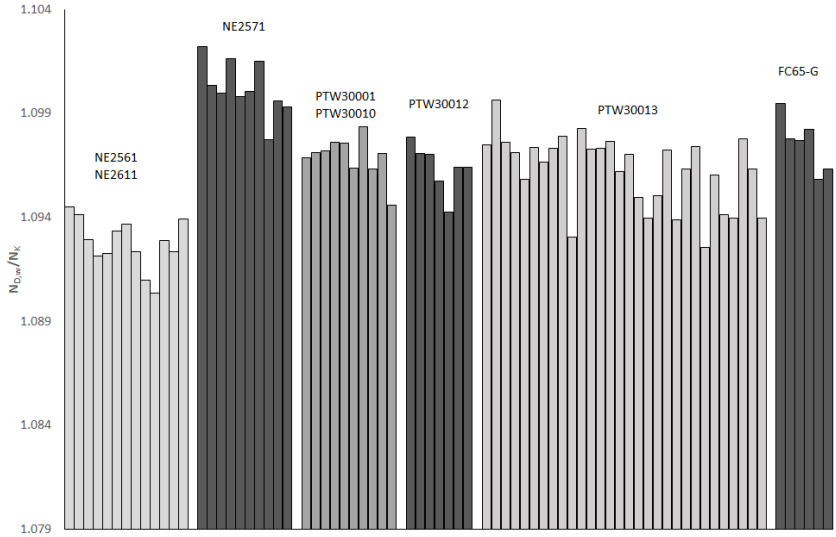

FIG. 2. The ratio of ^{60}Co calibration coefficients, $N_{D,w}/N_K$, is a useful indicator of the uniformity within a given type of chamber [59]. Chamber to chamber variations, demonstrated by differences in the ratio $N_{D,w}/N_K$ for chambers of a given type, are shown for a large number of cylindrical ionization chambers commonly used in radiotherapy dosimetry. Data measured in the IAEA Dosimetry Laboratory.

1.2.2.2. A more robust system of primary standards

Although the quantity of interest in radiation dosimetry is the absorbed dose to water, at the time of the release of the first edition of this international code of practice, most national, regional and international dosimetry recommendations were based on the use of an air kerma calibration coefficient for an ionization chamber; this calibration coefficient was traceable to a national or international primary standard of air kerma for ^{60}Co gamma radiation. Although international comparisons of these standards have exhibited very good agreement, a substantial drawback is that all such standards are based on measurements with ionization chambers and are therefore subject to potential common errors. In addition, depending on the method of evaluation, a factor related to the attenuation in the chamber wall entering the determination of air kerma has been found to vary by up to 0.7% for some primary standards [60]. In contrast, primary standards of absorbed dose to water are based on a number of different physical principles and they involve no assumptions or estimated correction factors common to all of them. Therefore, good agreement among these standards (see Section 2.2) gives much greater confidence in their accuracy.

1.2.2.3. Use of a simple formalism

The formalism given in Ref. [9], as well as in most air kerma based national and international dosimetry protocols for the determination of the absorbed dose to water in radiotherapy beams, was based on the application of several coefficients, perturbations and other correction factors. This was because of the practical difficulty in making the conversion from a quantity measured in air (air kerma) to an in-phantom quantity (absorbed dose to water). This complexity is best demonstrated by considering the equations needed and the procedures for selecting the appropriate data. Reliable information about certain physical characteristics of the ionization chamber used is also required. Many of these data, such as displacement correction factors and stopping power ratios, were derived from complex measurements or calculations based on theoretical models. A simplified procedure that starts from a calibration coefficient in terms of absorbed dose to water and applies correction factors for all influence quantities reduces the possibility of errors in the determination of absorbed dose to water in the radiation beam. The simplicity of the formalism related to absorbed dose to water is evident from the general equation used for the determination of absorbed dose to water (see Section 3).

1.2.3. Concluding remarks

Because of the advantages detailed in Section 1.2.2, calibrations in terms of absorbed dose to water and dosimetry procedures based on $N_{D,w,Q}$ (calibration coefficient in terms of absorbed dose to water for a dosimeter at a user beam quality Q) calibration coefficients are preferred in the dosimetry of radiotherapy high energy photon and electron beams and are implemented worldwide. The methodology has been extended to medium energy kilovoltage X ray and brachytherapy standards in some PSDLs and is in the development stage for proton beams in other standards laboratories.

It should be emphasized, however, that procedures based on air kerma calibrations are still of importance in a number of radiotherapy applications and other areas of radiation medicine. Of particular interest is the dosimetry of kilovoltage X rays: for low energy beams, no 'true' standards of absorbed dose to water exist or are in the process of being developed;[7] for medium energy beams, clinical implementation of $N_{D,w,Q}$ coefficients will take time to achieve. In proton and heavier ion beams, the use of $N_{D,w,^{60}Co}$ coefficients has become common, but most of the data used to derive the value of W_{air} for these beams are still

[7] For low energy X rays, there is no direct primary standard for this dose quantity. Instead, it is realized via air kerma and the use of calculated conversion factors.

based on N_K chamber calibrations. Although their use falls outside the scope of this international code of practice, most brachytherapy source calibrations worldwide are also based on air kerma standards, and so are ultimately all of the dosimetry procedures for radiation protection and radiodiagnostic and interventional radiology applications. The continued role and importance of air kerma calibrations should therefore not be underestimated.

Guidance and recommendations provided here in relation to identified good practices represent expert opinion but are not made on the basis of a consensus of all Member States.

1.3. SCOPE

This international code of practice provides a methodology for the determination of absorbed dose to water in the low, medium and high energy photon beams, electron beams, and proton and heavier ion beams used for external radiotherapy. It relies on the use of an ionization chamber or a dosimeter with an $N_{D,w}$ calibration coefficient and is applicable in all hospitals and facilities providing radiation treatment of cancer patients. Although the nature of these institutions may vary, this publication serves as a useful document for the medical physics and radiotherapy community and will help to achieve uniformity and consistency in radiation dose delivery throughout the world. It could also be of great value to the IAEA/World Health Organization (WHO) SSDL Network for improving the accuracy and consistency of their dose determination and thereby the standardization of radiation dosimetry in the countries served.

Compared with previous codes of practice or dosimetry protocols based on standards of air kerma (e.g. Refs [9, 10]) and with the first edition of this international code of practice, this publication introduces small differences in the value of the absorbed dose to water determined in clinical beams. Users who are not provided with calibrations in terms of absorbed dose to water may refer to the air kerma based international codes of practice, such as Refs [9, 10].

1.4. STRUCTURE

1.4.1. Range of beam qualities

The ranges of radiation qualities covered in this publication are given below (for a description of the beam quality index see the corresponding sections):

(a) Low energy X rays with generating potentials of up to 100 kV.[8]
(b) Medium energy X rays with generating potentials above 70 kV.[8]
(c) ^{60}Co gamma radiation.
(d) High energy photons generated by electrons with energies below 25 MeV, with $TPR_{20,10}$ values (see definition in Section 1.4.4) between approximately 0.6 and 0.8. Megavoltage photon beams generated with special accelerators or including magnetic resonance imaging techniques (e.g. CyberKnife, magnetic resonance linacs) are not included.
(e) Electrons in the energy interval 4–25 MeV with a half-value depth, R_{50}, of 1.4–10 g·cm^{-2}.
(f) Protons in the energy interval 50 MeV to ~250 MeV with a practical range, R_p, of 0.25–37 g·cm^{-2}.
(g) Light ions with atomic number Z between 2 (He) and 10 (Ne) with a practical range in water, R_p, of 2–30 g·cm^{-2} (for carbon ions, this corresponds to an energy range of 85–430 MeV/u, where u is the atomic mass unit).

1.4.2. Practical use of the international code of practice

Emphasis has been given to making the practical use of this document as simple as possible. The structure of this international code of practice differs from that of Ref. [9] and more closely resembles that of Ref. [10] in that the practical recommendations and data for each radiation type have been placed in an individual section devoted to that radiation type, and each section essentially forms an independent and self-contained code of practice, including detailed procedures and worksheets. The reader can perform a dose determination for a given beam by working through the appropriate section; the search for procedures or tables contained in other parts of the publication has been reduced to a minimum. Making the various codes of practice independent and self-contained has introduced unavoidable repetition of some portions of text, but this is expected to result in a publication that is simple and easy to use, especially for users with access to a limited number of radiation types. The first four sections contain general concepts that apply to all radiation types. The appendices provide complementary information.

[8] The boundary between low and medium energy kilovoltage X rays is not strict and there is an overlap in the range 70–100 kV. In this overlap region, the methods described in Sections 8 and 9 are equally satisfactory for determining absorbed dose, and whichever is more convenient should be used.

1.4.3. Expression of uncertainties

The evaluation of uncertainties in this international code of practice follows the guidance given by the International Organization for Standardization (ISO) [61]. Uncertainties of measurements are expressed as relative standard uncertainties and the evaluation of standard uncertainties is classified into type A and type B. Type A standard uncertainty is evaluated by statistical analysis of a series of observations, whereas the evaluation of type B standard uncertainty is based on means other than statistical analysis of a series of observations. A practical implementation of the ISO recommendations, based on the summaries provided in Refs [9, 62], is given for completeness in Appendix IV to this publication.

Estimates of the uncertainty in dose determination for the different radiation types are given in the appropriate sections. Compared with estimates in previous codes of practice, including the first edition of this international code of practice, the values given in this publication are generally smaller. This arises from the greater confidence in the determinations of absorbed dose to water based on D_w standards and, in some cases, from a more rigorous analysis of uncertainties in accordance with the ISO guidelines.

1.4.4. Quantities and symbols

Most of the symbols used in this publication are identical to those used in Refs [9, 10] and the first edition of this international code of practice. For completeness, a summary is provided in Table 1 for all quantities of relevance to the different methods discussed in this publication.

TABLE 1. QUANTITIES AND SYMBOLS USED IN THIS PUBLICATION

Symbol	Definition
B_w	Backscatter factor, defined as the ratio of the water collision kerma at a point on the beam axis at the surface of a full scatter water phantom to the water collision kerma at the same point in the primary (incident) beam with no phantom present.
c_{pl}	Material dependent scaling factor to convert ranges and depths measured in plastic phantoms into the equivalent values in water. This applies to electron, proton and light ion beams.[a]

TABLE 1. QUANTITIES AND SYMBOLS USED IN THIS PUBLICATION (cont.)

Symbol	Definition
$D_{w,Q}$	Absorbed dose to water at the reference depth, z_{ref}, in a water phantom irradiated by a beam of quality Q. The subscript Q is omitted when the reference beam quality is ^{60}Co. Unit: gray (Gy).
E_o, E_z	Mean energy of an electron beam at the phantom surface and at depth z, respectively. Unit: megaelectronvolt (MeV).
h_{pl}	Material dependent charged particle fluence scaling factor to correct for the difference in fluence in plastic compared with that in water at an equivalent depth.
HVL	Half-value layer, used as a beam quality index for low and medium energy X ray beams together with the kilovoltage.
$K_{air,Q}$	Air kerma at a reference point irradiated by a beam of quality Q.
k_i	General correction factor used in the formalism to correct for the effect of the difference in the value of an influence quantity between the calibration of a dosimeter under reference conditions in the standards laboratory and the use of the dosimeter in the user facility under different conditions.
k_{elec}	Calibration factor or coefficient of an electrometer.
k_h	Factor to correct the response of an ionization chamber for the effect of humidity if the chamber calibration coefficient is referred to dry air.
k_{pol}	Factor to correct the response of an ionization chamber for the effect of a change in polarity of the polarizing voltage applied to the chamber.
k_{Q,Q_o}	Factor to correct for the difference between the response of an ionization chamber to the reference beam quality Q_o used for calibrating the chamber in the standards laboratory and to the actual user beam quality Q. The subscript Q_o is omitted when the reference quality is ^{60}Co gamma radiation (i.e. the reduced notation k_Q always corresponds to the reference quality ^{60}Co).
k_s	Factor to correct the response of an ionization chamber for the lack of complete charge collection (due to ion recombination).

TABLE 1. QUANTITIES AND SYMBOLS USED IN THIS PUBLICATION (cont.)

Symbol	Definition
k_{TP}	Factor to correct the response of an ionization chamber for the effect of the difference that may exist between the standard reference temperature and pressure specified by the standards laboratory and the temperature and pressure of the chamber in the user facility under different environmental conditions.
k_{vol}	Factor to correct the response of an ionization chamber in flattening filter free photon beams for the volume averaging effect when the beam profile across the detector is not homogeneous.
M_Q	Reading of a dosimeter at quality Q, corrected for influence quantities other than beam quality. Unit: nanocoulomb (nC) or reading (rdg).
M_{em}	Reading of a dosimeter used as external monitor. Unit: nanocoulomb (nC) or reading (rdg).
$(\mu_{\mathrm{en}}/\rho)_{m_1,m_2}$	Ratio of the mean mass energy absorption coefficients of materials m_1 and m_2, averaged over a photon spectrum.
$N_{D,\mathrm{air}}$	Absorbed dose to air coefficient of an ionization chamber used in air kerma based dosimetry protocols (see Refs [9, 10]). This coefficient is denoted as N_{gas} in Ref. [18] and as N_D in Refs [9, 19], but the subscript 'air' was included in Ref. [10] to specify that it refers to the absorbed dose to the air of the chamber cavity. Care should be taken to avoid confusing $N_{D,\mathrm{air}}$ or N_D with the calibration coefficient in terms of absorbed dose to water, $N_{D,\mathrm{w}}$, described below. Unit: Gy/C or Gy/rdg.
$N_{D,\mathrm{w},Q}$	Calibration coefficient in terms of absorbed dose to water for a dosimeter at a beam quality Q. When the quality is taken as the reference beam quality Q_{o}, the notation becomes $N_{D,\mathrm{w},Q_{\mathrm{o}}}$. The product $M_{Q_{\mathrm{o}}} N_{D,\mathrm{w},Q_{\mathrm{o}}}$ yields the absorbed dose to water, $D_{\mathrm{w},Q_{\mathrm{o}}}$, at the reference depth z_{ref} and in the absence of the chamber. The subscript Q_{o} is omitted when the reference quality is a beam of ^{60}Co gamma rays (i.e. $N_{D,\mathrm{w}}$ always corresponds to the calibration coefficient in terms of absorbed dose to water for a ^{60}Co beam). The coefficient $N_{D,\mathrm{w}}$ was denoted N_D in Ref. [18], where a relationship between N_{gas} and N_D was given. The symbol N_D is also used in calibration certificates issued by some standards laboratories and manufacturers instead of $N_{D,\mathrm{w}}$. Users are strongly recommended to ascertain the physical quantity used for the calibration of their detectors in order to avoid serious mistakes.[b] Unit: Gy/C or Gy/rdg.

TABLE 1. QUANTITIES AND SYMBOLS USED IN THIS PUBLICATION (cont.)

Symbol	Definition
$N_{K_{air},Q}$	Calibration coefficient in terms of air kerma for a dosimeter at a beam quality Q. Unit: Gy/C or Gy/rdg.
p_{cav}	Factor that corrects the response of an ionization chamber for effects related to the air cavity, predominantly the in-scattering of electrons that makes the electron fluence inside a cavity different from that in the medium in the absence of the cavity.
p_{cel}	Factor that corrects the response of an ionization chamber for the effect of the central electrode during in-phantom measurements in high energy photon (including ^{60}Co), electron and proton beams. Note that this factor is not the same as that in Ref. [9], where the correction took into account the global effect of the central electrode both during the calibration of the chamber in air in a ^{60}Co beam and during subsequent measurements in photon and electron beams in a phantom. To avoid ambiguities, Ref. [10] called the correction factor used in Ref. [9] $p_{cel\text{-}gbl}$, keeping the symbol p_{cel} exclusively for in-phantom measurements.
PDD(z)	Percentage depth dose at depth z.
p_{dis}	Factor that accounts for the effect of replacing a volume of water with the detector cavity when the reference point of the chamber[c] is taken to be at the chamber centre. It is used as an alternative to the effective point of measurement of the chamber, P_{eff}. For plane parallel ionization chambers, p_{dis} is not required.
P_{eff}	The effective point of measurement of an ionization chamber. For the standard calibration geometry (i.e. a radiation beam incident from one direction), P_{eff} is shifted from the centre of the chamber towards the source by a distance that depends on the type of beam and chamber. For plane parallel ionization chambers, P_{eff} is usually assumed to be situated in the centre of the front surface of the air cavity.[d] The concept of the effective point of measurement of a cylindrical ionization chamber was used for all radiation types in Ref. [9], but in this international code of practice it is used only for electron and ion beams. For other beams, reference dosimetry is based on positioning the reference point of the chamber at the reference depth, z_{ref}, where the dose is determined. The reference point of an ionization chamber is specified for each radiation type in the corresponding section.

TABLE 1. QUANTITIES AND SYMBOLS USED IN THIS PUBLICATION (cont.)

Symbol	Definition
p_{ch}	Overall perturbation factor for an ionization chamber for in-phantom measurements at a beam quality Q. It is equal to the product of various factors correcting for different effects, each correcting for small perturbations; namely p_{cav}, p_{cel}, p_{dis} and p_{wall}.
p_{wall}	Factor that corrects the response of an ionization chamber for the non-medium equivalence of the chamber wall and any waterproofing material.
Q	General symbol indicating the quality of a radiation beam. A subscript 'o', that is Q_o, indicates the reference quality.
Q_{int}	Intermediate beam quality used to reduce the data required for managing the beam quality correction factors.
rdg	Value representing the reading of a dosimeter, in arbitrary units.
R_{50}	Half-value depth in water, used as the beam quality index for electron beams. This is the depth in water at which the absorbed dose is 50% of its value at the absorbed dose maximum. Unit: g/cm^2.
R_{csda}	Particle range under the continuous slowing down approximation.
R_p	Practical range for electron, proton and ion beams. Unit: g/cm^2.
R_{res}	Residual range for proton and ion beams. Unit: g/cm^2.
r_{cyl}	Cavity radius of a cylindrical ionization chamber.
SAD	Source–axis distance.
SCD	Source–chamber distance.
SOBP	Width of the spread-out Bragg peak in proton and heavier ion beams.
SSD	Source–surface distance.

TABLE 1. QUANTITIES AND SYMBOLS USED IN THIS PUBLICATION (cont.)

Symbol	Definition
$s_{m,\mathrm{air}}$	Stopping power ratio of medium to air, defined as the ratio of the mean restricted mass stopping power of material *m* and air, averaged over an electron spectrum. For all high energy radiotherapy beams in this international code of practice, except for light ion beams, stopping power ratios are of the Spencer–Attix type, with a cut-off energy of $\Delta = 10$ keV (see Ref. [19]).
TMR	Tissue–maximum ratio.
$\mathrm{TPR}_{20,10}$	Tissue–phantom ratio in water at depths of 20 g/cm^2 and 10 g/cm^2, for a field size of 10 cm × 10 cm and an SCD of 100 cm, used as the beam quality index for high energy photon radiation.
u_c	Combined standard uncertainty of a quantity.
W_{air}	Mean energy expended in dry air per ion pair formed.
$z_{\max}$	Depth of maximum dose. Unit: g/cm^2.
z_{ref}	Reference depth for in-phantom measurements. When specified at z_{ref}, the absorbed dose to water refers to $D_{\mathrm{w},Q}$ at the intersection of the beam central axis with the plane defined by z_{ref}. Unit: g/cm^2.

[a] In this international code of practice, depths and ranges are expressed in units of g/cm^2, in contrast to their definition in Ref. [10] for electron beams, where they are expressed in centimetres. As a result, the c_{pl} values for electrons given in this publication differ from those for C_{pl} in Ref. [6]. The use of a lowercase '*c*' in c_{pl} denotes this change.

[b] The difference between $N_{D,\mathrm{air}}$ and $N_{D,\mathrm{w}}$ is close to the value of the water to air stopping power ratio for ^{60}Co gamma rays. A confusion in the meaning of the factors could therefore result in an error in the dose delivered to patients of approximately 13%.

[c] In this publication, the reference point of a chamber is specified in each section for each type of chamber. It usually refers to the point of the chamber specified by a calibration document where the calibration coefficient applies [62].

[d] This assumption might fail if the chamber design does not follow certain requirements regarding the ratio of cavity diameter to cavity height, as well as that of guard ring width to cavity height (see Ref. [10]).

2. FRAMEWORK

2.1. THE INTERNATIONAL MEASUREMENT SYSTEM

The International Measurement System for radiation metrology provides the framework for consistency in radiation dosimetry by disseminating to users calibrated radiation instruments that are traceable to primary standards. This international arrangement for traceability is represented schematically in Fig. 3.

BIPM was set up by the Metre Convention (originally signed in 1875), which as of July 2021 has 63 Member States and 39 Associate States and Economies. It serves as the international centre for metrology, with its laboratory and offices in Sèvres (France), with the aim of ensuring worldwide uniformity in matters relating to metrology. In radiation dosimetry, BIPM and the PSDLs of many Member States of the Metre Convention have developed primary standards for radiation measurements (see Table 2 for guidance on the classification of instruments and standards laboratories). However, worldwide there are only some 20 countries with PSDLs involved in radiation dosimetry and they cannot calibrate the very large number of radiation dosimeters that are in use around the world. This demand is eased by the IAEA/WHO SSDL Network (see Section 2.1.2). Together, the IAEA, BIPM and PSDLs calibrate the secondary

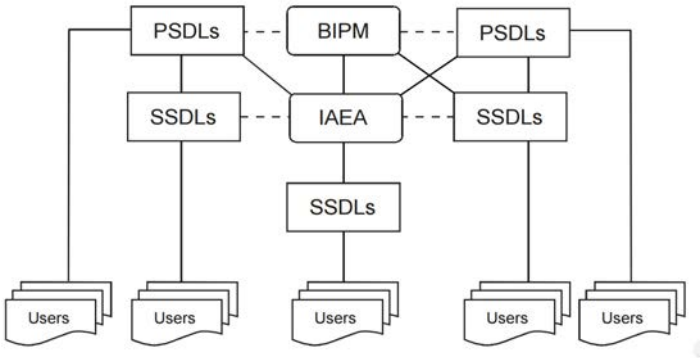

FIG. 3. The International Measurement System for radiation metrology, where the traceability of user reference instruments to primary standards is achieved either by direct calibration in a primary standards dosimetry laboratory (PSDL) or, more commonly, in a secondary standards dosimetry laboratory (SSDL) with a direct link to BIPM, to a PSDL or to the IAEA/WHO SSDL Network. Most SSDLs from countries that are not members of the Metre Convention achieve the traceability of their standards through the IAEA. The dashed lines indicate intercomparisons of primary and secondary standards.

TABLE 2. CLASSIFICATIONS OF INSTRUMENTS AND STANDARDS LABORATORIES *(adapted from Ref. [62])*

Classification of instruments	Standards laboratories
Primary standard An instrument of the highest metrological quality that permits the determination of a quantity from its definition without reference to other standards of the same quantity, the accuracy of which has been verified by comparison with standards for the same quantity maintained by other institutes participating in the International Measurement System	*Primary standards dosimetry laboratory* A national standardizing laboratory designated by the government for the purpose of developing, maintaining and improving primary standards in radiation dosimetry
Secondary standard An instrument with established precision and long term stability that has a calibration traceable to a primary standard	*Secondary standards dosimetry laboratory* A dosimetry laboratory designated by the competent authorities to provide calibration services, which is equipped with at least one secondary standard
National standard A standard recognized by an official national decision as the basis for fixing the value of all other standards of a given quantity in a country	
Reference instrument An instrument of the highest metrological quality available at a given location, with a traceable calibration from which measurements at that location are derived	
Field instrument An instrument used for routine measurements whose calibration is traceable to the reference instrument	

standards of SSDLs, and the SSDLs in turn calibrate the reference instruments of users (some PSDLs also calibrate the reference instruments of users in countries where a network of radiotherapy dosimetry oriented SSDLs is missing).

In addition to demonstrating traceability to primary standards, there is a need to validate the primary standards themselves, that is, to provide evidence that individual standards are operating at the level of the stated uncertainty. Validation of primary standards can involve many components, including the quality system

of the PSDL, but the clearest demonstration of the validity of a primary standard is comparison measurements with another national or international standard for the same quantity.

2.1.1. The mutual recognition arrangement of the International Committee for Weights and Measures

In 1999, CIPM established a mutual recognition arrangement (CIPM MRA) [63], the signatories of which were national metrology institutes and a number of international organizations, including the IAEA. As of July 2020, there are 106 signatories. Each signatory may choose to designate another laboratory in their country as the holder of the national standard for a particular quantity. This expands the CIPM MRA to cover a further 153 institutes (as of July 2020).[9]

The CIPM MRA has two main aims. The first is to make readily available the results of key international comparisons of standards and to establish the degree of equivalence between each standard and an agreed international reference value. These data are held on-line in the BIPM key comparison database (KCDB) [64]. For the dosimetry standards held at BIPM, national primary standards are compared on an ongoing basis with the relevant BIPM primary standard, which is taken to be the reference value. A structure of regional metrology organizations also exists within the CIPM MRA to extend comparisons of national standards, primary or secondary, beyond those undertaken by BIPM (and on an ad hoc basis by PSDLs and routinely by the IAEA). This includes comparisons for derived quantities or measurements that are considered to be supplementary rather than key.

The second main aim of the CIPM MRA is to enable the mutual recognition of the calibration and measurement capabilities stated by participating institutes. These capabilities are held on-line and take the form of a list of measurement services offered by each participating institute, including the stated uncertainty of each measurement [65]. As part of this declaration, each institute has to demonstrate that it has a suitable quality system in place. Before being made available in the KCDB, the calibration and measurement capabilities undergo a rigorous review process, firstly by the appropriate regional metrology organization and subsequently through an inter-regional review. Through this process, users can have confidence in the results and the stated uncertainties of the measurement services offered by participating national metrology institutes and international organizations throughout the world.

---

[9] Information on the current status of CIPM MRA is provided at http://www.bipm.org/en/cipm-mra/

2.1.2. The IAEA/WHO network of Secondary Standards Dosimetry Laboratories

The main role of the SSDLs is to bridge the gap between PSDLs and the users of ionizing radiation by enabling the transfer of dosimeter calibrations from the primary standard to user instruments [66]. In 1976, a network of SSDLs was established as a joint effort by the IAEA and WHO to improve accuracy in radiation dosimetry by providing a route for traceability to the International System of Units (système international d'unités (SI)) for national dosimetry standards, mainly for countries that are not members of the Metre Convention [67]. By 2020, the network included 87 SSDLs in 72 IAEA Member States, of which over half are in developing countries. The SSDL network also includes 22 collaborating organizations and affiliated members, among which is BIPM, several national PSDLs, the ICRU and other international organizations that provide support to the network [68].

As the organizer of the network, the IAEA has the responsibility to verify that the services provided by the member SSDLs follow internationally accepted metrological standards (including traceability for instruments used in radiation protection and diagnostic radiology). The first step in this process is the dissemination of dosimeter calibrations from BIPM or PSDLs through the IAEA to the SSDLs. Subsequently, bilateral comparisons and dose quality audits are implemented by the IAEA for the SSDLs to ensure that the standards disseminated to users remain within the levels of accuracy required by the International Measurement System [67].

One of the principal goals of the SSDL network in the field of radiotherapy dosimetry is to ensure that the dose delivered to patients undergoing radiotherapy treatment is within internationally accepted levels of accuracy. This is accomplished by ensuring that the calibrations of instruments provided by the SSDLs are within the stated uncertainties, emphasizing the need for SSDL participation in quality assurance programmes for radiotherapy, promoting the contribution of the SSDLs to support dosimetry quality audits in radiotherapy centres and assisting if needed in performing the calibration of radiotherapy equipment in hospitals.

2.2. STANDARDS FOR ABSORBED DOSE TO WATER

At present, there are only three basic methods that are sufficiently accurate to form the basis of primary standards for absorbed dose to water [58]: calorimetry, chemical dosimetry and ionization dosimetry. The PSDLs have developed various experimental approaches to establish standards for absorbed dose to water. These

standards are described briefly and the results of international comparisons are presented below.

Many PSDLs maintain a primary standard for absorbed dose to water operating in ^{60}Co gamma radiation and some PSDLs also maintain standards operating at other radiation qualities, such as megavoltage photons and electrons and kilovoltage X rays. Primary standards operating in ^{60}Co gamma radiation or in photon and electron beams produced by accelerators are based on one of the following methods:

(a) The graphite calorimeter developed by Domen and Lamperti [69], with certain modifications, is used by several PSDLs to determine the absorbed dose to graphite in a graphite phantom. The conversion to absorbed dose to water at the reference point in a water phantom can be performed in different ways [70], for example by application of the photon fluence scaling theorem [71, 72], by measurements based on the cavity ionization theory [73] or by direct Monte Carlo calculations [74].
(b) The water calorimeter offers a more direct determination of the absorbed dose to water at the reference point in a water phantom. The sealed water system [75, 76] consists of a small glass vessel containing high purity water and thermistor detectors. Water purity is important because the presence of impurities can result in exothermic or endothermic chemical reactions that modify the relationship between absorbed dose and temperature rise — the so called 'heat defect'. With the sealed water arrangement, high purity water can be saturated with various gases to create a mixture for which the heat defect has a well defined and stable value.
(c) The Fricke standard for absorbed dose to water determines the response of a known volume of Fricke solution to the total absorption of an electron beam in the volume [77]. Knowing the electron energy, the beam current and the mass of Fricke solution, the total absorbed energy can be determined and related to the change in absorbance of the Fricke solution as measured spectrophotometrically. In recent years, the use of the Fricke standard as a primary method to determine absorbed dose to water has diminished with the increasing adoption of water calorimetry.
(d) The ionization chamber primary standard consists of an air filled graphite cavity chamber with known cavity volume, designed to fulfil as far as possible the requirements of a Bragg–Gray detector. The chamber is placed in a water phantom and the absorbed dose to water at the reference point is derived from the mean specific energy imparted to the air of the cavity [78].

Until approximately 2015, absolute measurements for the determination of absorbed dose to water in kilovoltage X ray beams were based almost exclusively on extrapolation ionization chambers [79]. Water or graphite calorimetry is now

used at a number of PSDLs for the 100–250 kV X ray range [80], and BIPM has developed a primary standard for these beams based on the free air ionization chamber [81]. The availability of these standards enables calibrations in terms of absorbed dose to water for SSDL and user instruments in these X ray beams, the most direct route to absorbed dose determination in the clinic. However, there has been no significant development of primary standards for absorbed dose to water for X ray beam energies below 100 kV.

Comparisons of primary standards for absorbed dose to water in ^{60}Co gamma radiation have been carried out at BIPM since the 1990s; BIPM comparisons of air kerma primary standards have a longer history. Since the inception of the CIPM MRA, up to date results of these ongoing series of comparisons have been available on-line in BIPM KCDB[10]. Comparisons in terms of absorbed dose to water for ^{60}Co are registered as comparison series BIPM.RI(I)-K4. The results (as of July 2020) are shown in Fig. 4(a). The agreement is well within the standard uncertainty stated by each PSDL. Comparisons of air kerma primary standards for ^{60}Co gamma radiation, registered as BIPM.RI(I)-K1, exhibit a similar distribution despite smaller uncertainties, as shown in Fig. 4(b). The air kerma primary standards of all PSDLs are graphite cavity ionization chambers, and the associated correction factors are strongly correlated. In contrast, as noted above, the standards for absorbed dose to water use different methods that have uncorrelated, or only weakly correlated, uncertainties and constitute a system that is more robust and less susceptible to systematic influences.

Since 2009, BIPM has operated a travelling primary standard for absorbed dose to water, a graphite calorimeter [82] and dose conversion system, and between 2009 and 2016 this standard was used to make direct comparisons in the accelerator photon beams of PSDLs. Since 2017, comparisons have been made in reference beams maintained by BIPM at an external accelerator facility. The results of these comparisons are registered as BIPM.RI(I)-K6, and those for photon beams with $TPR_{20,10} = 0.63–0.71$ (as of July 2020) are shown in Fig. 4(c). The uncertainties are generally larger than those for ^{60}Co gamma radiation and agreement is again within the stated expanded uncertainties ($k = 2$).

Links to the published reports for all BIPM comparisons are available in BIPM KCDB. It should be noted that each result for a given PSDL shown in Fig. 4 is considered out of date when the PSDL makes a new comparison, typically every 10 years, although a maximum of 15 years between consecutive comparisons is agreed within CCRI. The up to date results are those available in BIPM KCDB.

[10] See http://kcdb.bipm.org/

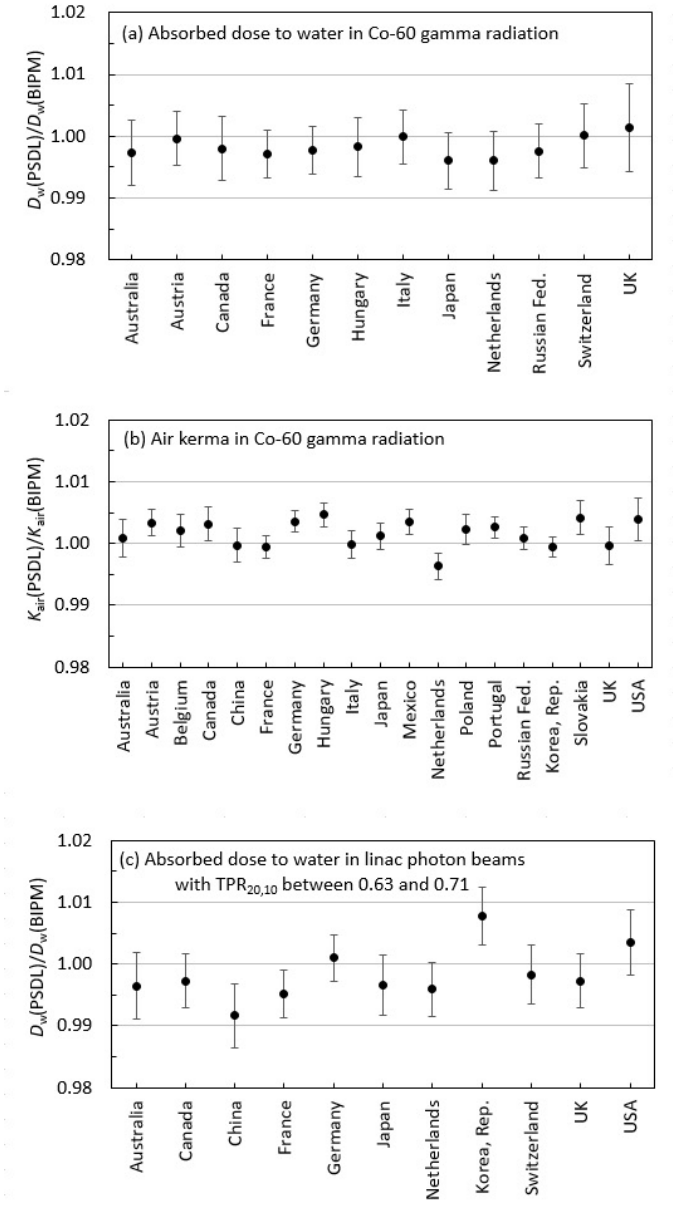

FIG. 4. Results of BIPM comparisons of standards for (a) absorbed dose to water in ^{60}Co gamma radiation, (b) air kerma in ^{60}Co gamma radiation and (c) absorbed dose to water in linac photon beams with $TPR_{20,10}$ between 0.63 and 0.71. Each result is relative to the corresponding BIPM determination. The uncertainty bars represent the standard uncertainty stated by each PSDL for their standard. All data were taken from BIPM KCDB in July 2020.

3. $N_{D,W}$ BASED FORMALISM

The formalism for the determination of absorbed dose to water in high energy photon and electron beams using an ionization chamber or a dosimeter calibrated in terms of absorbed dose to water in a ^{60}Co beam has been given in detail by Hohlfeld [55]. Complementary work on this topic and extensions of the formalism have been developed by Andreo [56] and Rogers [57]. The procedure for the determination of absorbed dose to water using standards of absorbed dose to water has been implemented in national dosimetry recommendations [83–85]. It was also included in the first edition of this international code of practice and in Ref. [10] for plane parallel ionization chambers.

3.1. FORMALISM

The absorbed dose to water at the reference depth z_{ref} in water for a reference beam of quality Q_{o} and in the absence of the chamber is given by the following equation:

$$D_{\text{w},Q_{\text{o}}} = M_{Q_{\text{o}}} N_{D,\text{w},Q_{\text{o}}} \tag{1}$$

where $M_{Q_{\text{o}}}$ is the reading of the dosimeter under the reference conditions used in the standards laboratory and N_{D,w,Q_o} is the calibration coefficient in terms of absorbed dose to water of the dosimeter obtained from a standards laboratory. In most clinical situations, the measurement conditions do not match the reference conditions used in the standards laboratory. This may affect the response of the dosimeter, and it is then necessary to differentiate between the reference conditions used in the standards laboratory and the clinical measurement conditions.

3.1.1. Reference conditions

The calibration coefficient for an ionization chamber irradiated under reference conditions is the ratio of the conventional true value of the quantity

to be measured to the indicated value.[11] Reference conditions are described by a set of values of influence quantities for which the calibration coefficient is valid without further correction factors. The reference conditions for calibrations in terms of absorbed dose to water are, for example, the geometrical arrangement (distance and depth), the field size, the material and dimensions of the irradiated phantom, and the ambient temperature, pressure and relative humidity.

3.1.2. Influence quantities

Influence quantities are defined as quantities that are not the subject of the measurement, but yet influence the quantity under measurement. They may be of different nature (e.g. pressure, temperature, polarization voltage); they may arise from the dosimeter (e.g. ageing, zero drift, warmup); or they may be quantities related to the radiation field (e.g. beam quality, dose rate, field size, depth in a phantom).

In calibrating an ionization chamber or a dosimeter, as many influence quantities as practicable are kept under control. However, many influence quantities can be difficult to control, for example air pressure and humidity, and dose rate in ^{60}Co gamma radiation. It is possible to correct for the effect of these influence quantities by applying appropriate correction factors. Assuming that influence quantities act independently from each other, a product of correction factors can be applied, $\prod k_i$, where each correction factor k_i is related to only one influence quantity. The independence of k_i holds for the common corrections for pressure, temperature, polarity, charge collection efficiency, etc., which are dealt with in Section 4.4.3.

A departure from the reference beam quality Q_o used to calibrate an ionization chamber can also be treated as an influence quantity. Measurements at radiation qualities other than the reference quality Q_o therefore require a correction factor. In this international code of practice, this is treated explicitly by the factor k_{Q,Q_o}, which is the correction for the radiation beam quality and is not included in the factors k_i discussed above.

---

[11] The ‘conventional true value’ of a quantity is the value attributed to a particular quantity and accepted, sometimes by convention, as having an uncertainty appropriate for a given purpose. The conventional true value is sometimes called ‘assigned value’, ‘best estimate of the value’, ‘conventional value’ or ‘reference’ [86]. At a given laboratory or hospital, the value measured by a reference standard may be taken as the conventional true value, and frequently the mean of a number of results of measurements of a quantity is used to establish the conventional true value.

3.2. CORRECTION FOR THE RADIATION QUALITY OF THE BEAM, k_{Q,Q_o}

When a dosimeter is used in a beam with a different quality Q from that used in its calibration, Q_o, the absorbed dose to water is given by the following equation:

$$D_{w,Q} = M_Q N_{D,w,Q_o} k_{Q,Q_o} \tag{2}$$

where the factor k_{Q,Q_o} corrects the calibration coefficient N_{D,w,Q_o} for the difference between the reference beam quality Q_o and the actual user quality Q, and the dosimeter reading M_Q has been corrected to the reference values of influence quantities other than the beam quality for which the calibration coefficient is valid.

The beam quality correction factor k_{Q,Q_o} is defined as the ratio of the calibration coefficients in terms of absorbed dose to water of the dosimeter at the qualities Q and Q_o, as follows:

$$k_{Q,Q_o} = \frac{N_{D,w,Q}}{N_{D,w,Q_o}} = \frac{D_{w,Q}/M_Q}{D_{w,Q_o}/M_{Q_o}} \tag{3}$$

The most common reference quality Q_o used for the calibration of ionization chambers and dosimeters is ^{60}Co gamma radiation, in which case the symbol k_Q is used in this international code of practice for the beam quality correction factor. In some PSDLs, high energy photon and electron beams are directly used for calibration purposes, and the symbol k_{Q,Q_o} is used in those cases.

Ideally, the beam quality correction factor should be measured directly for each chamber at the same quality as the user beam. However, this is not achievable in most standards laboratories. Such measurements can be performed only in laboratories with access to the appropriate beam qualities. For this reason, the technique is currently restricted to a few PSDLs globally. The procedure requires the availability of an energy independent dosimetry system, such as a calorimeter, operating at these qualities. A related problem is the difficulty in reproducing identical beam qualities to those produced by clinical accelerators in a standards laboratory [87, 88].

When no experimental data are available, or it is difficult to measure k_{Q,Q_o} directly for realistic clinical beams, in many cases the correction factors can be calculated (see Appendix II).

3.2.1. The concept of the intermediate quality Q_{int} and its use for photon beams

When the reference beam Q_o is ^{60}Co gamma radiation, k_{Q,Q_o} is denoted as k_Q and the data requirement is relatively straightforward; for each chamber type, k_Q values are provided for each beam quality Q of interest. However, with the availability of direct calibrations in accelerator photon and electron beams at standards laboratories, the situation can arise in which, for example, a reference chamber calibrated in a Q_o = 6 MV photon beam is to be used in a Q = 18 MV beam (for simplicity, the nominal megavoltage values, rather than $TPR_{20,10}$, are used here). This requires use of the factor $k_{18\ MV,6\ MV}$. More generally, the reference chamber might be calibrated in any of the accelerator beams available at the standards laboratory. This leads to the need for a two dimensional table of k_{Q,Q_o} values for each chamber type because both Q and Q_o are variables.

To reduce this problem to a manageable level, the concept of an 'intermediate quality', Q_{int}, is introduced. From the definition of k_{Q,Q_o} in Eq. (3), we can write the following:

$$k_{Q,Q_o} = \frac{N_{D,w,Q}}{N_{D,w,Q_o}} = \frac{N_{D,w,Q}}{N_{D,w,Q_{int}}} \frac{N_{D,w,Q_{int}}}{N_{D,w,Q_o}} = \frac{k_{Q,Q_{int}}}{k_{Q_o,Q_{int}}} \tag{4}$$

Here, an intermediate calibration coefficient $N_{D,w,Q_{int}}$ has been introduced in a way that transforms the required factor k_{Q,Q_o} into a ratio of two factors, $k_{Q,Q_{int}}$ and $k_{Q_o,Q_{int}}$. To demonstrate how this simplifies the data requirement, the example above is considered for megavoltage photons with Q_o = 6 MV and with ^{60}Co gamma radiation as the intermediate quality Q_{int}. Then, the factor $k_{18\ MV,6\ MV}$ is obtained as follows:

$$\begin{aligned} k_{18\ MV,6\ MV} &= \frac{N_{D,w,18\ MV}}{N_{D,w,6\ MV}} = \frac{N_{D,w,18\ MV}}{N_{D,w,^{60}Co}} \frac{N_{D,w,^{60}Co}}{N_{D,w,6\ MV}} \\ &= \frac{k_{18\ MV,^{60}Co}}{k_{6\ MV,^{60}Co}} = \frac{k_{18\ MV}}{k_{6\ MV}} \end{aligned} \tag{5}$$

where, in the final step, the subscript ^{60}Co is omitted following the notation adopted for k_Q. The factors $k_{18\ MV}$ and $k_{6\ MV}$ are taken from Section 6.5.1 as a function of $TPR_{20,10}$ and no additional data are required. Importantly, the need for a two dimensional table of k_{Q,Q_o} values for each chamber type is removed. Note that no measurements are made at the intermediate quality, ^{60}Co in this case, which is simply used as a tool to reduce the data required for each chamber type.

3.2.2. The intermediate quality for electron beams

The concept of the intermediate quality Q_{int}, introduced in Eq. (4) as follows:

$$k_{Q,Q_{\text{o}}} = \frac{k_{Q,Q_{\text{int}}}}{k_{Q_{\text{o}},Q_{\text{int}}}} \tag{6}$$

is also useful for electron dosimetry. However, in this case the best choice for Q_{int} is an electron beam rather than ^{60}Co gamma radiation because for some chamber types designed for use in electron beams no reliable data for k_Q are available. Furthermore, the uncertainty of the factors $k_{Q,Q_{\text{int}}}$ and $k_{Q_{\text{o}},Q_{\text{int}}}$ is reduced if Q_{int} is closer in energy and of the same beam type as Q and Q_{o}.

It would seem reasonable to choose Q_{int} in electron beams to be near the middle of the range; in this international code of practice it is chosen to be R_{50} = 7.5 g/cm^2, where R_{50} is the beam quality index in electron beams (see Section 7). Values for $k_{Q,Q_{\text{int}}}$ calculated on this basis are given in Section 7.6.2 for a series of chamber types. It is emphasized again that no measurements are made at Q_{int} — it is simply a tool to reduce the data required.

The calibration coefficient of the plane parallel chamber at the electron beam quality Q_{o} can be obtained in one of the following ways:

(a) By direct calibration at a standards laboratory in an electron beam of quality Q_{o};
(b) By calibration at a standards laboratory in ^{60}Co gamma radiation, followed by the application of the appropriate beam quality correction factor (see Section 7.6.2);
(c) By cross-calibration in the clinical electron beam of quality Q_{o} against a reference chamber with calibration coefficient $N_{D,\text{w},Q_{\text{o}}}^{\text{ref}}$ for this quality.

The process of cross-calibration in the clinic is described in Section 4.5.

3.2.3. The intermediate quality to convert between modalities

Equation (5) demonstrates the use of ^{60}Co as the intermediate quality in evaluating the factor $k_{18\text{ MV},6\text{ MV}}$ that converts calibration coefficients from a 6 MV photon beam to an 18 MV photon beam using existing k_Q factors based on ^{60}Co, although no user or calibration measurements are made in ^{60}Co gamma radiation. Generally, the concept of the intermediate quality provides a solution for the use of a chamber in any modality through its calibration in a different modality, as long as the relevant $k_{Q,Q_{\text{o}}}$ factors are available.

As an example, one can derive the calibration coefficient $N_{D,\mathrm{w},3\ \mathrm{g/cm^2}}$ for a proton beam with residual range $R_{\mathrm{res}} = 3\ \mathrm{g/cm^2}$ from a calibration with coefficient $N_{D,\mathrm{w},6\ \mathrm{MV}}$ in a 6 MV photon beam using the following:

$$N_{D,\mathrm{w},3\ \mathrm{g/cm^2}} = \frac{k_{3\ \mathrm{g/cm^2}}}{k_{6\ \mathrm{MV}}} N_{D,\mathrm{w},6\ \mathrm{MV}} \tag{7}$$

Values for $k_{3\ \mathrm{g/cm^2}}$ are provided in Section 10.7.2 and for $k_{6\ \mathrm{MV}}$ in Section 6.5.1. In this way, it is feasible to base reference dosimetry for proton and heavier ion beams on a chamber calibrated in an accelerator photon beam using only k_Q data available from the existing tables. The resulting uncertainty will be higher than that achievable through direct calibration in the radiation modality of interest.

4. IMPLEMENTATION

4.1. GENERAL

Early efforts in PSDLs concentrated on providing calibrations in terms of absorbed dose to water of ionization chambers in ^{60}Co gamma ray beams. This was followed by similar capabilities for high energy photon and electron beams [89–93]. Standards have been described for kilovoltage X ray beams [80] and for protons and light ions [94, 95], but to date few calibration services have been established for such modalities.

Depending on the standards laboratory and beam type (modality), users may be provided with $N_{D,w,Q}$ calibration coefficients according to different options. These options are clarified here in order to avoid the incorrect use of this international code of practice.

4.1.1. Calibrations in standards laboratories made at multiple beam qualities

Only laboratories with radiation sources and standards operating at different beam qualities can provide directly measured values of $N_{D,w,Q}$ or k_{Q,Q_o} for these qualities. The main advantage of this approach is that the individual chamber response in a water phantom irradiated by various beam types and qualities is intrinsically taken into account. Two approaches, differing only in the presentation of the data, are as follows:

(a) Users are provided with a series of $N_{D,w,Q}$ calibrations of the user ionization chamber at beam qualities Q. One of the beam qualities is selected by the user as the reference quality Q_o at the clinical site, with its calibration coefficient being denoted by N_{D,w,Q_o}. Values of k_{Q,Q_o} are derived by normalizing all calibration coefficients to N_{D,w,Q_o}, as defined in Eq. (3), which corresponds to directly measured values of k_{Q,Q_o}. The advantage of this approach is that, once directly measured values of k_{Q,Q_o} for a particular chamber have been obtained, it may not be necessary to recalibrate the chamber at all qualities Q, but only at the single reference quality Q_o. The quality dependence of that chamber can be verified less often by calibration at all qualities.[12] Furthermore, this single reference quality calibration does not need to be performed at the same laboratory where the k_{Q,Q_o} values were measured (usually a PSDL).

[12] See Section 4.3 for recommendations on the frequency of dosimeter calibrations.

(b) Users are provided with a calibration coefficient N_{D,w,Q_o} at a laboratory selected reference quality Q_o, together with a series of k_{Q,Q_o} factors directly measured for the user chamber at beam qualities Q. The criteria for the type and frequency of calibrations are as above.

A possible limitation of these two options resides in the difference between the beam qualities used at the standards laboratory and at the user facility. For megavoltage photon beams this has largely been circumvented through the installation of clinical linear accelerators in many standards laboratories. For kilovoltage beams, the large range of beam qualities available makes it challenging to match the conditions of calibration and use. It is worth noting that, despite decreasing clinical use, ^{60}Co remains the only 'universal' beam quality.

4.1.2. Calibrations in standards laboratories made at a single reference quality Q_o

Users are provided with a calibration coefficient N_{D,w,Q_o} (or $N_{D,w}$ when the reference quality is ^{60}Co). The values of k_{Q,Q_o} (or k_Q when the reference quality is ^{60}Co) to be used for this approach are generic, that is, they are common to a specific ionization chamber type and as such cannot take chamber to chamber differences for that chamber type into account. The current approaches for the beam quality correction factors are the following:

(a) Generic experimental values obtained from measurements at standards laboratories for a sample of ionization chambers of a given type. This approach is an alternative option to option (b) in Section 4.1.1 only when k_Q or k_{Q,Q_o} values have been obtained by a standards laboratory from a large sample of ionization chambers and the standard deviation of chamber to chamber differences is small. This is usually the case for secondary standard quality chambers (see Ref. [96]), such as those measured by the National Physical Laboratory in the United Kingdom (see Fig. 5) [97], and for a number of reference class chambers.[13] Generic experimental k_Q or k_{Q,Q_o} values not determined by a standards laboratory are not recommended, except as a secondary check on calculated values.
(b) Generic calculated values using the following:
    (i) The Bragg–Gray based analytical expression given in Eqs (91) and (92) in Appendix II. This procedure was used in the first edition of this

[13] The specifications for a reference class ionization chamber are given in Ref. [12], based on work conducted by McEwen at the National Research Council of Canada [98].

international code of practice and in Ref. [85] and is also used in this version for ions heavier than protons.

(ii) Detailed Monte Carlo simulations of a given chamber type. This technique was used in Ref. [99].

(c) Generic compound values, derived statistically from the combination of the following:

(i) Detailed Monte Carlo simulations of specific chamber types and PSDL based experimental values for a sample of chambers of that type, such as the 'consensus' k_Q data for megavoltage photon beams given in this publication [100].

(ii) Chamber specific Monte Carlo calculated values and analytical calculations using Eq. (92) in Appendix II, as for proton beams.

Approaches (c)(i) and (c)(ii) are used in this international code of practice.

It is emphasized that calculated beam quality correction factors for a given chamber type using either analytical or Monte Carlo techniques ignore chamber to chamber response variations with energy for that chamber

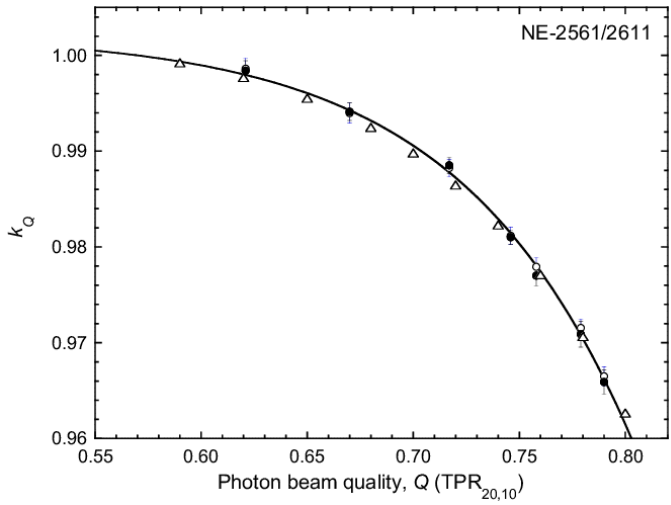

FIG. 5. Mean values of k_Q *at various photon beam qualities, measured at the National Physical Laboratory in the United Kingdom for secondary standard ionization chambers of types NE-2561 (open circles) and NE-2611 (NPL-2611) (filled circles) [97]. The solid line is a fit to the experimental data using Eq. (97) in Appendix II. The uncertainty bars represent chamber to chamber variations, determined as the standard deviations of samples of 13 NE-2561 and 11 NE-2611 (NPL-2611) chambers. The* k_Q *values are normalized to a* $TPR_{20,10}$ *of 0.568 (*^{60}*Co beam at the NPL). The* k_Q *values for these chambers given in Section 6.5.1 are included for comparison (triangles); note that these values are for both types of chamber.*

type. Calculations also rely heavily on chamber specifications provided by manufacturers. In most cases, the reference quality used is ^{60}Co.

4.1.3. Recommendations

On the basis of the descriptions in Sections 4.1.1 and 4.1.2, the following recommendations are given for compliance with this international code of practice:

(a) Approach (a), or its equivalent (b), in Section 4.1.1 are the preferred alternatives, although for beam qualities other than ^{60}Co such possibilities are at present restricted to a few calibration laboratories.
(b) Approach (c) in Section 4.1.2 is recommended when k_Q or k_{Q,Q_o} values directly measured for the user chamber at various beam qualities in a standards laboratory (approach in Section 4.1.1) are not available. The use of ^{60}Co as the reference quality for determining $N_{D,w}$ is particularly appropriate for SSDLs.
(c) For chamber calibrations in terms of absorbed dose to water and in terms of air kerma (see Sections 8 and 9), low and medium energy kilovoltage X ray dosimetry has to be based on approaches (a) or (b) in Section 4.1.1, with the range of Q values chosen to be as similar as possible to the qualities of the beams that will be used clinically.
(d) As long as there are restricted possibilities for standards laboratories to establish experimental $N_{D,w,Q}$ factors in proton and heavier ion beams, approaches (c)(ii) and (b)(i) in Section 4.1.2 are the only recommendations for protons and heavier ions, respectively.

4.2. EQUIPMENT

Only ionometric measurements are considered in this international code of practice for reference dosimetry. The basic requirements on equipment follow closely those in the first edition of this international code of practice and in Refs [9, 10, 12], as well as IEC Standard 60731 [96], for dosimeters with ionization chambers. The use of these documents, although developed for photon and electron radiation, can be extended to the other types of radiation field included in this publication.

This section provides only general requirements for equipment; specific details on instrumentation that apply to each radiation type will be discussed in the relevant section.

An ionometric dosimeter system for radiotherapy contains the following components:

(a) One or more ionization chamber assemblies, including the permanently attached cable and connector. It is advised that these ionization chambers be specifically designed for the intended purpose (e.g. modality, radiation quality).
(b) A measuring assembly (electrometer). This can be considered to form a system with the ionization chamber, and that system is calibrated as a unit, or the electrometer can be calibrated separately in terms of charge or current per scale division.
(c) One or more phantoms with waterproof sleeves (if required). A special holder might be required to position the chamber correctly within the phantom.
(d) Calibrated devices to measure the phantom temperature and air pressure, to correct the ionization chamber reading to reference conditions.
(e) One or more stability check devices. It is recognized, however, that in many facilities the use of radioactive check sources is actively discouraged. In such circumstances, and without access to a ^{60}Co beam, stability monitoring can be carried out through the regular comparison of duplicate dosimeters. Such an approach is also recommended from a quality assurance perspective to ensure that a robust dosimetry system is maintained.

4.2.1. Ionization chambers

A cylindrical ionization chamber type may be used for the calibration of radiotherapy beams of low and medium energy X rays above 70 kV, ^{60}Co gamma radiation, high energy photon beams, electron beams with energy above ~9 MeV, and therapeutic proton and heavier ion beams. This type of chamber is very convenient for measurements at these radiation qualities, as it is robust and simple to use for measurements in a water phantom. The chamber cavity volume should be between about 0.1 cm^3 and 1 cm^3. This size range is a compromise between the need for sufficient sensitivity and the ability to measure dose at a point. These requirements are met in cylindrical chambers with an air cavity of internal diameter not greater than ~7 mm and an internal length not greater than ~25 mm. In use, the radiation fluence should be approximately uniform over the cross-section of the chamber cavity. The chamber should not be used with the stem parallel to the beam direction, and therefore the cavity length is a limiting factor on the minimum field size in which measurements may be made (see Ref. [12]).

The construction of the chamber should be as homogeneous as possible, but it is recognized that for technical reasons the central electrode is likely to be

of a material different from that of the walls. Indeed, the choice of materials may play an important role in ensuring that the energy response of the chamber does not vary considerably. It is also necessary for the air cavity not to be sealed; it should be designed so that it will equilibrate rapidly with the ambient temperature and air pressure.

In choosing a cylindrical ionization chamber, the user should pay attention to whether it is to be used as a reference instrument (calibrated at a standards laboratory and used for beam calibration in the user beam) or as a field instrument (cross-calibrated against a reference chamber and normally used for routine measurements). Graphite walled ionization chambers usually have better long term stability and more uniform response than plastic walled chambers; however, the latter are mechanically more robust and therefore more suitable for routine measurements. Chambers with A-150 or nylon walls are explicitly not recommended as reference instruments because of the hygroscopic nature of the plastic [101]. As an ionization chamber is an instrument of high precision, attention should be paid to acquiring a chamber type whose performance has been tested sufficiently in radiotherapy beams. To aid the user, this international code of practice adopts the specification for a reference class ionization chamber given in Ref. [12], which is based on that in Ref. [98]. Specifications for reference class chambers are listed in Table 3. Guidelines on chamber specifications can be found in Ref. [96]. The characteristics of certain cylindrical ionization chambers that meet these specifications are given in Table 4. Other cylindrical chamber types, not listed in Table 4, may be suitable for reference dosimetry in one or more of the modalities covered in this publication if they have been shown to meet the same specifications.

The use of plane parallel ionization chambers in high energy electron and photon beams has been described in detail previously in Ref. [10]. Plane parallel chambers are recommended to be used at all electron energies, and below 8 MeV their use is mandatory. For photon beams, plane parallel chambers should not be used for reference dosimetry except in the very specific situation described in Section 6.2.1. However, they can be used for relative measurements. They are also suitable for reference and relative dosimetry for proton and heavier ion beams, especially for low energy beams and beams with a narrow spread-out Bragg peak (SOBP). The chamber should preferably be designed for use in water and the construction should be as homogeneous and water equivalent as possible. It is important to be aware of backscatter effects from the rear wall of the chamber, and chambers designed for measurements in solid phantoms should accordingly be as phantom equivalent as possible.

The diameter of the collecting electrode should not exceed 20 mm in order to reduce the influence of radial non-uniformities of the beam profile. The cavity height ought not to exceed 2 mm, and the collecting electrode should

TABLE 3. SPECIFICATIONS FOR REFERENCE CLASS IONIZATION CHAMBERS FOR REFERENCE DOSIMETRY [12]

Parameter	Specification
Chamber settling	Monitoring chamber response with accumulated dose: equilibrium is reached in <5 min; the initial and equilibrium readings agree within 0.5%
Leakage	<0.1% of the chamber reading[a]
Polarity effect	Less than 0.4% of the chamber reading; the polarity energy dependence is <0.3% between the energies of the ^{60}Co beam and 10 MV photon beam
Recombination correction	1. The correction is linear with the dose per pulse 2. Initial recombination (the part of the total charge recombination that is independent of the dose rate or the dose per pulse) is <0.2% at polarizing voltages of ~300 V 3. For pulsed beams, a plot of $1/M_Q$ (charge reading) versus $1/V$ is linear at least for practical values of V [b] 4. For continuous beams, the plot of $1/M_Q$ versus $1/V^2$ is linear, describing the effect of general recombination; the presence of initial recombination disturbs the linearity but this is normally a small effect, which may be neglected 5. The difference in the initial recombination correction obtained with opposite polarities is <0.1% 6. If the correction exceeds 1.05, other methods have to be used [102]
Chamber stability	Change in the calibration coefficient of <0.3% over a typical recalibration period of 2 years, as well as for long term (>5 years) stability
Chamber material	Wall material not exhibiting temperature and humidity effects

[a] In limited cases (e.g. small volume chambers in low dose rate beams) the leakage current may exceed this limit. In such circumstances, the leakage current has to be evaluated carefully and a correction needs to be applied to the raw ionization chamber reading.

[b] V: polarizing voltage.

be surrounded by a guard electrode with a width not smaller than 1.5 times the cavity height [10]. In addition, the thickness of the front window has to be restricted to ~0.1 g/cm^2 (or 1 mm of polymethyl methacrylate (PMMA)) to make measurements at shallow depths possible. It is also necessary for the air cavity to

TABLE 4. CHARACTERISTICS OF CYLINDRICAL CHAMBER TYPES *(as stated by manufacturers)*

Ionization chamber type	Cavity volume (cm^3)	Cavity length (mm)	Cavity radius (mm)	Wall material	Wall thickness (g/cm^2)	Central electrode material	Waterproof
NE 2571	0.69	24.1	3.2	Graphite	0.065	Aluminium	No
PTW 30010	0.6	23.0	3.1	PMMA/graphite	0.057	Aluminium	No
PTW 30012	0.6	23.0	3.1	Graphite	0.079	Aluminium	No
PTW 30013	0.6	23.0	3.1	PMMA/graphite	0.057	Aluminium	Yes
PTW 31010[a]	0.13	6.5	2.8	PMMA/graphite	0.078	Aluminium	Yes
PTW 31013	0.3	16.3	2.8	PMMA/graphite	0.078	Aluminium	Yes
PTW31021	0.07	4.8	2.4	PMMA/graphite	0.084	Aluminium	Yes
IBA CC13	0.13	5.8	3.0	C552	0.070	C552	Yes
IBA FC65-G	0.65	23.0	3.1	Graphite	0.073	Aluminium	Yes
IBA FC65-P	0.65	23.0	3.1	POM	0.057	Aluminium	Yes
Exradin A12	0.64	n.a.[b]	3.1	C-552	0.088	C-552	Yes
Exradin A19	0.62	n.a.[b]	3.1	C-552	0.088	C-552	Yes

[a] Although PTW 31010 does not meet the reference class specification, as demonstrated in Ref. [98], it is included here as an option for flattening filter free beams, where a shorter thimble is potentially advantageous. Use of this chamber type requires additional characterization and may result in a larger overall uncertainty in the determination of absorbed dose to water.

[b] n.a.: not applicable. Manufacturer data state 21.6 mm for the electrode length, and 26.5 mm (A12) and 26.2 mm (A19) for a so called ‘spot size’, defined as the smallest circle that inscribes the collecting volume and shell.

be vented so that it will equilibrate rapidly with the ambient temperature and air pressure. The characteristics of certain recommended plane parallel ionization chambers are given in Table 5. Other plane parallel chambers recommended for use in proton and heavier ion beams are given in Table 6. These chambers are usually called large area ionization chambers to specify the large size of the collecting electrode diameter (40–80 mm).

TABLE 5. CHARACTERISTICS OF PLANE PARALLEL CHAMBER TYPES FOR MEGAVOLTAGE PHOTON AND ELECTRON BEAMS *(adapted from Ref. [10])*

Ionization chamber type	Materials	Window thickness	Electrode spacing	Collecting electrode diameter	Guard ring width
Exradin A10 Markus type chamber	Kapton window C-552 body	3.86 mg/cm^2 0.05 mm	2 mm	5.4 mm	4.3 mm
Exradin 11[a] Roos type chamber	Wall and electrode in model P11: polystyrene equiv. model A11: C-552	1 mm polystyrene (P11) C-552 (A11)	2 mm	20 mm	4.4 mm
IBA PPC05	C-552 window and body Graphited (PEEK[b]) electrode	176 mg/cm^2 1 mm	0.5 mm	10 mm	3.5 mm
IBA PPC40 Roos type chamber	PMMA and graphite window Graphited electrode	118 mg/cm^2 1 mm	2 mm	16 mm	4 mm
IBA NACP	Mylar foil and graphite window, PMMA body Graphited electrode	104 mg/cm^2 0.6 mm	2 mm	10 mm	3 mm
PTW 34001 Roos type chamber	PMMA and graphite window Graphited electrode	132 mg/cm^2 1.13 mm	2 mm	16 mm	4 mm

TABLE 5. CHARACTERISTICS OF PLANE PARALLEL CHAMBER TYPES FOR MEGAVOLTAGE PHOTON AND ELECTRON BEAMS *(adapted from Ref. [10])* (cont.)

Ionization chamber type	Materials	Window thickness	Electrode spacing	Collecting electrode diameter	Guard ring width
PTW 34045 Advanced Markus type chamber	Polyethylene foil window PMMA cap, PMMA body	106 mg/cm^2 1.3 mm (incl. cap)	1 mm	5 mm	2 mm
PTW 23343[c] Markus type chamber	Polyethylene foil window PMMA cap, PMMA body	106 mg/cm^2 1.3 mm (incl. cap)	2 mm	5.3 mm	0.2 mm
Sun Nuclear SNC350p Roos type chamber	PMMA and graphite window Graphited electrode	n.a.[d]	2 mm	15.6 mm	4.1 mm

[a] Exradin T11 is no longer recommended because of the hygroscopic nature of A-150 plastic.
[b] Polyetheretherketone ($C_{19}H_{18}O_3$) 1.265 g/cm^3.
[c] The PTW 23343 (Markus) chamber is included here, despite having a narrower guard ring than specified in Section 4.2.1, as it is still commonly used for a range of beam modalities and applications.
[d] n.a.: not applicable

In most situations ionization chambers for measuring low energy X rays have to be of the plane parallel type specifically designed for this energy range (see Table 7). The plane parallel chamber has to have a thin entrance window (ideally with a thickness in the range 2–3 mg/cm^2) to provide full buildup of the primary beam and filter out secondary electrons generated in beam limiting devices (see Section 8.2.1). When used in beams above 40 kV it is necessary to add an additional 0.2 mm thickness of buildup material (PMMA, polyethylene or mylar foils). If a phantom is used, it should be supplied together with the chamber and buildup foils when it is sent for calibration. In addition, the same chamber should be used for the measurement of the HVL and the subsequent determination of absorbed dose. The characteristics of certain plane parallel ionization chambers used for X ray dosimetry for low energy therapy beams

TABLE 6. CHARACTERISTICS OF PLANE PARALLEL IONIZATION CHAMBERS USED FOR PROTONS AND HEAVIER ION BEAMS

Ionization chamber type	Cavity volume (cm^3)	Collecting electrode diameter (mm)	Window material	Window thickness (mm)
PTW 34070	10.5	81.6	PMMA	3.47
PTW 34080	10.5	81.6	PMMA	0.62
PTW 34073	2.5	39.6	PMMA	1.13

Note: For proton dosimetry, cylindrical chambers (Table 4) can also be used.

TABLE 7. CHARACTERISTICS OF PLANE PARALLEL IONIZATION CHAMBERS USED FOR X RAY DOSIMETRY AT LOW ENERGY

Ionization chamber type	Cavity volume (cm^3)	Collecting electrode diameter (mm)	Window material	Window thickness (mg/cm^2)
PTW 23342	0.02	5.1	Polyethylene	2.76
PTW 23344	0.20	15.9	Polyethylene	2.76

are given in Table 7. Note that there are plane parallel chambers designed for low energy diagnostic beams for which this international code of practice is not applicable.

4.2.2. Measuring assembly

The measuring assembly for the measurement of charge (or current) includes an electrometer and a power supply for the polarizing voltage of the ionization chamber. The electrometer should have a digital display and should be capable of four digit resolution (i.e. 0.1% resolution on the reading). The variation in the response should not exceed ±0.2% over one year (long term stability).

The electrometer and the ionization chamber may be calibrated together as a complete system or separately. The latter option can be useful in centres that have several electrometers and/or chambers.

It should be possible to reverse the polarity of the polarizing voltage, so that the polarity effect of the ionization chamber can be determined, and to vary the voltage in order to determine the collection efficiency, as described in Section 4.4.3.4. The available range of polarizing voltages should be 50–400 V for ionization chambers used for radiotherapy dosimetry.

4.2.3. Phantoms

Water is the reference medium for measurements of absorbed dose for medium energy X rays and photon, electron, proton and heavier ion beams. The phantom should extend to at least 5 cm beyond all four sides of the largest field size employed at the depth of measurement. There should also be a margin of at least 5 g/cm^2 beyond the maximum depth of measurement, except for medium energy X rays, in which case it should extend to at least 10 g/cm^2. In practice, these requirements can be met with a standard 30 cm × 30 cm × 30 cm acrylic walled phantom available from many suppliers.

Solid phantoms in slab form, such as polystyrene, PMMA, and certain water equivalent plastics such as Solid Water, Plastic Water and Virtual Water (see Refs [103, 104]) may **not** be used for reference dosimetry, except in the case of low energy X rays, where a PMMA phantom is permitted. However, Ref. [12] mentions the possibility of using solid phantoms for some treatment machines where the use of water phantoms is impractical. In these situations, only a water equivalent solid phantom material may be used for reference dosimetry and for the measurement of beam quality indices.

Plastic (slab) phantoms can be used for routine quality assurance measurements, provided that they have been suitably commissioned. This should include a determination of the mean thickness and density of each slab, as well as the thickness variation over a single slab, and an investigation by radiograph/CT scan for bubbles or voids in the plastic. The relationship between the dosimeter readings in plastic and water has to be established for the user beam. This involves a careful comparison of measurements performed in plastic with measurements carried out in water. Periodic checks at reasonable intervals might be also needed to assure the validity and consistency of the original comparison result [105]. Ionization chamber measurements in plastic water substitute phantoms are prone to effects such as charge storage[14] and temperature inhomogeneities, and it needs to be verified that these effects have no impact on the measurement. Plastics usually have low thermal conductivity; the dosimeter temperature needs to be determined by direct measurement at the

[14] To minimize this effect, the phantom should be constructed using thin slabs of plastic, in no case exceeding 2 cm [106].

position of the detector and/or by allowing sufficient time for the establishment of thermal equilibrium with the room [107].

4.2.4. Waterproof sleeve for the chamber

Unless the ionization chamber is designed so that it can be inserted directly into water, it has to be used with a waterproof sleeve. The sleeve should be made of PMMA, with a wall that is sufficiently thin (preferably not greater than 1.0 mm in thickness) to allow the chamber to achieve thermal equilibrium with the water in less than 10 min. The sleeve should be designed to allow the air pressure in the chamber to reach ambient air pressure quickly; an air gap of 0.1–0.3 mm between the chamber and the sleeve is adequate. This specification is consistent with Ref. [11] and with the first edition of this international code of practice. In order to reduce the buildup of water vapour around the chamber, a waterproof sleeve should not be left in water longer than is necessary to carry out the measurements. Additional accuracy is gained if the same sleeve that was used for the calibration of a chamber in the standards laboratory is also used for all subsequent measurements.

For ionization chambers that are waterproof, the use of a PMMA sleeve may still be a desirable option for positioning the chamber accurately at a given depth, although this depends on the positioning equipment used. For measurements in ^{60}Co it has been shown that a 1 mm thick PMMA sleeve has no significant impact on the reading of the ionization chamber, but for higher energy photon beams the sleeve has a measurable effect, as large as 0.3% for a >20 MV photon beam [98]. With the wide availability of waterproof ionization chambers and/or appropriate PMMA sleeves, the use of a thin rubber sheath is not recommended for reference or relative measurements.

4.2.5. Positioning of ionization chambers at the reference depth

In positioning a chamber at the reference depth in water, z_{ref} (expressed in g/cm^2), the perturbing effects of the chamber cavity and wall and of the waterproof sleeve or cover have to be considered. When the user quality Q is the same as the calibration quality Q_{o}, or when measured $k_{Q,Q_{\mathrm{o}}}$ values are used, these effects are accounted for in the chamber calibration, and it normally suffices to position the chamber at the same depth as at calibration (an exception is when a waterproof sleeve or cover of significantly different thickness is used at chamber calibration and at the user quality). This is also the case where measured $k_{Q,Q_{\mathrm{o}}}$ values are provided for a range of Q values and the user interpolates to their specific beam quality for the same modality.

In other situations, where no direct calibration at the user quality is available, calculated values for k_{Q,Q_o} have to be used. In this case, certain perturbing effects are accounted for in the k_{Q,Q_o} values and others have to be accounted for in the positioning of the chamber.[15] Account also has to be taken of the effect of any phantom window. The term 'water equivalent thickness' (in g/cm^2) refers to the product of the actual thickness (in cm) and the material density (in g/cm^3).

Note that the term 'reference point of the chamber' is used below and in the specification of reference conditions in each section. For cylindrical chambers, this refers to the centre of the cavity volume of the chamber on the chamber axis[16] and for plane parallel chambers (other than in low energy X rays) it refers to the inner surface of the entrance window, at the centre of the window. For the plane parallel chambers used in low energy X rays, it refers to the centre of the outer surface of the chamber window (or any buildup foils used).

4.2.5.1. Chamber cavity effects

Perturbation effects of different natures that are related to the chamber cavity are accounted for in calculated k_{Q,Q_o} factors (see Ref. [108] for a review). The finite size of the cavity introduces an uncertainty about the point where the chamber reading should be assigned and generally k_{Q,Q_o} factors are referred to the chamber cavity centre, as most chamber calibrations are made in photon beams. In analytical calculations, this perturbation is taken into account using the displacement factor p_{dis}, while the effect is intrinsically included in Monte Carlo calculations (see Appendix II). There are situations, however, where the alternative of using a chamber effective point of measurement is preferable.

For cylindrical chambers the method used depends on the radiation modality, and this is specified in the reference conditions in each section. In ^{60}Co, high energy photon beams and proton beams the chamber centre is positioned at z_{ref}, and values for p_{dis} are included in the calculation of k_{Q,Q_o}. In electron beams and in light ion beams ($Z > 1$), this method of positioning is not recommended, because of the steep dose gradients involved, and cylindrical

---

[15] Note that in clinical use it may be more practical to position chambers at a precisely known depth that is within a millimetre or so of the reference depth, and to correct the result to z_{ref} using the depth dose distribution of the user beam, rather than attempting to position a chamber to a fraction of a millimetre. However, motorized water phantoms generally provide the necessary positioning accuracy to avoid this extra step.

[16] The centre of the cavity volume should be taken to be that point on the chamber axis that is at a given distance, stated by the manufacturer, from the tip of the chamber (measured without the buildup cap). This information is usually provided in chamber manuals and data sheets.

chambers are positioned with the centre displaced from z_{ref}. For electron beams the chamber centre is positioned $0.5r_{cyl}$ deeper than z_{ref}, where r_{cyl} is the internal radius of the chamber cavity. For light ion ($Z > 1$) beams, a shift of $0.75r_{cyl}$ is recommended. Note that a number of studies have shown that these shift factors are approximations and there can be significant variations, depending on the chamber geometry and the depth of measurement [109]. However, for the chambers listed in Table 4, the factors given here are accurate enough to not affect the overall measurement uncertainty.

For plane parallel chamber types, the chamber reference point is assumed to be at the effective point of measurement; when this is placed at z_{ref}, no displacement correction factor p_{dis} is required. For cylindrical chambers, recent studies have shown that this is not technically correct [110], but the deviation from this assumption for the chambers listed in Tables 4 and 5 is small and can be neglected for the purposes of reference dosimetry.

4.2.5.2. Chamber wall effects

The factor p_{wall} included in the calculated k_{Q,Q_o} factors in the first edition of this international code of practice corrects for the difference in radiation response between the chamber wall material and the phantom material. However, p_{wall} does not include the effect of the different attenuation of the primary fluence by the chamber wall compared with that of the same thickness of phantom material. When the calibration quality Q_o and the user quality Q are the same, this attenuation is accounted for in the calibration of the chamber. Even when Q_o is not the same as Q, the wall attenuation in photon beams is sufficiently small that cancellation may be assumed. On the other hand, in charged particle beams, the energy loss due to the chamber wall can be significantly different from that caused by the same thickness of phantom material, and the water equivalent thickness of the chamber wall has to be taken into account when calculating where to position the chamber. For the chambers listed in Tables 4 and 5, the difference between physical and water equivalent thicknesses is generally small (<1 mm water).

4.2.5.3. Chamber waterproofing

For cylindrical chambers in photon beams, it is recommended that a multiplicative factor is applied to the chamber reading to account for any difference in the waterproofing sleeve thickness between calibration and use. Data are given in Ref. [98]. For plane parallel chambers requiring a waterproof front cover, it is recommended that a shift in the position of the chamber be applied to take into account any difference in the water equivalent cover thickness between calibration and use when positioning the chamber at z_{ref}.

4.2.5.4. Phantom window

For all modalities, when a horizontal beam is used, the water equivalent thickness of the phantom window should be taken into account. Note also that thin windows may be subject to an outward bowing due to the water pressure on the inner surface. This effect may occur as soon as the phantom is filled and can increase gradually over the next few hours. Any such effect increases the amount of water in front of a chamber and should also be accounted for in the positioning of the chamber at z_{ref}, particularly for medium energy X rays and low energy electron beams.

For a vertical beam set-up, there is no phantom window to consider, but the position of the water surface should be monitored. In low humidity environments, evaporation can lead to changes in the effective measurement depth, similar to window bowing for horizontal beam situations.

4.3. CALIBRATION OF IONIZATION CHAMBERS

When an ionization chamber or dosimeter is sent to a standards laboratory for calibration, stability check measurements should be carried out by the user before and after the calibration. This will determine whether the chamber response has been affected by the transportation and/or calibration process. A reference ionization chamber should be calibrated at a reference quality Q_o at intervals not exceeding three years or whenever the user suspects that the chamber has been damaged. If directly measured values of k_{Q,Q_o} (or $N_{D,w,Q}$) for the chamber have been obtained previously, a recalibration to verify the quality dependence of the chamber should be made at least every third time that the chamber is calibrated or every six years, whichever is shorter. However, because of the particular susceptibility of ionization chambers to change in energy response in low and medium energy X rays, it is preferable that chambers used for these beams are recalibrated at all relevant qualities each time. It is the responsibility of the user to increase the frequency of the calibrations for chambers whose long term stability has not been verified over a period exceeding five years.

4.3.1. Calibration in a ^{60}Co beam

Calibrations may be carried out either directly against a primary standard of absorbed dose to water at a PSDL or, more commonly, against a secondary standard at an SSDL. Only the latter case will be discussed here. Reference [11] provides general guidelines for the calibration of radiotherapy dosimeters in standards laboratories.

It is assumed that the absorbed dose to water, D_w, is known at the reference depth (usually 5 g/cm^2) in a water phantom for ^{60}Co gamma rays. This is realized at the SSDL by means of a calibrated ionization chamber performing measurements in a water phantom.[17] The user chamber is placed with its reference point at the same reference depth in a water phantom and its calibration coefficient $N_{D,w}$ is obtained from the following equation:

$$N_{D,w} = \frac{D_w}{M} \tag{8}$$

where M is the dosimeter reading, corrected for influence quantities, in order to correspond to the reference conditions for which the calibration coefficient is valid. The reference conditions recommended for the calibration of ionization chambers in ^{60}Co are given in Table 8.

TABLE 8. REFERENCE CONDITIONS RECOMMENDED FOR THE CALIBRATION OF IONIZATION CHAMBERS IN ^{60}Co GAMMA RADIATION IN STANDARDS LABORATORIES

Influence quantity	Reference value or reference characteristic
Phantom material	Water
Phantom size	30 cm × 30 cm × 30 cm (approximately)
Source–chamber distance[a]	100 cm
Air temperature[b]	20.0°C [c]
Air pressure	101.33 kPa
Reference point of the ionization chamber	For cylindrical chambers, on the chamber axis at the centre of the cavity volume For plane parallel chambers, on the inner surface of the entrance window, at the centre of the window

[17] Many primary laboratories also use this approach, since operating an absorbed dose primary standard for each calibration is not practicable.

TABLE 8. REFERENCE CONDITIONS RECOMMENDED FOR THE CALIBRATION OF IONIZATION CHAMBERS IN ^{60}Co GAMMA RADIATION IN STANDARDS LABORATORIES (cont.)

Influence quantity	Reference value or reference characteristic
Depth in phantom of the reference point of the chamber[a]	5 g/cm^2
Field size at the position of the reference point of the chamber	10 cm × 10 cm [d]
Relative humidity	50% [e]
Polarizing voltage and polarity	No reference values are recommended, but the values used should be stated in the calibration certificate
Dose rate	No reference values are recommended, but the dose rate used should always be stated in the calibration certificate. The certificate should also state whether a recombination correction has been applied and, if so, the value of the correction

[a] After a water phantom with a plastic window has been filled, its dimensions may slowly change with time. Evaporation may also be non-negligible. It may therefore be necessary to check the source–surface distance and the chamber depth every few hours.

[b] The temperature of the air in a chamber cavity should be taken to be that of the phantom, which should be measured; this is not necessarily the same as the temperature of the surrounding air.

[c] In some countries the reference air temperature is 22°C.

[d] Some laboratories use a set-up with a source–surface distance of 100 cm; in that case, the field size is defined at the phantom surface.

[e] For relative humidity values in the range 20%–80%, no correction for humidity is required (see Section 4.4.3.1).

4.3.2. Calibration in kilovoltage X rays

This international code of practice provides two different routes for the dosimetry of kilovoltage X rays (see Sections 8 and 9) based on chamber calibration coefficients in terms of absorbed dose to water and in terms of air kerma free in air. The formalism, including the relationship between $N_{D,w,Q}$ and

$N_{K,\mathrm{air},Q}$, is described in detail in Appendix I. The rationale for reinstating the $N_{K,\mathrm{air},Q}$ route is that, most X ray beam calibrations worldwide are still performed using air kerma. This constraint is linked to the lack of 'true' standards of absorbed dose to water for low energy X rays and to the limited number of PSDLs having these standards for medium energy X rays.

It is possible to derive calibration coefficients in terms of absorbed dose to water from air kerma calibration coefficients. The formulation is given in Appendix I and recommended dosimetric factors are to be obtained using the GUI web application[18]. Thus, any calibration laboratory with standards of air kerma can derive calibration coefficients in terms of absorbed dose to water. Even though this is formally equivalent to the user obtaining an air kerma calibration coefficient and applying the same dosimetric data, it has the advantage of permitting the widespread use of the unified methodology in a field of dosimetry where standards are notably lacking.

It is recommended that ionization chambers used for the dosimetry of low or medium energy X ray beams be calibrated in beams of similar quality to the user beams that will be measured (see Section 4.1.3). Because of the variety of auxiliary dosimetry equipment, such as buildup foils, phantoms and waterproof sleeves, and the variety of field sizes and source–surface distances (SSDs) that will be clinically relevant, it is important that the clinical measurement conditions are reproduced as closely as possible in the calibration process. When a chamber is sent for calibration, all relevant auxiliary equipment should be supplied as well, and the details of the clinical beams and geometry in which it will be used need to be clearly specified. This is generally more of a concern for kilovoltage X ray beams than for other modalities.

Plane parallel chambers are recommended for low energy X ray measurements, although cylindrical chambers can be used above 70 kV; for medium energy X rays only cylindrical chambers are recommended. All ionization chambers have to be able to provide electron equilibrium at the radiation qualities used. The wall thickness of cylindrical chambers is usually sufficient for this purpose, but plane parallel chambers require the addition of a buildup foil above 40 kV (see Section 4.2.1). The two chamber calibration modalities are described in detail in Ref. [11]. Air kerma calibrations are carried out free in air, typically with reference distances of 0.5–1 m and radiation field diameters of the order of 3–10 cm (at the lower end of these ranges for low energy X rays and at the higher end for medium energies) and reference values of temperature (20°C), pressure (101.3 kPa) and humidity (50% relative humidity). Typical reference conditions for calibrations in terms of absorbed dose to water are given in Table 9, where it should be noted that for low energy X rays only

[18] Available at https://kVx-rays.iaea.org

plane parallel chambers are calibrated at the surface of a PMMA phantom. For both low and medium energy X rays, the chamber support should be such that scattered radiation is avoided or minimized and the temperature sensor should be positioned just outside the radiation field.

TABLE 9. REFERENCE CONDITIONS RECOMMENDED FOR THE CALIBRATION OF IONIZATION CHAMBERS IN TERMS OF ABSORBED DOSE TO WATER IN LOW AND MEDIUM ENERGY X RAY BEAMS IN STANDARDS LABORATORIES

Influence quantity	Reference value or reference characteristic	
	Low energy X rays	Medium energy X rays
Phantom material	PMMA or water equivalent plastic designed for use in kilovoltage X rays	Water
Phantom size (approximate)	12 cm × 12 cm × 6 cm	30 cm × 30 cm × 30 cm
	The phantom has to extend in the beam direction beyond the ionization chamber by at least 5 g/cm^2 for low energy X rays and 10 g/cm^2 for medium energy X rays, and in the lateral direction far enough beyond the reference field size used to ensure that the entire primary beam exits through the rear face of the phantom	
Source–surface distance	Treatment distance as specified by the user[a]	
Air temperature[b]	20°C [c]	
Air pressure	101.3 kPa	
Reference point of the ionization chamber	For plane parallel chambers, at the centre of the outside surface of the chamber window (or of the buildup foil, if used)	For cylindrical chambers, on the central axis at the centre of the cavity volume
Depth in phantom of the reference point of the chamber	Surface of the phantom	2 g/cm^2

TABLE 9. REFERENCE CONDITIONS RECOMMENDED FOR THE CALIBRATION OF IONIZATION CHAMBERS IN TERMS OF ABSORBED DOSE TO WATER IN LOW AND MEDIUM ENERGY X RAY BEAMS IN STANDARDS LABORATORIES (cont.)

Influence quantity	Reference value or reference characteristic	
	Low energy X rays	Medium energy X rays
Field size at the position of the reference point of the chamber[d]	Dependent on standards laboratory; a minimum of 3 cm in diameter or 3 cm × 3 cm	10 cm × 10 cm or 10 cm diameter
Relative humidity[e]	50%	
Polarizing voltage and polarity	No reference values are recommended, but the values used should be stated in the calibration certificate	
Dose rate	No reference values are recommended, but the dose rate used should always be stated in the calibration certificate. The certificate should also state whether a recombination correction has been applied and, if so, the value of the correction	

[a] If more than one source–surface distance is used, the greatest should be chosen for calibration.

[b] The temperature of the air in a chamber cavity should be taken to be that of the phantom, which should be measured; this is not necessarily the same as the temperature of the surrounding air.

[c] In some countries the reference air temperature is 22°C.

[d] If these field sizes do not correspond to any of the user's clinical beams, then the closest field size to that of the beams used clinically should be used.

[e] For relative humidity values in the range 20%–80% no correction for humidity is required (see Section 4.4.3.1).

4.3.3. Calibration at other qualities

Standards laboratories with an accelerator can offer calibration services in high energy photon and electron beams. The user will be given either a series of calibration coefficients $N_{D,w,Q}$ at various beam qualities or a calibration coefficient N_{D,w,Q_o} plus measured values for k_{Q,Q_o}. Details on the calibration procedures at PSDLs are outside the scope of this publication.

It should be noted that standards of absorbed dose to water for protons and heavier ion beams are still under development and no laboratory based calibration services are currently available. However, a calibration coefficient in terms of absorbed dose to water can be obtained in the user proton (or light ion) beam when the standards laboratory is prepared to perform calibration measurements (with water calorimetry, for instance) in the proton or ion therapy centre. This approach is also possible for high energy photon and electron beams.

4.4. REFERENCE DOSIMETRY IN THE USER BEAM

4.4.1. Determination of the absorbed dose to water

It is assumed that the user has an ionization chamber or a dosimeter with a calibration coefficient $N_{D,\mathrm{w},Q_\mathrm{o}}$ in terms of absorbed dose to water at a reference quality Q_o. Following the formalism given in Section 3, the chamber is positioned according to the reference conditions and the absorbed dose to water is given by the following equation:

$$D_{\mathrm{w},Q} = M_Q N_{D,\mathrm{w},Q_\mathrm{o}} k_{Q,Q_\mathrm{o}} \tag{9}$$

where M_Q is the reading of the dosimeter incorporating the product $\prod k_\mathrm{i}$ of the correction factors for influence quantities and k_{Q,Q_o} is the correction factor that corrects for the difference between the reference beam quality Q_o and the actual quality Q being used. This equation is valid for all the radiation fields for which this international code of practice applies.

Details on the reference conditions to be used for radiotherapy beam calibrations and values for the factor k_{Q,Q_o} will be given in the individual sections dealing with the various radiation types. Recommendations on relative dosimetry, namely the determination of distributions of absorbed dose, will also be given in the respective sections. Although the correction factor k_{Q,Q_o} is not different in kind from all other correction factors for influence quantities, it is treated separately in each section because of its dominant role.

4.4.2. Practical considerations for measurements in the user beam

Precautions regarding the waterproof sleeve of a chamber when carrying out measurements in a water phantom are given in Section 4.2.4. Before measurements are made, the long term and short term stability of the dosimeter system should be verified. The simplest method, conceptually, to evaluate long term stability is to use a check source. Alternatively, the dosimeter system

could be compared with at least two other systems, with the assumption that three independent systems will not drift (or fail) in exactly the same way. Short term stability covers both warmup/stabilization and reproducibility for repeated measurements. Enough time should be allowed for the dosimeter to reach thermal equilibrium. Some AC powered electrometers have a very short warmup time (<10 min) but others are best switched on for 2 h or longer before use to allow stabilization. It is always recommended to preirradiate an ionization chamber to achieve charge equilibrium in the different materials. The minimum dose required to do this depends on a number of factors, but 10 Gy has been found to be generally sufficient for reference class ionization chambers [111]. It is especially important to operate the measuring system under stable conditions whenever the polarity or polarizing voltage are modified, which, depending on the chamber and sometimes on the polarity, might require several (up to 30) minutes and doses greater than 10 Gy. Indeed, failure to do so may result in errors that are larger than the effect for which one is correcting.

The leakage current is that generated by the complete measuring system in the absence of radiation. Leakage current can also be radiation induced; chambers may show no leakage prior to irradiation yet have a significant leakage after irradiation. The leakage current should always be measured before and after irradiation and should be small compared with the current obtained during the irradiation (less than approximately 0.1% of the measurement current and normally of the same sign). In some limited instances, for example small volume chambers or measurement at low dose rates, the relative leakage current may be significantly larger. If this is the case, the measurement current has to be corrected for leakage, paying attention to the sign of the leakage current. Chambers with a leakage current that is large (of the order of 1% of the measurement current) or variable in time should not be used.

Reproducibility is normally evaluated as part of the measurement of the absorbed dose. Repeated readings should be evaluated to ensure that there is no systematic drift in response, and the standard deviation of readings should be compared to historical data for the same chamber (or chambers of the same type). Any significant difference may indicate a problem with the measuring equipment or the radiation beam.

When relative measurements are carried out in accelerator and in kilovoltage X ray beams, it is strongly recommended that an additional monitoring dosimetry system be used during the experimental procedure to account for fluctuations in the radiation output. This is especially important when ratios of dosimeter

readings are used (e.g. cross-calibrations, measurements with different polarities or varying voltages). The following three options are used:

(a) A transmission type monitor chamber intercepting the beam prior to the phantom;
(b) A detector positioned in air between the radiation source and the phantom, a few centimetres from the central axis;
(c) A detector positioned within the phantom, a few centimetres from the central axis.

The third option provides a measure of the radiation output that corresponds most closely to the beam intercepting the chamber being measured, but all three geometries have been successfully used. If the monitor is positioned in air, the possible temperature drifts have to be taken into account. In this case, care should be taken to make sure that the temperature measured in the surroundings of the monitor chamber is representative of the temperature of the air inside the measuring volume of the monitor chamber itself, as there may be impedance-like effects when the temperature in the room varies.

4.4.3. Correction for influence quantities

The calibration coefficient for an ionization chamber is valid only for the reference conditions that apply to the calibration. Any departure from the reference conditions when using the ionization chamber in the user beam should be corrected for using appropriate factors. In the following, only general correction factors k_i are discussed, leaving items specific to each type of radiation beam to the relevant section.

4.4.3.1. Pressure, temperature and humidity

As all chambers recommended in this publication are open to the ambient air, the mass of air in the cavity volume is subject to atmospheric variations. The following correction factor:

$$k_{TP} = \frac{(273.15 + T)}{(273.15 + T_o)} \frac{P_o}{P} \tag{10}$$

should be applied to convert the cavity air mass to the reference conditions. In Eq. (10), P (in kPa) and T (in °C) are the cavity air pressure and temperature, respectively, at the time of the measurements, and P_o and T_o are the corresponding

reference values (generally 101.3 kPa and 20°C).[19] The temperature of the air in a chamber cavity should be taken to be that of the phantom, which should be measured; this is not necessarily the same as the temperature of the surrounding air.[20] For measurements in a water phantom, the chamber waterproof sleeve (if required) should be vented to the atmosphere in order to obtain rapid equilibrium between the ambient air and the air in the chamber cavity. For waterproof chambers, the air cavity is vented via the cable sleeve, so care is required to ensure that the cable is not sealed (e.g. using a clamping system or tape to fasten the cable in place).

No corrections for humidity are needed if the calibration coefficient refers to a relative humidity of 50% and is used in a relative humidity between 20% and 80%. If the calibration coefficient refers to dry air, a correction factor, k_h, should be applied [112]; for ^{60}Co calibrations $k_h = 0.997$.

4.4.3.2. Electrometer calibration

When the ionization chamber and the electrometer are calibrated separately, a calibration coefficient for each is given by the calibration laboratory. In this international code of practice, the electrometer calibration factor k_{elec} is treated as an influence quantity and is included in the product $\prod k_i$ of correction factors. Typically, the calibration coefficient $N_{D,w}$ for the ionization chamber will be given in units of Gy/nC and that for the electrometer k_{elec} either in units of nC/rdg or, if the electrometer readout is in terms of charge, as a dimensionless factor close to unity (effectively a calibration coefficient in units of nC/nC).

If the ionization chamber and the electrometer are calibrated together, then the combined calibration coefficient $N_{D,w}$ will typically be given in units of Gy/rdg or Gy/nC (depending on the electrometer readout) and no separate electrometer calibration coefficient k_{elec} is required. In this case, a value for k_{elec} of unity (dimensionless) should be recorded in the worksheets.

4.4.3.3. Polarity effect

The effect of using polarizing potentials of opposite polarity on a chamber reading should always be evaluated on commissioning. For most chamber types the effect will be small in photon beams (usually <0.2%), with a notable exception being the very thin window chambers used for low energy X rays. In

[19] In some countries the reference air temperature is 22°C.

[20] The equilibrium temperature of a water phantom that has been filled for some hours will always be lower than room temperature because of evaporation from the water surface. The exact difference from room temperature depends on the relative humidity of the room.

charged particle beams, particularly electrons[21], the effect may be significant. Polarity measurements that deviate significantly from the expectation value may be an indication of anomalous system behaviour and should be investigated.

When a chamber is used in a beam that produces a non-negligible polarity effect, the true reading is taken to be the mean of the absolute values of readings taken at both polarities. However, for the routine use of a given ionization chamber, a single polarizing potential and a single polarity are normally adopted. Therefore, the effect on the chamber reading of using polarizing potentials of opposite polarity for each user beam quality Q can be accounted for by using the following correction factor:

$$k_{\text{pol}} = \frac{|M_+| + |M_-|}{2|M|} \tag{11}$$

where M_+ and M_- are the electrometer readings obtained at positive and negative polarity, respectively, and M is the electrometer reading obtained with the polarity used routinely (positive or negative). The readings M_+ and M_- should be taken with care, ensuring that the chamber reading is stable following any change in polarity (some chambers can take tens of minutes to stabilize). To minimize the influence of fluctuations in the output of radiation generators (e.g. clinical accelerators, X ray therapy units), it is strongly recommended that all the readings be normalized to that of an external monitor (see Section 4.4.2 for recommendations regarding external monitors).

When the chamber is sent for calibration, the user usually informs the calibration laboratory regarding the polarizing potential and polarity to be adopted for the routine use of the chamber. The calibration should be carried out at this polarizing potential (and polarity, if only one polarity is used for the calibration); if not, this should be clearly stated. The calibration laboratory may or may not correct for the polarity effect at the calibration quality, Q_o. This should be stated in the calibration certificate.

If the calibration laboratory has already corrected for the polarity effect, then the user has to apply the correction factor k_{pol} derived using Eq. (11) to all measurements made using the routinely used polarity. This approach is the simplest in terms of formalism but requires additional measurements for every step, which are time consuming and require care to avoid errors. If the calibration laboratory has not corrected for the polarity effect, the subsequent treatment of

[21] For plane parallel chambers the polarity effect is generally more pronounced in low energy electron beams [10]. However, for certain chamber types it has been shown that the polarity effect increases with energy [113]. For this reason, the polarity effect should always be investigated at all electron energies.

the polarity effect depends on the facilities available to the user and on what beam qualities have to be measured. The following apply:

(a) If the user beam quality is the same as the calibration quality and the chamber is used at the same polarizing potential and polarity, then k_{pol} should be the same in both cases and the user should not apply a polarity correction for that particular beam (or equivalently k_{pol} is set equal to 1 in the worksheets). In the unusual situation where it is not possible to use the same polarizing potential as at calibration, the polarity effect will not be exactly the same in the two cases. The difference should be small and should be estimated and included as an uncertainty.

(b) If the user beam quality is not the same as the calibration quality, but it is possible to reproduce the calibration quality, then the polarity correction $\left[k_{pol}\right]_{Q_o}$ that was not applied at the time of calibration has to be estimated using Eq. (11) and with the same polarizing potential and polarity as those used at the calibration laboratory. The polarity effect at the user beam quality, $[k_{pol}]_Q$, also has to be determined from Eq. (11) using the polarizing potential and polarity adopted for routine use. A modified polarity correction k'_{pol} is then evaluated as follows:

$$k'_{pol} = \frac{\left[k_{pol}\right]_Q}{\left[k_{pol}\right]_{Q_o}} \tag{12}$$

This is then used to correct the dosimeter readings for polarity for each beam quality Q.

(c) If the user beam quality is not the same as the calibration quality and it is not possible to reproduce the calibration quality to estimate the correction $\left[k_{pol}\right]_{Q_o}$, then this has to be estimated from the chamber response to different beam qualities and polarities. If this cannot be done with a relative standard uncertainty (see Appendix IV) of <0.5%, then either the chamber should not be used or it should be sent to a calibration laboratory that can perform the required polarity correction.

It is worth noting that although it can be challenging to measure the polarity correction factor $[k_{pol}]_Q$ accurately, it is a self-consistent measurement, independent of any calibration laboratory or other equipment or radiation beam, and therefore a very useful quality assurance check on chamber performance. Deviations in the measured polarity correction from published data for the same chamber type, or variations in the polarity correction with time, may

indicate a problem with the chamber, connecting cable, electrometer or measurement procedure.

4.4.3.4. Ion recombination

The incomplete collection of charge in an ionization chamber cavity due to the recombination of ions requires the use of a correction factor k_s. The following two effects take place:

— The recombination of ions formed by separate ionizing particle tracks, termed 'general recombination' (or 'volume recombination'), which is dependent on the density of ionizing particles, and therefore on the dose rate for continuous beams or dose per pulse for pulsed beams;
— The recombination of ions formed by a single ionizing particle track, referred to as 'initial recombination', which is independent of the dose rate and the dose per pulse.

Both effects depend on the chamber geometry and on the applied polarizing voltage.

Initial recombination is generally small (<0.2%), except in proton and heavier ion beams. However, general recombination is often significant in pulsed radiation, and especially in pulsed–scanned beams, because the dose rate during a pulse is relatively high. It is possible to derive a correction factor using Boag's theory [114], but this does not account for chamber to chamber variations within a given chamber type. In addition, a slight offset of the central electrode in cylindrical chambers[22] might invalidate the application of Boag's theory. In special beams of very high intensity, space charge and other effects cannot be neglected, and a charge collection efficiency of >1.05 should be assessed by calibration against a dose rate independent system, such as a calorimeter [102].

(a) Pulsed photon and electron beams

For pulsed photon and electron beams, this international code of practice recommends that the correction factor k_s be derived using the two voltage method [116]. This method assumes a linear dependence of $1/M$ on $1/V$ (for both initial and general recombination) and uses the collected charges M_1 and M_2 at polarizing voltages V_1 and V_2, respectively, measured at the same irradiation

[22] This may be observed with a radiograph of the chamber. A radiograph should be taken at the time of commissioning and when performing quality control for dosimetry equipment [115].

conditions. V_1 is the normal operating voltage[23] and V_2 is a lower voltage; the ratio $n = V_1/V_2$ should ideally be equal to or larger than 3.[24] Strictly, the polarity effect may change with the voltage, and M_1 and M_2 should each be corrected for this effect using Eq. (11).[25] The recombination correction factor k_s at the normal operating voltage V_1 is obtained from the following equation:

$$k_s = a_0 + a_1\left(\frac{M_1}{M_2}\right) + a_2\left(\frac{M_1}{M_2}\right)^2 \tag{13}$$

where the constants a_i are given in Table 10. To minimize the influence of fluctuations in the output of clinical accelerators, all the readings should preferably be normalized to that of an external monitor (see Section 4.4.2).

For $k_s < 1.03$, the correction can be approximated to within 0.1% using the following relation:

$$k_s = \frac{n-1}{n - M_1/M_2} \tag{14}$$

This approximation [108] has the advantage of working for non-integral values of the voltage ratio n and also serves as a check on the evaluation using Eq. (13). Note that the correction factor k_s evaluated using the two voltage method in pulsed beams corrects for both general and initial recombination [117].

Caution is required regarding the use of the two voltage method. It has been shown [116–119] that for some chamber types, particularly plane parallel designs, the expected linear dependence of $1/M$ on $1/V$ (Jaffé plot) in pulsed photon and electron beams is not satisfied in the voltage interval used for the two voltage method. It is recommended best practice that the range of linearity of a chamber should be established by measuring the chamber response over a range of polarizing voltages up to the manufacturer's recommended maximum. This is a useful check on the performance of a chamber, which should always be performed when commissioning a new chamber. The chamber should be used

---

[23] The normal operating voltage should be chosen during characterization of the specific chamber at commissioning. It should never exceed the maximum polarizing voltage recommended by the manufacturer, nor be used in the region where charge multiplication is evident.

[24] This might not be possible for a specific combination of ionization chamber and electrometer. For example, some electrometers have a minimum value of V_2 of 100 V but the chamber may not be operating in the expected linear range for $1/M$ versus $1/V$ at 300 V.

[25] Alternatively, the recombination correction can be determined at each polarity separately and compared. Any significant difference in the values for k_{s+} and k_{s-} might indicate a problem with the chamber.

TABLE 10. QUADRATIC FIT COEFFICIENTS FOR THE CALCULATION OF k_s BY THE TWO VOLTAGE TECHNIQUE IN PULSED AND PULSED–SCANNED RADIATION AS A FUNCTION OF THE VOLTAGE RATIO V_1/V_2 [117]

V_1/V_2	Pulsed			Pulsed–scanned		
	a_0	a_1	a_2	a_0	a_1	a_2
2.0	2.337	−3.636	2.299	4.711	−8.242	4.533
2.5	1.474	−1.587	1.114	2.719	−3.977	2.261
3.0	1.198	−0.875	0.677	2.001	−2.402	1.404
3.5	1.080	−0.542	0.463	1.665	−1.647	0.984
4.0	1.022	−0.363	0.341	1.468	−1.200	0.734
5.0	0.975	−0.188	0.214	1.279	−0.750	0.474

subsequently only at voltages within the linear range, in which case the use of the two voltage method is valid, taking into account the requirements about recombination given in Table 3.

(b) Continuous beams

In continuous radiation, both for ^{60}Co gamma rays and kilovoltage X rays, the two voltage method may also be used. Although the effect of general recombination in continuous beams is described by a linear relation between $1/M$ and $1/V^2$, for the vast majority of beams found in clinical situations the dose rate is below 2 Gy/min and general recombination can be ignored. The dominant component is initial recombination and can be determined as for the overall recombination correction for pulsed beams using Eq. (13).

(c) Proton and heavier ion beams

For certain proton and heavier ion beam technologies, the pulsing regime (pulse length and pulse frequency) can be such that the time between pulses is long compared with the ion collection time, and the ionization chamber behaviour with respect to recombination resembles that for a pulsed beam. In

such a beam, a plot of $1/M$ versus $1/V$ (up to the manufacturer's recommended maximum voltage) should show a linear dependence, and the recombination correction can be determined either as described for pulsed beams using Eq. (13) or explicitly from the intercept $1/M_{sat}$ of a linear fit to the $1/M$ versus $1/V$ data using the following equation:

$$k_s = \frac{M_{sat}}{M_1} \tag{15}$$

where M_1 is the chamber reading at the operating voltage V_1. With linearity established, k_s can be obtained with the two voltage method and Eq. (13).

Conversely, for a much shorter time between beam pulses, the chamber behaviour might approach that for a continuous beam in which general recombination is dominant. In such a beam, a plot of $1/M$ versus $1/V^2$ should show a linear dependence, in which case the recombination correction can be determined from the intercept $1/M_{sat}$ of this linear fit, or once linearity is established using the two voltage method and the following relation [108]:

$$k_s = \frac{n^2 - 1}{n^2 - M_1/M_2} \tag{16}$$

In the most general case, the pulsing regime might be such that the chamber behaviour is intermediate and neither experimental plot is linear. This can also arise in a continuous beam for which initial recombination is not negligible. Such cases are evident during commissioning from the non-linearity of both plots ($1/M$ versus $1/V$ and $1/M$ versus $1/V^2$), and evaluation of the recombination correction requires a generalized approach.

(d) Generalized approach of De Almeida and Niatel

Under certain circumstances, neither experimental plot ($1/M$ versus $1/V$ or $1/M$ versus $1/V^2$) is linear and the accurate determination of k_s requires an alternative approach. This problem was first addressed by De Almeida and Niatel [120] and summarized by Boutillon [121]. Essentially, the two voltage method is used for a series of instantaneous dose rates[26] and a plot is made of the charge ratio M_1/M_2 as a function of the reading M_1. Expressing the intercept of

[26] This can be varied, for example, by changing the SSD or the depth in a phantom, or for certain beams by adding attenuating plates.

this plot as $(1 + b_0)$ and the gradient as b_1, the total recombination correction at the operating voltage V_1 is given by the following:

$$k_s = 1 + \frac{b_0}{(n-1)} + \frac{b_1}{(n^2-1)} M_1 \qquad (17)$$

where, as before, $n = V_1/V_2$. Using this relation, k_s can subsequently be evaluated for any reading M_1 measured at voltage V_1; that is, the recombination correction can be evaluated for any dose rate without the need to remeasure it.

This method can also be of use in pulsed radiation for which the coefficient of general recombination in Eq. (17) becomes $b_1/(n - 1)$ [122]. While no non-linearity should exist for pulsed beams, this has the advantage noted above of permitting the evaluation of k_s for any dose rate without the need to remeasure it. A derivation of Eq. (17) and information on its practical use can be found in Ref. [108].

(e) Additional considerations

It is not recommended that the ion recombination effect in a plane parallel chamber used for low energy X rays be measured by changing the polarization voltage. The recombination is normally negligible, and changing the polarizing voltage can distort the window and result in a change in sensitive volume and therefore in a response that exceeds any recombination effect.

For relative measurements, for example the determination of depth dose distributions and the measurement of output factors, the recombination correction should be determined in a subset of conditions that is sufficient for appropriate corrections to be derived. In pulsed beams, where general recombination is dominant, the recombination correction for a given chamber will scale approximately linearly with dose rate (strictly dose per pulse). In situations requiring k_s for a number of different dose rates, the method of De Almeida and Niatel can be an efficient solution. In continuous beams, the recombination correction is small and approximately constant.

For the calibration of ionization chambers in standards laboratories (see Tables 8 and 9) it is recommended that the calibration certificate states whether a recombination correction has or has not been applied. The preceding discussion and the worksheets in this international code of practice are based on the assumption that the calibration laboratory has applied a recombination correction, and therefore the procedure given for the determination of k_s refers only to recombination in the user beam. If the calibration laboratory has not applied a recombination correction, the correction factor determined for the user

beam quality Q has to be divided by that appropriate to the calibration quality Q_o, as follows:

$$k_s = \frac{k_{s,Q}}{k_{s,Q_o}} \tag{18}$$

When Q_o is a continuous beam, k_{s,Q_o} will normally be close to unity and the effect of not applying k_{s,Q_o} either at calibration or through Eq. (18) will be negligible in most cases. However, when Q_o is a pulsed beam, failure by the standards laboratory to apply k_{s,Q_o} at the time of calibration is a potential source of error, especially in the case where the dose per pulse in the user beam is very different from that used at calibration. If this is the case, the user has to determine k_{s,Q_o} in the clinic at a dose per pulse similar to that used at calibration (this may not be the dose per pulse normally used in the clinic). This determination does not need to be carried out at Q_o; what is important is the matching of the calibration dose per pulse. To avoid a recurrence of this problem, the user should request that a recombination correction be applied, or at least measured, at the next calibration at a standards laboratory, especially for calibration in pulsed beams.

4.4.3.5. Volume averaging correction (in flattening filter free beams)

The aim of reference dosimetry is the determination of the absorbed dose to water at the reference point in the water phantom in the absence of the detector. However, the signal obtained from an ionization chamber is proportional to the mean dose over the spatially extended measuring volume. If the beam profile is not homogeneous in the vicinity of the reference point, the dose determined from a chamber reading might differ from the 'true' dose value at the reference point.

Especially for high energy photon beams in flattening filter free (FFF) mode, non-uniformity of the lateral beam profile at the centre of the beam may result in an under-response of the ionization chamber. The magnitude of this effect depends on the lateral extent of the ionization chamber in relation to the variation of the beam profile around the point of measurement — namely on the beam profile variation across the projection of the sensitive volume of the ionization chamber on a plane orthogonal to the beam axis. Similar effects may influence dose measurements in the penumbra region of with flattening filter (WFF) and FFF beams; depending on the curvature of the lateral beam profile around the point of measurement, an over- or under-response of the ionization chamber may occur [123–133].

The deviation of the mean dose over the spatially extended measuring volume from the dose value at the reference point is taken into account using the volume averaging correction factor k_{vol}. This is defined as the ratio of the

absorbed dose to water at the reference point in the water phantom in the absence of the detector to the mean absorbed dose to water over a volume of water that coincides with the sensitive volume of the detector (still in the absence of the detector) [12]. It can generally be derived from an integration (averaging) of the 3-D dose distribution in an undisturbed water phantom over the volume occupied by the detector.

At the reference depth, the dose fall-off in the depth (axial) direction is nearly linear, so the mean dose value is mainly determined by the radial beam uniformity (i.e. the lateral beam profile). The 3-D integration can therefore be simplified to a 2-D integration of the lateral beam profile over the sensitive area of the detector facing the beam (i.e. the sensitive volume projected onto a plane orthogonal to the beam axis). The change in the lateral extent of the sensitive volume in the depth direction is taken into account by an appropriate weighting function [12].[27]

The correction factor k_{vol} can be calculated from measured lateral beam profiles as follows:

$$k_{\mathrm{vol}} = \frac{\iint_A w(x,y)\,\mathrm{d}x\mathrm{d}y}{\iint_A w(x,y)\,\mathrm{OAR}(x,y)\,\mathrm{d}x\mathrm{d}y} \tag{19}$$

where x and y are the coordinates on the axes orthogonal to the beam central axis; A is the area of the projection of the sensitive volume of the chamber on a plane orthogonal to the beam axis; OAR(x, y) is the off-axis ratio, which is the lateral dose profile at the measurement depth normalized to unity on the central axis; and $w(x, y)$ is a weighting function representing the extension of the air cavity of the ionization chamber along the beam axis (z) as a function of the lateral coordinates (x and y) of the beam. For plane parallel detectors $w(x, y)$ is unity over the integration area. For cylindrical chambers several weighting functions are proposed in appendix I of Ref. [12] that differ in the detail of the underlying chamber model. For the FFF beams of clinical accelerators considered in this international code of practice, all these models yield results within reasonable

[27] More generally, the (local) response varies over the volume of the ionization chamber; it can be expressed by the spatial response function [132–137]. The volume based weighting functions used here in the 2-D integration are an approximation of the spatial response function (see e.g. Ref. [133]).

agreement. For this reason, the simplest model for the weighting function is chosen, which assumes a line shaped (1-D) detector of cavity length L as follows:

$$w(x,y)=\begin{cases}1 & \text{for } x=0,-L/2\le y\le L/2\\ 0 & \text{otherwise}\end{cases} \tag{20}$$

The volume averaging correction factor is then calculated as follows:

$$k_{\mathrm{vol}}=\frac{L}{\int_{-L/2}^{L/2}\mathrm{OAR}(0,y)\,\mathrm{d}y} \tag{21}$$

Here it is assumed that the 1-D detector with length L is aligned along the y direction with its centre at the origin $(x, y) = (0, 0)$ so that the integration over the dose profile in the y direction, $\mathrm{OAR}(0, y)$, extends from $-L/2$ to $L/2$.

It has to be stressed that the off-axis ratio $\mathrm{OAR}(x, y)$ (i.e. the relative beam profile), which is required to calculate k_{vol}, has to be measured with a detector that itself is ideally not influenced by the volume averaging effect. To measure the beam profile, it is recommended to use a detector with a very small sensitive volume (e.g. a synthetic diamond detector, a semiconductor diode, a pinpoint ionization chamber). The 1-D relative dose profile should be measured with a high spatial resolution (typical step size of 1 mm), at least over the length L of the detector used for dose measurement (i.e. the reference class ionization chamber). The correction factor k_{vol} is then obtained either from a direct numerical integration of the data (averaging of the measured values according to Eq. (19)) or from the analytical integration of a polynomial fitting function to the measured relative dose values.

If no experimental data for the lateral dose profile are available (and no specific k_{vol} can be calculated), a generic value for the volume averaging correction factor in FFF beams at the reference point can be obtained from the numerical value equation (see equation (54) in Ref. [12]) as follows:

$$k_{\mathrm{vol}}=1+\left(0.0062\,\mathrm{TPR}_{20,10}-0.0036\right)\times\left(\frac{100}{\mathrm{SDD}}\right)^2\times L^2 \tag{22}$$

where $\mathrm{TPR}_{20,10}$ is the beam quality index for high energy photon radiation, L is the cavity length (in centimetres) of the thimble ionization chamber and SDD is the source–detector distance, which equals the SSD plus the measurement depth (also in centimetres). Table 11 shows volume averaging correction factors for different cavity lengths, calculated according to Eq. (22) for SDD = 110 cm.

TABLE 11. GENERIC VALUES FOR THE VOLUME AVERAGING CORRECTION FACTOR IN FLATTERING FILTER FREE BEAMS OF CLINICAL ACCELERATORS

Cavity length, L (cm)	Beam quality index, $TPR_{20,10}$					
	0.6	0.63	0.66	0.69	0.72	0.75
0.5	1.000	1.000	1.000	1.000	1.000	1.000
1.0	1.000	1.000	1.000	1.001	1.001	1.001
1.5	1.000	1.001	1.001	1.001	1.002	1.002
2.0	1.000	1.001	1.002	1.002	1.003	1.004
2.5	1.001	1.002	1.003	1.004	1.005	1.006

It can be seen from Table 11 that the volume averaging effect is most pronounced for ionization chambers with a long cavity (e.g. Farmer type chambers with $L \approx 2.5$ cm) and in FFF beams of higher energy. Therefore, it is recommended to use ionization chambers with a short cavity for dose measurements in FFF beams for which the correction factor k_{vol} is close to 1.0 and can often be neglected.

4.5. CROSS-CALIBRATION OF IONIZATION CHAMBERS

Traceability of reference dosimetry is obtained through the use of reference ionization chambers calibrated on a regular basis at a standards laboratory. While it is not desirable or practical to use a reference chamber in all clinical beams and for all routine measurements, any substitute field chamber that is used for this purpose also has to have a calibration traceable to a primary standard. This is achieved in the clinic through a process called cross-calibration, in which the calibration coefficient of the reference chamber for a reference beam of quality Q_o is used to determine the required calibration coefficient of the field chamber. This can be done either by using the substitution method — that is, positioning each chamber in turn at the reference point in the clinical beam and obtaining the two readings sequentially relative to an external beam monitor — or, when

the chambers are of similar design, by placing them side by side or tip to tip and obtaining the two readings simultaneously.[28]

Cross-calibration can be carried out in the clinical beam Q_o for which the reference chamber is calibrated, such as ^{60}Co gamma radiation, or in any other clinical photon, electron or proton beam of quality Q_{cross}. For electron and proton beams, the cross-calibration process (Section 4.5.2) and the subsequent use of the field chamber at a beam quality Q (Section 4.5.3) require beam quality correction factors $k_{Q,Q_{cross}}$ and k_{Q_{cross},Q_o} that have to be evaluated carefully. Figure 6 provides a flowchart summarizing the procedures for the correct evaluation of these factors. For simplicity, the flowchart includes only the photon and electron beam cases.

4.5.1. Cross-calibration in the reference beam Q_o

The simplest cross-calibration procedure is to obtain the calibration coefficient of a field chamber in the same quality Q_o as a reference chamber with calibration coefficient N^{ref}_{K,Q_o} or N^{ref}_{D,w,Q_o}. In the examples below, N^{ref}_{D,w,Q_o} is considered and the substitution method is used.

First, the reference chamber is positioned at the reference point in the water phantom and the absorbed dose to water is determined as follows:

$$D_{w,Q_o} = M^{ref}_{Q_o} N^{ref}_{D,w,Q_o} \tag{23}$$

where $M^{ref}_{Q_o}$ is the meter reading (per monitor unit or per unit time), corrected for influence quantities. The reference chamber is then removed and replaced by the field chamber. From the definition of a calibration coefficient, the following calibration coefficient is obtained for the field chamber:

$$N^{field}_{D,w,Q_o} = \frac{D_{w,Q_o}}{M^{field}_{Q_o}} \tag{24}$$

where $M^{field}_{Q_o}$ is the corresponding meter reading (per monitor unit or per unit time) for the field chamber, also corrected for influence quantities. Combining

[28] For the correct implementation of side by side (or tip to tip) cross-calibration, the chamber positions should be exchanged and remeasured and the mean value for each taken. This procedure has the advantage over substitution of not requiring an external beam monitor (for details see section 7.1.1 of Ref. [11]).

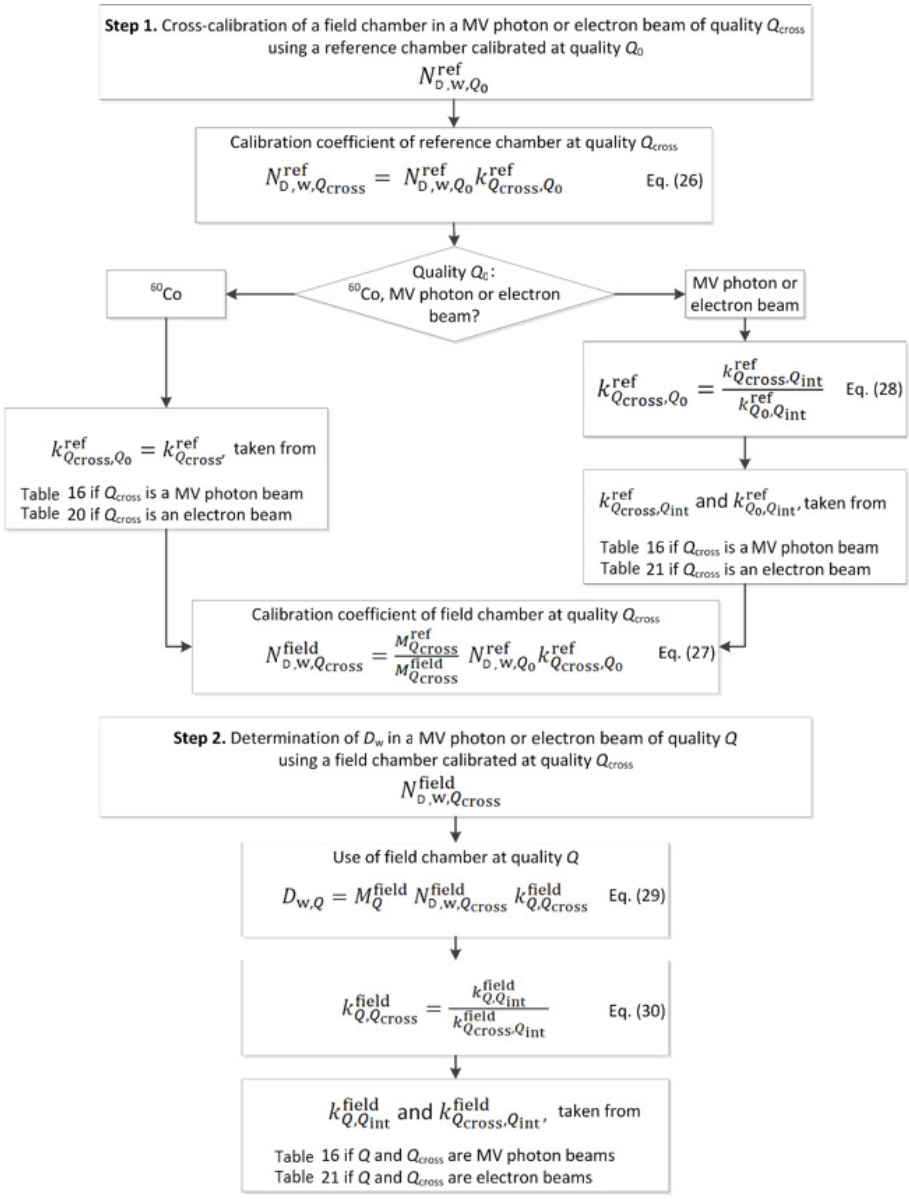

FIG. 6. Flowchart for megavoltage (MV) photon and electron dosimetry, indicating how the relevant beam quality factors are evaluated. In step 1, a field chamber is cross-calibrated in a megavoltage beam of quality Q_{cross} *using a reference cylindrical chamber with calibration coefficient* N^{ref}_{D,w,Q_o}. *In step 2, the field chamber is subsequently used to determine* $D_{w,Q}$ *in a megavoltage beam of quality* Q. *The logic of the flowchart can also be applied to proton dosimetry.*

Eqs (23, 24), it follows that the calibration coefficient of the field chamber is directly related to that of the reference chamber through the following relation:

$$N_{D,\mathrm{w},Q_\mathrm{o}}^{\mathrm{field}} = \frac{D_{\mathrm{w},Q_\mathrm{o}}}{M_{Q_\mathrm{o}}^{\mathrm{field}}} = \frac{M_{Q_\mathrm{o}}^{\mathrm{ref}}}{M_{Q_\mathrm{o}}^{\mathrm{field}}} N_{D,\mathrm{w},Q_\mathrm{o}}^{\mathrm{ref}} \tag{25}$$

The calibration coefficient $N_{D,\mathrm{w},Q_\mathrm{o}}^{\mathrm{field}}$ is applicable under the same reference conditions (e.g. Q_o, P_o, T_o) as the calibration coefficient of the reference chamber, $N_{D,\mathrm{w},Q_\mathrm{o}}^{\mathrm{ref}}$.

4.5.2. Cross-calibration in a beam Q_{cross} other than the reference beam Q_o

By incorporating the k_{Q,Q_o} concept for the reference chamber, the process of cross-calibration can be carried out in any clinical beam Q_{cross} and is therefore not restricted to the beam Q_o for which the reference chamber is calibrated. This might be useful, for example, if the user wants a field chamber cross-calibrated in a megavoltage photon, electron or proton beam for routine use, or for the cross-calibration of a plane parallel chamber, because a more reliable cross-calibration can be made in a high energy electron beam.

The procedure is based on obtaining the calibration coefficient $N_{D,\mathrm{w},Q_{\mathrm{cross}}}^{\mathrm{ref}}$ of the reference chamber for quality Q_{cross} from its calibration coefficient at quality Q_o, $N_{D,\mathrm{w},Q_\mathrm{o}}^{\mathrm{field}}$, using the appropriate beam quality correction factor $k_{Q_{\mathrm{cross}},Q_\mathrm{o}}^{\mathrm{ref}}$ for the reference chamber type, as follows:

$$N_{D,\mathrm{w},Q_{\mathrm{cross}}}^{\mathrm{ref}} = N_{D,\mathrm{w},Q_\mathrm{o}}^{\mathrm{ref}} k_{Q_{\mathrm{cross}},Q_\mathrm{o}}^{\mathrm{ref}} \tag{26}$$

For the cross-calibration measurements, the reference chamber and the field chamber are positioned alternately at the reference depth in water in the clinical beam of quality Q_{cross}. By expressing Eq. (25) in terms of Q_{cross} (rather than Q_o) and incorporating the result of Eq. (26), the calibration coefficient of the field chamber for the quality Q_{cross} is given by the following:

$$N_{D,\mathrm{w},Q_{\mathrm{cross}}}^{\mathrm{field}} = \frac{D_{\mathrm{w},Q_{\mathrm{cross}}}}{M_{Q_{\mathrm{cross}}}^{\mathrm{field}}} = \frac{M_{Q_{\mathrm{cross}}}^{\mathrm{ref}}}{M_{Q_{\mathrm{cross}}}^{\mathrm{field}}} N_{D,\mathrm{w},Q_\mathrm{o}}^{\mathrm{ref}} k_{Q_{\mathrm{cross}},Q_\mathrm{o}}^{\mathrm{ref}} \tag{27}$$

where the readings $M_{Q_{\mathrm{cross}}}^{\mathrm{ref}}$ and $M_{Q_{\mathrm{cross}}}^{\mathrm{field}}$ are corrected for influence quantities.

Figure 6 (step 1) provides clarifications on the evaluation of $k_{Q_{\mathrm{cross}},Q_\mathrm{o}}^{\mathrm{ref}}$. When the reference chamber calibration quality Q_o is ^{60}Co gamma radiation, $k_{Q_{\mathrm{cross}},Q_\mathrm{o}}^{\mathrm{ref}}$ reduces to $k_{Q_{\mathrm{cross}}}^{\mathrm{ref}}$, which is taken from Section 6.5.1 when Q_{cross} is a

megavoltage photon beam, from Section 7.6.2 when Q_{cross} is an electron beam and from Section 10.7.2 when Q_{cross} is a proton beam.

However, when Q_{o} is itself a megavoltage photon or electron beam (i.e. of the same modality as Q_{cross}), then $k^{\text{ref}}_{Q_{\text{cross}},Q_{\text{o}}}$ is obtained using the concept of the intermediate quality expressed by Eq. (6), as follows:

$$k^{\text{ref}}_{Q_{\text{cross}},Q_{\text{o}}} = \frac{k^{\text{ref}}_{Q_{\text{cross}},Q_{\text{int}}}}{k^{\text{ref}}_{Q_{\text{o}},Q_{\text{int}}}} \tag{28}$$

The evaluation of $k^{\text{ref}}_{Q_{\text{cross}},Q_{\text{int}}}$ and $k^{\text{ref}}_{Q_{\text{o}},Q_{\text{int}}}$ depends on the modality. For megavoltage photons, Q_{int} is taken to be ^{60}Co and the factors reduce to $k^{\text{ref}}_{Q_{\text{cross}}}$ and $k^{\text{ref}}_{Q_{\text{o}}}$, which are taken from Section 6.5.1. For electron dosimetry, $k^{\text{ref}}_{Q_{\text{cross}},Q_{\text{int}}}$ and $k^{\text{ref}}_{Q_{\text{o}},Q_{\text{int}}}$ are taken from Section 7.6.2.

4.5.3. Use of a cross-calibrated chamber

The field chamber can subsequently be used to determine the absorbed dose to water in any beam of quality Q of the same modality (photon, electron or proton) as that of Q_{cross}, and for which the value of the factor $k^{\text{field}}_{Q,Q_{\text{cross}}}$ is available, according to the following equation:

$$D_{\text{w},Q} = M^{\text{field}}_{Q} N^{\text{field}}_{D,\text{w},Q_{\text{cross}}} k^{\text{field}}_{Q,Q_{\text{cross}}} \tag{29}$$

where M^{field}_{Q} is the chamber reading, corrected for influence quantities, when the ionization chamber positioned in water in a beam of quality Q. The beam quality factor $k^{\text{field}}_{Q,Q_{\text{cross}}}$ is obtained using the intermediate quality Eq. (6) as follows:

$$k^{\text{field}}_{Q,Q_{\text{cross}}} = \frac{k^{\text{field}}_{Q,Q_{\text{int}}}}{k^{\text{field}}_{Q_{\text{cross}},Q_{\text{int}}}} \tag{30}$$

The evaluation of $k^{\text{field}}_{Q,Q_{\text{int}}}$ and $k^{\text{field}}_{Q_{\text{cross}},Q_{\text{int}}}$ again depends on the modality (see Fig. 6, step 2). For megavoltage photons, these reduce to k^{field}_{Q} and $k^{\text{field}}_{Q_{\text{cross}}}$ (from Section 6.5.1). For electron dosimetry these values are taken from Section 7.6.2 and for protons from Section 10.7.2.

5. CODE OF PRACTICE FOR ^{60}Co GAMMA RAY BEAMS

5.1. GENERAL

This section provides a code of practice for reference dosimetry (beam calibration) in the user's ^{60}Co gamma ray beam and recommendations for relative dosimetry. It is based on the use of a calibration coefficient in terms of absorbed dose to water N_{D,w,Q_o} for a dosimeter in a reference beam of quality Q_o, where Q_o is ^{60}Co. In this situation, $D_{w,Q}$ is denoted by D_w, k_{Q,Q_o} is denoted by k_Q, which has a value of unity, and N_{D,w,Q_o} is denoted by $N_{D,w}$.

5.2. DOSIMETRY EQUIPMENT

5.2.1. Ionization chambers

The recommendations regarding ionization chambers given in Section 4.2.1 should be followed. Both cylindrical and plane parallel[29] ionization chambers are recommended as reference instruments for the calibration of ^{60}Co gamma ray beams. The reference point of a cylindrical chamber for the purpose of calibration at the standards laboratory and for measurements under reference conditions in the user beam is taken to be on the chamber axis at the centre of the cavity volume. For plane parallel chambers, it is taken to be on the inner surface of the entrance window, at the centre of the window, and there is no need to scale the window thickness to its water equivalent. This point should be positioned at the reference depth in a water phantom. If a field instrument is used, this should be cross-calibrated against the calibrated reference chamber (see Section 5.5).

5.2.2. Phantoms and chamber sleeves

The recommendations regarding phantoms and chamber sleeves given in Sections 4.2.3 and 4.2.4 should be followed. Water is recommended as the reference medium for measurements of absorbed dose with ^{60}Co beams.[30] The phantom should extend to at least 5 cm beyond all four sides of the field

[29] Plane parallel chambers can be used for measurements under reference conditions in the user's ^{60}Co gamma ray beam when they are calibrated at the same quality.

[30] Plastic phantoms should not be used for reference dosimetry. However, they can be used for routine quality assurance measurements, provided that a transfer factor between plastic and water has been established.

size employed at the depth of measurement and to at least 5 g/cm^2 beyond the maximum depth of measurement.

In horizontal beams, the window of the phantom should be made of plastic and be of a thickness t_{win} of 0.2–0.5 cm.[31] The water equivalent thickness (in g/cm^2) of the phantom window should be taken into account when evaluating the depth at which the chamber is to be positioned; this thickness is calculated as the product $t_{win}\,\rho_{pl}$, where ρ_{pl} is the mass density of the plastic (in g/cm^3). For the commonly used plastics PMMA and clear polystyrene, the nominal values ρ_{PMMA} = 1.19 g/cm^3 and $\rho_{polystyrene}$ = 1.06 g/cm^3 [48] may be used for the calculation of the water equivalent thickness of the window.

For non-waterproof chambers, a waterproofing sleeve should be used, made of PMMA and preferably not thicker than 1.0 mm. The air gap between the chamber wall and the waterproofing sleeve should be sufficient (0.1–0.3 mm) to allow the air pressure in the chamber to equilibrate. The same waterproofing sleeve that was used for calibration of the user's ionization chamber should also be used for reference dosimetry; if this is not possible, then another sleeve of the same material and of similar thickness should be used. Plane parallel chambers, if not inherently waterproof or supplied with a waterproof cover, have to be used in a waterproof enclosure, preferably made of PMMA or a material that closely matches the chamber walls; ideally, there should be no more than 1 mm of added material in front of and behind the cavity volume.

5.3. BEAM QUALITY SPECIFICATION

Gamma ray spectra from ^{60}Co therapy sources used at hospitals or SSDLs have a substantial component of scattered low energy photons originating from the source itself or from the treatment head, but ionization chamber measurements are not expected to be influenced by ^{60}Co spectral differences by more than a few parts per mil [58]. For this reason, ^{60}Co gamma rays for radiotherapy dosimetry do not require a beam quality specifier other than the radionuclide.

[31] A window that is only a few millimetres thick may bow outwards slightly owing to water pressure on the inner surface. Any such effect should be accounted for when positioning the chamber at the depth of interest, particularly in low energy electron beams. According to experience, the time for such bowing to equilibrate after phantom filling is ~45 min.

5.4. DETERMINATION OF ABSORBED DOSE TO WATER

5.4.1. Reference conditions

The reference conditions for the determination of absorbed dose to water in a ^{60}Co gamma ray beam are given in Table 12.

5.4.2. Determination of absorbed dose under reference conditions

The absorbed dose to water at the reference depth z_{ref} in water, in the user ^{60}Co beam and in the absence of the chamber, is given by the following equation:

$$D_{w} = M \times N_{D,w} \tag{31}$$

where M is the reading of the dosimeter with the reference point of the chamber positioned at z_{ref}, in accordance with the reference conditions given in Table 12, and corrected for the influence quantities temperature and pressure, electrometer calibration, polarity effect and ion recombination, as described in the worksheet in Section 5.8 (see also Section 4.4.3). For ^{60}Co units, the timer error can influence M significantly. A method for calculating the timer error is given in the worksheet. $N_{D,w}$ is the calibration coefficient in terms of absorbed dose to water for the dosimeter at the reference quality ^{60}Co.

5.4.3. Absorbed dose at z_{max}

Section 5.4.2 provides a methodology for determining absorbed dose at z_{ref}. However, clinical dosimetry calculations are often referred to the depth of the dose maximum, z_{max}. To determine the absorbed dose at z_{max} for a given beam the user has to use the central axis percentage depth dose (PDD) data for SSD set-ups and tissue–maximum ratios (TMRs) for SAD set-ups.

5.5. CROSS-CALIBRATION OF FIELD IONIZATION CHAMBERS

As noted in Section 5.2.1, a field chamber (either cylindrical or plane parallel) may be cross-calibrated against a calibrated reference chamber in a ^{60}Co beam at the user facility. The chambers are compared by alternately placing each chamber in a water phantom with its reference point at z_{ref} in accordance with the reference conditions given in Table 12. A side by side chamber intercomparison is a possible alternative configuration. The calibration

TABLE 12. REFERENCE CONDITIONS FOR THE DETERMINATION OF ABSORBED DOSE TO WATER IN ^{60}Co GAMMA RAY BEAMS

Influence quantity	Reference value or reference characteristic
Phantom material	Water
Chamber type	Cylindrical or plane parallel
Measurement depth, z_{ref}	5 g/cm^2 (or 10 g/cm^2)[a]
Reference point of chamber	For cylindrical chambers, on the central axis at the centre of the cavity volume
	For plane parallel chambers, on the inner surface of the front wall at its centre[b]
Position of reference point of chamber	For cylindrical and plane parallel chambers, at the measurement depth z_{ref}
Source–surface distance or source–chamber distance	80 cm or 100 cm [c]
Field size	10 cm × 10 cm [d]

[a] In Ref. [138], the use of a single reference depth z_{ref} = 10 g/cm^2 for all high energy photon beam energies is recommended. The constancy of $N_{D,w}$ with depth reported by BIPM [59] validates this option. However, some users may prefer to use the same reference depth as that used for the calibration of ionization chambers in ^{60}Co beams, z_{ref} = 5 g/cm^2. The two options are therefore recommended in this international code of practice.

[b] The same approach for scaling of the plane parallel chamber front wall to the water equivalent thickness has to be followed for calibration and use in a ^{60}Co beam.

[c] The reference source–surface distance (SSD) or source–chamber distance (SCD) (for a source–axis distance (SAD) set-up) should be that used for clinical treatments.

[d] The field size is defined at the surface of the phantom for an SSD type set-up, whereas for an SAD type set-up it is defined at the plane of the detector, placed at the reference depth in the water phantom at the isocentre of the machine.

coefficient in terms of absorbed dose to water for the field ionization chamber is given by the following equation:

$$N_{D,\mathrm{w}}^{\mathrm{field}} = \frac{M^{\mathrm{ref}}}{M^{\mathrm{field}}} N_{D,\mathrm{w}}^{\mathrm{ref}} \tag{32}$$

where M_{ref} and M_{field} are the meter readings per unit time for the reference and field chambers, respectively, corrected for the influence quantities as described in Section 4.4.3, and $N_{D,\mathrm{w}}^{\mathrm{ref}}$ is the calibration coefficient in terms of absorbed dose to water for the reference chamber. The field chamber with calibration coefficient $N_{D,\mathrm{w}}^{\mathrm{field}}$ may be used subsequently for the determination of absorbed dose to water in the user ^{60}Co beam using the procedure described in Section 5.4.2, where $N_{D,\mathrm{w}}$ is replaced by $N_{D,\mathrm{w}}^{\mathrm{field}}$.

5.6. MEASUREMENTS UNDER NON-REFERENCE CONDITIONS

Clinical dosimetry requires the measurements of central axis PDD distributions, TPRs or TMRs, isodose distributions, transverse beam profiles and output factors as a function of field size and shape for both reference and non-reference conditions. Such measurements should be made for all possible combinations of field size and SSD or SAD used for radiotherapy treatment.

5.6.1. Central axis depth dose distributions

All measurements should follow the recommendations given in Section 4.2 regarding choices for phantoms and dosimeters, although other types of detector can also be used. Plane parallel ionization chambers are recommended for measurements of depth ionization curves. If a cylindrical ionization chamber is used instead, the effective point of measurement of the chamber has to be taken into account. This requires that the complete depth ionization distribution be shifted towards the surface by a distance equal to $0.6r_{\mathrm{cyl}}$ [9, 10]. To make measurements in the buildup region, well guarded plane parallel chambers (see Table 5) or extrapolation chambers should be used. Care should be taken in the use of certain solid state detectors (some types of diode and diamond detector) to measure depth dose distributions (e.g. Ref. [10]); only a solid state detector whose response has been regularly verified against a reference detector (ionization chamber) should be selected for these measurements.

Since the stopping power ratios and perturbation effects can be assumed to a reasonable accuracy to be independent of depth and field size [139], relative

ionization distributions can be used as relative distributions of absorbed dose, at least for depths at and beyond the depth of the dose maximum.

5.6.2. Field output factors

The field output factor may be determined as the ratio of corrected dosimeter readings measured under a given set of non-reference conditions to that measured under reference conditions. These measurements are typically performed at the reference depth [12, 138] and corrected to the depth of maximum dose using PDD data (or TMR). When field output factors are measured in open as well as wedged beams, special attention should be paid to the uniformity of the radiation fluence over the chamber cavity. For small fields, Ref. [12] should be followed.

In wedged beams, the radiation intensity varies strongly in the direction of the wedge. For output measurements in such beams, the detector dimension in the wedge direction should be as small as possible. Small thimble chambers aligned with their axis perpendicular to the wedge direction are recommended. The coincidence of the central axes of the beam, the collimator and the wedge should be ensured prior to making the output measurements.

5.7. ESTIMATED UNCERTAINTY IN THE DETERMINATION OF ABSORBED DOSE TO WATER UNDER REFERENCE CONDITIONS

When a reference dosimeter is used for the determination of absorbed dose to water in the user beam, the uncertainties in the different physical quantities or procedures that contribute to the dose determination can be determined in two steps. Step 1 includes uncertainties up to the calibration of the user reference dosimeter in terms of $N_{D,w}$ at the standards laboratory. Step 2 involves the calibration of the user beam and includes the uncertainties associated with the measurements at the reference point in a water phantom. Combining the uncertainties in the two steps in quadrature yields the combined standard uncertainty for the determination of the absorbed dose to water at the reference point.

It is the responsibility of the users to establish an uncertainty budget for their determination of absorbed dose to water. An example estimate of the uncertainties in the calibration of a ^{60}Co beam is given in Table 13. When the calibration of the reference dosimeter is carried out at an SSDL, the combined standard uncertainty in D_w is typically ~0.9%. This estimate may vary depending on the uncertainty quoted by the calibration laboratory, the care and experience of the user performing the measurement, and the quality and condition of the measurement equipment (e.g. regular recalibration of all measurement devices,

quality management system to ensure proper functioning). If a field dosimeter is used, the uncertainty in the dose determination increases (by approximately 0.2%) because of the additional step needed to cross-calibrate the field dosimeter against the calibrated reference dosimeter.

TABLE 13. ESTIMATED RELATIVE STANDARD UNCERTAINTY[a] OF D_w AT THE REFERENCE DEPTH IN WATER FOR A ^{60}Co BEAM

Physical quantity or procedure	Relative standard uncertainty (%)
Step 1: standards laboratory[b]	
$N_{D,w}$ calibration of secondary standard at PSDL	0.5
Long term stability of secondary standard	0.1
$N_{D,w}$ calibration of the user dosimeter at the standards laboratory	0.4
Combined uncertainty of step 1	0.6
Step 2: user ^{60}Co beam	
Long term stability of user dosimeter	0.2
Establishment of reference conditions	0.3
Dosimeter reading M_Q relative to timer or beam monitor	0.1
Correction for influence quantities k_i	0.3
Combined uncertainty of step 2	0.5
Combined standard uncertainty of D_w (steps 1 and 2)	0.8

[a] See Ref. [61] or Appendix IV for the expression of uncertainty. The estimates given in the table should be considered as typical values; these may vary depending on the uncertainty quoted by standards laboratories for calibration coefficients and on the experimental uncertainty at the user institution.

[b] If the calibration of the user dosimeter is performed at a PSDL then the combined standard uncertainty in step 1 is lower. The combined standard uncertainty in D_w should be adjusted accordingly.

5.8. WORKSHEET

Determination of the absorbed dose to water in a ^{60}Co gamma ray beam

User: _____ Date: _____

1. Radiation treatment unit and reference conditions for D_w determination

^{60}Co therapy unit: _____

Reference phantom: water Set-up: ☐ SSD ☐ SAD

Reference field size: 10 × 10 cm × cm Reference distance: _____ cm

Reference depth, z_{ref}: _____ g/cm^2

2. Ionization chamber and electrometer

Ionization chamber model: _____ Serial no.: Type: ☐ cyl ☐ pp

Chamber wall/window Material: _____ Thickness: _____ g/cm^2

Waterproof sleeve/cover Material: _____ Thickness: _____ g/cm^2

Phantom window Material: _____ Thickness: _____ g/cm^2

Absorbed dose to water cal. coefficient $N_{D,w}$ = _____ ☐ Gy/nC ☐ Gy/rdg

Reference conditions for calibration P_o = _____ kPa T_o = _____ °C Rel. humidity: ____%

Polarizing potential V_1: _____ V

Calibration polarity: ☐ positive ☐ negative ☐ corrected for polarity effect

User polarity: ☐ positive ☐ negative

Calibration laboratory: _____ Date: _____

Electrometer model: _____ Serial no.: _____

Calibrated separately from chamber: ☐ yes ☐ no Range setting: _____

If yes Calibration laboratory: Date: _____

3. Dosimeter reading[a] and correction for influence quantities

Uncorrected dosimeter reading at V_1 and user polarity: _____ ☐ nC ☐ rdg

Corresponding time: _____ min

Ratio of dosimeter reading and time[b]: M_1 = _____ ☐ nC/min ☐ rdg/min

(a) Pressure P = _____ kPa Temperature T = _____ °C Rel. humidity (if known): _____%

$$k_{TP} = \frac{(273.15+T)}{(273.15+T_o)}\frac{P_o}{P} = \_\_\_\_\_$$

(b) Electrometer calibration factor[c] k_{elec} = _____ ☐ nC/rdg ☐ dimensionless

(c) Polarity correction[d] Reading at $+V_1$: M_+ = _____ Reading at $-V_1$: M_- = _____

$$k_{pol} = \frac{|M_+| + |M_-|}{2M} = \_\_\_\_\_$$

(d) Recombination correction (two voltage method)

Polarizing voltages: V_1 (normal) = _____ V V_2 (reduced) = _____ V

Readings[e] at V_1, V_2: M_1 = _____ M_2 = _____

Voltage ratio V_1/V_2 = _____ Ratio of readings M_1/M_2 = _____

$$k_s = \frac{(V_1/V_2)^2 - 1}{(V_1/V_2)^2 - (M_1/M_2)} = \_\_\_\_\_$$ [f]

Corrected dosimeter reading at the voltage V_1:

$M = M_1 k_{TP} k_{elec} k_{pol} k_s$ = _____ ☐ nC/min ☐ rdg/min

4. Absorbed dose rate to water at the reference depth, z_{ref}

$D_w(z_{ref}) = MN_{D,w}$ = _____ Gy/min

5. Absorbed dose rate to water at the depth of dose maximum, z_{max}

Depth of dose maximum: z_{max} = 0.5 g/cm^2

(a) SSD set-up

PDD at z_{ref} for a 10 cm × 10 cm field size: PDD(z_{ref} = ____ g/cm^2) = _____ %

Absorbed dose rate calibration at z_{max}:

$D_w(z_{max}) = 100 D_w(z_{ref})/\text{PDD}(z_{ref})$ = _____ Gy/min

(b) SAD set-up

TMR at z_{ref} for a 10 cm × 10 cm field size: TMR(z_{ref} = ____ g/cm^2) = _____

Absorbed dose rate calibration at z_{max}:

$D_w(z_{max}) = D_w(z_{ref})/\text{TMR}(z_{ref})$ = _____ Gy/min

---

[a] All readings should be checked for leakage current and corrected if necessary.

[b] The timer error should be taken into account. The correction at voltage V_1 can be determined according to the following process:

M_A is the integrated reading at time t_A M_A = _____ t_A = _____ min

M_B is the integrated reading for n short exposures of time t_B/n each ($2 \le n \le 5$) M_B = _____ t_B = _____ min n = ___

Timer error: $\tau = (M_B t_A - M_A t_B)/(nM_A - M_B)$ = _____ min (the sign of τ has to be taken into account)

$M_1 = M_A/(t_A + \tau)$ = _____ ☐ nC/min ☐ rdg/min

[c] If the electrometer is not calibrated separately, set $k_{elec} = 1$.

[d] M in the denominator of k_{pol} denotes the reading at the user polarity. Preferably, each reading in the equation should be the average of the ratios of M (or M_+ or M_-) to the reading of an external monitor, M_{em}.

[e] Strictly, readings should be corrected for polarity effect (average from both polarities). Preferably, each reading in the equation should be the average of the ratios of M_1 or M_2 to the reading of an external monitor, M_{em}.

[f] It is assumed that the calibration laboratory has performed a recombination correction. Otherwise the factor $k'_s = k_s / k_{s,Q_0}$ should be used instead of k_s. When Q_0 is ^{60}Co, k_{s,Q_0} (at the calibration laboratory) will normally be close to unity, and the effect of not using this equation will be negligible in most cases.

Note: SAD: source–axis distance; SSD: source–surface distance; cyl: cylindrical; pp: plane parallel; PDD: percentage depth dose; TMR: tissue–maximum ratio.

6. CODE OF PRACTICE FOR HIGH ENERGY PHOTON BEAMS

6.1. GENERAL

This section provides a code of practice for reference dosimetry (beam calibration) in clinical high energy photon beams and recommendations for relative dosimetry. It applies to photon beams generated by clinical linear accelerators operating either in conventional mode WFF with nominal accelerating voltages in the range 1–25 MV or in FFF mode with nominal accelerating voltage up to ~10 MV.

The formalism presented here is not applicable to special FFF accelerator designs such as TomoTherapy and CyberKnife machines. The dosimetry procedures for such machines are described in Ref. [12].

For photon beams, the most common reference beam quality Q_o is ^{60}Co gamma rays. Some PSDLs can provide calibration coefficients $N_{D,w,Q}$ at other photon beam qualities, but ^{60}Co is the only quality available in most standards laboratories. For this reason, all data given in this section have ^{60}Co gamma rays as the reference quality. Users with access to high energy photon beam calibration qualities can still use this international code of practice by renormalizing the various $N_{D,w,Q}$ calibration coefficients to the value N_{D,w,Q_o} obtained for one of the reference qualities Q_o. The ratios of $N_{D,w,Q}$ to N_{D,w,Q_o} provide an experimental determination of the factors k_{Q,Q_o} (see Sections 4.1 and 6.5.2). Note that when the reference quality Q_o is ^{60}Co, k_{Q,Q_o} is denoted by k_Q and N_{D,w,Q_o} is denoted by $N_{D,w}$. If available, directly measured values of k_{Q,Q_o} or k_Q for a specific user chamber are the preferred option; if these are not available, the calculated values of k_Q for the appropriate chamber type given in this publication should be used.

6.2. DOSIMETRY EQUIPMENT

6.2.1. Ionization chambers

The recommendations regarding ionization chambers given in Section 4.2.1 should be followed. Only cylindrical ionization chambers are recommended for reference dosimetry in high energy photon beams; plane parallel chambers should

only be used for relative dosimetry.[32] For absorbed dose measurements in FFF beams, ionization chambers with a smaller collecting volume should be preferred because of their smaller volume averaging correction (see Section 4.4.3.5). The chamber types for which data are given in this international code of practice are listed in Section 6.5.1.

For high energy photon beams, the reference point of a cylindrical chamber for the purpose of calibration at the standards laboratory and for measurements under reference conditions in the user beam is taken to be on the chamber axis at the centre of the cavity volume. For plane parallel chambers, used only for relative dosimetry, it is taken to be on the inner surface of the entrance window, at the centre of the window. This point should be positioned at the reference depth in a water phantom. If a field instrument is used, this should be cross-calibrated against a calibrated reference chamber (see Sections 4.5 and 6.6).

6.2.2. Phantoms and chamber sleeves

The recommendations regarding phantoms and chamber sleeves given in Sections 4.2.3 and 4.2.4 should be followed. Water is the reference medium for measurements of absorbed dose and beam quality in photon beams.[33] The phantom should extend to at least 5 cm beyond all four sides of the field size employed at the depth of measurement and extend to at least 5 g/cm² beyond the maximum depth of measurement.

In horizontal beams, the window of the phantom should be made of plastic and be of a thickness t_{win} of 0.2–0.5 cm.[34] The water equivalent thickness (in g/cm²) of the phantom window should be taken into account when evaluating the depth at which the chamber is to be positioned; the thickness is calculated as the product $t_{win}\rho_{pl}$, where t_{win} is the geometrical thickness of the phantom window (in centimetres) and ρ_{pl} is the mass density of the plastic (in g/cm³).

---

[32] The behaviour of plane parallel chambers is still not adequate for their use for reference dosimetry of high energy photon beams; they show larger intratype variations of polarity correction, ion recombination, chamber leakage and k_{Q,Q_o} values than cylindrical ionization chambers, a change of calibration coefficient over time, etc. [140–143]. Only a recently calibrated plane parallel chamber with experimentally determined values for all necessary correction factors can be used for reference dosimetry.

[33] Plastic phantoms should not be used for reference dosimetry. However, they can be used for routine quality assurance measurements, provided that a transfer factor between plastic and water has been established.

[34] A window that is only a few millimetres thick may bow outwards slightly owing to water pressure on the inner surface. Any such effect should be accounted for when positioning the chamber at the depth of interest, particularly in low energy electron beams. According to experience, the time for such bowing to equilibrate after phantom filling is ~45 min.

For the commonly used plastics PMMA and clear polystyrene, the nominal values ρ_{PMMA} = 1.19 g/cm³ and $\rho_{polystyrene}$ = 1.06 g/cm³ [48] may be used for the calculation of the water equivalent thickness of the window.

For non-waterproof chambers, a waterproofing sleeve made of PMMA and preferably not thicker than 1.0 mm should be used.[35] The air gap between the chamber wall and the waterproofing sleeve should be sufficient (0.1–0.3 mm) to allow the air pressure in the chamber to equilibrate. The same waterproofing sleeve that was used for calibration of the user's ionization chamber should also be used for reference dosimetry. If it is not possible to use the same waterproofing sleeve that was used during calibration at the standardizing laboratory, then another sleeve of the same material and of similar thickness should be used.

6.3. BEAM QUALITY SPECIFICATION

6.3.1. Choice of beam quality index

For high energy photons produced by WFF clinical accelerators, the beam quality Q is specified by the tissue–phantom ratio $TPR_{20,10}$. This is the ratio of the absorbed doses at depths of 20 cm and 10 cm in a water phantom, measured with a constant SCD of 100 cm and a field size of 10 cm × 10 cm at the plane of the chamber.[36]

---

[35] For sleeves with thicknesses of 1 mm, the effect on the k_Q value (see Section 6.5) is known to be ~0.3% at the highest $TPR_{20,10}$ values. For different thicknesses, the change in the sleeve effect can be neglected in the clinical setting.

[36] For WFF beams, $TPR_{20,10}$ can also be obtained from the following simple relation [144]:

$$TPR_{20,10} = 1.2661PDD_{20,10} - 0.0595$$

where $PDD_{20,10}$ is the ratio of the PDD at 20 cm and 10 cm depths for a field size of 10 cm × 10 cm defined at the phantom surface with an SSD of 100 cm. This empirical equation was obtained from a sample of almost 700 accelerators and confirmed an earlier fit [145] used in Ref. [9]. Alternatively, $TPR_{20,10}$ can be estimated for WFF beams from a fit to the PDD data at 10 cm depth, PDD(10), measured for a 10 cm × 10 cm field size at an SSD of 100 cm. For the data published in Ref. [146], one obtains the following:

$$TPR_{20,10} = -0.7898 + 0.0329PDD(10) - 0.000166[PDD(10)]^2$$

The maximum deviation of the data about the fit is ~0.6% and occurs at PDD(10) = 75%. Because electron contamination at the depth of maximum absorbed dose might affect the PDD at 10 cm depth, the fit should be used only as an estimation of the relation between $TPR_{20,10}$ and PDD(10), and not for beam calibration. Note that above 10 MV, the PDD(10) value in the fit does not coincide with the $PDD(10)_X$ value used in Ref. [85], which refers exclusively to pure photon beams, namely without electron contamination. While the formulas given here have been determined for WFF beams, there is some evidence that they can also be used with reasonable accuracy for FFF beams [147]).

The most important characteristic of the beam quality index $TPR_{20,10}$ is its independence of the electron contamination in the incident beam. It is also a measure of the effective attenuation coefficient describing the approximately exponential decrease of a photon depth dose curve beyond the depth of maximum dose [148–150]. As $TPR_{20,10}$ is obtained as a ratio of doses, it does not require the use of displacement correction factors at two depths when cylindrical chambers are used. Furthermore, in most clinical set-ups, $TPR_{20,10}$ is not affected by small systematic errors in positioning the chamber at each depth, as the settings in the two positions will be affected in a similar manner.

Other beam quality specifiers, such as the PDD at 10 cm depth and the depth of the 80% depth dose, have been proposed in the literature. An overview of photon beam quality specifiers is given in Appendix III. It should be emphasized that there is no unique beam quality specifier that satisfies all possible requirements for the entire energy range covered in this international code of practice and for all possible accelerators used in hospitals and standards laboratories.

It has been shown that $TPR_{20,10}$ can also be used as a suitable beam quality index for FFF beams from clinical accelerators with nominal accelerating voltages up to ~10 MV [147, 151–153]. For photon beams with higher energy (which are less frequently used in clinical practice), other beam quality specifiers (e.g. $PDD(10)_X$ [152, 154], dual parameter beam quality specifiers [155–157]) might be advantageous. In this international code of practice, the nominal accelerating voltage for FFF beams is limited to 10 MV, so $TPR_{20,10}$ is used as the beam quality index for both WFF and FFF beams.

6.3.2. Measurement of beam quality index

The experimental set-up for measuring $TPR_{20,10}$ is shown in Fig. 7. The reference conditions of measurements are given in Table 14.

Although the definition of $TPR_{20,10}$ is strictly made in terms of ratios of absorbed dose, the use of ionization ratios provides acceptable accuracy because of the slow variation with depth of the water–air stopping power ratios and the assumed constancy of perturbation factors beyond the depth of dose maximum. The influence of recombination effects at the two depths should be investigated and taken into account if there is a variation with depth.

For FFF beams, corrections for volume averaging due to radial non-uniformity (see Section 4.4.3.5) and for the reduced equivalent square field size (see Ref. [12]) can be neglected [147, 153].

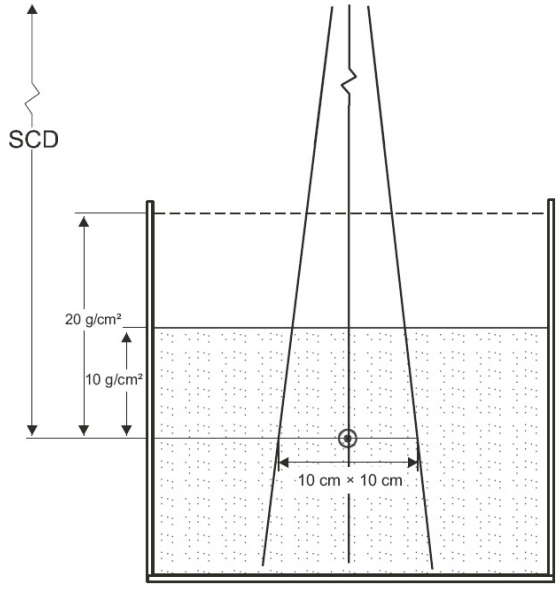

FIG. 7. Experimental set-up for the determination of the beam quality index Q *($TPR_{20,10}$). The source–chamber distance (SCD) is kept constant at 100 cm and measurements are made with 10 g/cm² and 20 g/cm² of water over the chamber. The field size at the position of the reference point of the chamber is 10 cm × 10 cm.*

TABLE 14. REFERENCE CONDITIONS FOR THE DETERMINATION OF THE PHOTON BEAM QUALITY ($TPR_{20,10}$)

Influence quantity	Reference value or reference characteristic
Phantom material	Water
Chamber type	Cylindrical or plane parallel
Measurement depths	20 g/cm² and 10 g/cm²
Reference point of the chamber	For cylindrical chambers, on the central axis at the centre of the cavity volume
	For plane parallel chambers, on the inner surface of the window at its centre

TABLE 14. REFERENCE CONDITIONS FOR THE DETERMINATION OF THE PHOTON BEAM QUALITY ($TPR_{20,10}$) (cont.)

Influence quantity	Reference value or reference characteristic
Position of the reference point of the chamber	For cylindrical and plane parallel chambers, at the measurement depths
Source–chamber distance	100 cm
Field size at source–chamber distance[a]	10 cm × 10 cm
Lateral beam profile	Homogeneous radial dose distribution over the sensitive volume of the ionization chamber

[a] The field size is defined at the plane of the reference point of the detector, at the recommended depths in the water phantom.

6.4. DETERMINATION OF ABSORBED DOSE TO WATER

6.4.1. Reference conditions

The reference conditions for determination of absorbed dose to water are given in Table 15.

6.4.2. Determination of absorbed dose under reference conditions

The absorbed dose to water at the reference depth z_{ref} in water in a photon beam of quality Q and in the absence of the chamber, is given by the following equation:

$$D_{w,Q} = M_Q N_{D,w,Q_o} k_{Q,Q_o} \tag{33}$$

where M_Q is the reading of the dosimeter obtained with the reference point of the chamber positioned at z_{ref} and at the reference conditions given in Section 6.4.1 and corrected for the influence quantities temperature and pressure, electrometer calibration, polarity effect, ion recombination and volume averaging (for FFF beams), as described in Section 4.4.3. N_{D,w,Q_o} is the calibration coefficient in terms of absorbed dose to water for the dosimeter at the reference quality Q_o

and k_{Q,Q_o} is a chamber specific factor that corrects the calibration coefficient for the difference between the reference beam quality Q_o and the actual quality being used, Q.

6.4.3. Absorbed dose at z_{max}

Section 6.4.2 provides a methodology for determining absorbed dose at z_{ref}. However, clinical dosimetry calculations are often referenced to the depth of the

TABLE 15. REFERENCE CONDITIONS FOR THE DETERMINATION OF ABSORBED DOSE TO WATER IN HIGH ENERGY PHOTON BEAMS

Influence quantity	Reference value or reference characteristic
Phantom material	Water
Chamber type	Cylindrical
Measurement depth, z_{ref}	10 g/cm²
Reference point of the chamber	On the central axis at the centre of the cavity volume
Position of the reference point of the chamber	At measurement depth z_{ref}
Source–surface distance or source–chamber distance[a]	100 cm
Field size[b]	10 cm × 10 cm
Lateral beam profile	Homogeneous radial dose distribution over the sensitive volume of the ionization chamber[c]

[a] If the reference dose has to be determined for an isocentric set-up, the source–axis distance (SAD) of the accelerator is to be used, even if this is not 100 cm.

[b] The field size is defined at the surface of the phantom for a source–surface distance type set-up, whereas for an SAD type set-up it is defined at the plane of the detector, placed at the reference depth in the water phantom at the isocentre of the machine.

[c] The radial dose distribution in the vicinity of the ionization chamber is mainly determined by the accelerator characteristics and cannot be easily modified by the user. When the radial dose distribution over the sensitive volume of the ionization chamber is non-uniform a correction for volume averaging has to be applied (see Section 4.4.3.5).

dose maximum z_{max} (or at some other depth). To determine the absorbed dose at the appropriate depth for a given beam, the user has to use the central axis PDD data for SSD set-ups and TPRs or TMRs for SAD set-ups. Section 6.7.1 describes how to generate central axis PDD data.

6.5. VALUES FOR k_{Q,Q_o}

6.5.1. Chamber calibrated in ^{60}Co

When the reference quality Q_o is ^{60}Co, k_{Q,Q_o} is denoted by k_Q and N_{D,w,Q_o} is denoted by $N_{D,w}$.Values for the factor k_Q at the reference depth (see Table 16) are calculated according to the following equation:

$$k_Q\left(\mathrm{TPR}_{20,10}\right)=\frac{1+\exp\left(\frac{a-0.57}{b}\right)}{1+\exp\left(\frac{a-\mathrm{TPR}_{20,10}}{b}\right)} \tag{34}$$

where $TPR_{20,10}$ is the beam quality index of the beam with quality Q, and a and b are chamber type specific constants, which are given in Appendix II for a number of chamber types suitable for reference dosimetry. These constants have been determined by regression analysis of k_Q values from recent Monte Carlo calculations and measurements [100]. The procedure for calculating k_Q is described in Appendix II. It is emphasized that calculated k_Q values do not account for chamber to chamber variations within a given chamber type and their use necessarily involves larger uncertainties than directly measured values (see Section 6.8). Calculated values for the factor k_Q are given in Table 16 for a series of beam qualities Q; a plot of k_Q versus Q for selected chamber types is shown in Fig. 8.

It should be noted that all k_Q values calculated according to Eq. (34) are equal to 1.000 at a beam quality index of Q = 0.57. This value corresponds (approximately) to the $TPR_{20,10}$ value of a ^{60}Co beam.[37] While this approach ensures that the formalism presented here consistently gives k_Q = 1.0 in the ^{60}Co beam, it is an approximation for low energy accelerator beams, because the response of a particular chamber in an accelerator beam of the same $TPR_{20,10}$ as a pure ^{60}Co spectrum ($Q \approx 0.57$) depends on its energy response over the entire spectrum and will not necessarily be the same as for ^{60}Co. However, the variation

[37] For a ^{60}Co beam, $TPR_{20,10}$ values of 0.568 [158], 0.57 [159], 0.572 [146, 160], 0.578 [161] and 0.579 [162] are found in the literature.

TABLE 16. CALCULATED VALUES[a] OF k_Q FOR HIGH ENERGY PHOTON BEAMS FOR VARIOUS CYLINDRICAL IONIZATION CHAMBERS AS A FUNCTION OF THE BEAM QUALITY INDEX $TPR_{20,10}$ *(see Eq. (34))*

Ionization chamber type	Beam quality index, $TPR_{20,10}$											
	0.56	0.59	0.62	0.65	0.68	0.70	0.72	0.74	0.76	0.78	0.80	0.82
Capintec PR-06C Farmer	1.0003	0.9993	0.9980	0.9961	0.9934	0.9909	0.9878	0.9839	0.9790	0.9727	0.9649	0.9551
Exradin A1SL Miniature	1.0006	0.9987	0.9965	0.9936	0.9901	0.9873	0.9840	0.9802	0.9759	0.9709	0.9652	0.9586
Exradin A12 Farmer	1.0004	0.9991	0.9973	0.9948	0.9915	0.9887	0.9852	0.9809	0.9756	0.9693	0.9615	0.9521
Exradin A12S Short Farmer	1.0004	0.9990	0.9972	0.9947	0.9913	0.9885	0.9850	0.9809	0.9758	0.9698	0.9624	0.9537
Exradin A18	1.0004	0.9991	0.9973	0.9949	0.9917	0.9889	0.9855	0.9814	0.9764	0.9702	0.9628	0.9538
Exradin A19 Classic Farmer	1.0005	0.9989	0.9968	0.9940	0.9904	0.9873	0.9836	0.9792	0.9738	0.9675	0.9599	0.9509
Exradin A26	1.0004	0.9991	0.9974	0.9951	0.9919	0.9891	0.9857	0.9816	0.9765	0.9702	0.9626	0.9533
Exradin A28	1.0004	0.9990	0.9972	0.9947	0.9914	0.9886	0.9853	0.9813	0.9764	0.9706	0.9636	0.9552

TABLE 16. CALCULATED VALUES[a] OF k_Q FOR HIGH ENERGY PHOTON BEAMS FOR VARIOUS CYLINDRICAL IONIZATION CHAMBERS AS A FUNCTION OF THE BEAM QUALITY INDEX $TPR_{20,10}$ *(see Eq. (34))* (cont.)

Ionization chamber type	Beam quality index, $TPR_{20,10}$											
	0.56	0.59	0.62	0.65	0.68	0.70	0.72	0.74	0.76	0.78	0.80	0.82
IBA CC13	1.0005	0.9989	0.9969	0.9942	0.9906	0.9876	0.9839	0.9795	0.9742	0.9678	0.9601	0.9510
IBA CC25	1.0004	0.9991	0.9974	0.9950	0.9918	0.9890	0.9855	0.9812	0.9760	0.9695	0.9617	0.9521
IBA FC23-C Short Farmer	1.0004	0.9991	0.9974	0.9950	0.9917	0.9888	0.9853	0.9810	0.9758	0.9693	0.9614	0.9519
IBA FC65-G Farmer	1.0004	0.9990	0.9972	0.9946	0.9912	0.9882	0.9846	0.9802	0.9748	0.9683	0.9603	0.9507
IBA FC65-P Farmer	1.0005	0.9988	0.9966	0.9936	0.9897	0.9865	0.9826	0.9780	0.9725	0.9660	0.9583	0.9491
NE 2561/2611A (NPL 2611A) Secondary standard	1.0003	0.9992	0.9977	0.9955	0.9925	0.9898	0.9865	0.9823	0.9771	0.9706	0.9627	0.9528
NE 2571 Farmer	1.0004	0.9991	0.9974	0.9951	0.9919	0.9891	0.9856	0.9813	0.9761	0.9697	0.9618	0.9522

TABLE 16. CALCULATED VALUES[a] OF k_Q FOR HIGH ENERGY PHOTON BEAMS FOR VARIOUS CYLINDRICAL IONIZATION CHAMBERS AS A FUNCTION OF THE BEAM QUALITY INDEX $TPR_{20,10}$ *(see Eq. (34))* (cont.)

Ionization chamber type	Beam quality index, $TPR_{20,10}$											
	0.56	0.59	0.62	0.65	0.68	0.70	0.72	0.74	0.76	0.78	0.80	0.82
PTW 30010 Farmer	1.0005	0.9989	0.9967	0.9938	0.9901	0.9869	0.9832	0.9787	0.9734	0.9671	0.9595	0.9506
PTW 30011 Farmer	1.0005	0.9989	0.9969	0.9942	0.9906	0.9875	0.9838	0.9793	0.9739	0.9674	0.9595	0.9501
PTW 30012 Farmer	1.0004	0.9990	0.9970	0.9944	0.9910	0.9881	0.9846	0.9804	0.9754	0.9694	0.9622	0.9536
PTW 30013 Farmer	1.0007	0.9984	0.9956	0.9920	0.9876	0.9840	0.9800	0.9753	0.9699	0.9636	0.9565	0.9484
PTW 31010 Semiflex	1.0008	0.9982	0.9952	0.9914	0.9869	0.9835	0.9795	0.9750	0.9700	0.9643	0.9579	0.9507
PTW 31013 Semiflex	1.0007	0.9985	0.9958	0.9924	0.9882	0.9848	0.9810	0.9765	0.9714	0.9655	0.9588	0.9511
PTW 31016 PinPoint 3D[b]	1.0006	0.9987	0.9962	0.9930	0.9888	0.9853	0.9812	0.9762	0.9703	0.9632	0.9549	0.9451

TABLE 16. CALCULATED VALUES[a] OF k_Q FOR HIGH ENERGY PHOTON BEAMS FOR VARIOUS CYLINDRICAL IONIZATION CHAMBERS AS A FUNCTION OF THE BEAM QUALITY INDEX $TPR_{20,10}$ *(see Eq. (34))* (cont.)

Ionization chamber type	Beam quality index, $TPR_{20,10}$											
	0.56	0.59	0.62	0.65	0.68	0.70	0.72	0.74	0.76	0.78	0.80	0.82
PTW 31021 Semiflex 3D[b]	1.0007	0.9984	0.9957	0.9925	0.9886	0.9856	0.9823	0.9786	0.9744	0.9697	0.9645	0.9587
PTW 31022 PinPoint 3D[b]	1.0005	0.9989	0.9968	0.9940	0.9905	0.9875	0.9840	0.9798	0.9749	0.9690	0.9621	0.9540
Sun Nuclear SNC125c	1.0005	0.9991	0.9971	0.9944	0.9908	0.9878	0.9840	0.9794	0.9739	0.9671	0.9590	0.9492
Sun Nuclear SNC600c Farmer	1.0004	0.9993	0.9978	0.9957	0.9926	0.9899	0.9866	0.9823	0.9770	0.9703	0.9620	0.9517

[a] Values are given to four decimal places to permit smooth interpolation of the data. This does not imply uncertainties of this order.

[b] Although the sensitive volume of the chamber is smaller than the recommendations given in Section 4.2.1, the chamber is included here because it is advantageous for dose measurements in FFF beams.

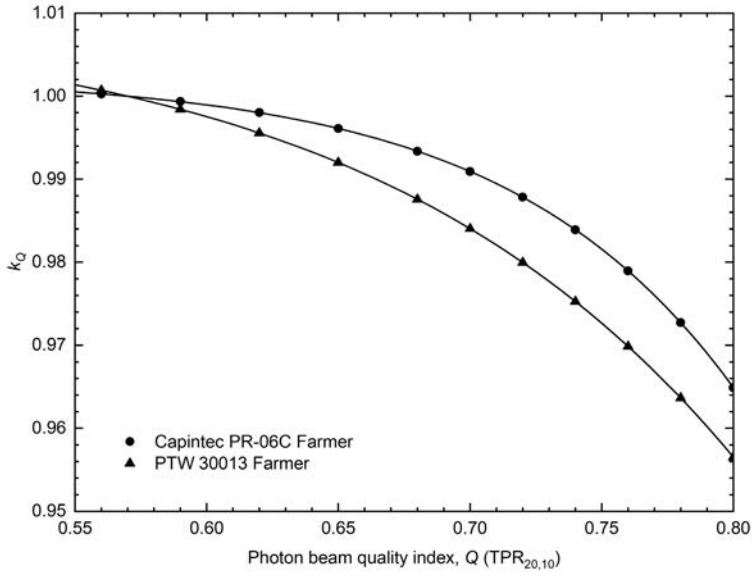

FIG. 8. Values of the k_Q *correction factor for two cylindrical ionization chambers of the Farmer type as a function of the photon beam quality* $TPR_{20,10}$. *The* k_Q *values for other types of ionization chamber given in Table 16 are (mostly) between the curves shown.*

of k_Q with $TPR_{20,10}$ in the vicinity of $Q = 0.57$ is small, so a small error in Q has a negligible influence on k_Q.

6.5.2. Chamber calibrated in a series of high energy photon beam qualities

For a chamber calibrated in a series of photon beam qualities, the data from the calibration laboratory are ideally presented in the form of a single calibration coefficient N_{D,w,Q_o} and a set of measured factors k_{Q,Q_o}. From the latter, a value for k_{Q,Q_o} at the user quality Q may be derived by interpolation. N_{D,w,Q_o} and the resulting k_{Q,Q_o} are then used directly in Eq. (33).

When the calibration laboratory provides a series of calibration coefficients $N_{D,w,Q}$, data first have to be converted to the above format by choosing one of the photon beam qualities used by the calibration laboratory as reference quality Q_o. The k_{Q,Q_o} factors are evaluated using the following equation:

$$k_{Q,Q_o} = \frac{N_{D,w,Q}}{N_{D,w,Q_o}} \tag{35}$$

Then, interpolation to determine k_{Q,Q_o} at the user quality Q proceeds as above. Note that when the reference quality Q_o is ^{60}Co, k_{Q,Q_o} is denoted by k_Q and N_{D,w,Q_o} is denoted by $N_{D,w}$.

Once experimental values for N_{D,w,Q_o} and k_{Q,Q_o} are obtained for a particular chamber, it may not be necessary for the user to calibrate the chamber every time at all qualities Q, but only at the reference quality Q_o. In this case, the new calibration coefficient N_{D,w,Q_o} should be used in conjunction with the existing values of k_{Q,Q_o}. The beam quality dependence of that chamber (k_{Q,Q_o} values) needs to be verified every third calibration cycle of the chamber or if the user suspects that the chamber has been damaged. The Q_o calibration does not need to be performed at the same laboratory where the experimental k_{Q,Q_o} values were measured. Note, however, that this procedure should not be repeated more than twice in succession; the chamber should be recalibrated at all qualities at least every six years.

6.5.3. Chamber calibrated at Q_o with generic experimental k_{Q,Q_o} values

Calibration laboratories sometimes provide generic experimental k_{Q,Q_o} values measured for a particular chamber type, together with a single experimental N_{D,w,Q_o} value for the user chamber, where the reference quality Q_o is usually ^{60}Co. Only those generic values of k_{Q,Q_o} that have been obtained by a standards laboratory from a large sample of ionization chambers are recommended for use in this international code of practice (see Section 4.1). Generic values not determined by a standards laboratory are not recommended.

It is emphasized that directly measured values of k_{Q,Q_o} for an individual chamber of a given chamber type are the preferred choice in this international code of practice, with the second option being using the calculated values of k_{Q,Q_o} for a given chamber type given in Table 16. Note that if generic values for k_{Q,Q_o} (measured for a particular chamber type) exist, these should be used only if they meet the criteria presented in Section 4.1.

6.6. CROSS-CALIBRATION OF FIELD IONIZATION CHAMBERS

As noted in Section 6.2.1, a field chamber may be cross-calibrated against a calibrated reference chamber at the reference quality Q_o (see also Section 4.5.1). The chambers are compared by alternately placing the chambers in a water phantom with their reference points at z_{ref} (a side by side chamber

intercomparison is a possible alternative configuration[38]). The calibration coefficient in terms of absorbed dose to water for the field ionization chamber is given by the following equation:

$$N_{D,\mathrm{w},Q_\mathrm{o}}^{\mathrm{field}} = \frac{M_{Q_\mathrm{o}}^{\mathrm{ref}}}{M_{Q_\mathrm{o}}^{\mathrm{field}}} N_{D,\mathrm{w},Q_\mathrm{o}}^{\mathrm{ref}} \tag{36}$$

where $M_{Q_\mathrm{o}}^{\mathrm{ref}}$ and $M_{Q_\mathrm{o}}^{\mathrm{field}}$ are the meter readings per monitor unit for the reference and field chambers, respectively, corrected for the influence quantities temperature and pressure, electrometer calibration, polarity effect and ion recombination, as described in the worksheet in Section 6.9 (see also Section 4.4.3), and $N_{D,\mathrm{w},Q_\mathrm{o}}^{\mathrm{ref}}$ is the calibration coefficient in terms of absorbed dose to water for the reference chamber. Preferably, the readings $M_{Q_\mathrm{o}}^{\mathrm{ref}}$ and $M_{Q_\mathrm{o}}^{\mathrm{field}}$ should be the averages $\overline{M_{Q_\mathrm{o}}^{\mathrm{ref}} / M_{Q_\mathrm{o}}^{\mathrm{em}}}$ and $\overline{M_{Q_\mathrm{o}}^{\mathrm{field}} / M_{Q_\mathrm{o}}^{\mathrm{em}}}$, where $\left(M_{Q_\mathrm{o}}^{\mathrm{ref}} / M_{Q_\mathrm{o}}^{\mathrm{em}}\right)_i$ and $\left(M_{Q_\mathrm{o}}^{\mathrm{field}} / M_{Q_\mathrm{o}}^{\mathrm{em}}\right)_i$ are, respectively, the ratios of reading i of the reference detector and the field instrument to the reading of an external monitor, M_{em}. The external monitor should preferably be positioned inside the phantom, approximately at depth z_{ref} but at a distance of 3–4 cm away from the chamber centre along the major axis in the transverse plane of the beam. Note that in the case of a side by side measurement, no external monitor is needed, provided that the beam profile is adequately uniform.

The field chamber with calibration coefficient $N_{D,\mathrm{w},Q_\mathrm{o}}^{\mathrm{field}}$ may be used subsequently for the determination of the absorbed dose to water in the user beam using the procedure described in Section 6.4.2, where $N_{D,\mathrm{w},Q_\mathrm{o}}$ is replaced by $N_{D,\mathrm{w},Q_\mathrm{o}}^{\mathrm{field}}$ (see also Section 4.5.3).

6.7. MEASUREMENTS UNDER NON-REFERENCE CONDITIONS

Clinical dosimetry requires the measurement of PDDs, TPRs or TMRs, isodose distributions, transverse beam profiles and field output factors as a function of field size and shape for both reference and non-reference conditions. Such measurements should be made for all possible combinations of energy, field size and SSD or SAD used for radiotherapy treatments.

[38] Additional information and practical hints for the calibration of dosimeters can be found in Ref. [11].

6.7.1. Central axis depth dose distributions

All measurements should follow the recommendations given in Section 4.2 regarding choices for phantoms and dosimeters, although other types of detector can also be used. Plane parallel ionization chambers are recommended for measurements of depth ionization curves. If a cylindrical ionization chamber is used, the effective point of measurement of the chamber has to be taken into account. This requires that the complete depth ionization distribution be shifted towards the surface by a distance equal to $0.6r_{cyl}$ [9, 10]. To make measurements in the buildup region, well guarded plane parallel chambers or extrapolation chambers should be used. Attention should be paid to the use of certain solid state detectors (some types of diode and diamond detector) to measure depth dose distributions (e.g. Ref. [10]); only a solid state detector whose response has been regularly verified against a reference detector (ionization chamber) should be selected for these measurements.

Since the stopping power ratios and perturbation effects can be assumed to a reasonable accuracy to be independent of depth for a given beam quality and field size, relative ionization distributions can be used as relative distributions of absorbed dose, at least for depths at and beyond the depth of dose maximum.

6.7.2. Field output factors

The field output factor may be determined as the ratio of corrected dosimeter readings obtained under a given set of non-reference conditions to those taken under reference conditions. These measurements are typically performed at the depth of maximum dose or at the reference depth [138] and corrected to the depth of the maximum dose using the PDD (or TMR).

When field output factors are measured in wedged beams or FFF beams (where the radiation fluence is not uniform over the chamber cavity), special attention should be paid to the volume averaging effect (see Section 4.4.3.5). The volume averaging correction in FFF beams usually varies with depth and field size. Because it is especially pronounced for large volume detectors, thimble chambers with large cavity lengths and plane parallel chambers with large collecting electrodes should be avoided for field output factor measurements in FFF beams.

In wedged photon beams, the radiation intensity varies strongly in the direction of the wedge. For output measurements in such beams, the detector dimension in the wedge direction should be as small as possible. A small thimble chamber aligned with its axis perpendicular to the wedge direction is recommended.

In all cases, the coincidence of the central axis of the beam and the collimator with the position of the reference point of the ionization chamber should be ensured prior to making the output measurements. This is of particular importance for FFF beams and for conventional (WFF) beams with field sizes smaller than approximately 5 cm × 5 cm. The measurement of field output factors in small fields is described in detail in Ref. [12].

6.8. ESTIMATED UNCERTAINTY IN THE DETERMINATION OF ABSORBED DOSE TO WATER UNDER REFERENCE CONDITIONS

When a reference dosimeter is used for the determination of absorbed dose to water in the user beam, the estimation of the uncertainties in the different physical quantities or procedures that contribute to the dose determination can be divided into two steps. Step 1 considers uncertainties up to the calibration of the user reference dosimeter in terms of $N_{D,w}$ at the standards laboratory. Step 2 deals with the calibration of the user beam and includes the uncertainties associated with the measurements at the reference point in a water phantom. Step 2 also includes the uncertainty of k_Q and the other influence quantities values. Combining the uncertainties in the two steps in quadrature yields the combined standard uncertainty for the determination of the absorbed dose to water at the reference point.

It is the responsibility of the user to establish an uncertainty budget for their determination of absorbed dose to water. An example estimate of the relative standard uncertainties in the calibration of a high energy photon beam is given in Table 17. When the calibration of the reference dosimeter is carried out in the ^{60}Co beam of an SSDL, the combined standard uncertainty in D_w is estimated to be typically ~1.0%, based on calculated values of k_Q. This estimate may vary depending on the uncertainty quoted by the calibration laboratory, the care and experience of the user doing the measurement, and the quality and condition of the measurement equipment (e.g. regular recalibration of all measurement devices, quality management system to ensure proper functioning). If the calibration of the reference dosimeter is carried out at a PSDL, but calculated values of k_Q are used, the final uncertainty in D_w is not expected to decrease significantly. If these k_Q values are measured at the PSDL for the user chamber, the uncertainty in D_w decreases to ~0.8%. If a field dosimeter is used, the uncertainty in dose determination increases somewhat (by approximately 0.2%) because of the additional step needed to cross-calibrate the field dosimeter against the calibrated reference dosimeter.

TABLE 17. ESTIMATED RELATIVE STANDARD UNCERTAINTY[a] OF $D_{w,Q}$ AT THE REFERENCE DEPTH IN WATER AND FOR A HIGH ENERGY PHOTON BEAM, BASED ON A CHAMBER CALIBRATION IN ^{60}Co GAMMA RADIATION

Physical quantity or procedure	Relative standard uncertainty (%)
Step 1: standards laboratory[b]	
$N_{D,w}$ calibration of secondary standard at PSDL	0.5
Long term stability of secondary standard	0.1
$N_{D,w}$ calibration of the user dosimeter at the standards laboratory	0.4
Combined uncertainty of step 1	0.6
Step 2: user's high energy photon beam	
Long term stability of user dosimeter	0.2
Establishment of reference conditions	0.3
Dosimeter reading M_Q relative to beam monitor	0.3[c]
Correction for influence quantities k_i	0.3
Beam quality factor, k_Q [100]	0.6[d]
Combined uncertainty of step 2	0.8
Combined standard uncertainty of $D_{w,Q}$ (steps 1 and 2)	1.0

[a] See Ref. [61] or Appendix IV for the expression of the uncertainty. The estimates given in the table should be considered typical values; these may vary depending on the uncertainty quoted by standards laboratories for calibration coefficients and on the experimental uncertainty at the user's institution.

[b] If the calibration of the user dosimeter is performed at a PSDL, then the combined standard uncertainty in step 1 is lower. The combined standard uncertainty in D_w should be adjusted accordingly.

[c] For the dosimeter reading, a smaller uncertainty has been assumed than in the first edition of this international code of practice to reflect the broader availability of high quality electrometers, the establishment of quality management systems and the improved education and experience of users.

[d] If k_Q is measured at a PSDL for the user chamber, this uncertainty is approximately of the order of 0.3%.

6.9. WORKSHEET

Determination of the absorbed dose to water in a high energy photon beam

User: _____ Date: _____

1. Radiation treatment unit and reference conditions for $D_{w,Q}$ determination

Accelerator: _____ Nominal accelerator potential: _____ MV

Nominal dose rate: _____ MU/min Beam quality, $Q(TPR_{20,10})$: _____

Reference phantom: water Set-up ☐ SSD ☐ SAD

Reference field size: 10 × 10 cm × cm Reference distance: _____ cm

Reference depth, z_{ref} = _____ g/cm^2

2. Ionization chamber and electrometer

Ionization chamber model: _____ Serial no.: _____

Chamber wall Material: _____ Thickness: _____ g/cm^2

Waterproof sleeve Material: _____ Thickness: _____ g/cm^2

Phantom window Material: _____ Thickness: _____ g/cm^2

Absorbed dose to water calibration coefficient[a] N_{D,w,Q_o} = _____ ☐ Gy/nC ☐ Gy/rdg

Calibration quality Q_o: ☐ ^{60}Co ☐ photon beam Calibration depth: _____ g/cm^2

If Q_o is photon beam, $TPR_{20,10}$ = _____

Reference conditions for calibration P_o = _____ kPa T_o = _____ °C Rel. humidity: _____%

Polarizing potential V_1 = _____ V

Calibration polarity: ☐ positive ☐ negative ☐ corrected for polarity effect

User polarity: ☐ positive ☐ negative

Calibration laboratory: _____ Date: _____

Electrometer model: Serial no.: _____

Calibrated separately from chamber: ☐ yes ☐ no Range setting: _____

If yes, calibration laboratory: Date: _____

3. Dosimeter reading[b] and correction for influence quantities

Uncorrected dosimeter reading at V_1 and user polarity: _____ ☐ nC ☐ rdg

Corresponding accelerator monitor units: _____ MU

Ratio of dosimeter reading and monitor units: M_1 = _____ ☐ nC/MU ☐ rdg/MU

(a) Pressure P = _____ kPa Temperature T = _____ °C Rel. humidity (if known): _____%

$$k_{TP} = \frac{(273.15+T)}{(273.15+T_o)}\frac{P_o}{P} = \_\_\_\_\_$$

(b) Electrometer calibration factor[c] k_{elec} = _____ ☐ nC/rdg ☐ dimensionless

(c) Polarity correction[d] Reading at $+V_1$: M_+ = _____ Reading at $-V_1$: M_- = _____

$$k_{pol} = \frac{|M_+| + |M_-|}{2M} = \_\_\_\_\_$$

(d) Recombination correction[e] (two voltage method)

Polarizing voltages: V_1 (normal) = _____ V V_2 (reduced) = _____ V

Readings[f] at V_1, V_2: M_1 = _____ M_2 = _____

Voltage ratio V_1/V_2 = _____ Ratio of readings M_1/M_2 = _____

Use Table 10 for a beam of type: ☐ pulsed ☐ pulsed–scanned

a_0 = _____ a_1 = _____ a_2 = _____

$$k_s = a_0 + a_1\left(\frac{M_1}{M_2}\right) + a_2\left(\frac{M_1}{M_2}\right)^2 = \_\_\_\_\_^{e}$$

(e) Volume averaging correction (in FFF beams)

SDD = _____ cm

Thimble length of ionization chamber L = _____ cm

$$k_{vol} = 1 + (0.0062Q - 0.0036)\left(\frac{100}{SDD}\right)^2 L^2 = \_\_\_\_\_$$

Corrected dosimeter reading at the voltage V_1:

$M_Q = M_1 k_{TP} k_{elec} k_{pol} k_s k_{vol}$ = _____ ☐ nC/MU ☐ rdg/MU

4. Absorbed dose to water at the reference depth, z_{ref}

Beam quality correction factor for user quality Q: k_{Q,Q_o} = _____

Taken from ☐ Table 16 ☐ other, specify:_____

$$D_{w,Q}(z_{ref}) = M_Q N_{D,w,Q_o} k_{Q,Q_o} = \_\_\_\_\_ \text{ Gy/MU}$$

5. Absorbed dose to water at the depth of dose maximum, z_{max}

Depth of dose maximum: z_{max} = _____ g/cm^2

(a) SSD set-up

PDD at z_{ref} for a 10 cm × 10 cm field size: PDD(z_{ref} = _____ g/cm^2) = _____ %

Absorbed dose calibration of monitor at z_{max}:

$D_{w,Q}(z_{max}) = 100\ D_{w,Q}(z_{ref})/PDD(z_{ref})$ = _____ Gy/MU

(b) SAD set-up

TMR at z_{ref} for a 10 cm × 10 cm field size: TMR(z_{ref} = _____ g/cm^2) = _____

Absorbed dose calibration of monitor at z_{max}:

$D_{w,Q}(z_{max}) = D_{w,Q}(z_{ref})/TMR(z_{ref})$ = _____ Gy/MU

[a] Note that if Q_o is ^{60}Co, N_{D,w,Q_o} is denoted by $N_{D,w}$.

[b] All readings should be checked for leakage and corrected if necessary.

[c] If the electrometer is not calibrated separately, set $k_{elec} = 1$.

[d] M in the denominator of k_{pol} denotes reading at the user polarity. Preferably, each reading in the equation should be the average of the ratios of M (or M_+ or M_-) to the reading of an external monitor, M_{em}. It is assumed that the calibration laboratory has performed a polarity correction. Otherwise, k_{pol} is determined according to the reading at $+V_1$ for quality Q_o: $M_+ =$ _____ and the reading at $-V_1$ for quality Q_o: $M_- =$ _____.

$$k_{pol} = \left[\left(|M_+| + |M_-|\right)/M\right]_{Q} \Big/ \left[\left(|M_+| + |M_-|\right)/M\right]_{Q_o} = \_\_\_\_\_$$

[e] It is assumed that the calibration laboratory has performed a recombination correction. Otherwise the factor $k'_s = k_s / k_{s,Q_o}$ should be used instead of k_s. When Q_o is ^{60}Co, k_{s,Q_o} (determined at the calibration laboratory) will normally be close to unity, and the effect of not using this equation will be negligible in most cases.

[f] Strictly, readings should be corrected for the polarity effect (average from both polarities). Preferably, each reading in the equation should be the average of the ratios of M_1 or M_2 to the reading of an external monitor, M_{em}.

Note: SAD: source–axis distance; SSD: source–surface distance; FFF: flattening filter free; PDD: percentage depth dose; TMR: tissue−maximum ratio; MU: monitor unit.

7. CODE OF PRACTICE FOR HIGH ENERGY ELECTRON BEAMS

7.1. GENERAL

This section provides a code of practice for reference dosimetry (beam calibration) and recommendations for relative dosimetry in clinical electron beams with energies in the range 3–25 MeV. It is based on a calibration coefficient in terms of absorbed dose to water, N_{D,w,Q_o}, for a dosimeter in a reference beam of quality Q_o. This reference quality may be either ^{60}Co gamma radiation or an electron beam quality.

7.2. DOSIMETRY EQUIPMENT

7.2.1. Ionization chambers

The recommendations regarding ionization chambers given in Section 4.2.1 should be followed. Plane parallel chambers are the recommended type for all beam qualities and have to be used for beam quality indexes of $R_{50} < 3$ g/cm^2 ($E_o \leq 8$ MeV).[39] Ideally, the chamber should be calibrated in an electron beam, either directly at a standards laboratory or by cross-calibration in a clinical electron beam. The reference point for plane parallel chambers is taken to be on the inner surface of the entrance window, at the centre of the window. This point should be positioned at the point of interest[40] in the phantom and the water equivalent thickness of the chamber window should be taken into account. Chamber window thicknesses (in millimetres and in mg/cm^2) for a variety of plane parallel chamber types are given in Table 5.

For beam qualities $R_{50} > 3$ g/cm^2 ($E_o > 8$ MeV), cylindrical chambers may be used. This represents a reduction in the energy limit for this chamber type and reflects the investigation by Muir and McEwen [163]. The reference point for cylindrical chambers is taken to be on the chamber axis at the centre of the cavity volume. For measurements in electron beams, this reference point

---

[39] The approximate relation $E_o = 2.33R_{50}$ is assumed, where E_o is the mean energy at the phantom surface in MeV and R_{50} is expressed in g/cm^2. The value stated for R_{50} takes precedence over that stated for E_o.

[40] 'Point of interest' is the term used to refer to a position within the water phantom where a measurement is to be made. Most commonly it refers to the reference depth, but equally it can mean any point along a depth ionization curve.

should be positioned a distance of $0.5r_{cyl}$ deeper than the point of interest in the phantom.[41] This is consistent with previous codes of practice, although several investigations [155–157] have shown that the factor that is multiplied by r_{cyl} is chamber dependent. The impact of using a common factor on the determination of the reference absorbed dose to water is not significant within the estimated combined uncertainties (see Section 7.10). Values for r_{cyl} for a variety of cylindrical chamber types are given in Table 4.

7.2.2. Phantoms and chamber sleeves

The recommendations regarding phantoms and chamber sleeves given in Sections 4.2.3 and 4.2.4 should be followed, both for the determination of the absorbed dose and for the beam quality specification. Water is recommended as the reference medium for measurements in all electron beams. The water phantom should extend to at least 5 cm beyond all four sides of the largest field size employed at the depth of measurement. There should also be a margin of at least 5 g/cm^2 beyond the maximum depth of measurement.

In a horizontal electron beam, the window of the phantom should be plastic and of a thickness t_{win} of 0.2–0.5 cm.[42] The water equivalent thickness of the phantom window (in g/cm^2) should be taken into account when positioning the chamber at the desired measurement depth. This thickness can be calculated as the product $t_{win}\rho_{pl}$, where ρ_{pl} is the density of the plastic (in g/cm^3). For the commonly used plastics PMMA and clear polystyrene, the nominal values ρ_{PMMA} = 1.19 g/cm^3 and $\rho_{polystyrene}$ = 1.06 g/cm^3 may be used, consistent with Section 7.8.1. However, for high accuracy measurements, particularly for low electron energies, it is recommended that the density of the window material is measured.[43] As noted in Section 4.2.3, solid phantoms cannot be used for the reference dosimetry of electron beams.[44]

It is recommended that waterproof chambers — plane parallel or cylindrical — be used, as these are now the most common types of reference

---

[41] This approach is taken to avoid the need for a fluence gradient correction.

[42] A window only a few millimetres thick may bow outwards slightly because of water pressure on the inner surface. Any such effect should be accounted for when positioning the chamber at the depth of interest, particularly in low energy electron beams. Based on experience, the time for such bowing to equilibrate after phantom filling is ~45 min.

[43] An alternative is to insert a sheet of the same thickness and material as the window in the water phantom and measure the impact on a depth ionization curve to determine the effective water equivalent thickness [164].

[44] Plastic phantoms can be used for routine quality assurance measurements, provided that a transfer factor between plastic and water has been established at the time of beam calibration.

chamber (this includes plane parallel chambers supplied with a waterproof cover). For non-waterproof chambers, any waterproof enclosure, preferably made from PMMA or a material that matches the chamber walls, should be no more than 1 mm thick on all sides around the ionization chamber air cavity. A small air gap between the chamber wall and the sleeve (0.1–0.3 mm) may be required to allow the air pressure in the chamber to follow the ambient air pressure (depending on the chamber design). For both chamber types, the same waterproofing should be used for the determination of absorbed dose to water at the user facility as was used for calibration at the standards laboratory.

7.3. BEAM QUALITY SPECIFICATION

7.3.1. Choice of beam quality index

For electron beams the beam quality index is the half-value depth in water, R_{50}. This is the depth in water (in g/cm^2) at which the absorbed dose is 50% of its value at the absorbed dose maximum, measured with a constant SSD of 100 cm and a field size of at least 10 cm × 10 cm at the phantom surface. The same applicator can be used for all beam energies up to 22 MeV for the measurement of the beam quality; there is no requirement to use a larger field size for higher energies.

7.3.2. Measurement of beam quality

The reference conditions for the determination of R_{50} are given in Table 18.

For all beam qualities, the preferred choice of detector for the measurement of R_{50} is a plane parallel chamber. For beam qualities $R_{50} > 3$ g/cm^2 ($E_o > 8$ MeV) a cylindrical chamber may be used, with the reference point positioned at the appropriate depth, deeper than the point of interest in the phantom.[45] A water phantom is the recommended choice. In a vertical beam, the direction of the scan should be towards the surface to reduce water–air interface effects.

Ideally, ion recombination and polarity corrections should be applied to the ionization chamber data at all depths (see Section 4.4.3). For consistency, the same polarizing voltage as for reference measurements should be used. It is recommended to obtain depth ionization curves at opposite polarities, as this is a quick and reliable check on system performance. For the purposes of correcting

[45] As for cylindrical chambers in photon beams [109, 165], the shift Xr_{cyl}, where $X = 0.5$, is an approximation. Actual values depend on the chamber geometry, and for beam quality measurements this can have a measurable effect.

TABLE 18. REFERENCE CONDITIONS FOR THE DETERMINATION OF THE ELECTRON BEAM QUALITY INDEX (R_{50})

Influence quantity	Reference value or reference characteristic
Phantom material	Water
Chamber type	For $R_{50} > 3$ g/cm^2, plane parallel or cylindrical For $R_{50} < 3$ g/cm^2, plane parallel
Reference point of chamber	For plane parallel chambers, on the inner surface of the window at its centre[a] For cylindrical chambers, on the central axis at the centre of the cavity volume
Position of reference point of chamber	For plane parallel chambers, at the point of interest[b] For cylindrical chambers, $0.5r_{cyl}$ deeper than the point of interest[c]
Source–surface distance	100 cm
Field size at phantom surface	At least 10 cm × 10 cm

[a] The entrance window should be scaled to the water equivalent thickness.

[b] 'Point of interest' refers to any point in the water phantom where data are to be obtained. In this case, it is at the inner surface of the entrance window.

[c] The shift Xr_{cyl}, where $X = 0.5$, is an approximation; the actual values depend on the chamber geometry. To achieve the highest accuracy, the actual shift should be taken into account for beam quality measurements [166, 167].

a depth ionization plot for ion recombination, published data for the relation between k_{ion} and dose per pulse for a particular chamber type may be used.[46] For measurements made over a short period of time (minutes), air temperature and pressure corrections need not be made, although it is recommended to monitor the environmental conditions.

When using an ionization chamber, the measured quantity is the half-value of the depth ionization distribution in water, $R_{50,ion}$. This is the depth in water (in g/cm^2) at which the ionization current is 50% of its maximum value. The

[46] For this purpose, the dose per pulse at each depth can be estimated from the nominal dose per pulse at the reference depth scaled by the per cent ionization at that depth.

half-value of the depth dose distribution in water R_{50} is obtained using the following relations[47] [168]:

$$R_{50} = \begin{cases} 1.029R_{50,\text{ion}} - 0.06\ \text{g/cm}^2 & \text{for } R_{50,\text{ion}} \le 10\ \text{g/cm}^2 \\ 1.059R_{50,\text{ion}} - 0.37\ \text{g/cm}^2 & \text{for } R_{50,\text{ion}} > 10\ \text{g/cm}^2 \end{cases} \quad (37)$$

As an alternative to the use of an ionization chamber, other detectors (e.g. diode, diamond) may be used to determine R_{50}. In this case, the user has to verify that the detector is suitable for depth dose measurements using test comparisons with an ionization chamber at a set of representative beam qualities.[48]

7.4. DETERMINATION OF ABSORBED DOSE TO WATER

7.4.1. Determination of absorbed dose under reference conditions

The absorbed dose to water at the reference depth z_{ref} in water, in an electron beam of quality Q and in the absence of the chamber, is given by the following equation:

$$D_{\text{w},Q} = M_Q N_{D,\text{w},Q_o} k_{Q,Q_o} \quad (38)$$

where M_Q is the reading of the dosimeter corrected for the influence quantities temperature and pressure, electrometer calibration, polarity effect and ion recombination, as described in the worksheet in Section 7.11 (see also Section 4.4.3). The chamber should be positioned in accordance with the reference conditions, as given in Table 19. N_{D,w,Q_o} is the calibration coefficient of the dosimeter in terms of absorbed dose to water at the reference quality Q_o, and k_{Q,Q_o} is a chamber specific factor that corrects for differences between the reference beam quality Q_o and the actual beam quality Q.

7.4.2. Reference conditions

The reference conditions for the determination of the absorbed dose to water in electron beams are given in Table 19. Because the precise choice of

[47] These relations remain unchanged with the adoption of recent stopping power data provided in Ref. [32].

[48] It has been shown [169–172] that plane parallel chambers have a depth dependent perturbation that may affect such a comparison. The impact of such effects, however, is generally <0.05 g/cm^2.

TABLE 19. REFERENCE CONDITIONS FOR THE DETERMINATION OF ABSORBED DOSE IN ELECTRON BEAMS

Influence quantity	Reference value or reference characteristic
Phantom material	Water
Chamber type	For $R_{50} \geq 3$ g/cm^2, plane parallel or cylindrical[a] For $R_{50} < 3$ g/cm^2, plane parallel
Measurement depth, z_{ref}	$0.6R_{50} - 0.1$ g/cm^2
Reference point of chamber	For plane parallel chambers, on the inner surface of the window at its centre[b] For cylindrical chambers, on the central axis at the centre of the cavity volume
Position of reference point of chamber	For plane parallel chambers, at z_{ref} For cylindrical chambers, $0.5r_{cyl}$ deeper than z_{ref}[c]
Source–surface distance	100 cm
Field size at phantom surface	10 cm × 10 cm

[a] This is a reduction from the previous recommendation, based on an analysis of clinical data.

[b] The entrance window of the chamber should be scaled to a water equivalent depth to determine the reference point.

[c] As noted in the previous text, the factor 0.5 is an approximation. Actual values depend on the chamber geometry but for reference positioning, the assumption of a shift of $0.5r_{cyl}$ does not introduce a significant error.

field size is not critical [10], a convenient choice for the reference field size is that which is used for the normalization of the field output factors, subject to the constraint that it should not be smaller than 10 cm × 10 cm at the phantom surface. The reference depth z_{ref} is given by the following equation [173]:

$$z_{ref} = 0.6R_{50} - 0.1 \text{ g/cm}^2 \quad \left(R_{50} \text{ in g/cm}^2\right) \tag{39}$$

This depth is close to the depth of the absorbed dose maximum z_{max} or greater, depending on the incident energy and the specifics of any field size defining system.

7.4.3. Absorbed dose at z_{max}

Clinical normalization most often takes place at the depth of the dose maximum z_{max}, which in this international code of practice does not always coincide with z_{ref}. To determine the absorbed dose at z_{max} for a given beam the user should use the measured central axis depth dose distribution to convert the absorbed dose at z_{ref} to that at z_{max}. The measurement of depth dose distributions is discussed in Section 7.7.1.

7.5. VALUES FOR k_{Q,Q_o}

The modified treatment of k_{Q,Q_o} for chambers cross-calibrated in a user electron beam, as described in Sections 3.2.1, 3.2.2 and 4.5, is discussed in Section 7.6 and may also be applied to chambers calibrated directly at a standards laboratory at a single electron beam quality.

7.5.1. Chamber calibrated in ^{60}Co

When the reference quality Q_o is ^{60}Co, the factor k_{Q,Q_o} is denoted by k_Q. Values for k_Q are given in Table 20 for a series of user qualities Q and for a number of chamber types; values for non-tabulated qualities may be obtained by interpolation. Data are presented in Fig. 9 for cylindrical chamber types. The number of chambers listed is significantly reduced from that in the first edition of this international code of practice for the following reasons:

(a) Only chambers that are currently manufactured are listed;
(b) Monte Carlo calculations have been validated only for limited k_{Q,Q_o} data (either via independent calculations or via experiments; see Appendix II).

7.5.2. Chamber calibrated at a series of electron beam qualities

For a chamber calibrated at a series of electron beam qualities, the data from the calibration laboratory will ideally be presented as both individual calibration coefficients, $N_{D,w,Q}$, determined at each calibration beam quality, and as measured factors k_{Q,Q_o} normalized to a reference beam quality Q_o.

TABLE 20. CALCULATED k_Q VALUES[a] FOR ELECTRON BEAMS, FOR VARIOUS CHAMBER TYPES CALIBRATED IN ^{60}Co GAMMA RADIATION, AS A FUNCTION OF BEAM QUALITY INDEX R_{50}

Ionization chamber type[b]	Beam quality index, R_{50} (g/cm^2)													
	1.0[c]	1.4	2.0	2.5	3.0	3.5	4.0	4.5	5.0	5.5	6.0	7.0	8.0	10.0
PTW 34001 Roos	0.9743	0.9645	0.9518	0.9428	0.9349	0.9281	0.9222	0.9171	0.9127	0.9088	0.9055	0.9001	0.8960	0.8907
IBA NACP-02	0.9679	0.9580	0.9451	0.9360	0.9281	0.9214	0.9155	0.9104	0.9061	0.9023	0.8990	0.8938	0.8899	0.8848
NE 2571					0.9297	0.9248	0.9210	0.9181	0.9157	0.9137	0.9121	0.9095	0.9075	0.9047
IBA FC65-G					0.9328	0.9279	0.9241	0.9210	0.9184	0.9163	0.9144	0.9114	0.9090	0.9055
Exradin A12					0.9353	0.9304	0.9264	0.9232	0.9205	0.9182	0.9163	0.9130	0.9104	0.9066
Exradin A19					0.9320	0.9273	0.9236	0.9205	0.9178	0.9156	0.9136	0.9103	0.9077	0.9036
PTW 30013					0.9300	0.9247	0.9210	0.9180	0.9155	0.9135	0.9118	0.9090	0.9068	0.9037
PTW 30012					0.9384	0.9331	0.9290	0.9257	0.9230	0.9207	0.9187	0.9156	0.9131	0.9094

TABLE 20. CALCULATED k_Q VALUES[a] FOR ELECTRON BEAMS, FOR VARIOUS CHAMBER TYPES CALIBRATED IN ^{60}Co GAMMA RADIATION, AS A FUNCTION OF BEAM QUALITY INDEX R_{50} (cont.)

Ionization chamber type[b]	Beam quality index, R_{50} (g/cm^2)													
	1.0[c]	1.4	2.0	2.5	3.0	3.5	4.0	4.5	5.0	5.5	6.0	7.0	8.0	10.0

Note: The data are derived from an analysis of experimental and Monte Carlo calculated factors and represent the best current estimate of values to be used for the listed ionization chamber types; see Appendix II.

[a] Values are given to four decimal places to permit smooth interpolation of the data. This does not imply uncertainties of this order.

[b] Only chambers demonstrating reference class performance are included in this table. Other chamber types may be suitable for relative dosimetry.

[c] Data are given for a beam quality of R_{50} = 1 g/cm^2 but the lack of experimental validation at this energy means that the uncertainty is greater than that given in Section 7.10. Use of experimentally determined $k_{Q,Q_{int}}$ factors for R_{50} < 1.4 g/cm^2 is recommended.

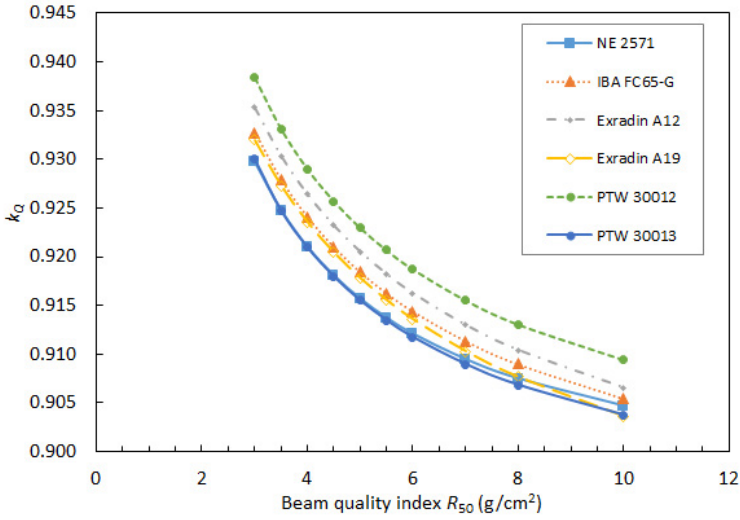

FIG. 9. Calculated k_Q *values for electron beams for various cylindrical chamber types calibrated in* ^{60}*Co gamma radiation.*

However, if the calibration data are in the form of a set of calibration coefficients $N_{D,w,Q}$, then one of the calibration qualities[49] should be chosen as the reference calibration quality Q_o. The corresponding calibration coefficient is denoted N_{D,w,Q_o} and the remaining calibration coefficients are given by the following relation:

$$k_{Q,Q_o} = \frac{N_{D,w,Q}}{N_{D,w,Q_o}} \tag{40}$$

If the quality of the user beam Q does not match any of the calibration qualities, the value for k_{Q,Q_o} to be used in Eq. (38) can be obtained by interpolation.[50]

A chamber calibrated at a series of beam qualities may be subsequently recalibrated only at the reference calibration quality Q_o. In this case, the new value for N_{D,w,Q_o} should be used in conjunction with the values for k_{Q,Q_o}

[49] The choice here is not critical. The quality corresponding to the $N_{D,w,Q}$ coefficient with the smallest relative uncertainty is appropriate; otherwise a quality close to the middle of the range.

[50] The type of interpolation (e.g. linear, polynomial, cubic spline) should be chosen to minimize any additional uncertainty arising from the procedure.

measured previously.[51] Note, however, that this procedure assumes that there is no change in the energy dependence of the ionization chamber, which has to be established before adopting this simpler recalibration method. In all cases, the chamber should be recalibrated at all qualities at least every six years, or if the user suspects that the chamber's response has changed or that the chamber has been damaged.

7.6. CROSS-CALIBRATION OF IONIZATION CHAMBERS

Cross-calibration refers to the calibration of a user chamber by direct comparison in a suitable user beam against a reference chamber that has previously been calibrated. A well known example of this procedure is the cross-calibration of a plane parallel chamber for use in electron beams against a reference cylindrical chamber calibrated in ^{60}Co gamma radiation.

7.6.1. Cross-calibration procedure

The highest energy electron beam available should be used; $R_{50} > 7$ g/cm^2 ($E_o > 16$ MeV) is recommended. The reference chamber and the chamber to be calibrated are compared by alternately positioning each at the reference depth z_{ref} in water in accordance with their reference conditions (see Table 19). The calibration coefficient in terms of absorbed dose to water for the chamber under calibration at the cross-calibration quality Q_{cross} is given by the following relation:

$$N^{field}_{D,w,Q_{cross}} = \frac{D_{w,Q_{cross}}}{M^{field}_{Q_{cross}}} = \frac{M^{ref}_{Q_{cross}}}{M^{field}_{Q_{cross}}} N^{ref}_{D,w,Q_o} k^{ref}_{Q_{cross},Q_o} \quad (41)$$

where $M^{ref}_{Q_{cross}}$ and $M^{field}_{Q_{cross}}$ are the dosimeter readings for the reference chamber and the chamber under calibration, respectively, corrected for the influence quantities temperature and pressure, electrometer calibration, polarity effect and ion recombination, as described in Section 4.4.3. N^{ref}_{D,w,Q_o} is the calibration coefficient in terms of absorbed dose to water for the reference chamber at quality Q_o and $k^{ref}_{Q_{cross},Q_o}$ is the beam quality correction factor for the reference chamber. The same superscript 'field' is used here as in Section 4.5.2 for consistency, although for electron beams the field chamber may be the reference detector that is used to calibrate all beams.

---

[51] In the case where the same reference beam quality is no longer available from the calibration laboratory, a beam quality close to the original Q_o should be chosen and a renormalization of Eq. (40) will be required.

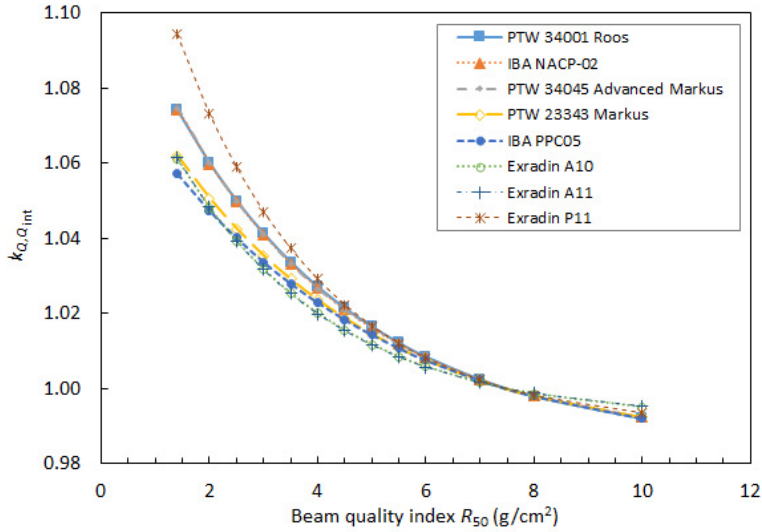

FIG. 10. Calculated $k_{Q,Q_{int}}$ *values for electron beams for various plane parallel chamber types using* Q_{int} *= 7.5 g/cm*^{2}*. Since* k_Q *factors are provided only for two plane parallel chambers (i.e. PTW 34001 Roos and IBA NACP-02), the relative energy dependence in electron beams is shown for a wider range of chamber types.*

When the reference chamber calibration quality Q_o is ^{60}Co gamma radiation, $k^{ref}_{Q_{cross},Q_o}$ reduces to $k^{ref}_{Q_{cross}}$. If Q_o is itself a megavoltage electron beam, then $k^{ref}_{Q_{cross},Q_o}$ is obtained using the concept of the intermediate quality, as follows:

$$k^{ref}_{Q_{cross},Q_o} = \frac{k^{ref}_{Q_{cross},Q_{int}}}{k^{ref}_{Q_o,Q_{int}}} \tag{42}$$

Values of $k_{Q,Q_{int}}$ are given in Table 21 and Fig. 10. These can also be used in conjunction with a calibration in one or more electron beam qualities, as described in Section 7.5.2.

7.6.2. Subsequent use of a cross-calibrated chamber

The field chamber can subsequently be used to determine the absorbed dose to water in any beam of quality Q of the same modality (photon, electron

TABLE 21. CALCULATED $k_{Q,Q_{int}}$ VALUES[a] FOR VARIOUS CHAMBER TYPES CALIBRATED IN ELECTRON BEAMS, AS A FUNCTION OF BEAM QUALITY INDEX R_{50} (Q_{int} = 7.5 g/cm^2)

Ionization chamber type[b]	Beam quality index, R_{50} (g/cm^2)													
	1.0[c]	1.4	2.0	2.5	3.0	3.5	4.0	4.5	5.0	5.5	6.0	7.0	8.0	10.0
PTW 34001 Roos	1.0851	1.0742	1.0600	1.0500	1.0412	1.0337	1.0271	1.0214	1.0164	1.0122	1.0084	1.0024	0.9979	0.9919
IBA NACP-02	1.0855	1.0743	1.0599	1.0497	1.0409	1.0332	1.0267	1.0210	1.0161	1.0119	1.0082	1.0023	0.9980	0.9923
PTW 34045 Advanced Markus	1.0861	1.0747	1.0601	1.0498	1.0409	1.0332	1.0266	1.0209	1.0160	1.0118	1.0082	1.0023	0.9980	0.9924
PTW 23343 Markus	1.0705	1.0620	1.0507	1.0425	1.0354	1.0291	1.0236	1.0188	1.0146	1.0108	1.0076	1.0022	0.9981	0.9924
IBA PPC40	1.0826	1.0721	1.0583	1.0485	1.0401	1.0327	1.0263	1.0208	1.0160	1.0118	1.0082	1.0024	0.9980	0.9922
IBA PPC05	1.0647	1.0572	1.0474	1.0401	1.0337	1.0279	1.0229	1.0183	1.0143	1.0107	1.0076	1.0022	0.9980	0.9921
Exradin A10	1.0714	1.0611	1.0482	1.0393	1.0317	1.0254	1.0200	1.0155	1.0117	1.0085	1.0058	1.0016	0.9986	0.9950
Exradin A11	1.0720	1.0615	1.0483	1.0393	1.0316	1.0252	1.0199	1.0154	1.0116	1.0084	1.0057	1.0016	0.9987	0.9952
Exradin P11	1.1113	1.0944	1.0733	1.0590	1.0472	1.0373	1.0291	1.0223	1.0167	1.0120	1.0081	1.0022	0.9982	0.9934
Sun Nuclear SNC350p	1.0851	1.0742	1.0600	1.0500	1.0412	1.0337	1.0271	1.0214	1.0164	1.0122	1.0084	1.0024	0.9979	0.9919

TABLE 21. CALCULATED $k_{Q,Q_{int}}$ VALUES[a] FOR VARIOUS CHAMBER TYPES CALIBRATED IN ELECTRON BEAMS, AS A FUNCTION OF BEAM QUALITY INDEX R_{50} (Q_{int} = 7.5 g/cm^2) (cont.)

Ionization chamber type[b]	Beam quality index, R_{50} (g/cm^2)													
	1.0[c]	1.4	2.0	2.5	3.0	3.5	4.0	4.5	5.0	5.5	6.0	7.0	8.0	10.0
NE 2571					1.0235	1.0180	1.0139	1.0106	1.0080	1.0059	1.0040	1.0012	0.9990	0.9959
IBA FC65-G					1.0249	1.0195	1.0154	1.0120	1.0091	1.0068	1.0047	1.0014	0.9988	0.9949
Exradin A12					1.0260	1.0205	1.0162	1.0127	1.0097	1.0072	1.0051	1.0015	0.9987	0.9944
Exradin A19					1.0254	1.0202	1.0161	1.0127	1.0098	1.0073	1.0051	1.0015	0.9986	0.9942
PTW 30013					1.0240	1.0186	1.0145	1.0112	1.0085	1.0062	1.0043	1.0012	0.9989	0.9955
PTW 30012					1.0264	1.0207	1.0162	1.0126	1.0096	1.0071	1.0049	1.0014	0.9987	0.9947

Note: The data are derived from an analysis of experimental and Monte Carlo calculated factors and represent the best current estimate of values to be used for the listed ionization chamber types.

[a] Values are given to four decimal places to permit smooth interpolation of the data. This does not imply uncertainties of this order.

[b] Only chambers demonstrating reference class performance are included in this table [98, 141, 174]. Other chamber types may be suitable for relative dosimetry.

[c] Data are given for a beam quality of R_{50} = 1 g/cm^2 but the lack of experimental validation at this energy means that the uncertainty is greater than that given in Section 7.10. Use of experimentally determined $k_{Q,Q_{int}}$ factors for R_{50} < 1.4 g/cm^2 is recommended.

or proton) as Q_{cross}, and for which the value of the factor $k^{\text{field}}_{Q,Q_{\text{cross}}}$ is available, according to the following equation:

$$D_{\text{w},Q} = M^{\text{field}}_{Q} N^{\text{field}}_{D,\text{w},Q_{\text{cross}}} k^{\text{field}}_{Q,Q_{\text{cross}}} \tag{43}$$

where M^{field}_{Q} is the chamber reading, corrected for influence quantities, when positioned in water in the beam of quality Q. The beam quality factor $k^{\text{field}}_{Q,Q_{\text{cross}}}$ is obtained using the intermediate quality in Eq. (6), in this case as follows:

$$k^{\text{field}}_{Q,Q_{\text{cross}}} = \frac{k^{\text{field}}_{Q,Q_{\text{int}}}}{k^{\text{field}}_{Q_{\text{cross}},Q_{\text{int}}}} \tag{44}$$

7.7. MEASUREMENTS UNDER NON-REFERENCE CONDITIONS

7.7.1. Central axis depth dose distributions

The measurement of a central axis depth dose distribution should follow the procedure given in Section 7.3.2 for the measurement of R_{50}. If an ionization chamber is used, the measured depth ionization distribution needs to be converted to a depth dose distribution.[52] For a beam of quality R_{50}, this is achieved by multiplying the ionization current or charge at each measurement depth z by the stopping power ratio $s_{\text{w,air}}$ at that depth. Values for $s_{\text{w,air}}$ are given in Table 22 as a function of R_{50} and of the relative depth z/R_{50}. The values provided in the first edition of this publication have been reviewed in light of the recommendations of Ref. [32] and have been found to be consistent with the updated I value for water. The multiparameter equation proposed in Ref. [173] and given in Appendix II may be simpler to implement in software.

Note that this procedure considers the variation in the perturbation factor with depth to be negligible. Various publications [169–172] have shown that this is not the case, even for well guarded plane parallel chambers, and if changes in the perturbation factor are significant they have to be accounted for. However, for the reference class chambers listed in Tables 20 and 21, the impact of a depth dependent perturbation correction on the determination of R_{50} is <0.05 g/cm^2.

[52] This conversion is required in electron beams because the water to air stopping power ratio $s_{\text{w,air}}$ changes rapidly with depth.

TABLE 22. SPENCER–ATTIX STOPPING POWER RATIOS ($\Delta = 10$ keV) OF WATER TO AIR ($s_{w,air}$) FOR ELECTRON BEAMS AS A FUNCTION OF BEAM QUALITY INDEX R_{50} AND RELATIVE DEPTH IN WATER, z/R_{50}

z/R_{50}	R_{50} (g/cm^2)													
	1.0	1.4	2.0	2.5	3.0	3.5	4.0	4.5	5.0	5.5	6.0	7.0	8.0	10.0
0.02	1.076	1.060	1.042	1.030	1.020	1.012	1.004	0.997	0.991	0.986	0.980	0.971	0.963	0.950
0.05	1.078	1.061	1.044	1.032	1.022	1.014	1.006	1.000	0.994	0.988	0.983	0.974	0.965	0.952
0.1	1.080	1.064	1.047	1.036	1.026	1.018	1.010	1.004	0.998	0.992	0.987	0.978	0.970	0.957
0.15	1.083	1.067	1.050	1.039	1.030	1.022	1.014	1.008	1.002	0.997	0.992	0.983	0.975	0.961
0.2	1.085	1.070	1.053	1.043	1.034	1.026	1.019	1.012	1.006	1.001	0.996	0.987	0.979	0.966
0.25	1.088	1.073	1.057	1.046	1.037	1.030	1.023	1.017	1.011	1.006	1.001	0.992	0.984	0.971
0.3	1.091	1.076	1.060	1.050	1.041	1.034	1.027	1.021	1.016	1.010	1.006	0.997	0.989	0.976
0.35	1.093	1.079	1.064	1.054	1.045	1.038	1.032	1.026	1.020	1.015	1.011	1.002	0.995	0.982
0.4	1.096	1.082	1.067	1.058	1.049	1.042	1.036	1.030	1.025	1.020	1.016	1.007	1.000	0.987
0.45	1.099	1.085	1.071	1.062	1.054	1.047	1.041	1.035	1.030	1.025	1.021	1.013	1.006	0.993
0.5	1.102	1.089	1.075	1.066	1.058	1.051	1.046	1.040	1.035	1.031	1.027	1.019	1.012	0.999
0.55	1.105	1.092	1.078	1.070	1.062	1.056	1.051	1.045	1.041	1.036	1.032	1.025	1.018	1.005
0.6	1.108	1.095	1.082	1.074	1.067	1.061	1.056	1.051	1.046	1.042	1.038	1.031	1.024	1.012
0.65	1.111	1.099	1.086	1.078	1.072	1.066	1.061	1.056	1.052	1.048	1.044	1.037	1.030	1.018
0.7	1.114	1.102	1.090	1.082	1.076	1.071	1.066	1.062	1.058	1.054	1.050	1.043	1.037	1.025
0.75	1.117	1.105	1.094	1.087	1.081	1.076	1.072	1.067	1.064	1.060	1.057	1.050	1.044	1.033

TABLE 22. SPENCER–ATTIX STOPPING POWER RATIOS (Δ = 10 keV) OF WATER TO AIR ($s_{w,air}$) FOR ELECTRON BEAMS AS A FUNCTION OF BEAM QUALITY INDEX R_{50} AND RELATIVE DEPTH IN WATER, z/R_{50} (cont.)

z/R_{50}	R_{50} (g/cm^2)													
	1.0	1.4	2.0	2.5	3.0	3.5	4.0	4.5	5.0	5.5	6.0	7.0	8.0	10.0
0.8	1.120	1.109	1.098	1.091	1.086	1.081	1.077	1.073	1.070	1.066	1.063	1.057	1.051	1.040
0.85	1.123	1.112	1.102	1.096	1.091	1.087	1.083	1.080	1.076	1.073	1.070	1.064	1.059	1.048
0.9	1.126	1.116	1.107	1.101	1.096	1.092	1.089	1.086	1.083	1.080	1.077	1.072	1.067	1.056
0.95	1.129	1.120	1.111	1.106	1.102	1.098	1.095	1.092	1.090	1.087	1.085	1.080	1.075	1.065
1	1.132	1.124	1.115	1.111	1.107	1.104	1.101	1.099	1.097	1.095	1.092	1.088	1.083	1.074
1.05	1.136	1.127	1.120	1.116	1.113	1.110	1.108	1.106	1.104	1.102	1.100	1.096	1.092	1.083
1.1	1.139	1.131	1.125	1.121	1.118	1.116	1.115	1.113	1.112	1.110	1.109	1.105	1.102	1.093
1.15	1.142	1.135	1.129	1.126	1.124	1.123	1.122	1.120	1.119	1.118	1.117	1.114	1.111	1.104
1.2	1.146	1.139	1.134	1.132	1.130	1.129	1.129	1.128	1.128	1.127	1.126	1.124	1.121	1.115
z_{ref} (g/cm^2)	0.5	0.7	1.1	1.4	1.7	2.0	2.3	2.6	2.9	3.2	3.5	4.1	4.7	5.9
$s_{w,air}$ (z_{ref})	1.102	1.09	1.078	1.07	1.064	1.058	1.053	1.048	1.044	1.04	1.036	1.029	1.022	1.01

Note: The data are derived using the approach described in Ref. [173], taking into account the recommendations of Ref. [32]).

7.7.2. Field output factors

For a given electron beam, field output factors should be measured at z_{max} for the non-reference field sizes and SSDs used for the treatment of patients. Field output factors may be determined as the absorbed dose at z_{max} for a given set of non-reference conditions relative to the absorbed dose at z_{ref} (or z_{max}) under the appropriate reference conditions. Users should be aware of the variation of the depth of maximum dose, z_{max}, particularly for small field sizes and high energies.

For detectors such as diodes and diamonds the field output factor is adequately approximated by the detector reading under non-reference conditions relative to that under reference conditions. If an ionization chamber is used, the measured ratio of corrected ionization currents or charges should be corrected for the variation in $s_{w,air}$ with depth using Table 22. The same considerations noted in Section 7.7.1 regarding perturbation effects also apply here.

7.8. USE OF PLASTIC PHANTOMS

Plastic phantoms may not be used for electron beam reference dosimetry, even at low electron energies. However, their use for quality assurance procedures or relative dosimetry is acceptable, where a solid phantom can provide a simpler experimental set-up without a loss in accuracy. Commercial water equivalent phantoms are preferred to generic plastics, as there is less chance of mistakes related to incorrect use of data or manufacturing defects, but both types are permitted.

7.8.1. Scaling of depths

Depths in plastic phantoms, z_{pl}, expressed in g/cm^2, are obtained by multiplying the depth in centimetres by the plastic density ρ_{pl} in g/cm^3. The density of the plastic, ρ_{pl}, should be measured for the batch of plastic in use rather than using a nominal value for the plastic type. Measurements made in a plastic phantom at depth z_{pl} (in g/cm^2) relate to the depth in water given as follows:

$$z_w = z_{pl} c_{pl} \quad \left(\text{g/cm}^2\right) \tag{45}$$

where c_{pl} is a depth scaling factor. Values for c_{pl} for certain plastics that are currently available are given in Table 23.[53] These are given only for guidance, and ideally the user should characterize a specific material prior to use. Data for legacy materials no longer manufactured but likely still in use can be found in the first edition of this international code of practice. Nominal values of the density ρ_{pl} for each plastic are also given in Table 23, and Refs [105, 175, 176] indicate how c_{pl} and h_{pl} can be determined.

TABLE 23. VALUES FOR THE DEPTH SCALING FACTOR, c_{pl}, THE FLUENCE SCALING FACTOR, h_{pl}, AND THE NOMINAL DENSITY, ρ_{pl}, FOR CERTAIN PLASTICS

Plastic phantom	c_{pl} [a]	h_{pl}	ρ_{pl} (g/cm^3)
Solid Water HE (Sun Nuclear)[b]	0.964	1.000	1.03
Wte (Bart's Health NHS Trust)[c]	0.973	0.999	1.04
Plastic Water (CIRS)	0.982	0.998	1.01
Virtual Water (Med-Cal)[d]	0.954	1.003	1.06
PMMA[e]	0.947	1.009	1.19
Clear polystyrene	0.930	1.026	1.06
White polystyrene[f]	0.933	1.019	1.06

[a] The IPEM Code of Practice for electron beams [106] uses the range scaling factor c_{pl}, which is equivalent to the product $c_{pl}\rho_{pl}$. For materials designed to be water equivalent, c_{pl} is generally within 1% of unity (i.e. 1 mm plastic, equivalent to 1 mm water).

[b] Taken from the manufacturer's data sheet. Solid Water was originally produced by Gammex.

[c] Taken from Ref. [176].

[d] Taken from Ref. [177].

[e] For PMMA and polystyrene, data are an average of values given in the first edition of this international code of practice and Ref. [106].

[f] Polystyrene with a small percentage of titanium oxide added (e.g. PTW RW3).

[53] For materials no longer available commercially (e.g. WT1) information can be found in the first edition of this international code of practice.

The relation between the ionization chamber measurement in a plastic phantom, $M_{Q_{pl}}$, and the measurement that would be obtained in a water phantom at the equivalent depth, M_Q, is given by the following relation:

$$M_Q = M_{Q_{pl}} h_{pl} \tag{46}$$

Note that h_{pl} is depth dependent, being unity at the phantom surface and increasing at larger depths. The values of h_{pl} given in Table 23 are applicable in the region around z_{max} to z_{ref}.

7.8.2. Plastic phantoms for beam quality specification

It is not recommended to use a plastic phantom to measure the beam quality specifier, as modern, automated water phantoms provide fast automated data acquisition of the full depth ionization or depth dose curve. Measuring a depth dose distribution requires that each measurement depth in plastic be scaled using Eq. (45) to give the appropriate depth in water. The ionization chamber reading should not only be corrected for the variation in water–air stopping power ratio, but should also be multiplied by the appropriate fluence scaling factor (which is also a function of depth). The anticipated increased accuracy due to positioning in a solid phantom is outweighed by these scaling factors.

7.9. NON-STANDARD ELECTRON BEAMS

A number of 'non-standard' electron beam delivery systems are either currently in use or at the early stages of development. As for megavoltage photon beam systems, these electron beams differ from standard electron beams produced by clinical linear accelerators in one or more of the following ways:

— Increased dose per pulse (which may or may not lead to a higher mean dose rate);
— Reduced maximum field size (often producing a degraded depth dose curve[54]);
— Maximum energy (energies >200 MeV have been proposed).

[54] In such beams, increased collimator scatter leads to z_{max} being much closer to the surface and farther from z_{ref} than for equivalent standard electron beams.

In the energy range covered in this international code of practice, the most common example of a non-standard beam is the IORT (intraoperative radiotherapy) linac. These mobile systems have been studied extensively over the last two decades, particularly in relation to their large dose per pulse values that lead to very high ion recombination corrections, which cannot be dealt with using the standard theory outlined in Section 4. The characteristics of these electron beams mean that it is not possible to use the formalism and approaches described here, and users of such systems are referred to the published literature [178–180].

7.10. ESTIMATED UNCERTAINTY IN THE DETERMINATION OF ABSORBED DOSE TO WATER UNDER REFERENCE CONDITIONS

It is the responsibility of the user to establish an uncertainty budget for their determination of absorbed dose to water. Example uncertainty estimates for the determination of absorbed dose to water using a ^{60}Co calibration coefficient are presented in Table 24, and for the determination of absorbed dose to water using calibration in a high energy electron beam with $R_{50} \approx 8$ g/cm^2 ($E_o \approx 20$ MeV) are given in Table 25. In each of these tables, estimates are given for both plane parallel and cylindrical chamber types (note that R_{50} cannot be <3 g/cm^2 when a cylindrical chamber is used). These estimates may vary depending on the uncertainty quoted by the calibration laboratory, the care and experience of the user performing the measurement, and the quality and condition of the measurement equipment (e.g. regular recalibration of all measurement devices, quality management system to ensure proper functioning). Uncertainty estimates are not given for the determination of absorbed dose at depths other than z_{ref}, although these may be large when plastic phantoms are used. The uncertainty of the k_{Q,Q_o} factors is discussed in Appendix II.

If measured values for k_{Q,Q_o} are used instead of calculated values, the combined uncertainty in the determination of absorbed dose to water may be considerably reduced. For example, if k_Q values (i.e. relative to ^{60}Co) are measured for a plane parallel chamber with a standard uncertainty of ~0.5%, the estimated overall uncertainty in the determination of the absorbed dose to water at z_{ref} in an electron beam is reduced from 1.2% to 0.7%.

The uncertainty in the determination of the absorbed dose to water using a plane parallel chamber cross-calibrated in a high energy electron beam (against a cylindrical chamber with an absorbed dose to water calibration coefficient determined in a ^{60}Co beam) deserves special attention because cancellations have to be taken into account. By combining Eq. (43) (the use of a cross-calibrated chamber), Eq. (41) (the cross-calibration coefficient) and Eq. (91) in Appendix II

(the basic equation for k_Q), the full expression for the absorbed dose to water becomes as follows:

$$D_{w,Q} = M_Q^{pp} \frac{M_{Q_{cross}}^{cyl}}{M_{Q_{cross}}^{pp}} N_{D,w}^{cyl} k_{Q_{cross}}^{cyl} k_{Q,Q_{cross}}^{pp} \quad (47)$$

Note that with Monte Carlo calculated k_Q factors, there is not the same explicit cancellation of stopping power ratios and W_{air} values as laid out in the first edition of this international code of practice.

TABLE 24. ESTIMATED RELATIVE STANDARD UNCERTAINTY[a] OF $D_{w,Q}$ AT THE REFERENCE DEPTH IN WATER AND FOR AN ELECTRON BEAM, BASED ON A CHAMBER CALIBRATION IN ^{60}Co GAMMA RADIATION

Physical quantity or procedure	Relative standard uncertainty (%)	
	Cylindrical $R_{50} \geq 3$ g/cm^2	Plane parallel $R_{50} \geq 2$ g/cm^2
Step 1: standards laboratory		
$N_{D,w}$ calibration of secondary standard at PSDL	0.5	0.5
Long term stability of secondary standard	0.1	0.1
$N_{D,w}$ calibration of user dosimeter at SSDL	0.4	0.4
Combined uncertainty of step 1[b]	0.6	0.6
Step 2: user electron beam		
Long term stability of user dosimeter	0.2	0.4
Establishment of reference conditions	0.3	0.3
Dosimeter reading M_Q relative to beam monitor	0.3	0.3
Correction for influence quantities k_i	0.3	0.3
Beam quality correction k_Q (see Appendix II)	0.7	0.7[c]
Applicability of k_Q to beam–chamber combination[d]	0.2	0.2

TABLE 24. ESTIMATED RELATIVE STANDARD UNCERTAINTY[a] OF $D_{w,Q}$ AT THE REFERENCE DEPTH IN WATER AND FOR AN ELECTRON BEAM, BASED ON A CHAMBER CALIBRATION IN ^{60}Co GAMMA RADIATION (cont.)

Physical quantity or procedure	Relative standard uncertainty (%)	
	Cylindrical $R_{50} \geq 3$ g/cm^2	Plane parallel $R_{50} \geq 2$ g/cm^2
Combined uncertainty of step 2	0.9	1.0
Combined standard uncertainty of $D_{w,Q}$ (steps 1 and 2)	1.1	1.2

[a] See Ref. [61] or Appendix IV for the expression of uncertainty. The estimates given in the table should be considered typical values; these may vary depending on the uncertainty quoted by standards laboratories for calibration coefficients and on the experimental uncertainty at the user institution.

[b] A user chamber calibrated directly at a PSDL will have a slightly smaller uncertainty for step 1. However, this has no significant effect on the combined uncertainty of the determination of the absorbed dose to water in the user reference beam.

[c] This increases to 0.8% for $R_{50} < 2$ g/cm^2.

[d] An extra term is added here to distinguish between the uncertainty taken purely from the k_Q calculation and the uncertainty in applying that factor to the user's beam and chamber.

Note: PSDL: primary standards dosimetry laboratory; SSDL: secondary standards dosimetry laboratory.

It is estimated that the overall uncertainty in the determination of the absorbed dose to water using a plane parallel ionization chamber cross-calibrated against a cylindrical chamber in a high energy beam approaches that given in Table 24 for a cylindrical chamber (i.e. a lower uncertainty than in a ^{60}Co calibration for the plane parallel chamber).

TABLE 25. ESTIMATED RELATIVE STANDARD UNCERTAINTY[a] OF $D_{w,Q}$ AT THE REFERENCE DEPTH IN WATER FOR AN ELECTRON BEAM, BASED ON A CHAMBER CALIBRATION IN A HIGH ENERGY ELECTRON BEAM

Physical quantity or procedure	Relative standard uncertainty (%)	
	Cylindrical $R_{50} \geq 3$ g/cm^2	Plane parallel $R_{50} \geq 2$ g/cm^2
Step 1: PSDL		
$N_{D,w}$ calibration of user dosimeter at PSDL	0.5	0.5
Combined uncertainty of step 1	0.5	0.5
Step 2: user electron beam		
Long term stability of user dosimeter	0.2	0.4
Establishment of reference conditions	0.3	0.3
Dosimeter reading M_Q relative to beam monitor	0.3	0.3
Correction for influence quantities k_i	0.3	0.3
Beam quality correction, k_{Q,Q_o} (calculated values)[b]	0.2	0.2 [c]
Applicability of k_Q to beam–chamber combination[d]	0.1	0.1
Combined uncertainty of step 2	0.6	0.7
Combined standard uncertainty of $D_{w,Q}$ (steps 1 and 2)	0.8	0.9

[a] See Ref. [61] or Appendix IV for the expression of uncertainty. The estimates given in the table should be considered typical values; these may vary depending on the uncertainty quoted by standards laboratories for calibration coefficients and on the experimental uncertainty at the user institution.

[b] The uncertainty in calculated k_{Q,Q_o} factors is reduced significantly because there is no conversion from ^{60}Co — only conversion from one electron beam to another.

[c] This increases to 0.4% for $R_{50} < 2$ g/cm^2.

[d] An extra term is added here to distinguish between the uncertainty taken purely from the k_{Q,Q_o} calculation and the uncertainty in applying that factor to the user's beam and chamber.

Note: PSDL: primary standards dosimetry laboratory.

7.11. WORKSHEET

Determination of the absorbed dose to water in an electron beam

User: _____ Date: _____

1. Radiation treatment unit and reference conditions for $D_{w,Q}$ determination

Accelerator: _____ Nominal energy: _____ MeV

Nominal dose rate: _____ MU/min Measured R_{50}: _____ g/cm^2

Reference phantom: ☐ water ☐ plastic Obtained from: ☐ ionization curves ☐ dose

Reference field size: _____ cm × cm Reference SSD: 100 cm

Beam quality, Q (R_{50} in water): _____ g/cm^2

Reference depth, $z_{ref} = 0.6R_{50} - 0.1$ = _____ g/cm^2

2. Ionization chamber and electrometer

Ionization chamber model: _____ Serial no.: _____ Type: ☐ pp ☐ cyl

Chamber wall/window Material: _____ Thickness: _____ g/cm^2

Waterproof sleeve/cover Material: _____ Thickness: _____ g/cm^2

Phantom window Material: _____ Thickness: _____ g/cm^2

Absorbed dose to water calibration coeff.[a] N_{D,w,Q_o} = _____ ☐ Gy/nC ☐ Gy/rdg

Calibration quality Q_o: ☐ ^{60}Co ☐ electron beam Calibration depth: _____ g/cm^2

If Q_o is an electron beam, R_{50} = _____ g/cm^2

Reference conditions for calibration P_o = _____ kPa T_o = _____ °C Rel. humidity: _____%

Polarizing potential V_1 = _____ V

Calibration polarity: ☐ positive ☐ negative ☐ corrected for polarity effect

User polarity: ☐ positive ☐ negative

Calibration laboratory: _____ Date: _____

Electrometer model: Serial no.: _____

Calibrated separately from chamber: ☐ yes ☐ no Range setting: _____

If yes Calibration laboratory: Date: _____

3. Phantom

Water phantom[b] Window material: _____ Thickness: _____ g/cm^2

4. Dosimeter reading[c] and correction for influence quantities

Uncorrected dosimeter reading at V_1 and user polarity: _____ ☐ nC ☐ rdg

Corresponding accelerator monitor units: _____ MU

Ratio of dosimeter reading and monitor units: M_1 = _____ ☐ nC/MU ☐ rdg/MU

(a) Pressure P = _____ kPa Temperature T = _____ °C Rel. humidity (if known): _____%

$$k_{TP} = \frac{(273.2+T)}{(273.2+T_o)}\frac{P_o}{P} = \_\_\_\_\_$$

(b) Electrometer calibration factor[d] $k_{\text{elec}} =$ _____ ☐ nC/rdg ☐ dimensionless

(c) Polarity correction[e] Reading at $+V_1$: $M_+ =$ _____ Reading at $-V_1$: $M_- =$ _____

$$k_{\text{pol}} = \frac{|M_+| + |M_-|}{2M} = \text{_____}$$

(d) Recombination correction (two voltage method)

Polarizing voltages: V_1 (normal) = _____ V V_2 (reduced) = _____ V

Readings[f] at V_1, V_2 : $M_1 =$ _____ $M_2 =$ _____

Voltage ratio $V_1/V_2 =$ _____ Ratio of readings $M_1/M_2 =$ _____

Use Table 10 for a beam of type: ☐ pulsed ☐ pulsed–scanned

$a_0 =$ _____ $a_1 =$ _____ $a_2 =$ _____ [g, h]

$$k_s = a_0 + a_1\left(\frac{M_1}{M_2}\right) + a_2\left(\frac{M_1}{M_2}\right)^2 = \text{_____}$$

Corrected dosimeter reading at the voltage V_1:

$$M_Q = M_1 h_{\text{pl}} k_{TP} k_{\text{elec}} k_{\text{pol}} k_s = \text{_____}$$ ☐ nC/MU ☐ rdg/MU

5. Absorbed dose to water at the reference depth, z_{ref}

Beam quality correction factor for user quality Q:

If Q_o is ^{60}Co, Table 20 gives: $k_{Q,Q_o} =$ _____

If Q_o is electron beam, Table 21 gives: $k_{Q,Q_{\text{int}}} =$ _____ $k_{Q_o,Q_{\text{int}}} =$ _____

$$k_{Q,Q_o} = \frac{k_{Q,Q_{\text{int}}}}{k_{Q_o,Q_{\text{int}}}} = \text{_____}$$

If k_{Q,Q_o} is derived from series of electron beam calibrations: $k_{Q,Q_o} =$ _____

Calibration laboratory: _____ Date: _____

$$D_{w,Q}(z_{\text{ref}}) = M_Q N_{D,w,Q_o} k_{Q,Q_o} = \text{_____ Gy/MU}$$

6. Absorbed dose to water at the depth of dose maximum, $z_{\max}$

Depth of dose maximum: $z_{\max} =$ _____ g/cm^2

PDD at z_{ref} for a field size of ____ cm × ____ cm: PDD(z_{ref} = ____ g/cm^2) = _____ %

Absorbed dose calibration of monitor at $z_{\max}$:

$$D_{w,Q}(z_{\max}) = 100\, D_{w,Q}(z_{\text{ref}})/\text{PDD}(z_{\text{ref}}) = \text{_____ Gy/MU}$$

---

[a] Note that if Q_o is ^{60}Co, N_{D,w,Q_o} is denoted by $N_{D,w}$.

[b] If a water phantom is used, the fluence scaling factor is set to $h_{\text{pl}} = 1$.

[c] All readings should be checked for leakage and corrected if necessary.

[d] If the electrometer is not calibrated separately, then $k_{\text{elec}} = 1$.

[e] M in the denominator of k_{pol} denotes reading at the user polarity. Preferably, each reading in the equation should be the average of the ratios of M (or M_+ or M_-) to the reading of an external monitor, M_{em}. It is assumed that the calibration laboratory has performed a polarity correction. Otherwise k_{pol} is determined according to the following procedure:

Reading at $+V_1$ for quality Q_o: $M_+ =$ _____ Reading at $-V_1$ for quality Q_o: $M_- =$ _____

$$k_{\text{pol}} = \left[\left(|M_+| + |M_-|\right)/|M|\right]_Q \Big/ \left[\left(|M_+| + |M_-|\right)/|M|\right]_{Q_o} = \text{_____}$$

[f] Strictly, readings should be corrected for the polarity effect (average from both polarities). Preferably, each reading in the equation should be the average of the ratios of M_1 or M_2 to the reading of an external monitor, M_{em}.

[g] Check that $k_s - 1 \approx (M_1/M_2 - 1)/(V_1/V_2 - 1)$.

[h] It is assumed that the calibration laboratory has performed a recombination correction. Otherwise the factor $k_s' = k_s/k_{s,Q_o}$ should be used instead of k_s. When Q_o is ^{60}Co, k_{s,Q_o} (at the calibration laboratory) will normally be close to unity and the effect of not using this equation will be negligible in most cases.

Note: cyl: cylindrical; pp: plane parallel; MU: monitor unit; PDD: percentage depth dose.

8. CODE OF PRACTICE FOR LOW ENERGY KILOVOLTAGE X RAY BEAMS

8.1. GENERAL

This section provides a code of practice for reference dosimetry (beam calibration) and recommendations for relative dosimetry in X ray beams with generating potentials between 10 kV and 100 kV (HVL: 0.03–5 mm Al). It is based on a calibration coefficient in terms of absorbed dose to water or air kerma obtained from a standards laboratory.

This range of beam qualities is referred to here as the low energy X ray range. The division into low and medium energy ranges (the latter presented in Section 9) is intended to reflect the two distinct types of radiotherapy for which kilovoltage X rays are used: 'superficial' and 'orthovoltage'. The boundary between the two ranges defined in this section and the next is not strict and the two ranges overlap between 80 kV and 100 kV. In the overlap region, the methods described in the two sections are equally satisfactory, and whichever is more suited to the clinical application should be used.

There is no direct primary standard of absorbed dose to water at the surface of a water phantom, as needed in the low energy X ray range. For this reason, the standard dosimetry is generally based on measurements of air kerma free in air, from which the absorbed dose to water is obtained by multiplication with factors that convert the air kerma free in air into the absorbed dose at the surface of a water phantom (see Appendix I).

This international code of practice provides two different methods to measure the absorbed dose in the user's beam. The in-air method (see Section 8.4.1) is based on a chamber calibrated in terms of air kerma free in air. The in-phantom method (see Section 8.4.2) is based on a plane parallel chamber mounted on the surface of a PMMA phantom calibrated in terms of absorbed dose to water at reference conditions.

The use of both air kerma and absorbed dose to water chamber calibrations for low energy kilovoltage X rays requires different types of beam quality factor, defined and denoted according to the chamber calibration modality. The air kerma beam quality factor is defined as the ratio of the calibration coefficients in terms of air kerma free in air (FIA) at qualities Q and Q_o, as follows:

$$k_{Q,Q_o}^{\mathrm{FIA}} = \frac{N_{K,\mathrm{air},Q}^{\mathrm{FIA}}}{N_{K,\mathrm{air},Q_o}^{\mathrm{FIA}}} \tag{48}$$

The absorbed dose to water beam quality factor is defined as the ratio of the calibration coefficients in terms of absorbed dose to water determined by calculation or measurement at the surface of a PMMA phantom at qualities Q and Q_o, as follows:

$$k_{Q,Q_o}^{\text{PMMA}} = \frac{N_{D,w,Q}^{\text{PMMA}}}{N_{D,w,Q_o}^{\text{PMMA}}} \tag{49}$$

8.2. DOSIMETRY EQUIPMENT

8.2.1. Ionization chambers

The recommendations regarding ionization chambers given in Section 4.2.1 should be followed. The chamber should be of a type designed for use with low energy X rays, as given in Table 7. These plane parallel chamber types can be used for both the in-phantom and in-air methods. The area density of the entrance windows of the plane parallel chambers listed in Table 7 provide full buildup of the secondary electron spectrum for beam qualities generated with tube voltages up to 40 kV. To ensure full buildup for qualities generated with tube voltages above 40 kV, it is necessary to add additional buildup material to the entrance window. It is recommended to use 0.2 mm thick PMMA, polyethylene or mylar foils (whatever is available) for this purpose. This causes an additional attenuation of these beams of <2%, whereby the photon fluence spectrum remains almost unchanged.

The reference point of the plane parallel chambers is taken to be on the outer surface of the chamber window at the window centre (or on the outer surface of the buildup foil, if one is used). The chamber, phantom and any buildup foils should be calibrated at the standards laboratory at the same SSD and field size used for reference dosimetry in the clinic. If the in-phantom method is adopted, the reference point is positioned so that it is flush with the front surface of the phantom. As there is a large chamber to chamber variation in energy response, it is not recommended to use a generic set of k_{Q,Q_o} values for this particular type of chamber.

Alternatively, if the in-air method is adopted at 70 kV and above, a cylindrical chamber type, as given in Table 4, can be used that has either a carbon wall and an aluminium central electrode or both electrodes made of conducting plastic that is approximately air equivalent. Chambers with graphite coated nylon or PMMA walls may be vulnerable to sudden changes of response at low energies [181] and should be used only with appropriate precautions. The

long axis of the chamber should be either parallel to or at a right angle to the anode–cathode axis of the X ray tube, depending on which of these orientations leads to the smallest dose gradient along the length of the chamber. The reference point of the cylindrical chamber is taken to be on the chamber axis at the centre of the cavity volume.

8.2.2. Phantoms

The recommendations regarding phantoms given in Section 4.2.3 should be followed. The phantom has to permit the plane parallel chamber to be mounted with the outside face of the chamber window flush with the phantom surface. This is normally not possible using a water phantom and therefore plastic phantoms are used instead. Note that when they are employed in this way, the plane parallel chamber types listed in Table 7 are intended to be used in a specially designed PMMA phantom that is supplied optionally together with the chamber. The use of a water equivalent material designed for use in kilovoltage X rays is ideal but PMMA (e.g. Perspex, Lucite) is acceptable.[55] Because the phantom–chamber unit is calibrated in terms of absorbed dose to water at the surface, no dose or depth conversions are needed, irrespective of the type of plastic used. However, corrections are necessary if the SSDs and field sizes in the clinical beam differ significantly from those used for the calibration at the standards laboratory (see Section 8.4.2). The phantom has to extend in the beam direction by at least 5 g/cm^2 and in the lateral direction far enough beyond the reference field size to ensure that the entire primary beam exits through the rear face of the phantom.

[55] PMMA is acceptable for a phantom that is used only for measurements at the surface. This is because the phantom needs to reproduce only the backscatter, and not the attenuation or scatter at depth. The chamber is calibrated in the phantom under the reference conditions of field size and SSD, so as long as these are similar to the reference conditions in the clinic, any difference between PMMA and water will be very small. For the measurement of field output factors at other field sizes and SSDs, only the ratio of the backscatter at the different geometries has to be similar to that of water. Even though PMMA is not water equivalent, the backscatter is typically an order of magnitude less than the absorbed dose at the surface, and the difference in backscatter between water and PMMA is another order of magnitude smaller. Hence the overall disagreement is typically no more than 1%.

8.3. BEAM QUALITY SPECIFICATION

8.3.1. Choice of beam quality index

It has long been known that it is desirable to use more than one beam quality parameter to characterize a kilovoltage X ray spectrum for dosimetry [182–184]. The usual quantities used are the kilovoltage generating potential and the HVL. Where possible, it is preferable to have the dosimeter calibrated at the same combinations of kilovoltage potential and HVL as those of the user's clinical beams.

8.3.2. Measurement of beam quality

The conventional material used for the determination of the HVL in low energy X ray beams is aluminium. The HVL is defined as the thickness of an absorber (usually copper or aluminium) required to attenuate a narrow X ray beam at a reference point distant from the absorbing layer to half of the air kerma rate of the incident radiation.

Because of the absorption of low energy X rays in air, and the consequent beam hardening through air, the HVL increases with the distance from the X ray target. Therefore, the HVL for low energy X ray beams should, as far as possible, be measured with the chamber at the same SCD as that used for the HVL measurement at the standards dosimetry laboratory. The ideal experimental arrangement is to place at approximately half the distance between the X ray target and the chamber a collimating aperture that reduces the field size to just enough to cover the ionization chamber, with a small margin of typically 5–10 mm around the chamber. The total beam size defined by the lead diaphragm should not exceed 4 cm [185–187]. Strictly, the HVL corresponds to narrow beam geometry, and Refs [11, 182] describe the method to derive the zero field area by measuring the HVL at two or three diaphragm sizes and extrapolating the HVL–diaphragm size plot to the zero area value (see also Ref. [108]). The typical distance from the X ray focal spot to the ionization chamber is 100 cm. The collimating aperture should be placed immediately after the foils used in the measurement [185]. The measurement of HVL requires scatter free conditions and therefore positioning the ionization chamber <1 m from any walls, floors and ceilings needs to be avoided. It is good practice to expose a piece of radiochromic film behind the detector to ensure that the ionization chamber is correctly centred in the radiation field. It is also vital to ensure that the chamber axis is perpendicular to both the filament–target direction of the X ray tube and the beam central axis to minimize the influence of the heel effect on the readings of the ionization chamber.

The filters added for the HVL measurement are placed in combinations of thickness that span the thickness range in which the HVL is expected to be.

The thickness of the filters that reduces the air kerma rate to one half is then obtained by interpolation, preferably using an exponential, or using a straight line if the added thicknesses are close to the HVL value. The purity of aluminium or copper should be at least 99.9%. For further guidance on HVL determination, see Refs [185, 187–189].

A suitable ionization chamber has to be used. In particular, the energy dependence of the air kerma response should be known for the application range of radiation qualities needed for the HVL measurements. Note that it may be necessary to correct for the energy dependence when the chamber is used in the X ray beam with and without the additional aluminium filters used for the HVL measurements.

A monitor chamber should be used to prevent incorrect results due to variations in the X ray output. Care has to be taken to avoid the response of the monitor chamber being affected by increasing scatter as more filters are placed in the beam. If a monitor chamber is not available, the effects of output variation can be minimized by randomizing the measurement sequence and measuring the air kerma rate without additional filters at both the beginning and the end of the measurements.

8.4. DETERMINATION OF ABSORBED DOSE TO WATER

8.4.1. In-air method

The absorbed dose to water at the surface of a water phantom for a radiation quality Q, $D_{w,Q}^{surface}$, is obtained from an air kerma measurement free in air, $K_{air,Q}^{FIA}$, using the following equation:

$$D_{w,Q}^{surface}(f,\mathrm{SSD})_{clin} = K_{air,Q}^{FIA}\left[\mu_{en}(Q)/\rho\right]_{w,air}^{FIA} B_{w,Q}(f,\mathrm{SSD})_{clin} \quad (50)$$

where $\left[\mu_{en}(Q)/\rho\right]_{w,air}^{FIA}$ is the water to air ratio of mass energy absorption coefficients averaged over the photon spectrum free in air and B_w is the backscatter factor, defined as the ratio of the water collision kerma at a point on the beam axis at the surface of a full scatter water phantom to the water collision kerma at the same point in the primary (incident) beam with no phantom present. It is dependent on the beam quality Q, the field size f and the SSD. Values of $\left[\mu_{en}(Q)/\rho\right]_{w,air}^{FIA}$ and $B_{w,Q}(f, \mathrm{SSD})_{clin}$ are obtained from the data provided in Ref. [54]; it is recommended to use the GUI web application[56]. Note that for this purpose Q has to be specified by the beam kilovoltage and HVL, which therefore

[56] See footnote 18 on p. 51.

have to be known or measured by the user. The air kerma free in air, $K_{\mathrm{air},Q}^{\mathrm{FIA}}$, in the clinical beam is obtained as follows:

$$K_{\mathrm{air},Q}^{\mathrm{FIA}} = M_{Q}^{\mathrm{FIA}}\, N_{K,\mathrm{air},Q_{\mathrm{o}}}^{\mathrm{FIA}} k_{Q,Q_{\mathrm{o}}}^{\mathrm{FIA}} \tag{51}$$

where M_{Q}^{FIA} is the reading of the chamber free in air corrected for temperature, pressure, electrometer calibration, polarity effect and ion recombination, as described in Section 4.4.3; $N_{K,\mathrm{air},Q_{\mathrm{o}}}^{\mathrm{FIA}}$ is the air kerma calibration coefficient for the reference beam quality; and $k_{Q,Q_{\mathrm{o}}}^{\mathrm{FIA}}$ is the air kerma beam quality factor. The chamber should be positioned in accordance with the reference conditions given in Table 26. The effective point of measurement is assumed to coincide with the reference point of the chamber.

The calibration certificate of the reference chamber needs to contain the air kerma calibration coefficient $N_{K,\mathrm{air},Q_{\mathrm{o}}}^{\mathrm{FIA}}$ measured at a suitable reference radiation quality Q_{o} and values for $k_{Q,Q_{\mathrm{o}}}^{\mathrm{FIA}}$ as a function of HVL obtained from

TABLE 26. REFERENCE CONDITIONS FOR THE DETERMINATION OF ABSORBED DOSE IN LOW ENERGY X RAY BEAMS USING THE IN-AIR METHOD

Influence quantity	Reference value or reference characteristic
Chamber type	Plane parallel for low energy X rays (up to 100 kV) Cylindrical chamber for X ray energies above 70 kV
Measurement point	Free in air at the end of the applicator
Reference point of the chamber	Plane parallel chamber: at the centre of the outside surface of the chamber window (or foil, if used) Cylindrical chamber: the reference point of the cylindrical chamber is taken to be on the chamber axis at the centre of the cavity volume
Source–surface distance	Defined by the end of the reference applicator
Field size, f	Parallel plate chamber: 10 cm diameter (or 10 cm × 10 cm)[a] Cylindrical chamber: 5 cm diameter (or 5 cm × 5 cm)

[a] If this field size is not available in the clinical beam, the air kerma calibration coefficients can be corrected for other field sizes using the data shown in Fig. 11.

a set of selected standard radiation qualities characterized by their generating tube voltages U (in kilovolts) and HVL (in millimetres of aluminium). The latter values should span the entire HVL range of the clinical beams of interest. Thus, the clinical beam air kerma quality factor, k_{Q,Q_o}^{FIA}, can be obtained by interpolation with respect to the HVL values.

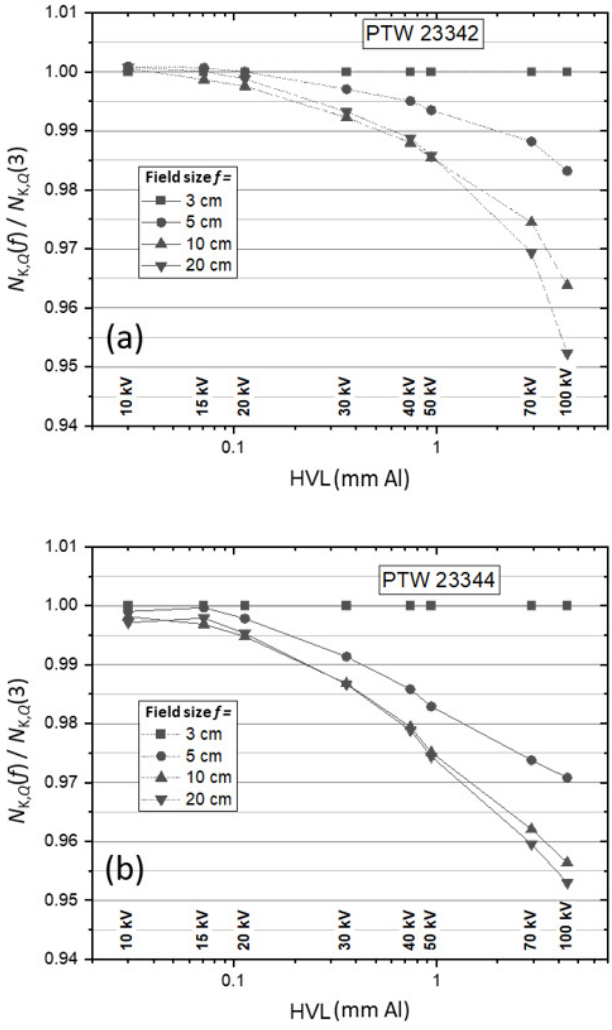

FIG. 11. Air kerma calibration coefficients measured free in air at Physikalisch-Technische Bundesanstalt at a source–surface distance of 30 cm and field sizes f = *3, 5, 10 and 20 cm (diameter of the circular beam), normalized to* f = *3 cm, for ionization chambers of the PTB TW series [190]: (a) PTW 23342 and (b) PTW 23344.*

When the plane parallel chamber types PTW 23342 and PTW 23344 listed in Table 7 are used for free in air measurements of the air kerma, they demonstrate a significant dependence of the calibration coefficients on field size at radiation qualities generated with tube voltages of ≥30 kV. This is shown in Fig. 11, which shows air kerma calibration coefficients measured free in air at different field sizes normalized to a field size of 3 cm plotted against the HVL values for a set of standard beam qualities Q. This behaviour is caused by the large PMMA housing of these chamber types surrounding a small sensitive volume. Photons scattered from the housing into the sensitive volume contribute to the chamber reading. Therefore, the reading increases if the field size is increased. If the field size is ≥10 cm in diameter, almost the entire housing is covered by the cross-section of the beam and the reading changes only moderately if the field size is increased further (see Fig. 11). Therefore, it is recommended to use a reference field of 10 cm diameter (or of an area of 10 cm × 10 cm) when these chambers are calibrated and used for air kerma measurements in the clinical beam. If this field size is not available in the clinical beam, the air kerma calibration coefficients can be corrected for other field sizes using the data shown in Fig. 11.

At ≥70 kV, the cylindrical chamber types given in Table 4 can be used for the in-air method. The minimum field size used for these chamber types is be 5 cm diameter (or 5 cm × 5 cm). The dependence of the calibration coefficients on larger field sizes is small and can usually be neglected.

8.4.2. In-phantom method

The absorbed dose to water at the surface of a water phantom, $D_{w,Q}^{surface}(f,SSD)_{clin}$, for a clinical radiation quality Q at clinical beam conditions $(f, SSD)_{clin}$ is obtained from the following equation:

$$D_{w,Q}^{surface}(f,SSD)_{clin} = M_Q^{PMMA}(f,SSD)_{clin}\, N_{D,w,Q_o}^{PMMA}(f,SSD)_{lab} \times k_{Q,Q_o}^{PMMA}(f,SSD)_{lab}\, k_{g,Q}^{PMMA}(f,SSD)_{clin} \quad (52)$$

where:

$M_Q^{PMMA}(f,SSD)_{clin}$ is the reading of a plane parallel chamber mounted on the surface of a PMMA phantom at the clinical beam quality Q under clinical beam conditions $(f, SSD)_{clin}$, corrected for temperature, pressure, electrometer calibration, polarity effect and ion recombination, as described in Section 4.4.3;

$N_{D,w,Q_o}^{PMMA}(f,SSD)_{lab}$ is the calibration coefficient in terms of absorbed dose to water for the reference quality Q_o at the standards

laboratory under reference beam conditions $(f, \mathrm{SSD})_{\mathrm{lab}}$ (see Table 27);

$k_{Q,Q_o}^{\mathrm{PMMA}}(f,\mathrm{SSD})_{\mathrm{lab}}$ is the absorbed dose to water beam quality factor at the standards laboratory under reference beam conditions $(f, \mathrm{SSD})_{\mathrm{lab}}$;

$k_{g,Q}^{\mathrm{PMMA}}(f,\mathrm{SSD})_{\mathrm{clin}}$ is the geometry correction factor, which corrects for effects due to differences between the clinical and standards laboratory beam conditions.

The calibration coefficient $N_{D,w,Q_o}^{\mathrm{PMMA}}(f,\mathrm{SSD})_{\mathrm{lab}}$ is obtained from the calibration certificate of the standards laboratory. The absorbed dose to water beam quality factor $k_{Q,Q_o}^{\mathrm{PMMA}}(f,\mathrm{SSD})_{\mathrm{lab}}$ for the clinical beam quality is obtained (usually by interpolation) from those provided by the standards laboratory as a function of the HVL for a set of reference beam qualities Q measured at the standards laboratory beam conditions (examples for several PTW 23342 chambers are given in Fig. 12).

The geometry correction factors can be provided by the standards laboratory. Examples of values used at PTB for the two most frequently used chamber types (PTW 23342 and PTW 23344) are given in Tables 28 and 29. Note that these corrections were determined for SSD = 30 cm. The geometry correction factor depends mainly on the field size f and only moderately on the SSD. Therefore, the values given in the tables can reasonably be used for the range of SSDs typically used in clinical applications. Note that the values given in the tables are normalized to the reference quality Q_o = 30 kV, a first HVL of 0.36 mm Al and a field size of 3 cm (diameter). If other reference conditions or reference qualities are chosen, the corresponding values need to be calculated accordingly.

TABLE 27. REFERENCE CONDITIONS FOR THE DETERMINATION OF ABSORBED DOSE IN LOW ENERGY X RAY BEAMS USING THE IN-PHANTOM METHOD

Influence quantity	Reference value or reference characteristic
Phantom material	Water equivalent plastic or PMMA
Chamber type	Plane parallel for low energy X rays (up to 100 kV)
Measurement depth	Phantom surface
Reference point of the chamber	At the centre of the outside surface of the chamber window (or foil, if used)
Source–surface distance	Defined by the end of the reference applicator
Field size	Same field size as that used for the calibration at the standards laboratory

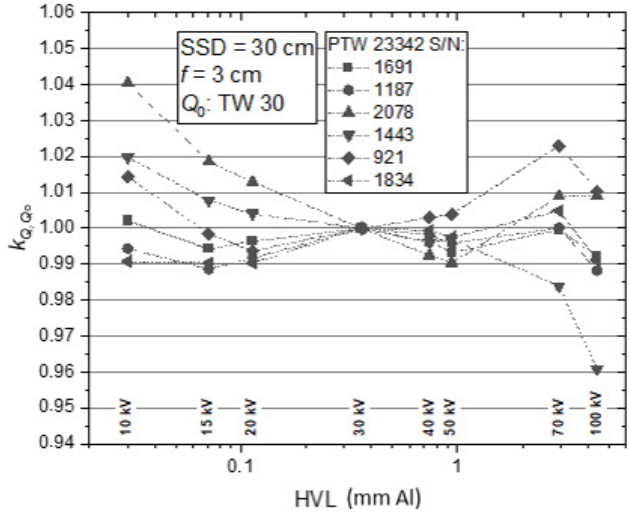

FIG. 12. Beam quality factors k_{Q,Q_o}^{PMMA} *(Q_o = 30 kV, 0.36 mm Al) in terms of absorbed dose to water at the surface of a water phantom measured at Physikalisch-Technische Bundesanstalt for several chambers of type PTW 23342 (the serial numbers (S/N) are shown in the key). The chambers were calibrated at the surface of a PMMA phantom under reference conditions, as shown in Table 27. SSD: source–surface distance.*

TABLE 28. GEOMETRY CORRECTION FACTORS FOR THE CHAMBER TYPE PTW 23342 AT DIFFERENT FIELD SIZES FOR THE PTB TW SERIES [190], NORMALIZED TO THE REFERENCE CONDITIONS Q_o = 30 kV, 0.36 mm Al AND f = 3 cm

f (cm)	Geometry correction factor						
	10 kV	20 kV	30 kV	40 kV	50 kV	70 kV	100 kV
2	1.00	1.00	1.01	1.01	1.01	1.02	1.02
3	1.00	1.00	1.00	1.00	1.00	1.00	1.00
5	1.00	1.00	1.00	0.98	0.98	0.97	0.98
6	1.00	1.00	1.00	0.99	0.99	0.97	0.96
8	1.00	1.00	1.00	0.98	0.98	0.95	0.94
10	1.00	1.00	1.00	0.97	0.97	0.93	0.93

TABLE 28. GEOMETRY CORRECTION FACTORS FOR THE CHAMBER TYPE PTW 23342 AT DIFFERENT FIELD SIZES FOR THE PTB TW SERIES [190], NORMALIZED TO THE REFERENCE CONDITIONS Q_o = 30 kV, 0.36 mm Al AND f = 3 cm (cont.)

f (cm)	Geometry correction factor						
	10 kV	20 kV	30 kV	40 kV	50 kV	70 kV	100 kV
15	1.00	1.00	1.00	0.98	0.95	0.93	0.92
20	1.00	1.00	1.00	0.98	0.96	0.92	0.91

TABLE 29. GEOMETRY CORRECTION FACTORS FOR THE CHAMBER TYPE PTW 23344 AT DIFFERENT FIELD SIZES FOR THE PTB TW SERIES [190], NORMALIZED TO THE REFERENCE CONDITIONS Q_o = 30 kV, 0.36 mm Al AND f = 3 cm

f (cm)	Geometry correction factor						
	10 kV	20 kV	30 kV	40 kV	50 kV	70 kV	100 kV
2	1.00	1.00	1.01	1.02	1.02	1.03	1.04
3	1.00	1.00	1.00	1.00	1.00	1.00	1.00
5	1.00	1.00	0.99	0.98	0.98	0.96	0.96
6	1.00	1.00	0.99	0.98	0.97	0.95	0.95
8	1.00	1.00	0.99	0.98	0.96	0.94	0.93
10	1.00	1.00	0.99	0.97	0.95	0.93	0.92
15	1.00	1.00	0.99	0.97	0.95	0.92	0.90
20	1.00	1.00	0.99	0.96	0.95	0.90	0.90

8.5. MEASUREMENTS UNDER NON-REFERENCE CONDITIONS

8.5.1. Central axis depth dose distributions

A nominal depth dose distribution for the beam quality of interest may be obtained from the literature [146]. However, if desired, the depth dose distribution can be measured using the same chamber as that used for the in-phantom reference dosimetry method and a water equivalent phantom [191].

Thin sheets of water equivalent phantom material designed for use with kilovoltage X rays are placed over the chamber and in the phantom, and the phantom is moved back by the same distance as the thickness of the sheets added to maintain a constant SSD. The manufacturer's specifications for the material should state that it is equivalent to water within a few per cent in the energy range of interest. This should be verified by comparison with published data. PMMA is not suitable for measurement of depth dose distributions, although it is used as a phantom material for reference dosimetry. Strictly, this procedure provides a depth ionization distribution rather than a depth dose distribution. However, if the percentage variation of the response of the chamber is constant with beam quality at the 5% level, the error introduced by assuming that a depth dose distribution is the same as the depth ionization distribution is not likely to be more than a few

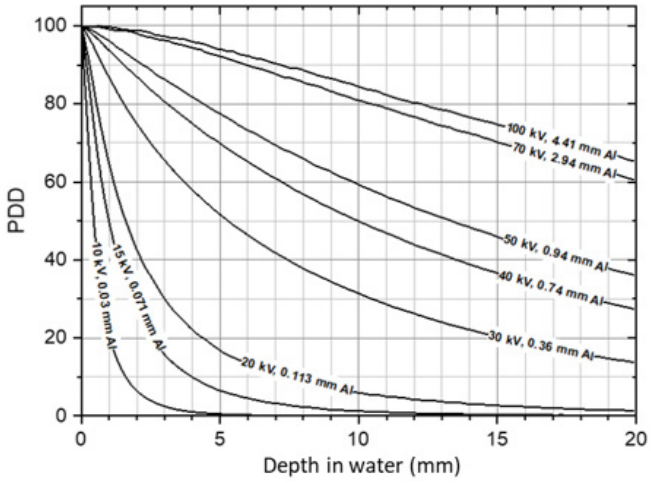

FIG. 13. Percentage depth dose (PDD) in water calculated for the PTB TW series for SSD = 30 cm and f *= 3 cm using the DOSRZnrc/EGSnrc code.*

per cent at any clinically relevant depth. Examples of relative depth dose profiles in water for a set of standard beam qualities Q are given in Fig. 13[57].

8.5.2. Field output factors

For clinical applications, the field output factors Ω are required for all combinations of SSD and field size used for radiotherapy treatment. For low energy X rays, Ω is the ratio of the absorbed dose at the surface of a water phantom for each combination of field size and SSD used in clinical conditions, $D_{w,Q}(f,\mathrm{SSD})_{clin}$, to that under reference conditions, $D_{w,Q}(f,\mathrm{SSD})_{ref}$. It can be estimated from Eq. (50) as follows:

$$\Omega = \frac{D_{w,Q}(f,\mathrm{SSD})_{clin}}{D_{w,Q}(f,\mathrm{SSD})_{ref}} \approx \frac{K^{FIA}_{air,Q}(f,\mathrm{SSD})_{clin}\, B_{w,Q}(f,\mathrm{SSD})_{clin}}{K^{FIA}_{air,Q}(f,\mathrm{SSD})_{ref}\, B_{w,Q}(f,\mathrm{SSD})_{ref}} \tag{53}$$

The air kerma free in air at clinical and reference conditions is determined according to Eq. (51). The corresponding backscatter factors are determined using the data given in Ref. [54]. It is recommended to use the GUI web application (see footnote 18 on p. 51) to calculate dosimetric quantities. Alternatively, Ω can be determined by in-phantom measurements at clinical and reference conditions according to Eq. (53).

8.6. ESTIMATED UNCERTAINTY IN THE DETERMINATION OF ABSORBED DOSE TO WATER UNDER REFERENCE CONDITIONS

It is the responsibility of users to establish an uncertainty budget for their determination of absorbed dose to water. Examples of relative uncertainties for the determination of the absorbed dose to water at the surface of a water phantom in the user beam, estimated according to the in-air method (see Section 8.4.1) and the in-phantom method (see Section 8.4.2), are presented in Table 30. These estimates may vary depending on the uncertainty quoted by the calibration laboratory, the care and experience of the user performing the measurement, and the quality and condition of the measurement equipment (e.g. regular recalibration of all measurement devices, quality management system to ensure proper functioning).

The relative uncertainty of the air kerma calibration coefficient of a secondary standard at the PSDL is taken to be 0.5%. Calibration of the user dosimeter at the SSDL adds another 0.5%, which results in a combined

[57] For the DOSRZnrc/EGSnrc code, see https://doi.org/10.4224/40001303

uncertainty of 0.7% for the calibration of the user chamber. In the user beam, the calibration coefficient has to be interpolated, which is assumed to introduce an uncertainty of 0.5%. Using the data and methods in Ref. [54], the uncertainties of the calculation of the water to air ratio of the mean mass energy absorption coefficient and of the backscatter factor are estimated to be 0.5% and 1%, respectively. These uncertainties also depend on the uncertainties in the beam specifications (kilovoltage, HVL) and irradiation conditions (SSD, *f*) of the user.

The relative uncertainty of the absorbed dose to water calibration coefficient of a plane parallel chamber mounted in an PMMA phantom is estimated to be 1.4% (as determined at PTB) at the PSDL and 1.5% at the SSDL. The uncertainty of the interpolation of the calibration coefficient to the user beam quality is estimated to be 0.5%. The relative uncertainty of the geometry correction factor is estimated to be 1%.

The stability of a good dosimeter over a series of readings is typically better than 0.1%, but the temperature of the chamber may be uncertain to at least ±1°C because of heating from the X ray tube. The X ray output from some machines depends on the line voltage, tube temperature and operator control of the tube current and voltage. This variation is minimized when the exposures are controlled by a monitor chamber, but this is rarely the case for dedicated low energy X ray machines, where the variation in output over a series of identical exposure times may be as much as 5%. This uncertainty should be estimated separately by the user from the standard deviation of a set of at least five exposures of typical treatment length. It is not included in this analysis.

Because the SSD is often very short on a low energy X ray machine, there may be difficulty in achieving a positioning reproducibility that results in an uncertainty better than 1% in the determination of absorbed dose to water, so this uncertainty is assigned to the establishment of reference conditions.

TABLE 30. ESTIMATED RELATIVE STANDARD UNCERTAINTY[a] OF $D_{w,Q}$ AT THE REFERENCE DEPTH IN WATER FOR A LOW ENERGY X RAY BEAM

Physical quantity or procedure	Relative standard uncertainty (%)	
	$N_{D,w}$ based	N_K based
Step 1: standards laboratory	SSDL	SSDL
Calibration of secondary standard (N_D or N_K) at PSDL	1.4	0.5

TABLE 30. ESTIMATED RELATIVE STANDARD UNCERTAINTY[a] OF $D_{w,Q}$ AT THE REFERENCE DEPTH IN WATER FOR A LOW ENERGY X RAY BEAM (cont.)

Physical quantity or procedure	Relative standard uncertainty (%)	
	$N_{D,w}$ based	N_K based
Long term stability of secondary standard	0.1	0.1
Calibration of the user dosimeter at the standards laboratory	0.5	0.5
Combined uncertainty in step 1	1.5	0.7
Step 2: user X ray beam		
Interpolation of the calibration coefficient to the user beam	0.5	0.5
Ratio of the mean mass energy absorption coefficient water to air		0.5
Backscatter factor		1.0
Geometry correction factor	1.0	
Long term stability of the user dosimeter	0.3	0.3
Dosimeter reading M_Q relative to timer or beam monitor	0.1	0.1
Establishment of reference conditions[b]	1.0	1.0
Correction for influence quantities k_i	0.8	0.8
Combined uncertainty in step 2	1.7	1.8
Combined standard uncertainty of $D_{w,Q}$ (steps 1 and 2)	2.3 (2.2)[c]	1.9 (1.9)[c]

[a] See Ref. [61] or Appendix IV for the expression of uncertainty. The estimates given in the table should be considered typical values; these may vary depending on the uncertainty quoted by standards laboratories for calibration coefficients and on the experimental uncertainty at the user institution.

[b] Uncertainties due to difficulties in achieving a good positioning reproducibility at short distances from the source and those caused by the possible difference between the reference point and effective point of measurement of the chamber.

[c] Combined standard uncertainty when the user dosimeter is calibrated directly at the PSDL.

8.7. WORKSHEET

Determination of the absorbed dose to water in a low energy X ray beam

User: _____ Date: _____

1. Radiation treatment unit and reference conditions for $D_{w,Q}$ determination

X ray machine: _____ Nominal tube potential: _____ kV

Nominal tube current: _____ mA Beam quality, Q(HVL) = _____ mm Al

Reference phantom: _____ Reference depth: phantom surface

Added foil material: _____ Thickness: _____ mm

Reference field size f: _____ cm × cm Reference SSD: _____ cm

2. Ionization chamber and electrometer

Ionization chamber model: _____ Serial no.:_____

Chamber wall material: _____ Thickness:_____ g/cm^2

Air kerma calibration coefficient $N_{K,\mathrm{air},Q_o}^{\mathrm{FIA}}$ = _____ □ Gy/nC □ Gy/rdg

Absorbed dose calibration coefficient $N_{D,\mathrm{w},Q_o}^{\mathrm{PMMA}}(f,\mathrm{SSD})_{\mathrm{lab}}$ = _____ □ Gy/nC □ Gy/rdg

Reference beam quality, Q_o(HVL) = _____ mm Al

Reference conditions for calibration P_o = _____ kPa T_o = _____ °C Rel. humidity: _____%

Polarizing potential V = _____ V

Calibration polarity: □ positive □ negative □ corrected for polarity effect

User polarity: □ positive □ negative

Calibration laboratory: _____ Date: _____

Electrometer model: Serial no.: _____

Calibrated separately from chamber: □ yes □ no Range setting: _____

If yes Calibration laboratory: Date: _____

3. Dosimeter reading[a] and correction for influence quantities

Uncorrected dosimeter reading at V and user polarity: _____ □ nC □ rdg

Corresponding time: _____ min

Ratio of dosimeter reading and time[b]: M = _____ □ nC/min □ rdg/min

(a) Pressure P = _____ kPa Temperature T = _____ °C Rel. humidity (if known): _____%

$$k_{TP} = \frac{(273.2+T)}{(273.2+T_o)}\frac{P_o}{P} = \_\_\_\_\_$$

(b) Electrometer calibration coefficient[c]: k_{elec} = _____ □ nC/rdg □ dimensionless

Corrected dosimeter reading at the voltage V:

$M_Q = Mk_{TP}k_{\mathrm{elec}}$= _____ □ nC/min □ rdg/min

4. Absorbed dose rate to water at the phantom surface

Beam quality correction factor for user quality Q (free in air): k_{Q,Q_o}^{FIA} = _____

(in phantom): $k_{Q,Q_o}^{\mathrm{PMMA}}(f,\mathrm{SSD})_{\mathrm{lab}}$ = _____

at Q_o(HVL) = _____ mm Al

Calibration laboratory: _____ Date: _____

Or beam quality correction factor interpolated:

$\left(k_{Q,Q_o}\right)_1$ = _____ at HVL_1 = _____ mm Al Date: _____

$\left(k_{Q,Q_o}\right)_2$ = _____ at HVL_2 = _____ mm Al Date: _____

$$k_{Q,Q_o} = \left(k_{Q,Q_o}\right)_1 + \left[\left(k_{Q,Q_o}\right)_2 - \left(k_{Q,Q_o}\right)_1\right]\left[\frac{\ln(\mathrm{HVL}) - \ln(\mathrm{HVL}_1)}{\ln(\mathrm{HVL}_2) - \ln(\mathrm{HVL}_1)}\right] = \_\_\_\_\_$$

Absorbed dose rate calibration at the phantom surface:

$\left[\mu_{\mathrm{en}}(Q)/\rho\right]_{\mathrm{w,air}}^{\mathrm{FIA}}$ = _____ $B_{\mathrm{w},Q}(f, \mathrm{SSD})$ = _____

$k_{\mathrm{g},Q}^{\mathrm{PMMA}}(f,\mathrm{SSD})_{\mathrm{clin}}$ = _____

In-air method (Section 8.4.1):

$$D_{\mathrm{w},Q}^{\mathrm{surface}}(f,\mathrm{SSD})_{\mathrm{clin}} =$$

$$M_Q^{\mathrm{FIA}}\, N_{\mathrm{K,air},Q_o}^{\mathrm{FIA}}\, k_{Q,Q_o}^{\mathrm{FIA}} \left[\mu_{\mathrm{en}}(Q)/\rho\right]_{\mathrm{w,air}}^{\mathrm{FIA}} B_{\mathrm{w},Q}(f,\mathrm{SSD})_{\mathrm{clin}} = \_\_\_\_\_ \text{ Gy/min}$$

In-phantom method (Section 8.4.2):

$$D_{\mathrm{w},Q}^{\mathrm{surface}}(f,\mathrm{SSD})_{\mathrm{clin}} =$$

$$M_Q^{\mathrm{PMMA}}(f,\mathrm{SSD})_{\mathrm{clin}}\, N_{\mathrm{D,w},Q_o}^{\mathrm{PMMA}}(f,\mathrm{SSD})_{\mathrm{lab}}\, k_{Q,Q_o}^{\mathrm{PMMA}}(f,\mathrm{SSD})_{\mathrm{lab}}\, k_{\mathrm{g},Q}^{\mathrm{PMMA}}(f,\mathrm{SSD})_{\mathrm{clin}} = \_\_\_\_\_ \text{ Gy/min}$$

---

[a] All readings should be checked for leakage and corrected if necessary.

[b] The timer error should be taken into account. The correction at voltage V can be determined according to the following:

M_A is the integrated reading in a time t_A M_A = _____ t_A = _____ min

M_B is the integrated reading in n short exposures of time t_B/n each ($2 \le n \le 5$) M_B = _____ t_B = _____ min n = ___

Timer error: $\tau = (M_B t_A - M_A t_B)/(nM_A - M_B)$ = _____ min (the sign of τ has to be taken into account)

$M = M_A/(t_A + \tau)$ = _____ ☐ nC/min ☐ rdg/min

[c] If the electrometer is not calibrated separately, set $k_{\mathrm{elec}} = 1$.

Note: HVL: half-value layer; SSD: source–surface distance; PDD: percentage depth dose.

9. CODE OF PRACTICE FOR MEDIUM ENERGY KILOVOLTAGE X RAY BEAMS

9.1. GENERAL

This section provides a code of practice for reference dosimetry (beam calibration) and recommendations for relative dosimetry in X ray beams with an HVL greater than 2 mm of aluminium and generating potentials between 80 kV and 300 kV. It is based on determining a calibration coefficient in terms of absorbed dose to water or air kerma obtained from a standards laboratory.

This range of beam qualities is referred to here as the medium energy X ray range. The division into low and medium energy ranges (the former covered in Section 8) is intended to reflect the two distinct types of radiotherapy for which kilovoltage X rays are used, 'superficial' and 'orthovoltage'. The boundary between the two ranges is not strict and has an overlap between 80 kV and 100 kV. In the overlap region, the methods presented in either section are equally satisfactory, and whichever is more suited to the clinical application should be used.

Although a key comparison was carried out at BIPM in 2017 for the measurement of absorbed dose to water in medium energy X ray beams [64], there is still limited availability of national standards for absorbed dose to water in this energy range. However, it is possible to derive calibration coefficients in terms of absorbed dose to water from air kerma calibration coefficients (see Appendix I for details). Therefore, this international code of practice discusses both routes to obtain the absorbed dose in a user's beam: using chamber calibration in terms of air kerma free in air and in terms of absorbed dose to water.

This international code of practice considers the absorbed dose to be measured at a reference depth of 2 g/cm^2 in water. The absorbed dose to water at other depths can be obtained using PDD data.

Air kerma and absorbed dose to water chamber calibrations for medium energy kilovoltage X rays require different types of beam quality factor, defined and denoted according to the chamber calibration modality. The air kerma beam quality factor is defined as the ratio of the calibration coefficients in terms of air kerma free in air at the qualities Q and Q_o (reference quality), as follows:

$$k_{Q,Q_o}^{\mathrm{FIA}} = \frac{N_{K,\mathrm{air},Q}^{\mathrm{FIA}}}{N_{K,\mathrm{air},Q_o}^{\mathrm{FIA}}} \tag{54}$$

The absorbed dose to water beam quality factor is defined as the ratio of calibration coefficients in terms of absorbed dose to water determined by calculation or measurement at a depth of 2 g/cm^2 in a water phantom, as follows:

$$k_{Q,Q_o}^{z=2} = \frac{N_{D,w,Q}^{z=2}}{N_{D,w,Q_o}^{z=2}} \tag{55}$$

9.2. DOSIMETRY EQUIPMENT

9.2.1. Ionization chambers

The recommendations regarding ionization chambers given in Section 4.2.1 should be followed. Only cylindrical ionization chambers with a cavity volume in the range 0.1–1.0 cm^3 are recommended for reference dosimetry in medium energy X ray beams. Farmer type chambers with a graphite or PMMA–graphite wall and an aluminium central electrode are used most frequently (see Table 4).

The reference point of a cylindrical chamber for the purpose of calibration at the standards laboratory and for measurements under reference conditions in the user beam is taken to be on the chamber axis at the centre of the cavity volume. This point is positioned at a reference depth of 2 g/cm^2 in the water phantom.

This international code of practice provides guidance based on a calibration coefficient of the reference ionization chamber in terms of absorbed dose to water or air kerma free in air. Some examples of the k_{Q,Q_o}^{FIA} and $k_{Q,Q_o}^{z=2}$ beam quality factors measured at PTB against their corresponding primary standards [192] are shown in Fig. 14. Note that the values of the beam quality factor for the chamber type PTW 30013 with respect to air kerma are almost independent of the X ray beam quality Q but vary significantly (by up to 8%) with respect to the absorbed dose to water. This difference has physical reasons that are independent of the chamber type (see Section 9.4 for an explanation). Despite these significant radiation quality dependences of the beam quality factor for some of the chamber types, all of these chambers can be used for reference dosimetry.

For a given chamber type, chamber to chamber variations in energy response can be significant and, as for low energy X rays, each individual dosimeter should be calibrated at a range of beam qualities that allow interpolation to the clinical beam qualities. In general, it is not recommended that a generic set of k_{Q,Q_o} values (see Section 3.2) for a particular type of chamber be used, because significant chamber to chamber variations cannot always be excluded. The chamber should be calibrated at the reference conditions given in Table 31.

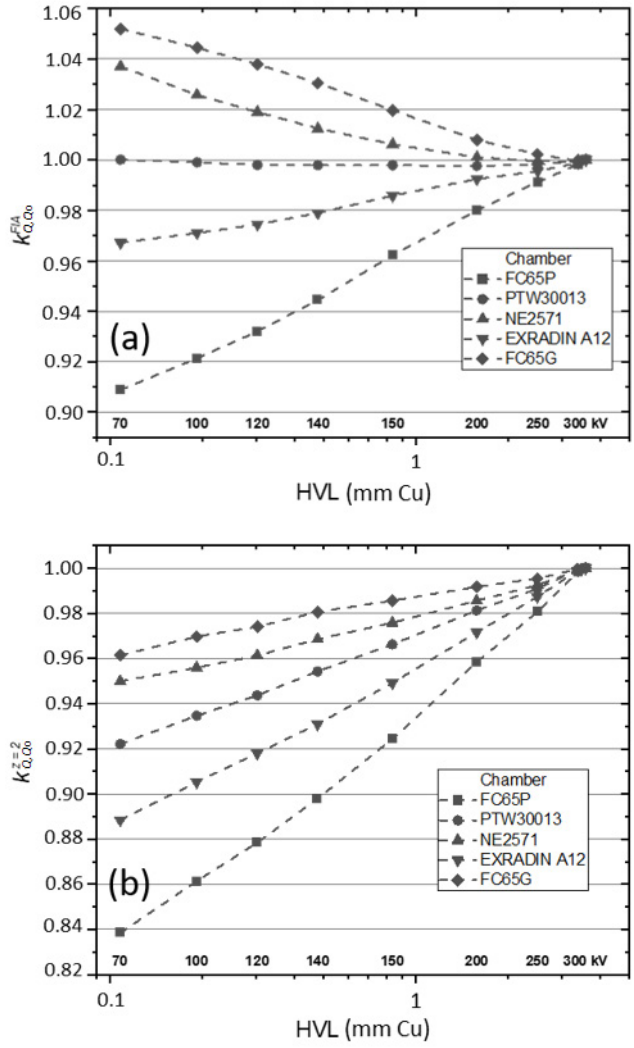

FIG. 14. Beam quality factors (a) k_{Q,Q_o}^{FIA} *in terms of air kerma free in air and (b)* $k_{Q,Q_o}^{z=2}$ *in terms of absorbed dose to water at a depth of 2 cm, measured at Physikalisch-Technische Bundesanstalt for the TH series (medium energy kilovoltage X ray beam qualities), with* Q_o *= TH 300 [192]. Note that the response of the chamber type PTW 30013 with respect to air kerma is almost independent of the X ray beam quality but varies by up to 8% with respect to absorbed dose to water (see Section 9.4).*

9.2.2. Phantoms and chamber sleeves

The recommendations regarding phantoms and chamber sleeves given in Sections 4.2.3 and 4.2.4 should be followed. Water is recommended as the reference medium for measurements of absorbed dose with medium energy X ray beams. The phantom should extend to at least 5 cm beyond all four sides of the largest field size employed at the depth of measurement. There should be a margin of at least 10 g/cm^2 beyond the maximum depth of measurement for both the calibrations and depth dose measurements.

In the clinic, it is recommended that vertical beams be used for all dosimetry measurements. This is to minimize any issues with the X ray beam having to pass through the thick plastic wall of the water phantom if the beam is directed horizontally.

For non-waterproof chambers, a waterproofing sleeve made of PMMA and preferably not thicker than 1.0 mm should be used. The air gap between the chamber wall and the waterproofing sleeve should be sufficiently thick (0.1–0.3 mm) to allow the air pressure in the chamber to equilibrate. The same waterproofing sleeve that was used for calibration of the user's ionization chamber in terms of absorbed dose to water at the standardizing laboratory should also be used for reference dosimetry in the clinical beam. If this is not possible, then another sleeve of the same material and of similar thickness should be used. The waterproofing sleeve should not be applied for calibration of the chamber in terms of air kerma free in air.

For relative dosimetry, some solid phantoms have good radiological water equivalence for kilovoltage X ray beams and may be used for measurements of quantities such as depth doses or field output factors [193–195]. It has been found that RMI457 Solid Water, Virtual Water and Plastic Water can be considered radiologically water equivalent even for lower energy X ray beams for such purposes. Other solid phantoms should be used with care, as their particular attenuation or scattering properties may be very different to those of water. Solid phantoms used in the clinic have to be checked by performing a dosimetric comparison with water [196].

9.3. BEAM QUALITY SPECIFICATION

9.3.1. Choice of beam quality index

It has long been known that it is desirable to use more than one beam quality parameter to characterize a kilovoltage X ray spectrum for dosimetry [182–184]. Typical quantities used are the kilovoltage generating potential and

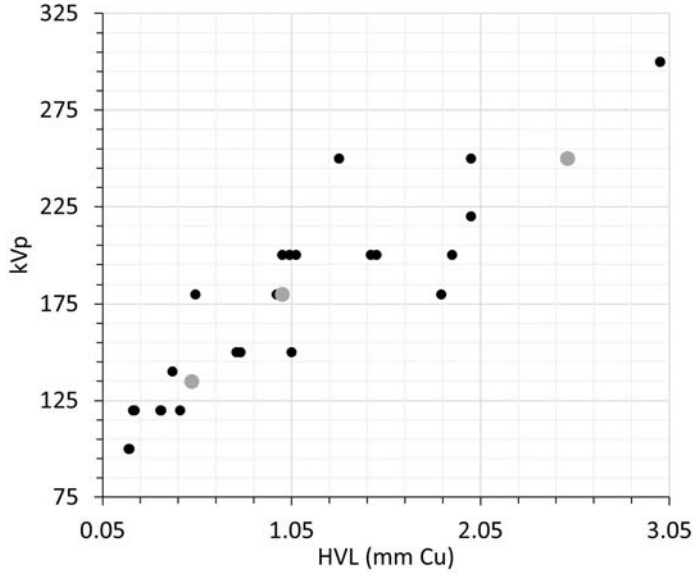

FIG. 15. Peak kilovoltage (kVp) versus half-value layer (HVL) (mm Cu) for medium energy kilovoltage X ray beams. Data are from the IAEA (gray circles) and from several centres worldwide (black circles) (from an IAEA survey).

the HVL, but neither uniquely defines the quality of the beam. For example, a kilovoltage X ray beam with a particular HVL may be produced either by light filtration of high voltage radiation or by heavy filtration of low voltage radiation. It is also not feasible to match both the kilovoltage and the HVL of each clinical beam precisely with the beams of the standards laboratories (see Fig. 15). In this international code of practice, the data are presented using both parameters, HVL and kilovoltage, for both low and medium energy X ray beams (see footnote 18 on p. 51).

So far, there have been insufficient experimental data available to determine how $N_{D,w,}$ and N_K vary independently with HVL and generating potential for a medium energy X ray chamber. Therefore, it is preferable, where possible, to have the dosimeter calibrated at similar combinations of kilovoltage and HVL as those of the user's reference clinical beams.

9.3.2. Determination of beam quality

In medium energy X ray beams, both aluminium and copper filters are used to determine the HVL. The HVL is defined as the thickness of an absorber

(usually copper or aluminium) required to attenuate a narrow beam to half the air kerma rate of the incident radiation.

The ideal arrangement is to place a collimating aperture at approximately half the distance between the X ray target and the chamber. The collimating aperture should reduce the field size to just enough to cover the ionization chamber with a small margin around the chamber, for instance 5–10 mm, and the total beam size defined by the lead diaphragm should not exceed 4 cm [185–187]. Because strictly the HVL corresponds to narrow beam geometry, the method described in Refs [11, 182] is used to derive the zero field area by measuring the HVL at two or three diaphragm sizes and extrapolating the plot of HVL versus diaphragm size to the zero area value (see also Ref. [108]). If possible, the HVL should be measured at the same distance as that used by the PSDL or SSDL to measure HVLs. The typical distance from the X ray focal spot to the ionization chamber is 100 cm. The collimating aperture should be placed immediately after the foils used in the measurement [185]. The measurement of HVL requires scatter free conditions and therefore positioning the ionization chamber at <1 m from any walls, floors and ceilings needs to be avoided. It is good practice to expose a piece of radiochromic film behind the detector to ensure that the ionization chamber is correctly centred in the radiation field. It is also vital to ensure that the chamber axis is perpendicular to both the filament–target direction of the X ray tube and to the beam central axis to minimize the influence of the heel effect on the readings of the ionization chamber.

The filters added for the HVL measurement are placed in combinations of thickness that span the range of HVL thickness to be determined. The thickness of the filters that reduces the air kerma rate to one half of the air kerma rate of the incident beam is then obtained by interpolation, preferably using an exponential, or a straight line if the added thicknesses are close to the HVL value. The purity of the aluminium or copper used for HVL measurements should be at least 99.9%. For further guidance on HVL determination, see Refs [185, 187–189].

Measurements are performed in air with ionization chambers that are suitable for this purpose. Strictly, it is the ionization current or the integrated charge per irradiation time that is measured, not the air kerma rate. This distinction is particularly relevant for lightly filtered beams. An ionization chamber with an energy response that varies by <2% over the quality range measured should be used.[58]

[58] HVL measurement errors of up to 10% can result from using a Farmer type chamber in a lightly filtered 100 kV beam. If the chamber energy response varies by more than 2% over the quality range, then each measurement has to be converted to an air kerma measurement using an air kerma calibration coefficient that is appropriate for each filtered or unfiltered beam. This is an iterative process because the calibration coefficient itself is determined by the HVL.

It is recommended that a monitor chamber be used to prevent misleading results due to variation in the X ray output. Care has to be taken to ensure that the response of the monitor chamber is not affected by increasing scatter as more filters are placed in the path of the beam. If a monitor chamber is not available, the effects of output variation can be minimized by measuring the air kerma rate without additional filters at the beginning, middle and end of the measurement sequence. Any changes in the air temperature and pressure during the measurements need to be considered in the readings of the ionization chamber.

9.4. DETERMINATION OF ABSORBED DOSE TO WATER

9.4.1. Reference conditions

The reference conditions for the determination of absorbed dose to water are given in Table 31.

TABLE 31. REFERENCE CONDITIONS FOR THE DETERMINATION OF ABSORBED DOSE IN MEDIUM ENERGY X RAY BEAMS

Influence quantity	Reference value or reference characteristic
Phantom material	Water
Chamber type	Cylindrical
Measurement depth[a], z_{ref}	2 g/cm^2
Reference point of the chamber	On the central axis at the centre of the cavity volume
Position of the reference point of the chamber	At the measurement depth z_{ref}
Source–surface distance	Usual treatment distance, as determined by the reference applicator[b]
Field size	10 cm × 10 cm or a diameter of 10 cm [c]

[a] z_{ref} is the reference depth in the phantom at which the reference point (see Section 9.2.1) of the chamber is positioned.

[b] If applicators resulting in different source–surface distances (SSDs) are used, then the one that defines the greatest SSD should be chosen as the reference applicator.

[c] When the X ray machine has an adjustable rectangular collimator, a 10 cm × 10 cm field should be set. Otherwise, if the field is defined by fixed applicators, a reference applicator of comparable size should be chosen.

Some clinics may only have applicators that are smaller in dimension than the ones listed in Table 31. In that case, the largest square or circular applicator should be chosen as the reference applicator, provided that the field size encompasses the entire ionization chamber.

9.4.2. Determination of absorbed dose under reference conditions

The absorbed dose to water at the reference depth z_{ref} in water, in a medium energy X ray beam of quality Q and in the absence of the chamber, is given by the following equation:

$$D_{\mathrm{w},Q} = M_Q N_{D,\mathrm{w},Q} \tag{56}$$

where M_Q is the reading of the dosimeter with the reference point of the chamber positioned at z_{ref} in accordance with the reference conditions given in Section 9.4.1 and corrected for the influence quantities temperature and pressure, electrometer calibration, polarity effect and ion recombination, as described in the worksheet in Section 9.7 (see also Section 4.4.3). The ionic recombination is negligible when the absorbed dose rate is lower than a few grays per minute (see Ref. [197]). $N_{D,\mathrm{w},Q}$ is the calibration coefficient in terms of absorbed dose to water for the dosimeter at the quality Q. Note also that the correction for the timer error may be significant; this is not a multiplicative correction and is therefore treated separately in the worksheet. The absorbed dose to water $D_{\mathrm{w},Q}$ at the X ray beam quality Q can be obtained using a reference chamber calibrated in terms of air kerma free in air (see Section 9.4.3) or absorbed dose to water (see Section 9.4.4).

9.4.3. Chamber calibrated in terms of air kerma free in air

If the chamber is calibrated in terms of air kerma free in air at a reference quality Q_{o} with calibration coefficient $N^{\mathrm{FIA}}_{K,\mathrm{air},Q_{\mathrm{o}}}$, the absorbed dose to water at the clinical X ray beam quality Q is obtained from the following equation (see Appendix I):

$$\begin{aligned} D^{z=2}_{\mathrm{w},Q}(f,\mathrm{SSD})_{\mathrm{clin}} = {} & M^{z=2}_{Q}(f,\mathrm{SSD})_{\mathrm{clin}}\, N^{\mathrm{FIA}}_{K,\mathrm{air},Q_{\mathrm{o}}}\, k^{\mathrm{FIA}}_{Q,Q_{\mathrm{o}}} \\ & \times \left[\mu_{\mathrm{en}}(Q)/\rho\right]^{z=2}_{\mathrm{w,air}} (f,\mathrm{SSD})_{\mathrm{clin}}\, p_{\mathrm{ch},Q}(f,\mathrm{SSD})_{\mathrm{clin}} \end{aligned} \tag{57}$$

where $M^{z=2}_{Q}(f,\mathrm{SSD})_{\mathrm{clin}}$ is the reading of the chamber at the reference point in the water phantom at the beam quality Q, $k^{\mathrm{FIA}}_{Q,Q_{\mathrm{o}}}$ is the air kerma beam quality factor, $\left[\mu_{\mathrm{en}}(Q)/\rho\right]^{z=2}_{\mathrm{w,air}}$ is the mean value of the water to air ratio of the mass energy absorption coefficients averaged over the spectrum at 2 cm depth in water and $p_{\mathrm{ch},Q}$ corrects for the difference in the response of the chamber between

its calibration free in air and its use at 2 cm depth in water (see Appendix I). Both $\left[\mu_{\mathrm{en}}(Q)/\rho\right]_{\mathrm{w,air}}^{z=2}$ and $p_{\mathrm{ch},Q}$ depend on the field size f and the SSD, whereas $N_{K,\mathrm{air},Q}^{\mathrm{FIA}}$ is considered to be largely independent of these parameters. The clinical beam generating potential and HVL, as well as the field size and source–surface distance $(f, \mathrm{SSD})_{\mathrm{clin}}$, should therefore be known.

The calibration certificate of the reference chamber should contain the air kerma calibration coefficient $N_{K,\mathrm{air},Q_{\mathrm{o}}}^{\mathrm{FIA}}$, measured at a suitable reference radiation quality Q_{o}, and values of $k_{Q,Q_{\mathrm{o}}}^{\mathrm{FIA}}$ as a function of the HVL obtained from a set of selected standard radiation qualities. These radiation qualities should be characterized by their generating tube voltage U (in units of kilovolt) and the HVL and have values close to those used in the clinic. Figure 16 shows that the $k_{Q,Q_{\mathrm{o}}}^{\mathrm{FIA}}$ values at a constant HVL vary only weakly (by less than ~0.5%) with kilovoltage. A similar behaviour can be expected for the ionization chamber types listed in Table 4. Thus, the air kerma beam quality factor $k_{Q,Q_{\mathrm{o}}}^{\mathrm{FIA}}$ can be obtained by interpolation with respect to the HVL values. The other values given for fixed kilovoltage and varying HVL are calculated as mean values of the monoenergetic air kerma response function[59] of the chambers for various X ray spectra.

The relative uncertainty for $k_{Q,Q_{\mathrm{o}}}^{\mathrm{FIA}}$ interpolated using only HVL is 0.5%. The relative standard uncertainty of $N_{K,\mathrm{air},Q_{\mathrm{o}}}^{\mathrm{FIA}}$ is given in the certificate and is usually not greater than ~0.5% (one standard deviation). Thus, the relative standard uncertainty of $N_{K,\mathrm{air},Q}^{\mathrm{FIA}}$ in the clinical beam is 0.7%.

Values of the ratios $\left[\mu_{\mathrm{en}}(Q,f,\mathrm{SSD})/\rho\right]_{\mathrm{w,air}}^{z=2}$ are obtained from the data of Andreo [54]. It is recommended to use the GUI web appplication[60] to obtain calculated data for kilovoltage X rays as a function of kilovoltage and HVL. Note that Q has to be specified by the two beam parameters, kilovoltage and HVL, for this purpose. As these ratios vary only moderately with small changes in kilovoltage and HVL (see Fig. 17), it is sufficient if both values are known within relative uncertainties of ~4%. Then, the relative standard uncertainty of the ratios under these conditions is not greater than 0.5%.

The overall chamber perturbation factor $p_{\mathrm{ch},Q}$ can be obtained from published data. Table 32 shows values recommended for frequently used chamber types. These are mean values of measured and calculated data reported by Bancheri et al. [192]. It is recommended to use interpolated values with respect

---

[59] The monoenergetic air kerma response function was determined from measured calibration coefficients of the chamber in terms of air kerma at the ISO 4037 narrow spectrum series in the range of beam qualities N-10 to N-300. The differently filtered X ray spectra were obtained using almost unfiltered X ray spectra measured in the range 70–300 kV by calculational addition of aluminium and copper layers of different thicknesses. In this way, sets of X ray spectra were obtained that largely cover the range of typical clinical beams.

[60] See footnote 18 on p.51.

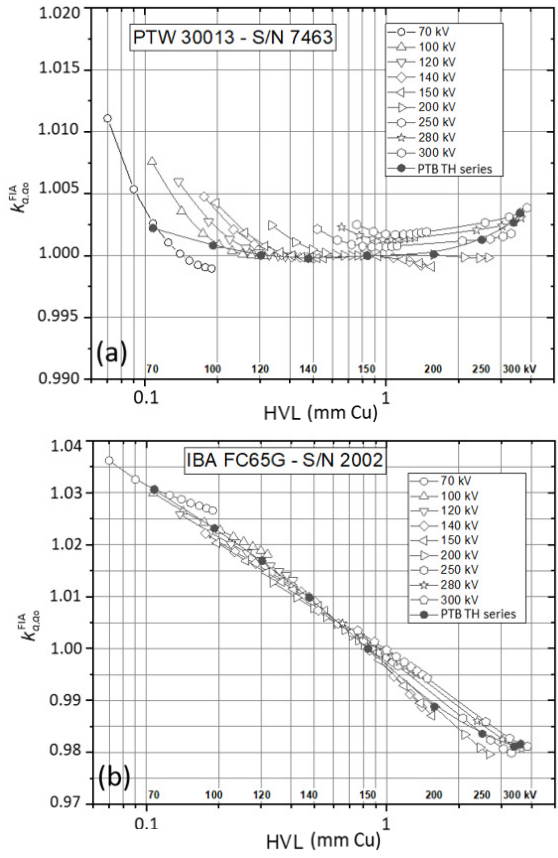

FIG. 16. Air kerma based beam quality factor k_{Q,Q_o}^{FIA} *as a function of HVL for* Q_o *= TH 150 [192] for ionization chambers of the PTB TH series: (a) PTW 30013 and (b) IBA FC65-G. The dependence of* k_{Q,Q_o}^{FIA} *on kilovoltage and HVL is shown for a series of beam qualities generated with selected tube high voltages of 70–300 kV and different filtrations, which largely cover the range of typical clinical beams.*

to HVL for the clinical qualities. The relative standard uncertainty is estimated at 1.0%. The data of Czarnecki et al. [198] are consistent with Table 32 within the stated uncertainties. It is noted that $p_{ch,Q}$ depends on the field size f [185]. If the clinical beam diameter deviates significantly from 10 cm, a correction according to Ref. [185] can be applied. If this correction is ignored, an additional uncertainty of 0.5% should be taken into account.

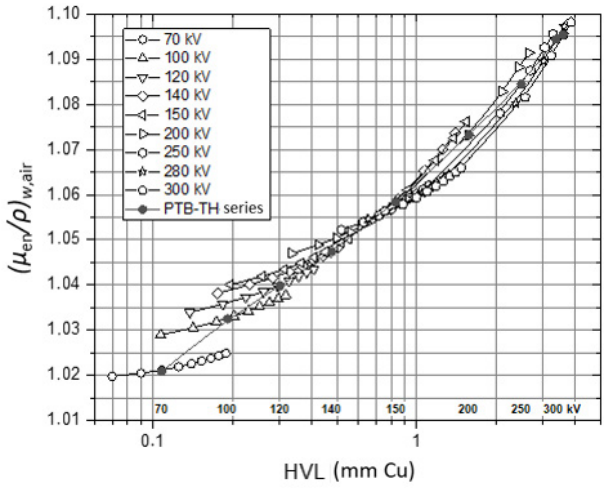

FIG. 17. Dependence of $\left[\mu_{en}(Q)/\rho\right]_{w,air}^{z=2}$ *on HVL and kilovoltage for SSD = 100 cm and* f *= 10 cm. Data are shown for the PTB therapy reference radiation qualities and for a series of qualities generated with tube high voltages of 70–300 kV and different filtrations for each fixed kilovoltage, which largely cover the range of typical clinical beams characterized by the kilovoltage and HVL.*

TABLE 32. RECOMMENDED VALUES OF $p_{ch,Q}$ (f = 10 cm, SSD = 100 cm) FOR VARIOUS CYLINDRICAL IONIZATION CHAMBERS AT A DEPTH OF 2 cm

Quality	70 kV	100 kV	120 kV	140 kV	150 kV	200 kV	250 kV	280 kV	300 kV
HVL (mm Cu)	0.108	0.192	0.303	0.477	0.838	1.581	2.498	3.384	3.592
IBA FC65-P	0.991	0.997	1.000	0.999	0.997	0.994	0.994	0.995	0.995
PTW 30013	1.001	1.008	1.014	1.016	1.016	1.011	1.008	1.006	1.006
NE 2571	0.994	1.004	1.011	1.015	1.017	1.012	1.009	1.007	1.007
Exradin A12	0.990	1.000	1.005	1.006	1.008	1.005	1.004	1.003	1.003
IBA FC65-G	0.995	1.004	1.011	1.014	1.018	1.015	1.011	1.009	1.009

9.4.4. Chamber calibrated in terms of absorbed dose to water

If the chamber is calibrated in terms of absorbed dose to water, the absorbed dose to water in the clinical X ray beam quality Q is obtained from the following equation:

$$D_{\mathrm{w},Q}^{z=2}(f,\mathrm{SSD})_{\mathrm{clin}} = M_{Q}^{z=2}(f,\mathrm{SSD})_{\mathrm{clin}}\, N_{D,\mathrm{w},Q_{\mathrm{o}}}^{z=2}(f,\mathrm{SSD})_{\mathrm{lab}} \times k_{Q,Q_{\mathrm{o}}}^{z=2}(f,\mathrm{SSD})_{\mathrm{lab}}\, k_{\mathrm{g},Q}^{z=2}(f,\mathrm{SSD})_{\mathrm{clin}} \tag{58}$$

where $M_{Q}^{z=2}(f,\mathrm{SSD})_{\mathrm{clin}}$ is the reading of the chamber at the reference position in the water phantom at the clinical radiation quality Q and at the clinical field size and SSD, $(f, \mathrm{SSD})_{\mathrm{clin}}$, $N_{D,\mathrm{w},Q_{\mathrm{o}}}^{z=2}(f,\mathrm{SSD})_{\mathrm{lab}}$ is the absorbed dose to water calibration coefficient at the reference radiation quality Q_{o} measured at the standards laboratory field size and SSD, $(f, \mathrm{SSD})_{\mathrm{lab}}$, and $k_{Q,Q_{\mathrm{o}}}^{z=2}(f,\mathrm{SSD})_{\mathrm{lab}}$ is the corresponding absorbed dose to water beam quality factor. $k_{\mathrm{g},Q}^{z=2}(f,\mathrm{SSD})_{\mathrm{clin}}$ is the geometry correction factor at the radiation quality Q given by the ratio of the calibration coefficients under $(f, \mathrm{SSD})_{\mathrm{clin}}$ and $(f, \mathrm{SSD})_{\mathrm{lab}}$ conditions (see Appendix I). The clinical beam generating voltage and HVL $(\mathrm{kV}, \mathrm{HVL})_{\mathrm{clin}}$, as well as $(f, \mathrm{SSD})_{\mathrm{clin}}$, should be known.

The calibration certificate of the reference chamber should contain the calibration coefficient $N_{D,\mathrm{w},Q_{\mathrm{o}}}^{z=2}$ measured at the stated reference radiation quality Q_{o} and values $k_{Q,Q_{\mathrm{o}}}^{z=2}$ obtained from a set of selected standard radiation qualities characterized by their generating tube voltage U (in units of kilovolt) and the HVL. The beam quality correction factor can be obtained by interpolation with respect to the HVL values. Examples of $k_{Q,Q_{\mathrm{o}}}^{z=2}$ as a function of HVL and kilovoltage are shown in Fig. 18 for the chamber types PTW 30013 and IBA FC65G. It can be seen that at a constant HVL the $k_{Q,Q_{\mathrm{o}}}^{z=2}$ values vary only weakly (less than ~0.5%) for different kilovoltage values. A similar behaviour can be expected for the other ionization chamber types listed in Table 4. Therefore, it is acceptable that the interpolation is based on the HVL, and these differences can be taken into account by considering a relative uncertainty of 0.5% in the interpolated value. The absorbed dose to water calibration coefficient issued by standards laboratories operating a water calorimeter is usually ~1% [80]. Thus, the relative standard uncertainty of $N_{D,\mathrm{w},Q_{\mathrm{o}}}^{z=2} k_{Q,Q_{\mathrm{o}}}^{z=2}$ in the clinical beam is 1.1%.

The geometry correction factor in Eq. (58) can be assumed to be essentially proportional to the chamber independent differences in $(f, \mathrm{SSD})_{\mathrm{lab}}$ and $(f, \mathrm{SSD})_{\mathrm{clin}}$ for values of $\left[\mu_{\mathrm{en}}(Q,f,\mathrm{SSD})/\rho\right]_{\mathrm{w,air}}^{z=2}$, which can be calculated using the GUI web application[60]. The relative uncertainty of the calculated geometry correction factor is estimated to be 0.2%.

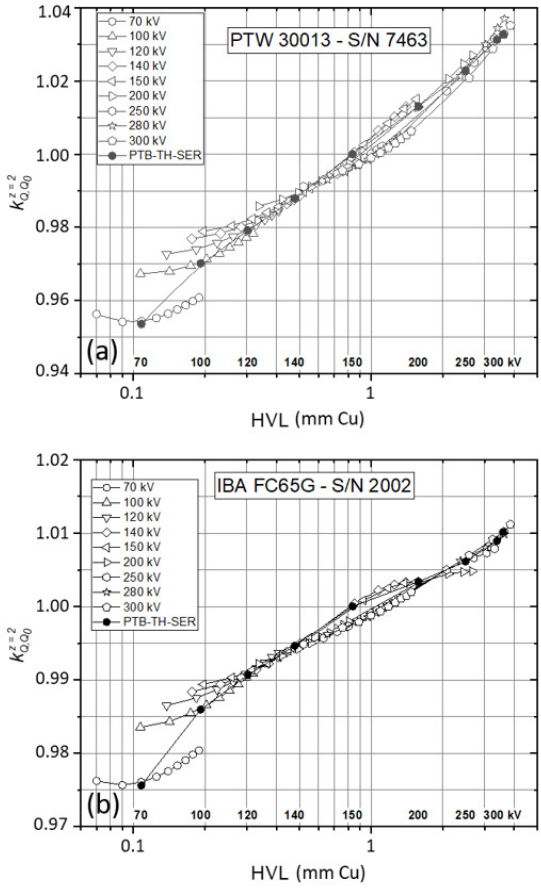

FIG. 18. Absorbed dose to water based beam quality factor $k_{Q,Q_o}^{z=2}$ *as a function of HVL for* Q_o *= TH 150 [192] for chambers of the PTB TH series: (a) PTW 30013 and (b) IBA FC65G. The dependence of* $k_{Q,Q_o}^{z=2}$ *on kilovoltage and HVL is shown for a series of qualities generated with tube high voltages of 70–300 kV and different filtrations that largely cover the range of typical clinical beams.*

9.5. MEASUREMENTS UNDER NON-REFERENCE CONDITIONS

9.5.1. Central axis depth dose distributions

The measurements under reference conditions prescribed in this international code of practice provide the absorbed dose at a depth of 2 g/cm^2 in water. In order to relate this measurement to the dose at other depths, it is necessary to obtain the central axis depth dose distribution. An estimate of the

depth dose distribution may be obtained from the literature [146]. However, it is unlikely that the published data will match the exact kilovoltage and HVL of the clinical beam. Therefore, it is recommended that the depth dose distributions be measured for all clinical beam qualities and for all applicators.

Depth doses should be measured with a suitable ionization chamber that has minimal energy response variations and good spatial resolution. A Farmer type cylindrical ionization chamber that is suitable for reference dosimetry should have a response in a phantom that is reasonably independent of depth and field size. However, a chamber of this type cannot be used accurately in a phantom at depths of less than ~0.5 cm [186, 193, 199, 200], owing to the size of the cavity and the effects from the chamber being partially above the water surface. Depending on the field size and beam energy, there may be a significant variation in the absorbed dose in the first few millimetres of the depth dose distribution. It should be noted that applicators with high atomic number materials or lead cutouts can generate significant electron contamination and appropriate thin plastic foils should be used to absorb these electrons.

It is possible to measure depth dose distributions using either a small ionization chamber in a scanning tank, as used for relative dosimetry in high energy electron and photon beams, or a plane parallel chamber of the type used for high energy electron dosimetry [201]. The latter has the advantage of allowing measurements in a water phantom at depths of <0.5 cm. This type of plane parallel chamber was not designed for use with kilovoltage X rays, but NACP, PTW Markus, PTW Advanced Markus and PTW Roos chambers have been shown to be suitably accurate for depth dose measurements at beam energies of 50–300 kV with uncertainties of <3% [193, 201, 202]. It is also noted that some older plane parallel chambers, such as Capintec PS-033, have been shown not to be suitably accurate for depth dose measurements. Small scanning ionization chambers have similar issues to Farmer type chambers when measuring the dose at the surface.

As neither small scanning ionization chambers nor plane parallel chambers were designed for kilovoltage X rays, the relationship between the depth ionization distribution and the depth dose distribution (at depths >0.5 cm) has to be determined through comparison with a Farmer type cylindrical chamber at several suitable depths. The depth of measurement of a Farmer type chamber in a phantom is taken to be the depth of the central axis of the chamber. In most cases, the differences between chamber types are typically no more than a few per cent [202, 203].

Dose measurements near the water phantom surface are challenging, and the preferred method for the extrapolation is to perform high resolution depth dose measurements using a plane parallel chamber at 0.1 mm intervals with a depth of water in the tank of up to 2 mm, and then extrapolate to the surface dose. When

making measurements near the surface, there always has to be sufficient material thickness to ensure full buildup of secondary electrons. The total thickness required can be estimated using the continuous slowing down approximation range of the maximum energy of electrons in the material used [48]. For all depth dose measurements, the effective point of measurement of the ionization chamber should be used, otherwise the PDD curves may need to be shifted to account for the differences in depth. This allows depth doses to be measured with appropriate spatial resolution close to the water phantom surface. The effective point of measurement for both parallel plate and cylindrical chambers is the centre of the sensitive air cavity of the chamber [185]. Typical examples of PDDs can be found in Ref. [146].

Another method is to perform the near surface dose measurements in a suitable solid phantom and those for the remainder of the depth dose curve in water using a Farmer type chamber. In such cases, corrected dose measurements near the surface can be combined with the measured dataset for the other depths.

Verification of the surface doses can also be achieved by using a chamber calibrated in terms of air kerma free in air and employing the method described in Section 8. Values for the ratio of mass energy absorption coefficients over the medium energy X ray range can be found in the GUI web application[60].

Some detectors that are used routinely for scanning high energy beams are not suitable for use in medium energy X rays because of excessive variation in their response as a function of beam quality in kilovoltage energies. There are other detectors that can be considered for possible use in verifying depth doses for kilovoltage X ray beams. Synthetic diamond detectors have been shown to give good agreement with ionization chamber readings and therefore may be useful for the measurement of PDDs for small fields [204]. Radiochromic film has also been used with some success but it relies on a suitable film dosimetry quality assurance process to achieve accurate results [205, 206]. In comparison, solid state diode detectors may not be suitable for PDD measurements, as they have been found to give significant differences in response, particularly for higher energy beams and larger field sizes [201, 204].

9.5.2. Field output factors

For clinical applications, field output factors Ω are required for all combinations of SSDs and field sizes used for radiotherapy treatment. For medium energy X rays, Ω is given by the ratio of the absorbed dose to water for each combination of field size and SSD, $D_{w,Q}(f, \mathrm{SSD})_{clin}$, relative to the absorbed dose under reference conditions, $D_{w,Q}(f, \mathrm{SSD})_{ref}$, measured at the depth of 2 g/cm^2 in water as follows:

$$\Omega = \frac{D_{w,Q}(f,\mathrm{SSD})_{\mathrm{clin}}}{D_{w,Q}(f,\mathrm{SSD})_{\mathrm{ref}}} \cong \frac{M_Q^{z=2}(f,\mathrm{SSD})_{\mathrm{clin}}\left[\mu_{\mathrm{en}}(Q)/\rho\right]_{w,\mathrm{air}}^{z=2}(f,\mathrm{SSD})_{\mathrm{clin}}}{M_Q^{z=2}(f,\mathrm{SSD})_{\mathrm{ref}}\left[\mu_{\mathrm{en}}(Q)/\rho\right]_{w,\mathrm{air}}^{z=2}(f,\mathrm{SSD})_{\mathrm{ref}}} \tag{59}$$

In Eq. (59) it is assumed that the calibration coefficients and the overall chamber perturbation factor $p_{\mathrm{ch},Q}$ are largely independent of f and SSD, and thus cancel. Ω has to be measured for each beam quality and each individual applicator. The edge of the active volume of the chamber should be enclosed within the full width at half-maximum of the field size.

9.6. ESTIMATED UNCERTAINTY IN THE DETERMINATION OF ABSORBED DOSE TO WATER UNDER REFERENCE CONDITIONS

It is stated above that the absorbed dose to water calibration coefficient at X ray beam quality Q can be obtained from the chamber calibration in terms of air kerma free in air (see Section 9.4.3) or absorbed dose to water (see Section 9.4.4). It is the responsibility of users to establish an uncertainty budget for their determination of absorbed dose to water. Examples of uncertainty estimates for the two routes are given in Table 33. These estimates may vary depending on the uncertainty quoted by the calibration laboratory, the care and experience of the user performing the measurement, and the quality and condition of the measurement equipment (e.g. regular recalibration of all measurement devices, quality management system to ensure proper functioning).

The relative standard uncertainty (coverage factor k = 1) of the air kerma calibration coefficient at the PSDL is taken here to be 0.5%, which can be regarded as an upper limit [207]. Interpolation of the calibration coefficient to the user beam quality contributes an additional relative uncertainty of 0.5%. The relative uncertainty of the water to air ratio of the mean mass energy absorption coefficient is estimated to be 0.5% [54]. The uncertainty of the chamber perturbation factor is estimated to be ~1% from the uncertainty of mean values obtained from measurements and calculations. An additional uncertainty of 0.5% has to be considered if the field size dependence of the chamber perturbation factor is ignored.

The relative standard uncertainty (coverage factor k = 1) in the absorbed dose to water calibration coefficient determined directly from a primary standard is taken here to be 1% [207, 208]. An additional relative uncertainty

of 0.5% is taken into account in the interpolation to the user beam quality. The relative uncertainty of the geometry correction factor is estimated to be 0.2% [54].

The X ray output from some machines depends on the line voltage, the tube temperature and the operator control of the tube current and voltage. This uncertainty should be estimated separately by the user from the standard deviation of a set of at least five exposures of typical treatment length. It is not included in this analysis. Because the dose gradient from beams at the lower end of the energy range may be as large as 1% per millimetre, there may be difficulty in achieving a depth positioning reproducibility better than 1%, so this uncertainty is assigned to the establishment of reference conditions. The uncertainties are summarized in Table 33.

It can be seen from Table 33 that the calibration of the reference ionization chamber — whether it is in terms of absorbed dose to water or in terms of air kerma free in air — does not make a significant difference to the uncertainties in the absorbed dose to water in the user beam. The more convenient method in the clinic may be chosen by the user.

TABLE 33. ESTIMATED RELATIVE STANDARD UNCERTAINTY[a] OF $D_{w,Q}$ AT THE REFERENCE DEPTH IN WATER FOR A MEDIUM ENERGY X RAY BEAM

Physical quantity or procedure	Relative standard uncertainty (%)	
	$N_{D,w}$ based	N_K based
Step1: standards laboratory		
Calibration of secondary standard (N_D or N_K) at PSDL	1.0	0.5
Long term stability of secondary standard	0.1	0.1
Calibration of the user dosimeter at the standards laboratory	0.5	0.5
Combined uncertainty in step 1	1.1	0.7
Step 2: User X ray beam		
Procedure to obtain the calibration coefficient in the user beam	0.5	0.5
Chamber perturbation correction		1.0

TABLE 33. ESTIMATED RELATIVE STANDARD UNCERTAINTY[a] OF $D_{w,Q}$ AT THE REFERENCE DEPTH IN WATER FOR A MEDIUM ENERGY X RAY BEAM (cont.)

Physical quantity or procedure	Relative standard uncertainty (%)	
	$N_{D,w}$ based	N_K based
Field size dependence of the chamber perturbation factor		0.5
Ratio of the mean mass energy absorption coefficient water to air		0.5
Geometry correction factor	0.2	
Long term stability of the user dosimeter	0.3	0.3
Dosimeter reading M_Q relative to timer or beam monitor	0.1	0.1
Establishment of reference conditions	1.0	1.0
Correction for influence quantities k_i	0.8	0.8
Combined uncertainty in step 2	1.4	1.9
Combined standard uncertainty of $D_{w,Q}$ (steps 1 and 2)	1.8 (1.7)[b]	2.0 (1.9)[b]

[a] See Ref. [7] or Appendix IV for the expression of uncertainty. The estimates given in the table should be considered typical values; these may vary depending on the uncertainty quoted by standards laboratories for calibration coefficients and on the experimental uncertainty at the user institution.

[b] Combined standard uncertainty with the user dosimeter calibrated directly at the PSDL.

9.7. WORKSHEET

Determination of the absorbed dose to water in a medium energy X ray beam

User: _____ Date: _____

1. Radiation treatment unit and reference conditions for $D_{w,Q}$ determination

X ray machine: _____ Nominal tube potential : _____ kV

Nominal tube current: _____ mA Beam quality, Q(HVL): ____ mm ☐ Al ☐ Cu

Reference phantom: water Reference depth: __2__ g/cm^2

Reference field size: _____ cm × cm Reference SSD: _____ cm

2. Ionization chamber and electrometer

Ionization chamber model: _____ Serial no:_____

Chamber wall Material: _____ Thickness = _____ g/cm^2

Waterproof sleeve Material: _____ Thickness = _____ g/cm^2

Phantom window Material: _____ Thickness = _____ g/cm^2

Air kerma free in air calibration coefficient $N_{K,\mathrm{air},Q_o}^{\mathrm{FIA}}$ = _____ ☐ Gy/nC ☐ Gy/rdg

Absorbed dose calibration coefficient $N_{D,\mathrm{w},Q_o}^{z=2}(f,\mathrm{SSD})_{\mathrm{lab}}$ = __ ☐ Gy/nC ☐ Gy/rdg

Reference beam quality, Q_o (HVL): _____ mm ☐ Al ☐ Cu

Reference conditions for calibration P_o = _____ kPa T_o = _____ °C Rel. humidity: ___%

Polarizing potential V = ____ V

Calibration polarity: ☐ positive ☐ negative ☐ corrected for polarity effect

User polarity: ☐ positive ☐ negative

Calibration laboratory: _____ Date: _____

Electrometer model: Serial no.: _____

Calibrated separately from chamber: ☐ yes ☐ no Range setting: _____

If yes Calibration laboratory: Date: _____

3. Dosimeter reading[a] and correction for influence quantities

Uncorrected dosimeter reading at V and user polarity: _____ ☐ nC ☐ rdg

Corresponding time: _____ min

Ratio of dosimeter reading and time[b]: M = _____ ☐ nC/min ☐ rdg/min

(a) Pressure P = _____ kPa Temperature T = _____ °C Rel. humidity (if known): ____%

$$k_{TP} = \frac{(273.2+T)}{(273.2+T_o)}\frac{P_o}{P} = \_\_\_\_\_$$

(b) Electrometer calibration factor[c] k_{elec} = _____ ☐ nC/rdg ☐ dimensionless

(c) Polarity correction[d] Reading at $+V$: M_+ = _____ Reading at $-V$: M_- = ____

$$k_{\text{pol}} = \frac{|M_+| + |M_-|}{2M} = \_\_\_\_\_$$

Corrected dosimeter reading at voltage V:

$M_Q = M k_{TP} k_{\text{elec}} k_{\text{pol}}$ = _____ ☐ nC/min ☐ rdg/min

4. Absorbed dose rate to water at the reference depth, z_{ref}

$\left[\mu_{\text{en}}(Q)/\rho\right]_{\text{w,air}}^{z=2}(f,\text{SSD})_{\text{clin}}$ = _____ $p_{\text{ch},Q}(f,\text{SSD})_{\text{clin}}$ = _____ cm

$k_{\text{g},Q}^{z=2}(f,\text{SSD})_{\text{clin}}$ = _____

Beam quality correction factor for user quality Q (free in air): k_{Q,Q_o}^{FIA} = _____

(in phantom): $k_{Q,Q_o}^{z=2}(f,\text{SSD})_{\text{lab}}$ = _____

at Q_o(HVL) = _____ mm ☐ Al ☐ Cu

Calibration laboratory: _____ Date: _____

Or beam quality correction factor interpolated:

$\left(k_{Q,Q_o}\right)_1$ = _____ at HVL_1 = _____ mm ☐ Al ☐ Cu Date: _____

$\left(k_{Q,Q_o}\right)_2$ = _____ at HVL_2 = _____ mm ☐ Al ☐ Cu Date: _____

$$k_{Q,Q_o} = \left(k_{Q,Q_o}\right)_1 + \left[\left(k_{Q,Q_o}\right)_2 - \left(k_{Q,Q_o}\right)_1\right] \left[\frac{\ln(\text{HVL}) - \ln(\text{HVL}_1)}{\ln(\text{HVL}_2) - \ln(\text{HVL}_1)}\right] = \_\_\_\_\_$$

Absorbed dose rate calibration at z_{ref}:

Chamber calibrated in terms of air kerma free in air (Section 9.4.3):

$D_{\text{w},Q}^{z=2}(f,\text{SSD})_{\text{clin}}$ =

$M_Q^{z=2}(f,\text{SSD})_{\text{clin}}\, N_{K,\text{air},Q_o}^{\text{FIA}}\, k_{Q,Q_o}^{\text{FIA}} \left[\mu_{\text{en}}(Q)/\rho\right]_{\text{w,air}}^{z=2}(f,\text{SSD})_{\text{clin}}\, p_{\text{ch},Q}(f,\text{SSD})_{\text{clin}}$ = _____ Gy/min

Chamber calibrated in terms of absorbed dose to water (Section 9.4.4):

$D_{\text{w},Q}^{z=2}(f,\text{SSD})_{\text{clin}}$ =

$M_Q^{z=2}(f,\text{SSD})_{\text{clin}}\; N_{\text{D,w},Q_o}^{z=2}(f,\text{SSD})_{\text{lab}}\; k_{Q,Q_o}^{z=2}(f,\text{SSD})_{\text{lab}}\; k_{\text{g},Q}^{z=2}(f,\text{SSD})_{\text{clin}}$ = _____ Gy/min

5. Absorbed dose rate to water at the depth of dose maximum, z_{max}

Depth of dose maximum: z_{max} = _____ g/cm^2

PDD at z_{ref} for ___ cm × ___ cm field size: PDD(z_{ref} = 2 g/cm^2) = _____%

Absorbed dose rate calibration at z_{max}:

$D_{\text{w},Q}(z_{\text{max}}) = 100 \times D_{\text{w},Q}(z_{\text{ref}})/\text{PDD}(z_{\text{ref}})$ = _____ Gy/min

---

[a] All readings should be checked for leakage and corrected if necessary.

[b] The timer error should be taken into account. The correction at voltage V can be determined according to

M_A is the integrated reading in a time t_A M_A = _____ t_A = _____ min

M_B is the integrated reading in n short exposures of time t_B/n each ($2 \le n \le 5$) M_B = _____ t_B = _____ min

n = _____

Timer error: $\tau = (M_B t_A - M_A t_B)/(n M_A - M_B)$ = _____ min (the sign of τ has to be taken into account)

$M = M_A/(t_A + \tau)$ = _____ ☐ nC/min ☐ rdg/min

[c] If the electrometer is not calibrated separately, then set $k_{\text{elec}} = 1$.

[d] M in the denominator of k_{pol} denotes a reading at the user polarity. Preferably, each reading in the equation should be the average of the ratios of M (or M_+ or M_-) to the reading of an external monitor, M_{em}.

Note: HVL: half-value layer; SSD: source–surface distance; PDD: percentage depth dose.

10. CODE OF PRACTICE FOR PROTON BEAMS

10.1. GENERAL

This section provides a code of practice for reference dosimetry (beam calibration) and recommendations for relative dosimetry in proton beams with energies in the range from 50 MeV to 250 MeV. It is based on a calibration coefficient in terms of absorbed dose to water N_{D,w,Q_o} for a dosimeter in a reference beam of quality Q_o.[61]

A typical depth dose distribution for a pristine[62] proton beam is shown in Fig. 19. This consists of a region where the dose increases only slowly with depth,

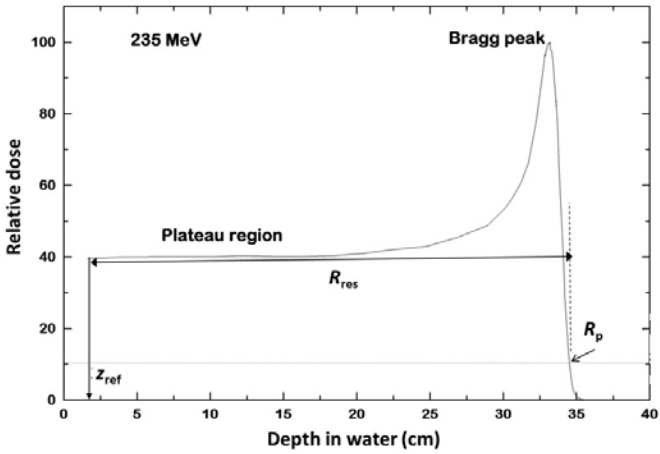

FIG. 19. Percentage depth dose distribution for a 235 MeV pristine proton beam, illustrating the plateau region and the Bragg peak. Indicated on the figure are the reference depth, z_{ref} (plateau), the residual range at z_{ref} used to specify the quality of the beam, R_{res}, and the practical range, R_p.

---

[61] As no primary standard of absorbed dose to water for proton beams is yet available, ^{60}Co gamma rays will be used as the reference beam quality Q_o for proton dosimetry (see Section 10.5). If primary standards of absorbed dose to water, based for example on a water or graphite calorimeter, become available at PSDLs, then a solution similar to those for other modalities can be used.

[62] The term 'pristine' is commonly used in proton therapy and means a non-scattered monoenergetic beam [209].

called the ‘plateau’, and a region where the dose rises rapidly to a maximum, called the ‘Bragg peak’.

Because clinical applications require a relatively uniform dose to be delivered to the volume to be treated, the pristine proton beam has to be spread out both laterally and in depth. This is obtained at a treatment depth by the superposition of Bragg peaks of different intensities and energies. This technique is called ‘range modulation’ and creates a region of high dose uniformity, the SOBP (see Fig. 20). Currently, two types of proton beam delivery system are used in the clinic: the broad beam delivery system, which uses scattered or uniformly scanned beams, and the pencil beam scanning (PBS) delivery system, which uses intensity modulated scanned beams [210]. In the broad beam delivery system, the beam is spread uniformly and then conformed to the target by customized devices, such as a collimator and a range compensator. In the PBS delivery system, a narrow beam is scanned electromagnetically over the target volume in a sequence specifically designed for each target with a treatment planning system. This international code of practice includes recommendations for the determination of absorbed dose for both the PBS and the broad beam delivery systems. The reference dosimetry procedures for the two systems are substantially different. During PBS, the dose is delivered to the patient by a large number of small pencil beams and the number of particles for each of these pencil beams has to be specified and controlled by the dose monitor. In contrast, with broad beam delivery systems, the dose is delivered by spreading out a pristine proton beam both laterally and in depth.

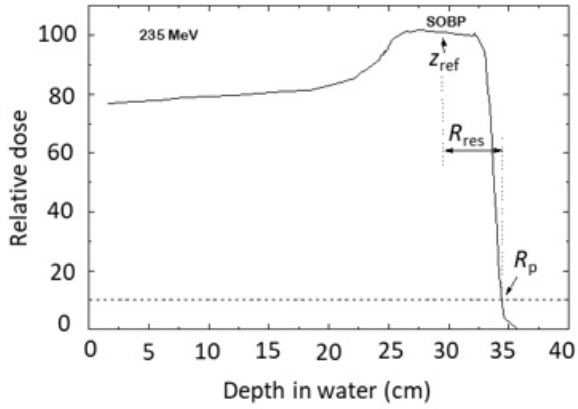

FIG. 20. Percentage depth dose distribution for a modulated proton beam. Indicated on the figure are the reference depth, z_{ref} *(middle of the spread-out Bragg peak (SOBP)), the residual range at* z_{ref} *used to specify the quality of the beam,* R_{res}*, and the practical range,* R_p*.*

10.2. DOSIMETRY EQUIPMENT

10.2.1. Ionization chambers

The recommendations regarding ionization chambers given in Section 4.2.1 should be followed. Both cylindrical and plane parallel ionization chambers are recommended for use as reference instruments for the calibration of clinical broad beam and PBS delivery. The use of cylindrical ionization chambers is limited to broad proton beams with qualities $R_{res} \geq 0.5$ g/cm^2 and to scanned pencil proton beams with beam qualities $R_{res} \geq 15$ g/cm^2 at the reference depth. Graphite walled cylindrical chambers are preferable to plastic walled chambers because of their better long term stability and smaller chamber to chamber variations (see Section 4.2.1 and Fig. 2). The reference point for these chambers is taken to be on the central axis of the chamber, at the centre of the cavity volume. Plane parallel ionization chambers can be used for reference dosimetry in all proton beams, either with an absorbed dose to water calibration coefficient in a ^{60}Co gamma radiation reference beam or with a cross-calibration coefficient obtained in a high energy proton beam (with $R_{res} \geq 15$ g/cm^2; see Section 10.6). For plane parallel ionization chambers, the reference point is taken to be on the inner surface of the entrance window, at the centre of the window; this point is positioned at the point of interest in the phantom. The cavity diameter of the plane parallel ionization chamber or the cavity length of the cylindrical ionization chamber should not be larger than approximately half the reference field size. Moreover, the outer diameter for cylindrical ionization chambers should not be larger than half of the SOBP width.

For relative dosimetry, plane parallel ionization chambers and small volume cylindrical ionization chambers (<0.1 cm^3) are recommended. The chamber types for which data are given in this international code of practice are listed in Section 10.7.2.

10.2.2. Phantoms and chamber sleeves

The recommendations regarding phantoms and chamber sleeves given in Sections 4.2.3 and 4.2.4 should be followed. Water is recommended as the reference medium for the determination of absorbed dose and for beam quality measurements with proton beams. The phantom should extend to at least 5 cm beyond all four sides of the field size employed at the depth of measurement and to at least 5 g/cm^2 beyond the maximum depth of measurement.

In horizontal beams, the window of the phantom should be made of plastic and be of a thickness t_{win} of 0.2–0.5 cm. The water equivalent thickness (in g/cm^2) of the phantom window should be taken into account when evaluating

the depth at which the chamber is to be positioned; the thickness is calculated as the product $t_{win}\rho_{pl}$, where ρ_{pl} is the mass density of the plastic (in g/cm^3). For the commonly used plastic PMMA, the nominal value ρ_{PMMA} = 1.19 g/cm^3 [48] may be used for the calculation of the water equivalent thickness of the window. For window thicknesses larger than 0.5 cm, the water equivalent thickness should be calculated as described in Section 10.7.3 rather than by scaling by density.

For non-waterproof ionization chambers, a waterproofing sleeve made of PMMA and preferably not thicker than 1.0 mm should be used. The air gap between the chamber wall and the waterproofing sleeve should be sufficient (0.1–0.3 mm) to allow the air pressure in the chamber to equilibrate. The same waterproofing sleeve that was used for calibration of the user's ionization chamber should also be used for reference dosimetry; if this is not possible, then another sleeve of the same material and of similar thickness should be used. Plane parallel ionization chambers, if not inherently waterproof or supplied with a waterproof cover, have to be used in a waterproof enclosure, preferably made from PMMA or a material that closely matches the chamber walls; ideally, there should be no more than 1 mm of added material in front of and behind the cavity volume.

Plastic phantoms should not be used for reference dosimetry in proton beams since the required water to plastic fluence correction factors, h_{pl}, are not known with sufficient accuracy. They depend on nuclear interaction cross-sections that have large uncertainties [211]. Information on the use of plastic phantoms for relative dosimetry is given in Section 10.7.3.

10.3. BEAM QUALITY SPECIFICATION

10.3.1. Choice of beam quality index

In this international code of practice, the residual range, R_{res}, is chosen as the beam quality index for both broad beams and scanned proton beams, because it has the advantage of being easily measurable. Although this choice will slightly underestimate the stopping power ratios in the middle of the SOBP, this effect is unlikely to exceed 0.3% [212, 213] for $R_{res} > 2$ g/cm^2 but can reach 0.6% for $R_{res} \leq 2$ g/cm^2 [214].

The residual range R_{res} (in g/cm^2) at a measurement depth z is defined as follows:

$$R_{res} = R_p - z \tag{60}$$

where z is the depth of measurement and R_p is the practical range (both expressed in g/cm^2), which is defined as the depth at which the absorbed dose beyond the

Bragg peak (for a single energy static pencil beam) or the SOBP (for a modulated beam) falls to 10% of its maximum value [212] (see Figs 19 and 20). Unlike the other radiation types covered in this publication, in the case of protons, the quality Q is not unique to a particular beam but is also determined by the reference depth z_{ref} chosen for measurement.

10.3.2. Measurement of beam quality

The residual range R_{res} should be derived from a measured depth dose distribution, obtained using the reference conditions given in Table 34. The preferred choice of detector for the measurement of central axis depth dose distributions for broad beams is a plane parallel ionization chamber. For scanned pencil beams, it should be a large area plane parallel ionization chamber that measures an integrated radial profile[63] as a function of depth for a single energy static pencil beam. Additional information on the measurement of depth dose distributions is given in Section 10.7.

TABLE 34. REFERENCE CONDITIONS FOR THE DETERMINATION OF PROTON BEAM QUALITY, R_{res}

Influence quantity	Reference value or reference characteristic
Phantom material	Water
Chamber type	Plane parallel
Reference point of the chamber	On the inner surface of the window at its centre
Position of the reference point of the chamber	At the point of interest
Source–surface distance	Clinical treatment distance

[63] The term ‘integrated depth dose curve’ is used in practice to describe the depth dose distribution for a single static pencil beam measured with a large area plane parallel ionization chamber. The more correct term ‘integrated radial profile as a function of depth’ should be used instead.

TABLE 34. REFERENCE CONDITIONS FOR THE DETERMINATION OF PROTON BEAM QUALITY, R_{res} (cont.)

Influence quantity	Reference value or reference characteristic
Field size at the phantom surface	For broad beams, 10 cm × 10 cm For small field applications (i.e. eye treatments), 10 cm × 10 cm or the largest field clinically available For scanned beams, the spot size of a single energy static pencil beam

10.4. DETERMINATION OF ABSORBED DOSE TO WATER

10.4.1. Reference conditions

Reference conditions for the determination of absorbed dose to water in proton beams are given in Tables 35 and 36.

10.4.2. Determination of absorbed dose under reference conditions

The absorbed dose to water at the reference depth z_{ref} in water in a proton beam of quality Q and in the absence of the chamber is given by the following equation:

$$D_{w,Q}(z_{ref}) = M_Q N_{D,w,Q_o} k_{Q,Q_o} \quad (61)$$

where M_Q is the reading of the dosimeter with the reference point of the chamber positioned at z_{ref} in accordance with the reference conditions given in Tables 35 and 36, corrected for the influence quantities pressure and temperature, electrometer calibration, polarity effect and ion recombination, as described in the worksheet in Section 10.9 (see also Section 4.4.3). N_{D,w,Q_o} is the calibration coefficient in terms of absorbed dose to water for the dosimeter at the reference quality Q_o and k_{Q,Q_o} is a chamber specific factor that corrects for differences between the reference beam quality, Q_o, and the actual quality being used, Q.

For broad beams, the determination of the absorbed dose to water is performed in the centre of the SOBP, while for scanned beams it is generally performed in the initial plateau region for a single energy pencil beam using a single layer scanned field (see Fig. 21). However, in some institutions with a PBS

TABLE 35. REFERENCE CONDITIONS FOR THE DETERMINATION OF ABSORBED DOSE TO WATER IN BROAD PROTON BEAMS CALIBRATED IN A SPREAD-OUT BRAGG PEAK

Influence quantity	Reference value or reference characteristic
Phantom material	Water
Chamber type	For $R_{res} > 0.5$ g/cm^2, cylindrical and plane parallel For $R_{res} < 0.5$ g/cm^2, plane parallel
Measurement depth, z_{ref}	Middle of the spread out Bragg peak
Reference point of the chamber	For plane parallel chambers, on the inner surface of the window, at its centre For cylindrical chambers, on the central axis, at the centre of the cavity volume
Position of the reference point of the chamber	For plane parallel and cylindrical chambers, at the measurement depth z_{ref}
Source–surface distance	Clinical treatment distance
Field size at the phantom surface	10 cm × 10 cm, or the size used for the normalization of the field output factors, whichever is larger For small field applications (i.e. eye treatments), 10 cm × 10 cm or the largest field clinically available

TABLE 36. REFERENCE CONDITIONS FOR THE DETERMINATION OF ABSORBED DOSE TO WATER IN SCANNED PROTON BEAMS CALIBRATED IN A SINGLE ENERGY PENCIL BEAM USING A SINGLE ENERGY LAYER SCANNED FIELD

Influence quantity	Reference value or reference characteristic
Phantom material	Water
Chamber type	For $R_{res} \geq 15$ g/cm^2, cylindrical and plane parallel For $R_{res} < 15$ g/cm^2, plane parallel

TABLE 36. REFERENCE CONDITIONS FOR THE DETERMINATION OF ABSORBED DOSE TO WATER IN SCANNED PROTON BEAMS CALIBRATED IN A SINGLE ENERGY PENCIL BEAM USING A SINGLE ENERGY LAYER SCANNED FIELD (cont.)

Influence quantity	Reference value or reference characteristic
Measurement depth, z_{ref}	The plateau region, at a depth of 2 g/cm^2, for beams with $R_p \geq 5.0$ g/cm^2 The plateau region, at a depth of 1 g/cm^2, for beams with $R_p > 5.0$ g/cm^2
Reference point of the chamber	For plane parallel chambers, on the inner surface of the window at its centre For cylindrical chambers, on the central axis at the centre of the cavity volume
Position of the reference point of the chamber	For cylindrical and plane parallel chambers, at the measurement depth z_{ref}
Source–surface distance	Clinical treatment distance
Reference field size at the phantom surface	Uniform scanned field, large enough to achieve at least 99.5% of lateral charged particle equilibrium (i.e. the field output factor changes by <0.5% for fields larger than the reference field)

delivery system, the calibration may also be performed in the centre of the SOBP if all passive beam shaping elements (e.g. range shifters) are placed downstream of the beam monitoring system [215–217]. In this case, the determination of absorbed dose to water is not performed in the plateau part of the dose distribution, but in the centre of a scanning volume.

The reference conditions for the calibration of scanned proton beams in a single energy pencil beam using a single layer scanned field are given in Table 36. The limit in terms of R_{res} for the use of cylindrical ionization chambers is the result of the constraint that assuming the displacement correction factor p_{dis} to be unity does not introduce an uncertainty of more than 0.5% [218].

The set-up for the determination of the absorbed dose to water with a cylindrical chamber and a plane parallel chamber for a single energy pencil beam using a single layer scanned field is shown in Fig. 21. The schematic spot pattern for a square reference scanned field indicates that the scanning is performed with

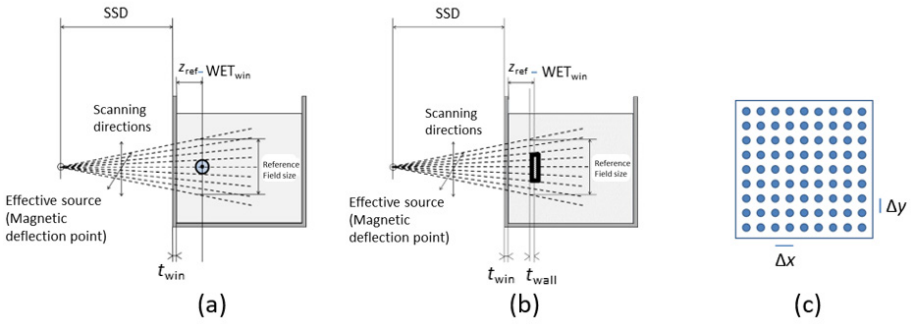

FIG. 21. Illustration of the set-up for the determination of the absorbed dose to water for a single energy pencil beam using a single layer scanned field: (a) cylindrical chamber; (b) plane parallel chamber; (c) schematic spot pattern for a square reference scanned field, with the constant spot spacing Δx and Δy indicated. SSD: source–surface distance; t_{win}*: phantom window thickness;* WET_{win}*: water equivalent thickness;* t_{wall}*: water equivalent thickness of the chamber wall; and* z_{ref}*: reference depth.*

the constant spot spacing Δx, Δy and with a constant number of particles per spot, providing symmetry of 1% and flatness of 2% [219].

10.4.3. Recombination corrections

Different approaches to determine recombination corrections for continuous and pulsed beams are described in Section 4. For clinical proton beams, it is important to establish whether the beam behaves as a continuous beam or as a pulsed beam with respect to recombination. Both cyclotrons and slow extraction synchrotrons provide pulsed beams but the time between pulses is very short compared to the ion collection time of most ionization chambers [210], and therefore most beams are considered to be of the continuous type. Beams from a synchrocyclotron behave as pulsed beams but, depending on the pulse length, the regime could be intermediate. In case of doubt, this should be investigated by making a full Jaffé plot ($1/M$ versus $1/V$). According to the general recombination theory described in Section 4, if the data are well described by a linear fit, then the conditions of a pulsed beam are met. If the data are well described by a linear fit in a plot of $1/M$ versus $1/V^2$, then the conditions for continuous radiation are met.

10.5. VALUES FOR k_{Q,Q_o}

Ideally, the values for k_{Q,Q_o} should be obtained by direct measurement of the absorbed dose at the qualities Q and Q_o (see Eq. (3)) under reference conditions for the user's ionization chamber used for proton dosimetry. However, at present no primary standard of absorbed dose to water for proton beams is available. Therefore all values for k_{Q,Q_o} given in this publication for proton beams are derived by calculation and are based on ^{60}Co gamma radiation as the reference beam quality Q_o. The notation k_Q denotes this exclusive use of ^{60}Co as the reference quality.

Table 37a (for $R_{res} \leq 4$ g/cm^2) and Table 37b (for $R_{res} \geq 4$ g/cm^2) give calculated values for k_Q as a function of R_{res} for cylindrical and plane parallel ionization chambers [220]. Values for k_Q for cylindrical chambers for scanned proton beams with $R_{res} \geq 15$ g/cm^2 are presented in italics, as these chambers are not recommended for scanned beams with $R_{res} < 15$ g/cm^2. Values for k_Q for non-tabulated qualities may be obtained by interpolation between tabulated values. Details of calculations and discussion of the influence of new data [32] on the calculated values of k_Q are provided in Appendix II. The deviation of the updated values from those given in the first edition of this international code of practice is within 1% for the chambers listed in Tables 37a and 37b.

10.6. CROSS-CALIBRATION OF IONIZATION CHAMBERS

Cross-calibration refers to the calibration of a user ionization chamber by direct comparison in a suitable user beam against a reference ionization chamber that has previously been calibrated (see Section 4). An example is the cross-calibration of a plane parallel ionization chamber for use in proton beams against a reference cylindrical ionization chamber calibrated in ^{60}Co gamma radiation. Despite the additional step, such a cross-calibration generally results in a determination of absorbed dose to water using the plane parallel ionization chamber, which is more reliable than that achieved using a plane parallel ionization chamber calibrated directly in ^{60}Co. This is mainly because the problems associated with the p_{wall} correction for plane parallel ionization chambers in ^{60}Co, which enters the determination of k_{Q,Q_o}, are avoided [221].

10.6.1. Cross-calibration procedure

The highest energy proton beam ($R_{res} > 15$ g/cm^2) should be used with the chamber placed in the relatively homogeneous plateau region. For scanned beams, a single layer scanned field should be used. The reference chamber and

the field chamber to be calibrated are compared by alternately positioning each at the reference depth z_{ref} in water in accordance with the reference conditions for each (see Tables 35 and 36). The calibration coefficient in terms of absorbed dose to water for the chamber under calibration, at the proton cross-calibration quality Q_{cross}, is given by the following equation:

$$N_{D,w,Q_{cross}}^{field} = \frac{M_{Q_{cross}}^{ref}}{M_{Q_{cross}}^{field}} N_{D,w,Q_o}^{ref} k_{Q_{cross},Q_o}^{ref} \quad (62)$$

where $M_{Q_{cross}}^{ref}$ and $M_{Q_{cross}}^{field}$ are the dosimeter readings for the reference chamber and the field chamber under calibration, respectively, corrected for the influence quantities temperature and pressure, electrometer calibration, polarity effect and ion recombination, as described in Section 4.4.3. N_{D,w,Q_o}^{ref} is the calibration coefficient in terms of absorbed dose to water for the reference chamber at quality Q_o (i.e. ^{60}Co gamma radiation) and k_{Q_{cross},Q_o}^{ref} is the beam quality correction factor for the reference chamber.

10.6.2. Subsequent use of a cross-calibrated chamber

The cross-calibrated chamber with calibration coefficient $N_{D,w,Q_{cross}}^{field}$ may be used subsequently for the determination of absorbed dose in a user beam of quality Q using the basic Eq. (61), as follows:

$$D_{w,Q} = M_Q^{field} N_{D,w,Q_{cross}}^{field} k_{Q,Q_{cross}}^{field} \quad (63)$$

The values for $k_{Q,Q_{cross}}^{field}$ are derived as follows:

$$k_{Q,Q_{cross}}^{field} = \frac{k_Q^{field}}{k_{Q_{cross}}^{field}} \quad (64)$$

where k_Q^{field} and $k_{Q_{cross}}^{field}$ are taken from Tables 37a and 37b.

10.7. MEASUREMENTS UNDER NON-REFERENCE CONDITIONS

Clinical dosimetry requires the measurement of central axis PDD distributions, transverse beam profiles, field output factors, etc. Such measurements should be made for all possible combinations of energy, field size

TABLE 37a. CALCULATED k_Q VALUES[a] FOR PROTON BEAMS FOR VARIOUS CYLINDRICAL AND PLANE PARALLEL IONIZATION CHAMBERS AS A FUNCTION OF BEAM QUALITY, R_{res}, FOR 0.25 g/cm^2 ≤ R_{res} ≤ 4 g/cm^2 *(see Table 37b for 4 g/cm^2 ≤ R_{res} ≤ 40 g/cm^2)*

Chamber type[b]	Beam quality, R_{res} (g/cm^2)								
	0.25	0.5	1	1.5	2	2.5	3	3.5	4
Cylindrical chambers									
Capintec PR-06C Farmer		1.0366	1.0347	1.0340	1.0337	1.0335	1.0334	1.0333	1.0332
Exradin A1SL Miniature		1.0284	1.0266	1.0259	1.0256	1.0254	1.0253	1.0252	1.0251
Exradin A12 Farmer		1.0382	1.0364	1.0357	1.0354	1.0352	1.0351	1.0350	1.0349
Exradin A12S Short Farmer		1.0363	1.0344	1.0338	1.0334	1.0332	1.0331	1.0330	1.0329
Exradin A18		1.0364	1.0345	1.0338	1.0335	1.0333	1.0332	1.0331	1.0330
Exradin A19 Classic Farmer		1.0380	1.0361	1.0355	1.0351	1.0349	1.0348	1.0347	1.0346
Exradin A28		1.0315	1.0296	1.0290	1.0287	1.0285	1.0283	1.0282	1.0282
IBA CC13		1.0314	1.0295	1.0289	1.0285	1.0283	1.0282	1.0281	1.0280
IBA CC25		1.0369	1.0350	1.0343	1.0340	1.0338	1.0337	1.0336	1.0335

TABLE 37a. CALCULATED k_Q VALUES[a] FOR PROTON BEAMS FOR VARIOUS CYLINDRICAL AND PLANE PARALLEL IONIZATION CHAMBERS AS A FUNCTION OF BEAM QUALITY, R_{res}, FOR 0.25 g/cm^2 ≤ R_{res} ≤ 4 g/cm^2 *(see Table 37b for 4 g/cm^2 ≤ R_{res} ≤ 40 g/cm^2) (cont.)*

Chamber type[b]	Beam quality, R_{res} (g/cm^2)								
	0.25	0.5	1	1.5	2	2.5	3	3.5	4
IBA FC23-C Short Farmer		1.0334	1.0316	1.0309	1.0306	1.0304	1.0303	1.0302	1.0301
IBA FC65-G Farmer		1.0259	1.0240	1.0234	1.0231	1.0229	1.0228	1.0227	1.0226
IBA FC65-P Farmer		1.0303	1.0284	1.0278	1.0274	1.0272	1.0271	1.0270	1.0269
NE 2561/2611A (NPL 2611A) Sec. Std		1.0284	1.0265	1.0259	1.0256	1.0254	1.0252	1.0251	1.0251
NE 2571 Farmer		1.0254	1.0236	1.0229	1.0226	1.0224	1.0223	1.0222	1.0221
PTW 30010 Farmer		1.0265	1.0246	1.0240	1.0237	1.0235	1.0233	1.0232	1.0232
PTW 30011 Farmer		1.0213	1.0194	1.0188	1.0185	1.0183	1.0182	1.0181	1.0180
PTW 30012 Farmer		1.0333	1.0314	1.0308	1.0304	1.0302	1.0301	1.0300	1.0299
PTW 30013 Farmer		1.0284	1.0265	1.0259	1.0256	1.0254	1.0252	1.0251	1.0251
PTW 31010 Semiflex		1.0259	1.0240	1.0234	1.0231	1.0229	1.0228	1.0227	1.0226

TABLE 37a. CALCULATED k_Q VALUES[a] FOR PROTON BEAMS FOR VARIOUS CYLINDRICAL AND PLANE PARALLEL IONIZATION CHAMBERS AS A FUNCTION OF BEAM QUALITY, R_{res}, FOR 0.25 g/cm^2 ≤ R_{res} ≤ 4 g/cm^2 *(see Table 37b for 4 g/cm^2 ≤ R_{res} ≤ 40 g/cm^2) (cont.)*

Chamber type[b]	Beam quality, R_{res} (g/cm^2)								
	0.25	0.5	1	1.5	2	2.5	3	3.5	4
PTW 31013 Semiflex		1.0226	1.0207	1.0201	1.0198	1.0196	1.0194	1.0193	1.0193
PTW 31016 PinPoint 3D		1.0073	1.0055	1.0049	1.0046	1.0044	1.0042	1.0041	1.0041
PTW 31021 Semiflex 3D		1.0342	1.0323	1.0317	1.0314	1.0312	1.0311	1.0310	1.0309
Plane parallel chambers									
Exradin A10	1.0335	1.0298	1.0279	1.0273	1.0270	1.0268	1.0266	1.0265	1.0265
Exradin A11	1.0283	1.0246	1.0228	1.0222	1.0218	1.0216	1.0215	1.0214	1.0213
Exradin A11TW	1.0435	1.0397	1.0378	1.0372	1.0369	1.0367	1.0366	1.0365	1.0364
IBA NACP-02	0.9909	0.9874	0.9856	0.9850	0.9847	0.9845	0.9844	0.9843	0.9842
IBA PPC05	0.9987	0.9951	0.9933	0.9927	0.9924	0.9922	0.9921	0.9920	0.9919
IBA PPC40	1.0018	0.9982	0.9964	0.9957	0.9954	0.9952	0.9951	0.9950	0.9949

TABLE 37a. CALCULATED k_Q VALUES[a] FOR PROTON BEAMS FOR VARIOUS CYLINDRICAL AND PLANE PARALLEL IONIZATION CHAMBERS AS A FUNCTION OF BEAM QUALITY, R_{res}, FOR 0.25 g/cm^2 ≤ R_{res} ≤ 4 g/cm^2 *(see Table 37b for 4 g/cm^2 ≤ R_{res} ≤ 40 g/cm^2) (cont.)*

Chamber type[b]	Beam quality, R_{res} (g/cm^2)								
	0.25	0.5	1	1.5	2	2.5	3	3.5	4
PTW 34045 Adv. Markus	1.0114	1.0077	1.0059	1.0053	1.0050	1.0048	1.0046	1.0046	1.0045
PTW 23343 Markus	1.0119	1.0083	1.0064	1.0058	1.0055	1.0053	1.0052	1.0051	1.0050
PTW 34001 Roos	1.0033	0.9997	0.9979	0.9973	0.9970	0.9968	0.9967	0.9966	0.9965

[a] Values are given to four decimal places to permit smooth interpolation of the data. This does not imply uncertainties of this order.

[b] Some of the chambers listed in this table fail to meet some of the minimum requirements described in Section 4.2.1. However, they have been included in this table because of their current clinical use.

TABLE 37b. CALCULATED k_Q VALUES[a] FOR PROTON BEAMS FOR VARIOUS CYLINDRICAL AND PLANE PARALLEL IONIZATION CHAMBERS AS A FUNCTION OF BEAM QUALITY, R_{res}, FOR 4 g/cm^2 $\leq R_{res} \leq$ 40 g/cm^2 *(see Table 37a for 0.25 g/cm^2 $\leq R_{res} \leq$ 4 g/cm^2)*

Chamber type[b]	Beam quality, R_{res} (g/cm^2)									
	4	4.5	5	7.5	10	15	20	25	30	40
Cylindrical chambers										
Capintec PR-06C Farmer	1.0332	1.0332	1.0331	1.0329	1.0328	*1.0326*	*1.0319*	*1.0315*	*1.0313*	*1.0311*
Exradin A1SL Miniature	1.0251	1.0250	1.0250	1.0248	1.0247	*1.0245*	*1.0240*	*1.0237*	*1.0235*	*1.0234*
Exradin A12 Farmer	1.0349	1.0348	1.0348	1.0346	1.0345	*1.0343*	*1.0336*	*1.0332*	*1.0330*	*1.0328*
Exradin A12S Short Farmer	1.0329	1.0329	1.0328	1.0326	1.0325	*1.0324*	*1.0317*	*1.0313*	*1.0310*	*1.0309*
Exradin A18	1.0330	1.0329	1.0329	1.0327	1.0326	*1.0324*	*1.0320*	*1.0318*	*1.0316*	*1.0314*
Exradin A19 Classic Farmer	1.0346	1.0346	1.0345	1.0343	1.0342	*1.0340*	*1.0333*	*1.0330*	*1.0327*	*1.0326*
Exradin A28	1.0282	1.0281	1.0281	1.0279	1.0278	*1.0276*	*1.0269*	*1.0266*	*1.0263*	*1.0262*
IBA CC13	1.0280	1.0280	1.0279	1.0277	1.0276	*1.0275*	*1.0268*	*1.0264*	*1.0262*	*1.0260*
IBA CC25	1.0335	1.0335	1.0334	1.0332	1.0331	*1.0329*	*1.0323*	*1.0319*	*1.0317*	*1.0315*

TABLE 37b. CALCULATED k_Q VALUES[a] FOR PROTON BEAMS FOR VARIOUS CYLINDRICAL AND PLANE PARALLEL IONIZATION CHAMBERS AS A FUNCTION OF BEAM QUALITY, R_{res}, FOR 4 g/cm^2 ≤ R_{res} ≤ 40 g/cm^2 *(see Table 37a for 0.25 g/cm^2 ≤ R_{res} ≤ 4 g/cm^2) (cont.)*

Chamber type[b]	Beam quality, R_{res} (g/cm^2)									
	4	4.5	5	7.5	10	15	20	25	30	40
IBA FC23-C Short Farmer	1.0301	1.0300	1.0300	1.0298	1.0297	*1.0295*	*1.0288*	*1.0284*	*1.0282*	*1.0280*
IBA FC65-G Farmer	1.0226	1.0225	1.0225	1.0223	1.0222	*1.0220*	*1.0213*	*1.0209*	*1.0207*	*1.0205*
IBA FC65-P Farmer	1.0269	1.0269	1.0268	1.0266	1.0265	*1.0264*	*1.0257*	*1.0253*	*1.0251*	*1.0249*
NE 2561/2611A (NPL 2611A) Sec. Std	1.0251	1.0250	1.0249	1.0248	1.0246	*1.0245*	*1.0237*	*1.0232*	*1.0230*	*1.0228*
NE 2571 Farmer	1.0221	1.0221	1.0220	1.0218	1.0217	*1.0215*	*1.0208*	*1.0205*	*1.0202*	*1.0201*
PTW 30010 Farmer	1.0232	1.0231	1.0230	1.0229	1.0228	*1.0226*	*1.0219*	*1.0215*	*1.0213*	*1.0211*
PTW 30011 Farmer	1.0180	1.0179	1.0179	1.0177	1.0176	*1.0174*	*1.0167*	*1.0164*	*1.0161*	*1.0160*
PTW 30012 Farmer	1.0299	1.0299	1.0298	1.0296	1.0295	*1.0294*	*1.0287*	*1.0283*	*1.0281*	*1.0279*
PTW 30013 Farmer	1.0251	1.0250	1.0249	1.0248	1.0246	*1.0245*	*1.0238*	*1.0234*	*1.0232*	*1.0230*
PTW 31010 Semiflex	1.0226	1.0225	1.0225	1.0223	1.0222	*1.0220*	*1.0214*	*1.0210*	*1.0208*	*1.0206*

TABLE 37b. CALCULATED k_Q VALUES[a] FOR PROTON BEAMS FOR VARIOUS CYLINDRICAL AND PLANE PARALLEL IONIZATION CHAMBERS AS A FUNCTION OF BEAM QUALITY, R_{res}, FOR 4 g/cm^2 ≤ R_{res} ≤ 40 g/cm^2 *(see Table 37a for 0.25 g/cm^2 ≤ R_{res} ≤ 4 g/cm^2) (cont.)*

Chamber type[b]	Beam quality, R_{res} (g/cm^2)									
	4	4.5	5	7.5	10	15	20	25	30	40
PTW 31013 Semiflex	1.0193	1.0192	1.0192	1.0190	1.0189	*1.0187*	*1.0181*	*1.0177*	*1.0175*	*1.0173*
PTW 31016 PinPoint 3D	1.0041	1.0040	1.0039	1.0038	1.0037	*1.0035*	*1.0031*	*1.0029*	*1.0027*	*1.0025*
PTW 31021 Semiflex 3D	1.0309	1.0308	1.0308	1.0306	1.0305	*1.0303*	*1.0297*	*1.0294*	*1.0292*	*1.0290*
Plane parallel chambers										
Exradin A10	1.0265	1.0264	1.0263	1.0262	1.0261	1.0259	1.0257	1.0256	1.0255	1.0253
Exradin A11	1.0213	1.0213	1.0212	1.0210	1.0209	1.0208	1.0206	1.0205	1.0204	1.0202
Exradin A11TW	1.0364	1.0363	1.0363	1.0361	1.0360	1.0358	1.0357	1.0355	1.0354	1.0352
IBA NACP-02	0.9842	0.9841	0.9841	0.9839	0.9838	0.9836	0.9835	0.9834	0.9833	0.9831
IBA PPC05	0.9919	0.9919	0.9918	0.9916	0.9915	0.9914	0.9912	0.9911	0.9910	0.9908
IBA PPC40	0.9949	0.9949	0.9948	0.9947	0.9946	0.9944	0.9943	0.9941	0.9940	0.9938

TABLE 37b. CALCULATED k_Q VALUES[a] FOR PROTON BEAMS FOR VARIOUS CYLINDRICAL AND PLANE PARALLEL IONIZATION CHAMBERS AS A FUNCTION OF BEAM QUALITY, R_{res}, FOR 4 g/cm^2 ≤ R_{res} ≤ 40 g/cm^2 *(see Table 37a for 0.25 g/cm^2 ≤ R_{res} ≤ 4 g/cm^2) (cont.)*

Chamber type[b]	Beam quality, R_{res} (g/cm^2)									
	4	4.5	5	7.5	10	15	20	25	30	40
PTW 34045 Adv. Markus	1.0045	1.0044	1.0044	1.0042	1.0041	1.0039	1.0038	1.0037	1.0035	1.0033
PTW 23343 Markus	1.0050	1.0049	1.0049	1.0047	1.0046	1.0044	1.0043	1.0042	1.0041	1.0038
PTW 34001 Roos	0.9965	0.9964	0.9964	0.9962	0.9961	0.9959	0.9958	0.9957	0.9956	0.9953

[a] Values are given to four decimal places to permit smooth interpolation of the data. This does not imply uncertainties of this order.

[b] Some of the chambers listed in this table fail to meet some of the minimum requirements described in Section 4.2.1. However, they have been included in this table because of their current clinical use.

Note: k_Q values for cylindrical chambers for scanned proton beams with R_{res} ≥ 15 g/cm^2 are presented in italics.

and SSD used for radiotherapy treatments (or a representative subset in the case of scanning beams). For the measurement of transverse profiles or three dimensional dose distributions, very small ionization chambers with a cavity volume smaller than ~0.1 cm^3 should be used. For dosimeters other than ionization chambers, the energy and/or depth dependence of the detector response should be checked against ionization chambers. For scanned proton beams, a particular requirement is the measurement of integrated radial profiles as a function of depth for single static pencil beams. Such measurements should be made for a representative subset of energies, field sizes, spot sizes and SSDs used for radiotherapy treatments [210]. The recommendations given in Section 10.2 for the selection of ionization chambers and phantoms should be followed.

10.7.1. Central axis depth dose distributions

For measurements of depth dose distributions of broad proton beams, the use of plane parallel ionization chambers is recommended. The measured depth ionization distribution has to be converted to a depth dose distribution because of the depth dependence of the stopping power ratio $s_{w,air}$, particularly in the low energy region. This is achieved by multiplying the measured ionization charge or current at each depth z by the stopping power ratio $s_{w,air}$ and the perturbation factor at that depth. Values for $s_{w,air}$ as a function of R_{res} can be calculated from Eq. (100) in Appendix II. Perturbation factors are assumed to have a value of unity (see Appendix II). The influence of ion recombination and polarity effects on the depth ionization distribution should be investigated and taken into account if there is a variation with depth.

If the field size for which measurements are to be performed is smaller than twice the diameter of the cavity of the plane parallel chamber, then a detector with a better spatial resolution (e.g. mini-chamber, diode, diamond detector) is recommended [222, 223]. The resulting distribution also has to be converted using the appropriate stopping power ratios (e.g. water to air, water to silicon, water to graphite). For this purpose, the necessary stopping power values can be found in Ref. [210]. The suitability of such detectors for depth dose measurements should be verified by test comparisons with a plane parallel ionization chamber at a larger field size.

For clinical proton beams produced by PBS delivery systems, measurements for pencil beams are performed with large area plane parallel ionization chambers in a similar way to the measurement of depth dose curves using plane parallel ionization chambers in broad beams. However, the result for scanned beams is an integrated radial profile as a function of depth.

10.7.2. Field output factors

The field output factor may be determined as the ratio of the corrected dosimeter reading at the reference depth z_{ref} measured under a given set of non-reference conditions to that measured under reference conditions (reference conditions are given in Tables 35 and 36).

10.7.3. Use of plastic phantoms for relative dosimetry

The use of plastic phantoms is strongly discouraged, as in general they introduce discrepancies in the determination of the absorbed dose. Plastic phantoms should not be used for reference dosimetry in proton beams, because the required water to plastic fluence correction factors, h_{pl}, are not well known. Nevertheless, when accurate chamber positioning in water is not possible or when no waterproof chamber is available, their use is permitted for the measurement of depth dose distributions for low energy proton beams (below ~100 MeV). In this case, the dosimeter reading at each plastic depth should be scaled using the fluence correction factor h_{pl}. It is assumed that h_{pl} has a constant value of unity at all depths.

The criteria determining the choice of plastic materials are discussed in Section 4.2.3. The density of the plastic, ρ_{pl}, should be measured for the batch in use instead of using a nominal value for the type of plastic. Each measurement depth in plastic z_{pl} (expressed in g/cm^2) also has to be scaled to give the corresponding depth in water z_w by the following equation:

$$z_w = z_{pl} c_{pl} \tag{65}$$

where c_{pl} is a depth scaling factor and z_w is expressed in units of g/cm^2. In proton dosimetry, the product $z_{pl}c_{pl}$ is commonly referred to as the water equivalent thickness of the slab. For proton beams, c_{pl} can be calculated, to a good approximation, as the ratio of the continuous slowing down approximation ranges (expressed in g/cm^2) [49] in water and in plastic. The depth scaling factor c_{pl} has a value of 0.974 for PMMA and 0.981 for clear polystyrene. The procedure described in Section 10.7.1 should be followed to generate central axis depth dose distributions from the measured depth ionization distributions.

If a plastic phantom is used to measure the beam quality index, the measured quantity is the residual range in the plastic, $R_{res,pl}$. The residual range, R_{res}, in water is also obtained using the scaling Eq. (65).

10.8. ESTIMATED UNCERTAINTY IN THE DETERMINATION OF ABSORBED DOSE TO WATER UNDER REFERENCE CONDITIONS

The uncertainties associated with the physical quantities and procedures involved in the determination of the absorbed dose to water in the user proton beam can be estimated separately for broad proton beams calibrated in the SOBP and for scanned proton beams calibrated in a single energy pencil beam using a single energy layer scanned field. For both types of beam, each of these uncertainties can be determined in two steps. Step 1 considers uncertainties up to the calibration of the user chamber in terms of $N_{D,w}$ at a standards laboratory. Step 2 deals with the subsequent calibration of the user proton beam using this chamber and includes the uncertainty of k_Q as well as that associated with measurements at the reference depth in a water phantom.

It is the responsibility of users to establish an uncertainty budget for their determination of the absorbed dose to water. Table 38 provides estimates of the relative standard uncertainties in these two steps for broad proton beams calibrated in the SOBP and for scanned proton beams calibrated in a single energy pencil beam using single energy layer scanned field, which yield a combined relative standard uncertainty of 1.7% for the determination of the absorbed dose to water with cylindrical and plane parallel ionization chambers. These estimates may vary depending on the uncertainty quoted by the calibration laboratory, the care and experience of the user performing the measurement, and the quality and condition of the measurement equipment (e.g. regular recalibration of all measurement devices, quality management system to ensure proper functioning). The uncertainty component ‘establishment of reference conditions’ includes uncertainty due to potential ripple effects in the SOBP (effects produced by modulators) and dose gradient corrections. This uncertainty is slightly smaller for scanned beams because the calibration is made in the plateau region, but this has no significant effect on the combined uncertainty.

TABLE 38. ESTIMATED RELATIVE STANDARD UNCERTAINTY[a] (%) OF $D_{w,Q}$ AT THE REFERENCE DEPTH IN WATER FOR A CLINICAL PROTON BEAM BASED ON A CHAMBER CALIBRATION IN ^{60}Co GAMMA RADIATION

Physical quantity or procedure	Cylindrical and plane parallel chambers
Step 1: standards laboratory	
$N_{D,w}$ calibration of secondary standard at PSDL	0.5[b]
Long term stability of secondary standard	0.1
$N_{D,w}$ calibration of the user dosimeter at the standards laboratory	0.4
Combined uncertainty in step 1	0.6
Step 2: user proton beam	
Long term stability of user dosimeter	0.3
Establishment of reference conditions	0.4 (0.3)[c]
Dosimeter reading M_Q relative to beam monitor	0.3
Correction for influence quantities k_i	0.3
Beam quality correction, k_Q (see Appendix II)	1.4
Combined uncertainty in step 2	1.6
Combined standard uncertainty in $D_{w,Q}$ (steps 1 and 2)	1.7

[a] See Ref. [61] or Appendix IV for the expression of uncertainty. The estimates given in the table should be considered typical values; these may vary depending on the uncertainty quoted by standards laboratories for calibration coefficients and on the experimental uncertainty at the user's institution.

[b] If the calibration of the user's dosimeter is performed at a PSDL, then the combined standard uncertainty in step 1 is lower. The combined standard uncertainty in D_w should be adjusted accordingly.

[c] Estimated relative standard uncertainties for a scanned clinical beam calibrated in a single energy pencil beam using a single energy layer scanned field are shown in parentheses.

Table 39 shows estimates of the relative standard uncertainties for the determination of the absorbed dose to water in a clinical proton beam using a cylindrical ionization chamber cross-calibrated against a reference chamber in a proton beam, which yield a combined relative standard uncertainty of 2.0%. As stated above, this estimate may vary depending on the uncertainty quoted by the calibration laboratory, the care and experience of the user performing the measurement, and the quality and condition of the measurement equipment. In this case, the uncertainty is higher owing to the contribution of the cross-calibration step. As in Table 38, the uncertainty for the establishment of reference conditions is slightly smaller for scanned beams because the calibration is made in the plateau regions, but this has no significant effect on the combined uncertainty. Details on the uncertainty estimation for the various physical parameters entering the calculation of k_Q are given in Appendix II.

TABLE 39. ESTIMATED RELATIVE STANDARD UNCERTAINTY (%)[a] OF $D_{w,Q}$ AT THE REFERENCE DEPTH IN WATER FOR A CLINICAL PROTON BEAM BASED ON A CHAMBER CROSS-CALIBRATED IN A PROTON BEAM AGAINST A REFERENCE CHAMBER

Physical quantity or procedure	Reference cylindrical chamber
Step 1: standards laboratory	
N_{D,w,Q_o} calibration in a ^{60}Co beam at a secondary standards dosimetry laboratory	0.6 [b]
Step 2: cross-calibration of plane parallel chamber in user's proton beam	
Ratio of dosimeter readings $M^{ref}_{Q_{cross}} \Big/ M^{field}_{Q_{cross}}$	0.6
Long term stability of user's dosimeter	0.3
Establishment of reference conditions	0.4 (0.3) [c]
Correction for influence quantities k_i	0.3
k_{Q_{cross},Q_o} for reference chamber (Q_o is ^{60}Co beam)	1.6
Combined uncertainty in step 2	1.7

TABLE 39. ESTIMATED RELATIVE STANDARD UNCERTAINTY (%)[a] OF $D_{w,Q}$ AT THE REFERENCE DEPTH IN WATER FOR A CLINICAL PROTON BEAM BASED ON A CHAMBER CROSS-CALIBRATED IN A PROTON BEAM AGAINST A REFERENCE CHAMBER (cont.)

Physical quantity or procedure	Reference cylindrical chamber
Step 3: user's clinical proton beam	
Dosimeter reading M_Q relative to the beam monitor	0.3
Long term stability of user dosimeter	0.3
Establishment of reference conditions	0.4 (0.3) [c]
Correction for influence quantities k_i	0.3
Beam quality correction, $k_{Q,Q_{cross}}$	0.6
Combined uncertainty in step 3	0.9
Combined standard uncertainty in $D_{w,Q}$ (steps 1, 2 and 3)	2.0

[a] See Ref. [7] or Appendix IV for the expression of uncertainty. The estimates given in the table should be considered typical values; these may vary depending on the uncertainty quoted by standards laboratories for calibration coefficients and on the experimental uncertainty at the user's institution.

[b] If the calibration of the user dosimeter is performed at a PSDL, then the combined standard uncertainty in step 1 is lower. The combined standard uncertainty in D_w should be adjusted accordingly.

[c] Estimated relative standard uncertainties for a scanned clinical beam calibrated in a single energy pencil beam using a single layer scanned field are shown in parentheses.

10.9. WORKSHEET

Determination of the absorbed dose to water in a proton beam

User: _____ Date: _____

1. Radiation treatment unit and reference conditions for $D_{w,Q}$ determination

Proton therapy unit: _____ Nominal energy: _____ MeV

Nominal dose rate: _____ MU/min Practical range, R_p = _____ g/cm^2

Reference phantom: Water Width of the SOBP: _____ g/cm^2

Reference field size: _____ cm × cm Reference SSD: _____ cm

Reference depth, z_{ref} = _____ g/cm^2 Beam quality, $Q(R_{res})$ = _____ g/cm^2

2. Ionization chamber and electrometer

Ionization chamber model: _____ Serial no.: Type: ☐ cyl ☐ pp

Chamber wall/window Material: _____ Thickness: _____ g/cm^2

Waterproof sleeve/cover Material: _____ Thickness: _____ g/cm^2

Phantom window Material: _____ Thickness: _____ g/cm^2

Absorbed dose to water calibration coefficient, $N_{D,w}$ = _____ ☐ Gy/nC ☐ Gy/rdg

Reference conditions for calibration P_o = _____ kPa T_o = _____ °C Rel. humidity: _____%

Polarizing potential V_1: _____ V

Calibration polarity: ☐ positive ☐ negative ☐ corrected for polarity effect

User polarity: ☐ positive ☐ negative

Calibration laboratory: _____ Date: _____

Electrometer model: Serial no.: _____

Calibrated separately from chamber: ☐ yes ☐ no Range setting: _____

If yes Calibration laboratory: Date: _____

3. Dosimeter reading[a] and correction for influence quantities

Uncorrected dosimeter reading at V_1 and user polarity: _____ ☐ nC ☐ rdg

Corresponding accelerator monitor units: _____ MU

Ratio of dosimeter reading and monitor units: M_1 = _____ ☐ nC/MU ☐ rdg/MU

(a) Pressure P = _____ kPa Temperature T = _____ °C Rel. humidity (if known): _____%

$$k_{TP} = \frac{(273.2+T)}{(273.2+T_o)}\frac{P_o}{P} = \_\_\_\_\_$$

(b) Electrometer calibration factor[b] k_{elec} = _____ ☐ nC/rdg ☐ dimensionless

(c) Polarity correction[c] Reading at $+V_1$: M_+ = _____ Reading at $-V_1$: M_- = _____

$$k_{pol} = \frac{|M_+| + |M_-|}{2M} = \_\_\_\_\_$$

(d) Recombination correction

(i) If the two voltage method is applicable:

Polarizing voltages: V_1 (normal) = _____V V_2 (reduced) = _____V

Readings[d] at V_1, V_2: M_1 = _____ M_2 = _____

Voltage ratio V_1/V_2 = _____ Ratio of readings M_1/M_2 = _____

Use Table 10 for a beam of type: ☐ pulsed ☐ pulsed–scanned

a_0 = _____ a_1 = _____ a_2 = _____[e, f]

$$k_s = a_0 + a_1\left(\frac{M_1}{M_2}\right) + a_2\left(\frac{M_1}{M_2}\right)^2 = \_\_\_\_\_$$

(ii) If the two voltage method is not applicable:

k_s = _____

Corrected dosimeter reading at the voltage V_1:

$M_Q = M_1 k_{TP} k_{elec} k_{pol} k_s$ = _____ ☐ nC/MU ☐ rdg/MU

4. Absorbed dose to water at the reference depth, z_{ref}

Beam quality correction factor for user quality Q: k_Q = _____

Taken from ☐ Table 37a, 37b ☐ other, specify: _____

Absorbed dose calibration of monitor at z_{ref}:

$$D_{w,Q}(z_{ref}) = M_Q N_{D,w} k_Q = \_\_\_\_\_ \text{ Gy/MU}$$

---

[a] All readings should be checked for leakage and corrected if necessary.

[b] If the electrometer is not calibrated separately, then set $k_{elec} = 1$.

[c] M in the denominator of k_{pol} denotes the reading at the user's polarity. Preferably, each reading in the equation should be the average of the ratios of M (or M_+ or M_-) to the reading of an external monitor, M_{em}.

It is assumed that the calibration laboratory has performed a polarity correction. Otherwise k_{pol} is determined according to the following:

Reading at $+V_1$ for quality Q_o: M_+ = _____ Reading at $-V_1$ for quality Q_o: M_- = _____

$$k_{pol} = \left[\left(|M_+| + |M_-|\right)/|M|\right]_Q \Big/ \left[\left(|M_+| + |M_-|\right)/|M|\right]_{Q_o} = \_\_\_\_\_$$

[d] Strictly, readings should be corrected for the polarity effect (average from both polarities). Preferably, each reading in the equation should be the average of the ratios of M_1 or M_2 to the reading of an external monitor, M_{em}.

[e] It is assumed that the calibration laboratory has performed a recombination correction. Otherwise the factor $k_s' = k_s / k_{s,Q_o}$ should be used instead of k_s. When Q_o is ^{60}Co, k_{s,Q_o} (at the calibration laboratory) will normally be close to unity and the effect of not using this equation will be negligible in most cases.

[f] Check that $k_s - 1 \approx (M_1/M_2 - 1)/(V_1/V_2 - 1)$.

Note: SOBP: spread-out Bragg peak; SSD: source–surface distance; cyl: cylindrical; pp: plane parallel; MU: monitor unit.

11. CODE OF PRACTICE FOR LIGHT ION BEAMS

11.1. GENERAL

According to the recommendations of the IAEA and ICRU [29, 30], any nucleus with an atomic number equal to, or smaller than, that of neon (Z = 10) is called a 'light ion', and the term 'heavy ions' is used for heavier nuclei. This section provides a code of practice for reference dosimetry and recommendations for relative dosimetry for light ions heavier than protons. The recommendations are based on a calibration coefficient in terms of absorbed dose to water for an ionization chamber in a reference beam that, owing to the lack of primary standards for light ions, is taken to be ^{60}Co gamma rays; however, other beam types, such as a proton or a megavolt photon beam, could also be used as the reference quality (see Section 3.2.3). The code of practice applies to light ion beams that have ranges of 2–30 g/cm^2 in water. For a carbon beam, this corresponds to an energy range of 85–430 MeV/u.

As for proton beams, the depth dose distribution of a monoenergetic light ion beam in water, shown in Fig. 22, has a sharp Bragg peak near the region where primary particles stop. For clinical applications of light ion beams, SOBPs include the complete target volume. In contrast to most therapeutic radiation beams (excluding neutrons and protons), owing to the strong dependence of the biological response on the energy of light ions in clinical applications, it is common to use absorbed dose multiplied by the relative biological effectiveness

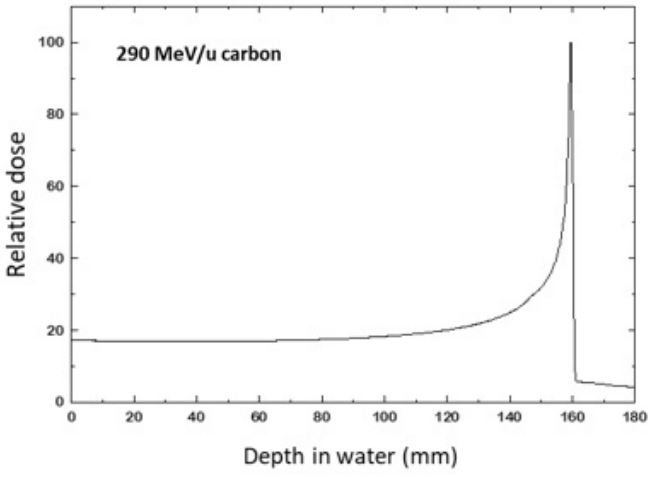

FIG. 22. Depth dose distribution of a monoenergetic 290 MeV/u carbon beam in water.

(RBE) of the beam for the tissue under consideration, or the RBE weighted dose [30, 224], in prescribing, recording and reporting light ion beam therapy. The difference between the two kinds of distribution can be seen in Figs 23 and 24, where the modulation of the absorbed dose distribution in the SOBP is obvious. In the case of clinical neutron and proton beams, a fixed RBE value is typically used throughout the irradiation field. In the case of light ions, the RBE varies

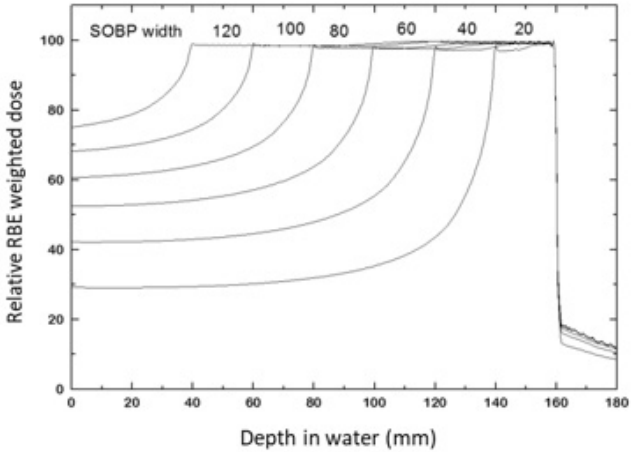

FIG. 23. Relative biological effectiveness (RBE) weighted dose distributions of therapeutic 290 MeV/u carbon beams. The spread out Bragg peak (SOBP) widths of 20–120 mm are designed to yield a uniform biological effect in the peaks [224, 225].

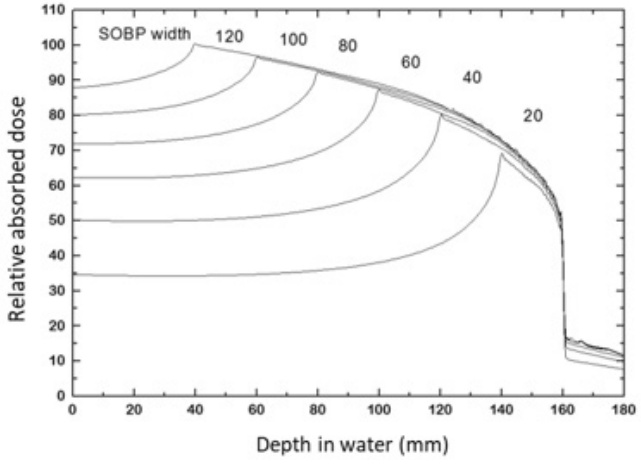

FIG. 24. Absorbed dose distributions of the beams shown in Fig. 23 [224, 225].

with depth and with the dose delivered to the tissue, as well as with tissue type, endpoint and some other parameters. In principle, the same is true for protons, but owing to the smaller RBE variation, a constant RBE value of 1.1 is recommended by ICRU [210]. The use of an RBE weighted dose is an attempt to achieve a homogenous biological effect in the target volume and allows the comparison of clinical results obtained with conventional radiotherapy to those obtained using light ion radiotherapy.

In this international code of practice, however, the dosimetry of light ions is restricted to the determination of the absorbed dose and does not include radiobiological considerations. The reason for this approach is the feasibility of using the same formalism and procedures for all the radiotherapy beams used throughout the world in order to achieve international consistency in dosimetry. The robustness of a common framework for radiotherapy dosimetry will encourage correlated comparisons of the delivery of absorbed dose to patients, reducing the number of degrees of freedom in comparing the outcome of a radiotherapy treatment. Biological studies can then be made on the basis of uniform dosimetry procedures.

Light ion beams used in radiotherapy have a distinct physical characteristic for radiation dosimetry compared to other therapeutic radiation beams [226]. In the case of high energy protons, incident particles interact with target nuclei and produce low energy protons or heavier ions through recoil. When light ions pass through beam modulating devices or human tissues, they produce highly energetic fragments of the projectile and low energetic fragments of the target nuclei. The projectile fragments have approximately the same velocity as the incident light ions at the point of production and, because of their lower charge, have a longer range than the incident particles. Many kinds of atomic nuclei are produced, all with different energy distributions. In the case of carbon ions, nuclei with $Z = 1$ (protons) up to $Z = 5$ (beryllium) are produced as secondary nuclei during projectile fragmentation. This fragmentation of projectiles and (to a lesser extent) target nuclei has a considerable effect on the response of both biological samples and dosimeters to light ion beams. Compared with the depth dose distribution of a proton beam (see Fig. 19), the distribution in Fig. 22 shows a tail at the distal end of the Bragg peak, which is due to the fragmentation of the incident particles.

As for proton beams, two types of light ion beam delivery system are currently available: the broad beam delivery system, which uses scattered or uniformly scanned beams, and the PBS delivery system, which uses intensity modulated scanned beams [210]. In broad beam delivery systems, the beam is spread uniformly and then conformed to the target using customized devices such as a collimator and a range compensator. In PBS delivery systems, a narrow beam is electromagnetically scanned over the target volume in a sequence specifically designed for each target with a treatment planning

system. Recommendations for ionization chamber dosimetry for broad light ion beams based on absorbed dose to water standards were provided by the first edition of this international code of practice. However, reference dosimetry for beams delivered by intensity modulated scanning, which is becoming routine practice in light ion beam therapy, was not covered. This publication includes recommendations for the determination of absorbed dose for broad and scanned light ion beams. The procedures for reference dosimetry for the PBS delivery system are substantially different from those for the broad beam delivery system. This is because during PBS the dose is delivered to the patient by a large number of small pencil beams and the number of particles in each of these pencil beams has to be specified and controlled by the dose monitor. It should be noted that only a few comparisons of carbon beam dosimetry have been performed: three were made before the publication of the first edition of this international code of practice [227–229] and only one was performed more recently, between Japanese centres [230].

11.2. DOSIMETRY EQUIPMENT

11.2.1. Ionization chambers

The recommendations regarding ionization chambers given in Section 4.2.1 should be followed. Cylindrical and plane parallel ionization chambers are recommended for use as reference instruments in clinical broad and scanning light ion beams. The use of cylindrical ionization chambers is limited to light ion beams with a range of ≥ 0.5 g/cm^2, if measurements are performed in the entrance plateau (typically for monoenergetic beams). Graphite walled cylindrical chambers are preferred to plastic walled chambers because of their better long term stability and smaller chamber to chamber variations (see Section 4.2.1 and Fig. 2). The reference point for these chambers is taken to be on the central axis of the chamber at the centre of the cavity volume. In the case of light ion beams, an effective point of measurement of the chamber, P_{eff}, should be used because the depth dose distribution in the SOBP is not flat and the slope depends on the width of the SOBP and on the RBE variation within the SOBP [227]. The reference point of the cylindrical chamber should be positioned at a distance of $0.75r_{\text{cyl}}$ deeper than the point of interest in the phantom [231].

Plane parallel ionization chambers can be used for reference dosimetry in all light ion beams and have to be used for light ion beams with a range of <0.5 g/cm^2. For plane parallel ionization chambers, the reference point is taken on the inner surface of the entrance window, at the centre of the window. This point is positioned at the point of interest in the phantom. The cavity diameter

of the plane parallel ionization chamber or the cavity length of the cylindrical ionization chamber should not be larger than approximately half of the reference field size. The diameter of a cylindrical ionization chamber should not be larger than approximately half of the width of the SOBP for measurements in the SOBP.

For relative dosimetry, plane parallel ionization chambers are recommended for depth dose measurements, while small volume cylindrical ionization chambers should be used for profile and specific quality assurance measurements, such as dosimetric plan verification. The ionization chamber types for which data are given in this publication are listed in Section 11.6.

11.2.2. Phantoms and chamber sleeves

The recommendations regarding phantoms and chamber sleeves given in Sections 4.2.3 and 4.2.4 should be followed. Water is recommended as the reference medium for measurements of absorbed dose in light ion beams. The phantom should extend to at least 5 cm beyond all four sides of the field size employed at the depth of measurement and to at least 5 g/cm^2 beyond the maximum depth of measurement.

In horizontal beams, the window of the phantom should be made of plastic and be of a thickness t_{win} of 0.2–0.5 cm. The water equivalent thickness (in g/cm^2) of the phantom window should be taken into account when evaluating the depth at which the chamber is to be positioned; this thickness is calculated approximately as the product $t_{win}\rho_{pl}$. For the commonly used plastic PMMA, the nominal value r_{PMMA} = 1.19 g/cm^3 [48] may be used for the calculation of the water equivalent thickness of the window. For window thicknesses larger than 0.5 cm, the water equivalent thickness should be calculated in accordance to Section 10.7.3 rather than by scaling by density. For PMMA, a depth scaling factor of c_{pl} = 0.974 is typically used.

For non-waterproof chambers, a waterproofing sleeve made of PMMA and preferably not thicker than 1.0 mm should be used. The air gap between the chamber wall and the waterproofing sleeve should be sufficient (0.1–0.3 mm) to allow the air pressure in the chamber to equilibrate. The same waterproofing sleeve that was used for calibration of the user's ionization chamber should also be used for reference dosimetry; if this is not possible, then another sleeve of the same material and of similar thickness should be used. Plane parallel ionization chambers, if not inherently waterproof or supplied with a waterproof cover, have to be used in a waterproof enclosure (preferably made of PMMA or a material that closely matches the chamber walls); ideally, there should be no more than 1 mm of added material in front of and behind the cavity volume. The water equivalent thickness of the enclosure and sleeves should be calculated with the relative stopping power, as for the windows.

Plastic phantoms should not be used for reference dosimetry in light ion beams at larger depths (i.e. above 2 g/cm^2), since the required water to plastic fluence correction factors, h_{pl}, are not accurately known [232]. However, plastic phantoms can be used for routine quality assurance measurements at larger depths, provided that a transfer factor between plastic and water has been established.

11.3. BEAM QUALITY SPECIFICATION

Beam quality specifiers for all radiotherapy beams are described in Appendix III. Monte Carlo studies [233–238] have shown that most of the effects of fragment spectra on dosimetric quantities in light ion beams can be described reasonably well by using some simplified physical parameters. For light ions, the residual range R_{res} may be used rather than a characterization by the atomic number, mass number, energy of the incident light ion beam, width of the SOBP and range, as suggested in the previous edition of this international code of practice. This is in accordance with the procedure for proton beams (Section 10). However, the uncertainty related to light ion dosimetry is larger than the influence of the beam quality. Therefore, in contrast to the recommendations for proton beams, the residual range is not used as a beam quality specifier for light ion beams in this publication.

11.4. DETERMINATION OF ABSORBED DOSE TO WATER

11.4.1. Reference conditions

For broad beams the absorbed dose to water is determined in the centre of the SOBP, while for scanning beams it is generally determined in the plateau region at a depth of 10 mm in water for a single energy pencil beam using a single layer scanned field (see Fig. 25). If, owing to technical reasons, a depth of 10 mm is not convenient, 20 mm may be used. As shown in Fig. 24, the SOBP of a light ion depth dose distribution is not flat, and the dose at the distal end of the SOBP is smaller than that at the proximal part. The slope near the centre of a broad SOBP is rather small, whereas that of a narrow SOBP is steep. The reference depth for calibration should be taken at the centre of the SOBP, which is typically also the centre of the target volume.

Reference conditions for the determination of absorbed dose to water are given in Tables 40 and 41.

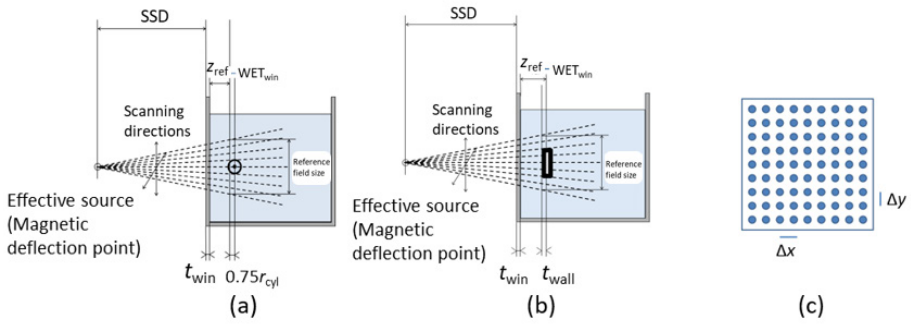

FIG. 25. Illustration of the set-up for the determination of the absorbed dose to water for a single energy pencil beam using a single layer scanned field: (a) cylindrical chamber; (b) plane parallel chamber; (c) schematic spot pattern for a square reference single layer scanned field, with the constant spot spacing Δx and Δy indicated. SSD: source–surface distance; t_{win}*: thickness of the phantom window;* WET_{win} *water equivalent thickness of the phantom window;* z_{ref}*: shallow reference depth;* r_{cyl}*: radius of the cylindrical ionization chamber cavity.*

11.4.2. Determination of absorbed dose under reference conditions

The absorbed dose to water at the reference depth z_{ref} in water, in a light ion beam of quality Q and in the absence of the chamber is given by the following equation:

$$D_{\mathrm{w},Q} = M_Q N_{D,\mathrm{w},Q_\mathrm{o}} k_{Q,Q_\mathrm{o}} \tag{66}$$

where M_Q is the reading of the dosimeter corrected for the influence quantities temperature and pressure, electrometer calibration, polarity effect and ion recombination, as described in the worksheet in Section 11.8 (see also Section 4.4.3). The chamber should be positioned in accordance with the reference conditions, as given in Table 40 or Table 41. $N_{D,\mathrm{w},Q_\mathrm{o}}$ is the calibration coefficient in terms of absorbed dose to water for the dosimeter at the reference quality Q_o, and k_{Q,Q_o} is a chamber specific factor that corrects $N_{D,\mathrm{w},Q_\mathrm{o}}$ for the differences between the reference beam quality Q_o and the actual beam quality Q. When Q_o corresponds to ^{60}Co, the beam quality correction factor is denoted by k_Q.

The set-up for the determination of the absorbed dose to water with a cylindrical chamber and parallel plane chamber for a single energy pencil beam using a single layer scanned field is shown in Fig. 25. The schematic spot pattern for a square reference scanned field is also shown in this figure to indicate that the scanning is performed typically with the constant spot spacing Δx and Δy, providing a symmetry of 1% and a flatness of 2% [30, 219].

TABLE 40. REFERENCE CONDITIONS FOR THE DETERMINATION OF ABSORBED DOSE IN BROAD LIGHT ION BEAMS CALIBRATED IN THE SPREAD-OUT BRAGG PEAK

Influence quantity	Reference value or reference characteristic
Phantom material	Water
Chamber type	For SOBP width ≥2.0 g/cm^2, cylindrical and plane parallel For SOBP width <2.0 g/cm^2, plane parallel
Measurement depth, z_{ref}	Middle of the SOBP
Reference point of chamber	For plane parallel chambers, on the inner surface of the window at its centre For cylindrical chambers, on the central axis at the centre of the cavity volume
Position of reference point of chamber	For plane parallel chambers, at the measurement depth z_{ref} For cylindrical chambers, $0.75r_{cyl}$ deeper than z_{ref}
Source–surface distance	Clinical treatment distance
Field size at the phantom surface	10 cm × 10 cm, or that used for normalization of the field output factors, whichever is larger

Note: SOBP: spread-out Bragg peak.

11.4.3. Recombination correction in light ion beams

Different approaches for determining recombination corrections for continuous and pulsed beams are described in Section 4.4.3.4. As for proton beams, for clinical light ion beams it is important to establish whether the beam behaves as a continuous beam or as a pulsed beam with respect to recombination. All currently known clinical light ion beams behave as continuous beams, but in case of doubt, this should be investigated by making a Jaffé plot ($1/M$ versus $1/V$). If the data are well described by a linear fit, then the conditions for a pulsed scanned beam are met. If the data are well described by a quadratic linear fit in a plot of $1/M$ versus $1/V^2$, then the conditions for continuous radiation are met.

For plane parallel ionization chambers in continuous scanned and broad light ion beams, the two voltage method should not be used, because initial

TABLE 41. REFERENCE CONDITIONS FOR THE DETERMINATION OF ABSORBED DOSE IN SCANNED LIGHT ION BEAMS CALIBRATED IN A SINGLE ENERGY PENCIL BEAM USING A SINGLE LAYER SCANNED FIELD

Influence quantity	Reference value or reference characteristic
Phantom material	Water
Chamber type	Cylindrical and plane parallel
Measurement depth z_{ref}	The plateau region, preferentially at a depth of 1 g/cm^2 (alternatively 2 g/cm^2)
Reference point of chamber	For plane parallel chambers, on the inner surface of the window at its centre For cylindrical chambers, on the central axis at the centre of the cavity volume
Position of reference point of chamber	For plane parallel chambers, at the measurement depth z_{ref} For cylindrical chambers, $0.75r_{cyl}$ deeper than z_{ref}
Source–surface distance	Clinical treatment distance
Reference field size[a] at the phantom surface	10 cm × 10 cm or that used for normalization of the field output factors, whichever is larger

[a] The reference field is a uniform scanned field, large enough to achieve at least 99.5% of lateral charged particle equilibrium (i.e. the field output factor changes by <0.5% for fields larger than the reference field).

recombination is not negligible and is a complex function of $1/V$ [239]. In contrast to proton beams, it cannot be assumed that initial recombination is small at high voltages; however, it becomes approximately linear with voltage and for most systems it is the dominant contribution to recombination. It is therefore advised to produce a full Jaffé plot, as explained in Section 4, to determine the linear region in the plot of $1/M$ versus $1/V$. It may be advisable to operate at higher voltage; otherwise, the initial recombination is unacceptably large. A linear extrapolation method in which the reading at the operating voltage V_o is not one of the data points used to determine recombination should then be used. This linear extrapolation method can either be based on a linear fit to multiple data points

in a plot of $1/M$ versus $1/V$ or be an alternative two voltage method in which the operating voltage V_o is not one of the two data points in the linear region.

For cylindrical ionization chambers in continuous scanned and broad light ion beams, the two voltage method may be used with care. If initial recombination is not negligible, the recombination correction determined with the two voltage method will not be accurate. Initial recombination can be minimized by operating at higher voltage. For continuous scanned light ion beams, it may also be advisable to operate at higher voltage; otherwise, general recombination becomes unacceptably large. In both cases, the recombination correction determined can be incorrect if charge multiplication or any another type of distortion of the Jaffé plot occurs at the operating voltage. It is then advised to produce a full Jaffé plot, as explained in Section 4, to determine the linear region of the plot of $1/M$ versus $1/V^2$. A linear extrapolation method in which the reading at the operating voltage V_o is not one of the data points used to determine recombination should then be used. This linear extrapolation method can either be based on a linear fit to multiple data points in a plot of $1/M$ versus $1/V^2$ or be an alternative two voltage method in which the operating voltage V_o is not one of the two data points in the linear region. If the initial recombination has to be quantified, it can be determined separately from the volume recombination using the method of De Almeida and Niatel (see Section 4.4.3.4). A quadratic fit to a Jaffé plot will also reveal the recombination behaviour, but it is less sensitive in separating initial and volume recombination.

For pulsed ion beams (i.e. short pulse length), there is currently no information available, but it should not be assumed that the two voltage method can be applied, since initial recombination is a complex function of $1/V$ [239].

11.5. VALUES FOR k_{Q,Q_o}

Since beam quality specifications are not currently used for the dosimetry of light ion beams, k_Q values depend solely on the chamber type used. Experimental values of the factor k_{Q,Q_o} are available for very few situations and no values from Monte Carlo simulations with detailed chamber geometries are available yet. The beam quality correction factor is therefore defined by Eq. (91) in Appendix II as follows:

$$k_Q = \frac{\left(s_{w,air}\right)_Q p_Q}{\left(s_{w,air} p\right)_{Q_o}} \frac{\left(W_{air}\right)_Q}{\left(W_{air}\right)_{Q_o}} \tag{67}$$

At present, no primary standard of absorbed dose to water for light ion beams is available and the k_{Q,Q_o} values for light ions given in this international

code of practice are based on the use of ^{60}Co gamma radiation as the reference beam quality Q_o. The notation k_Q denotes use of ^{60}Co as the reference quality.

The factors appearing in the numerator have to be evaluated for the light ion beam of quality Q and, because of the complexity of the physical processes involved, their determination represents a considerable effort. There is currently no information available on perturbation factors for ionization chambers in light ion beams, and in what follows they will be assumed to be unity. Since the secondary electrons produced by light ions have on average extremely low energies, their effects are expected to be less important than for high energy photons and of similar magnitude as for proton beams. For ^{60}Co gamma radiation, results from detailed Monte Carlo simulations for the combined effect of stopping power ratio and perturbation factors are available (see Appendix II) and were used for the computation of the k_{Q,Q_o} factors shown in Table 42.

The stopping power ratios and W_{air} values for light ion beams are taken to be independent of beam quality, owing to the current lack of experimental data [235, 240]. Existing calculations [241] demonstrate that if R_{res} is selected as the beam quality specifier, then the variation with R_{res} down to 1 g/cm^2 is smaller (~0.3%) than the uncertainty related to the data. Constant values of the stopping power ratio and W_{air} are therefore adopted here for all light ion beams. The recommended values are 1.126 and 34.71 eV, respectively. Note that the W_{air} value corresponds to dry air. As the stopping power ratio $s_{w,air}$ of light ions is close to that of ^{60}Co (1.127 [242]), the k_Q values for light ions are dominated by the ratio of W_{air} values and the chamber specific perturbation factors at ^{60}Co.

Table 42 gives values of k_Q for various cylindrical and plane parallel ionization chambers in common use. This publication includes only one set of k_{Q,Q_o} values for carbon ions.

11.6. MEASUREMENTS UNDER NON-REFERENCE CONDITIONS

For clinical use, the depth dose distributions, the transverse beam profiles, the penumbra size of the radiation fields and the field output factors for the various conditions of treatments with light ion beams should be measured.

Plane parallel ionization chambers are recommended for the measurement of depth dose distributions. For the measurement of transverse profiles or three dimensional dose distributions, very small ionization chambers with a cavity volume of less than ~0.1 cm^3 should be used. For dosimeters other than ionization chambers, the energy and/or depth dependence of the detector response should be checked against ionization chambers.

TABLE 42. CALCULATED VALUES OF k_Q FOR CARBON ION BEAMS[a] FOR VARIOUS CYLINDRICAL AND PLANE PARALLEL IONIZATION CHAMBERS

Ionization chamber type[b]	k_Q
Cylindrical chambers	
Capintec PR-06C Farmer	1.042
Exradin A1SL Miniature Shonka	1.043
Exradin A12 Farmer	1.040
Exradin A12S Farmer	1.042
Exradin A18	1.044
Exradin A19 Classic Farmer	1.039
Exradin A28	1.037
IBA CC13	1.027**
IBA CC25	1.030**
IBA FC23-C Short Farmer	1.030**
IBA FC65-G Farmer[c]	1.028*
IBA FC65-P Farmer	1.026**
NE 2561/2611A (NPL 2611A) Secondary Standard	1.040
NE 2571 Farmer	1.031**
PTW 30010 Farmer	1.030**
PTW 30011 Farmer	1.027**
PTW 30012 Farmer	1.037**
PTW 30013 Farmer[c]	1.028*

TABLE 42. CALCULATED VALUES OF k_Q FOR CARBON ION BEAMS[a] FOR VARIOUS CYLINDRICAL AND PLANE PARALLEL IONIZATION CHAMBERS (cont.)

Ionization chamber type[b]	k_Q
PTW 31010 Semiflex	1.039
PTW 31013 Semiflex	1.036
Plane parallel chambers	
Exradin A10	1.033
Exradin A11	1.035
Exradin A11TW	1.047
IBA NACP-02	0.998
IBA PPC05	0.993**
IBA PPC40	0.993**
PTW 34045 Advanced Markus	1.006
PTW 23343 Markus	1.009
PTW 34001 Roos	0.997**

[a] k_Q factors for chambers for which experimental values from direct measurements and cross-calibration exist [95, 243–245] are given as an average of the calculated and the experimental value, marked by * for direct calibration and by ** for cross-calibration.

[b] Some of the chambers listed in this table fail to meet some of the minimum requirements described in Section 4.2.1. However, they have been included in this table because of their current clinical use.

[c] Corrected data, according to a new analysis [245]. Experimental data were averaged when several direct measurements were available.

11.7. ESTIMATED UNCERTAINTY IN THE DETERMINATION OF ABSORBED DOSE TO WATER UNDER REFERENCE CONDITIONS

At present, the uncertainties in the dosimetry of light ions are rather large compared with those in the dosimetry of other radiotherapy beams. For the calculated k_Q factors given in this international code of practice, the uncertainties are dominated by those of the stopping power ratio and the W_{air} value. Detailed comparisons between ionization chamber dosimetry and water calorimetry, as in Ref. [95], are still necessary for further developments in the field. The influence of projectile and target fragmentation on the overall uncertainty, however, seems to be minor (see Appendix II).

The example estimate of the relative standard uncertainties given in Table 43 should therefore be regarded as preliminary. Estimates of the uncertainties for scanned ion beams calibrated in a single energy layer are given in Table 43 in parentheses, yielding a slightly higher combined standard uncertainty of 2.6% and 2.7% for the determination of the absorbed dose to water in a clinical light ion beam with a cylindrical and plane parallel ionization chamber, respectively. These estimates may vary depending on the uncertainty quoted by the calibration laboratory, the care and experience of the user performing the measurement, and the quality and condition of the measurement equipment (e.g. regular recalibration of all measurement devices, quality management system to ensure proper functioning). In this case, the uncertainty component 'establishment of reference conditions' includes additional uncertainty due to potential inhomogeneity in depth dose and dose gradient corrections. Note that Table 43 is provided as an example, and it is the responsibility of users to establish their uncertainty budget for the determination of absorbed dose to water.

TABLE 43. ESTIMATED RELATIVE STANDARD UNCERTAINTY[a] OF $D_{w,Q}$ AT THE REFERENCE DEPTH IN WATER AND FOR A CLINICAL LIGHT ION BEAM, CALIBRATED AT THE SPREAD-OUT BRAGG PEAK AND IN A SINGLE ENERGY LAYER, BASED ON A CHAMBER CALIBRATION IN ^{60}Co GAMMA RADIATION

Physical quantity or procedure	Relative standard uncertainty (%)	
	User chamber type	
	Cylindrical	Plane parallel
Step 1: standards laboratory		
$N_{D,w}$ calibration of secondary standard at a primary standards dosimetry laboratory	0.5	0.5
Long term stability of secondary standard	0.1	0.1
$N_{D,w}$ calibration of the user dosimeter at the standard laboratory	0.4	0.4
Combined uncertainty in step 1	0.6[b]	0.6[b]
Step 2: user light ion beam		
Long term stability of user dosimeter	0.2	0.4
Establishment of reference conditions	0.4 (0.6)[c]	0.6 (0.7)[c]
Dosimeter reading M_Q relative to beam monitor	0.3	0.3
Correction for influence quantities k_i	0.3	0.3
Beam quality correction, k_Q (calculated)	2.4	2.4
Combined uncertainty in step 2	2.5	2.6
Combined standard uncertainty in $D_{w,Q}$ (steps 1 and 2)	2.6	2.7

TABLE 43. ESTIMATED RELATIVE STANDARD UNCERTAINTY[a] OF $D_{w,Q}$ AT THE REFERENCE DEPTH IN WATER AND FOR A CLINICAL LIGHT ION BEAM, CALIBRATED AT THE SPREAD-OUT BRAGG PEAK AND IN A SINGLE ENERGY LAYER, BASED ON A CHAMBER CALIBRATION IN ^{60}Co GAMMA RADIATION (cont.)

Physical quantity or procedure	Relative standard uncertainty (%)	
	User chamber type	
	Cylindrical	Plane parallel

[a] See Ref. [61] or Appendix IV for the expression of uncertainty. The estimates given in the table should be considered typical values; these may vary depending on the uncertainty quoted by standards laboratories for calibration coefficients and on the experimental uncertainty at the user's institution.

[b] If the calibration of the user dosimeter is performed at a PSDL, then the combined standard uncertainty in step 1 is lower. The combined standard uncertainty in D_w should be adjusted accordingly.

[c] The estimated relative standard uncertainties for a scanned clinical beam calibrated in a single energy pencil beam using a single layer scanned field are shown in parentheses. If an RBE weighted SOBP is used for reference dosimetry in a passive beam, an additional uncertainty has to be included, which is due to the absorbed dose gradient in such an SOBP.

11.8. WORKSHEET

Determination of the absorbed dose to water in a light ion beam

User: _____ Date: _____

1. Radiation treatment unit and reference conditions for $D_{w,Q}$ determination

Ion species: _____ Nominal energy: _____ MeV/u

Beam type: ☐ scanned ☐ broad

Nominal dose rate: _____ MU/min Practical range, R_p = _____ g/cm^2

Reference phantom: water Width of the SOBP: _____ g/cm^2

Reference field size: _____ cm × cm Reference SSD: _____ cm

Reference depth, z_{ref} = _____ g/cm^2

2. Ionization chamber and electrometer

Ionization chamber model: _____ Serial no.: _____ Type: ☐ cyl ☐ pp

Chamber wall/window Material: _____ Thickness: _____ g/cm^2

Waterproof sleeve/cover Material: _____ Thickness: _____ g/cm^2

Phantom window Material: _____ Thickness: _____ g/cm^2

Absorbed dose to water calibration coefficient, $N_{D,w}$ = _____ ☐ Gy/nC ☐ Gy/rdg

Reference conditions for calibration P_o = _____ kPa T_o = _____ °C Rel. humidity: ____%

Polarizing potential V_1 = ____ V

Calibration polarity: ☐ positive ☐ negative ☐ corrected for polarity effect

User polarity: ☐ positive ☐ negative

Calibration laboratory: _____ Date: _____

Electrometer model: Serial no.: _____

Calibrated separately from chamber: ☐ yes ☐ no Range setting: _____

If yes Calibration laboratory: Date: _____

3. Dosimeter reading[a] and correction for influence quantities

Uncorrected dosimeter reading at V_1 and user polarity: _____ ☐ nC ☐ rdg

Corresponding accelerator monitor units: _____ MU

Ratio of dosimeter reading and monitor units: M_1 = _____ ☐ nC/MU ☐ rdg/MU

(a) Pressure P = _____ kPa Temperature T = _____ °C Rel. humidity (if known): _____%

$$k_{TP} = \frac{(273.2+T)}{(273.2+T_o)}\frac{P_o}{P} = \_\_\_\_\_$$

(b) Electrometer calibration factor[b] k_{elec} = _____ ☐ nC/rdg ☐ dimensionless

(c) Polarity correction[c] Reading at $+V_1$: M_+ = _____ Reading at $-V_1$: M_- = ____

$$k_{pol} = \frac{|M_+|+|M_-|}{2M} = \_\_\_\_\_$$

(d) Recombination correction (two voltage method)

(i) If the two voltage method is applicable:

Polarizing voltages: V_1 (normal) = _____V V_2 (reduced)= _____V

Readings[d] at V_1, V_2: M_1 = _____ M_2 = _____

Voltage ratio V_1/V_2 = _____ Ratio of readings M_1/M_2 = _____

Use Table 10 for a beam of type: ☐ pulsed ☐ pulsed–scanned

a_o = _____ a_1 = _____ a_2 = _____

e, f

$$k_s = a_0 + a_1\left(\frac{M_1}{M_2}\right) + a_2\left(\frac{M_1}{M_2}\right)^2 = \_\_\_\_\_$$

(ii) If the two voltage method is not applicable:

k_s = _____

Corrected dosimeter reading at voltage V_1:

$M_Q = M_1 k_{TP} k_{elec} k_{pol}\, k_s$ = _____ ☐ nC/MU ☐ rdg/MU

4. Absorbed dose to water at the reference depth, z_{ref}

Beam quality correction factor for user quality Q: k_Q = _____

Taken from ☐ Table 37a, 37b ☐ Other, specify: _____

Absorbed dose calibration of monitor at z_{ref}:

$$D_{w,Q}(z_{ref}) = M_Q N_{D,w} k_Q = \_\_\_\_\_ \text{ Gy/MU}$$

---

[a] All readings should be checked for leakage and corrected if necessary.

[b] If the electrometer is not calibrated separately, set $k_{elec} = 1$.

[c] M in the denominator of k_{pol} denotes reading at the user polarity. Preferably, each reading in the equation should be the average of the ratios of M (or M_+ or M_-) to the reading of an external monitor, M_{em}.

It is assumed that the calibration laboratory has performed a polarity correction. Otherwise k_{pol} is determined according to the following:

Reading at $+V_1$ for quality Q_o: M_+ = _____ Reading at $-V_1$ for quality Q_o: M_- = _____

$$k_{pol} = \left[\left(|M_+| + |M_-|\right)/|M|\right]_Q \Big/ \left[\left(|M_+| + |M_-|\right)/|M|\right]_{Q_o} = \_\_\_\_\_$$

[d] Strictly, readings should be corrected for the polarity effect (average with both polarities). Preferably, each reading in the equation should be the average of the ratios of M_1 or M_2 to the reading of an external monitor, M_{em}.

[e] It is assumed that the calibration laboratory has performed a recombination correction. Otherwise the factor $k'_s = k_s / k_{s,Q_o}$ should be used instead of k_s. When Q_o is ^{60}Co, k_{s,Q_o} (at the calibration laboratory) will normally be close to unity and the effect of not using this equation will be negligible in most cases.

[f] Check that $k_s - 1 \approx (M_1/M_2 - 1)/(V_1/V_2 - 1)$.

Note: SOBP: spread-out Bragg peak; SSD: source–surface distance; cyl: cylindrical; pp: plane parallel; MU: monitor unit.

Appendix I

FORMALISM FOR THE DOSIMETRY OF KILOVOLTAGE X RAY BEAMS

I.1. INTRODUCTION

The formalism for the dosimetry of kilovoltage X ray beams based on standards of absorbed dose to water follows the formulation developed in Section 3 of this international code of practice. However, as emphasized throughout this publication, the availability of such standards and $N_{D,w,Q}$ calibrations of user ionization chambers is limited. For low energy X rays, $N_{D,w,Q}$ calibrations rely on measurements of air kerma calibration coefficients at the surface of a PMMA phantom, with a subsequent numerical calculation of $N_{D,w,Q}$ being performed by the standards laboratory, and very few facilities provide this service. For medium energy X rays, standards are in the process of being developed and user calibrations are not yet widely available. For these reasons, the most common procedure still relies on air kerma calibrations.

There is also an important constraint in the use of $N_{D,w,Q}$ calibrations when determining absorbed dose to water for beam qualities and geometry conditions (field size and SSD) that are different from those used for the instrument calibration, as is the case in most clinical institutions. This is due to the often significant dependence of dosimetric quantities on beam quality and geometry, which makes a modified formalism that accounts for these dependences necessary.

This appendix details the extended formalism for the dosimetry of kilovoltage X ray beams based on air kerma and absorbed dose to water calibrations and their relationships. Although for kilovoltage X rays the recommendation is to specify the beam quality in terms of kilovoltage and HVL (in millimetres of aluminium or copper), for simplicity the beam quality will be denoted as Q.

I.2. BACKGROUND

The absorbed dose to water in kilovoltage X ray beams can be determined from either in-air or in-phantom measurements. The former are generally used for the determination of absorbed dose to water at a phantom surface for low energy X rays, and the latter for a dose determination at a given reference depth in a phantom for medium energy X rays. Strictly, what is determined is water kerma, which is assumed to be equivalent to the absorbed dose to water for the energies

involved in kilovoltage X ray dosimetry. Both methods can use an ionization chamber calibrated in terms of air kerma or in terms of absorbed dose to water; although different, these two routes are intrinsically related in the absorbed dose to water formalism used in this international code of practice and are considered separately in Sections I.3 and I.4.

Using basic dosimetry theory, for the in-air method the absorbed dose to water at the surface of a water phantom ($D_{w,Q}^{surface}$) for a beam quality Q is given by the following expression:

$$D_{w,Q}^{surface} = K_{air,Q}^{FIA} \left[\mu_{en}(Q)/\rho \right]_{w,air}^{FIA} B_{w,Q} \tag{68}$$

where:

$K_{air,Q}^{FIA}$ is the air kerma free in air at the measuring position (i.e. the air kerma arising from the incident radiation, in the absence of the phantom), obtained by multiplying the chamber reading free in air (corrected for influence quantities) by the corresponding air kerma calibration coefficient.

$\left[\mu_{en}(Q)/\rho \right]_{w,air}^{FIA}$ is the water to air ratio of the mean mass energy absorption coefficients, averaged over the photon spectrum free in air. This ratio converts the air kerma measured free in air to water kerma at the same position (i.e. free in air), $K_{w,Q}^{FIA}$, and is practically independent of field size and distance.

$B_w(Q)$ is the backscatter factor, defined as the ratio of water kerma with and without the phantom present. It converts the water kerma free in air to the water kerma at the phantom entrance surface, $K_{w,Q}^{surface}$, which is taken to be equal to the absorbed dose to water at the same position. In contrast to $\left[\mu_{en}(Q)/\rho \right]_{w,air}^{FIA}$, the backscatter factor shows a strong field size and distance dependence.

For the in-phantom method the absorbed dose to water at a reference depth z_{ref} is given by the following equation:

$$D_{w,Q}^{z_{ref}} = K_{air,Q}^{z_{ref}} \left[\mu_{en}(Q)/\rho \right]_{w,air}^{z_{ref}} p_{ch,Q} \tag{69}$$

where:

$K_{\text{air},Q}^{z_{\text{ref}}}$ is the air kerma at the reference depth in the phantom, obtained to a first approximation by multiplying the chamber reading at z_{ref} (corrected for influence quantities) by the air kerma calibration coefficient free in air (the influence on the calibration coefficient of the different spectra in air and water is treated later as a perturbation correction);

$\left[\mu_{\text{en}}(Q)/\rho\right]_{\text{w,air}}^{z_{\text{ref}}}$ is the water to air ratio of the mean mass energy absorption coefficients, averaged over the photon spectrum at z_{ref}; it converts the air kerma at the reference depth in the phantom to water kerma at the same position, $K_{\text{w},Q}^{z_{\text{ref}}}$, and depends on the field size and the distance from the source to the measuring position;

$p_{\text{ch},Q}$ accounts for the change in the response of the chamber between its calibration free in air and its use at the reference depth in the phantom.

Because the air kerma at the reference depth already includes the scatter contribution from the phantom, no backscatter factor is involved in Eq. (69).

Equations (70) and (71) form the basis of the absorbed dose to water formalism for the dosimetry of kilovoltage low energy X ray beams. Each method can be used in conjunction with an $N_{K,\text{air}}$ or an $N_{D,\text{w}}$ chamber calibration, thus offering four different cases. Section I.3 describes the $N_{K,\text{air}}$ route using the in-air method for low energy X rays in the range 10–100 kV to determine the absorbed dose at the surface of a water phantom. Section I.4 describes the $N_{D,\text{w}}$ route for the two methods, that is, the in-phantom method for medium energy X rays in the range 70–300 kV to determine the absorbed dose at the reference depth of 2 cm in water.

I.3. CHAMBER CALIBRATED IN TERMS OF AIR KERMA FREE IN AIR

This is the most widely used route for chamber calibration, both for low and medium energy X rays. Standards laboratories provide air kerma calibration coefficients $N_{K,\text{air},Q}^{\text{FIA}}$ for the user chamber, measured free in air, for a series of standardized beam qualities.

I.3.1. Low energy X rays

For a low energy beam of quality Q with measurements made free in air, Eq. (68) can be written as follows:

$$D_{\mathrm{w},Q}^{\mathrm{surface}} = K_{\mathrm{air},Q}^{\mathrm{FIA}} \left[\mu_{\mathrm{en}}(Q)/\rho\right]_{\mathrm{w,air}}^{\mathrm{FIA}} B_{\mathrm{w},Q}(f,\mathrm{SSD}) \tag{70}$$

where the explicit dependence of the backscatter factor on Q, f and SSD has been included.

Dividing Eq. (70) by the chamber reading free in air, $M_Q^{\mathrm{FIA}}(f,\mathrm{SSD})$, yields the following calibration coefficient in terms of absorbed dose to water at the surface of a water phantom:

$$N_{D,\mathrm{w},Q}^{\mathrm{surface}}(f,\mathrm{SSD}) = N_{K,\mathrm{air},Q}^{\mathrm{FIA}}(f,\mathrm{SSD}) \left[\mu_{\mathrm{en}}(Q)/\rho\right]_{\mathrm{w,air}}^{\mathrm{FIA}} B_{\mathrm{w},Q}(f,\mathrm{SSD}) \tag{71}$$

which is the general expression that relates $N_{D,\mathrm{w},Q}^{\mathrm{surface}}$ and $N_{K,\mathrm{air},Q}^{\mathrm{FIA}}$ for low energy beams of quality Q. Equation (71) is also valid for low energy X rays if the chamber is calibrated while inserted in its own phantom (e.g. Ref. [108]).

The air kerma calibration coefficients $N_{K,\mathrm{air},Q}^{\mathrm{FIA}}$ of the user chamber for clinical qualities are obtained (usually by interpolation) from those provided by the calibration laboratory for a set of standard $(Q, f, \mathrm{SSD})_{\mathrm{lab}}$ conditions; as the in-air calibration coefficients have a negligible dependence on f and SSD[64] for the limited range of values used at the calibration laboratory, only the beam quality needs to be considered for their derivation.

In contrast, it is possible that for the range of field sizes and SSDs used in the clinic certain chambers might show a change in response in air, depending on the extent to which the chamber body is covered by the field (stem effect). In this case, the following more general expression is used:

$$N_{D,\mathrm{w},Q}^{\mathrm{surface}}(f,\mathrm{SSD})_{\mathrm{clin}} = N_{D,\mathrm{w},Q}^{\mathrm{surface}}(f,\mathrm{SSD})_{\mathrm{lab}}\, p_{\mathrm{ch},Q}(f,\mathrm{SSD})_{\mathrm{clin}} \tag{72}$$

where a chamber perturbation correction factor $p_{\mathrm{ch},Q}$ is included to account for the modified influence of the stem. This correction should be determined experimentally for the specific chamber and $(f, \mathrm{SSD})_{\mathrm{clin}}$ conditions

[64] The independence of $N_{K,\mathrm{air},Q}^{\mathrm{FIA}}$ from f requires a field that covers the chamber body. The independence of $N_{K,\mathrm{air},Q}^{\mathrm{FIA}}$ from f and SSD should be demonstrated for a given chamber type.

(e.g. Ref. [185]). The coefficient $N_{D,\mathrm{w},Q}^{\mathrm{surface}}(f,\mathrm{SSD})_{\mathrm{clin}}$ has to be calculated for each clinical quality and geometry condition.

The absorbed dose to water at the surface of a water phantom is then determined using the general formalism of this international code of practice according to the following equation:

$$D_{\mathrm{w},Q}^{\mathrm{surface}}(f,\mathrm{SSD})_{\mathrm{clin}} = M_Q^{\mathrm{FIA}}(f,\mathrm{SSD})_{\mathrm{clin}}\ N_{D,\mathrm{w},Q}^{\mathrm{surface}}(f,\mathrm{SSD})_{\mathrm{clin}} \tag{73}$$

If for a given f and SSD, a specific clinical quality is selected as the reference quality Q_{o}, Eq. (73) can be written for any other beam quality Q at the same f and SSD as follows (for simplicity, the subscript 'clin' is omitted):

$$D_{\mathrm{w},Q}^{\mathrm{surface}}(f,\mathrm{SSD}) = M_Q^{\mathrm{FIA}}(f,\mathrm{SSD})\ N_{D,\mathrm{w},Q_{\mathrm{o}}}^{\mathrm{surface}}(f,\mathrm{SSD})\ k_{Q,Q_{\mathrm{o}}}(f,\mathrm{SSD}) \tag{74}$$

where

$$k_{Q,Q_{\mathrm{o}}}(f,\mathrm{SSD}) = \frac{N_{D,\mathrm{w},Q}^{\mathrm{surface}}(f,\mathrm{SSD})}{N_{D,\mathrm{w},Q_{\mathrm{o}}}^{\mathrm{surface}}(f,\mathrm{SSD})} \tag{75}$$

It should be noted that in addition to the beam quality, Eqs (70)–(75) for low energy X rays include the specific dependence on f and SSD. The reason is that, in contrast to the quantities used in broad beam megavoltage photon dosimetry, backscatter factors depend substantially on f and SSD and the geometry conditions have to always be taken into account; this is also why $N_{D,\mathrm{w},Q}$ values cannot be used at different (f, SSD) values from those for which they were derived.

It is emphasized that backscatter factors are chamber independent (by definition), and for a given clinical beam in the range 30–100 kV, field diameters of 3–20 cm and SSDs of 30–100 cm, $B_{\mathrm{w},Q}(f,\mathrm{SSD})$ varies in the range 1–20% (the contribution of the variation with SSD is ~0.1–2%) [54].

I.3.2. Medium energy X rays

For a medium energy beam of quality Q with measurements made at $z_{\mathrm{ref}} = 2$ cm in water, Eq. (69) can be written as follows:

$$D_{\mathrm{w},Q}^{z=2}(f,\mathrm{SSD}) = K_{\mathrm{air},Q}^{z=2}\left[\mu_{\mathrm{en}}(Q,f,\mathrm{SSD})/\rho\right]_{\mathrm{w,air}}^{z=2} \tag{76}$$

As with Eq. (71), this can be expressed for a given chamber in terms of calibration coefficients as follows:

$$N_{D,\mathrm{w},Q}^{z=2}(f,\mathrm{SSD}) = N_{K,\mathrm{air},Q}^{\mathrm{FIA}}(f,\mathrm{SSD})\left[\frac{\mu_{\mathrm{en}}(Q,f,\mathrm{SSD})}{\rho}\right]_{\mathrm{w,air}}^{z=2} p_{\mathrm{ch},Q}(f,\mathrm{SSD}) \quad (77)$$

However, in this case, the perturbation correction p_{ch} has to account for the following:

(a) The effect on the chamber response of the difference between the spectra obtained at the chamber position for the calibration free in air and those measured at the reference depth in the water phantom;
(b) The replacement of water by air and the chamber wall material;
(c) The influence of the stem on the chamber response in water and free in air;
(d) The effect on the chamber response of the waterproof sleeve, if used.

The air kerma calibration coefficients $N_{K,\mathrm{air},Q}^{\mathrm{FIA}}$ of the user chamber for clinical qualities are obtained (usually by interpolation) from those provided by the calibration laboratory for a set of standard $(Q, f, \mathrm{SSD})_{\mathrm{lab}}$ conditions; as the air kerma calibration coefficients have a reduced dependence on f and SSD, only the beam quality needs to be considered for their derivation. In contrast, the coefficient $N_{D,\mathrm{w},Q}^{z=2}(f,\mathrm{SSD})$ has to be calculated for each clinical quality and geometry condition using Eq. (77).

The absorbed dose to water at a depth of 2 cm in water is determined using the general formalism of this international code of practice according to the following equation:

$$D_{\mathrm{w},Q}^{z=2}(f,\mathrm{SSD}) = M_{Q}^{z=2}(f,\mathrm{SSD})\, N_{D,\mathrm{w},Q}^{z=2}(f,\mathrm{SSD}) \quad (78)$$

If a specific clinical quality is selected as reference quality Q_{o}, Eq. (78) can be written for any other beam quality Q at the same field size f and SSD as follows:

$$D_{\mathrm{w},Q}^{z=2}(f,\mathrm{SSD}) = M_{Q}^{z=2}(f,\mathrm{SSD})\, N_{D,\mathrm{w},Q_{\mathrm{o}}}^{z=2}(f,\mathrm{SSD})\, k_{Q,Q_{\mathrm{o}}}(f,\mathrm{SSD}) \quad (79)$$

where

$$k_{Q,Q_{\mathrm{o}}}(f,\mathrm{SSD}) = \frac{N_{D,\mathrm{w},Q}^{z=2}(f,\mathrm{SSD})}{N_{D,\mathrm{w},Q_{\mathrm{o}}}^{z=2}(f,\mathrm{SSD})} \quad (80)$$

Note that, in addition to the beam quality, Eqs (76)–(80) for medium energy X rays include the specific dependence on field size f and SSD. The reason is that, in contrast to the case of broad megavoltage photon beams, the water to air ratio of the mean mass energy absorption coefficients may depend on these variables (although to a much lesser extent than backscatter factors for low energy beams) and their geometry conditions should strictly be taken into account.

It is of interest to note that $\left[\mu_{\text{en}}(Q)/\rho\right]_{\text{w,air}}^{z=2}$ is chamber independent (by definition), and for a given clinical beam in the range 120–280 kV, field diameters of 3–20 cm and SSDs of 30–100 cm, values vary only by up to ~1% (the contribution of the variation with SSD is practically negligible, i.e. ≤0.1%). Owing to these small variations, $N_{D,\text{w},Q}^{z=2}$ values could be used at different (f, SSD) values from those for which they were derived, after verifying that the corresponding $\left[\mu_{\text{en}}(Q)/\rho\right]_{\text{w,air}}^{z=2}$ values are not too different.

I.4. CHAMBER CALIBRATED IN TERMS OF ABSORBED DOSE TO WATER

This route is less common than that based on $N_{K,\text{air}}^{\text{FIA}}$ owing to the reduced availability of $N_{D,\text{w}}$ laboratory calibrations, as noted previously. For both low and medium energies, the formalism described in Sections 8 and 9 is applicable for the specific conditions under which the chamber was calibrated. An important constraint, however, is that the measuring conditions (Q, f, SSD) at the standards laboratory do not match those used in the clinic and sometimes are substantially different. This discrepancy presents the potential risk of large errors if $N_{D,\text{w}}$ interpolations are made by the user, as the calibration and clinical conditions have to be properly accounted for. The solution is provided by a modified formalism that introduces an additional geometry correction factor to account for different (f, SSD) for a given Q, making their dependence on laboratory and clinical conditions in the different expressions explicit.

I.4.1. Low energy X rays

For low energy X rays the few laboratories providing absorbed dose to water calibrations do so for a chamber positioned at the surface of a PMMA phantom, where an air kerma coefficient $N_{K,\text{air},Q}^{\text{PMMA}}$ is measured and $N_{D,\text{w},Q}^{\text{PMMA}}$ is derived by calculation at the calibrating laboratory (using a method analogous to Eq. (71) for calibrations free in air). The main advantage of this procedure is that it harmonizes the backscatter factors and $\left[\mu_{\text{en}}(Q)/\rho\right]_{\text{w,air}}^{z=2}$ values (those used by the calibrating laboratory) among all users, who do not require specific data for the derivation of $N_{D,\text{w},Q}^{\text{PMMA}}$.

Clinical $N_{D,\mathrm{w},Q_{\mathrm{clin}}}^{\mathrm{PMMA}}$ coefficients are derived by interpolation from the $N_{D,\mathrm{w},Q_{\mathrm{lab}}}^{\mathrm{PMMA}}$ values supplied by the calibration laboratory, but it is emphasized that these coefficients are exclusively applicable to the (f, SSD) conditions under which they were derived, that is, $(f, \mathrm{SSD})_{\mathrm{lab}}$.

To extend the formalism used in Eq. (73) for air kerma to absorbed dose to water, making it applicable to any $(f, \mathrm{SSD})_{\mathrm{clin}}$ condition, a geometry correction factor is introduced for a given chamber type at a clinical quality Q that will convert $N_{D,\mathrm{w},Q}^{\mathrm{PMMA}}$ from a condition $(f, \mathrm{SSD})_{\mathrm{lab}}$ to the general condition $(f, \mathrm{SSD})_{\mathrm{clin}}$. Hence, the absorbed dose to water at the surface of a water phantom is determined using a modified formalism according to the following equation:

$$D_{\mathrm{w},Q}^{\mathrm{surface}}(f,\mathrm{SSD})_{\mathrm{clin}} = M_{Q}^{\mathrm{PMMA}}(f,\mathrm{SSD})_{\mathrm{clin}} \times N_{D,\mathrm{w},Q}^{\mathrm{PMMA}}(f,\mathrm{SSD})_{\mathrm{lab}}\ k_{\mathrm{g},Q}^{\mathrm{PMMA}}(f,\mathrm{SSD})_{\mathrm{clin}} \tag{81}$$

where Q corresponds to any of the Q_{clin} values available, and tables of the geometry correction factor values $k_{\mathrm{g},Q}^{\mathrm{PMMA}}(f,\mathrm{SSD})$ should ideally be provided by the calibrating laboratory or be available from another source for the specific chamber type.

If one of the clinical qualities is selected as the reference Q_{o}, the clinical beam quality factors are defined as follows:

$$k_{Q,Q_{\mathrm{o}}}^{\mathrm{PMMA}}(f,\mathrm{SSD})_{\mathrm{lab}} = \frac{N_{D,\mathrm{w},Q}^{\mathrm{PMMA}}(f,\mathrm{SSD})_{\mathrm{lab}}}{N_{D,\mathrm{w},Q_{\mathrm{o}}}^{\mathrm{PMMA}}(f,\mathrm{SSD})_{\mathrm{lab}}} \tag{82}$$

where Q corresponds to any of the Q_{clin} values available and the explicit $(f, \mathrm{SSD})_{\mathrm{lab}}$ dependence has been included. Equation (81) then becomes the following:

$$D_{\mathrm{w},Q}^{\mathrm{surface}}(f,\mathrm{SSD})_{\mathrm{clin}} = M_{Q}^{\mathrm{PMMA}}(f,\mathrm{SSD})_{\mathrm{clin}}\ N_{D,\mathrm{w},Q_{\mathrm{o}}}^{\mathrm{PMMA}}(f,\mathrm{SSD})_{\mathrm{lab}} \times k_{Q,Q_{\mathrm{o}}}^{\mathrm{PMMA}}(f,\mathrm{SSD})_{\mathrm{lab}}\ k_{\mathrm{g},Q}^{\mathrm{PMMA}}(f,\mathrm{SSD})_{\mathrm{clin}} \tag{83}$$

I.4.1.1. The geometry correction factor

For low energy X rays the geometry correction factor entering Eqs (81, 83) is defined as follows:

$$k_{\mathrm{g},Q}^{\mathrm{PMMA}}(f,\mathrm{SSD})_{\mathrm{clin}} = \frac{N_{D,\mathrm{w},Q}^{\mathrm{PMMA}}(f,\mathrm{SSD})_{\mathrm{clin}}}{N_{D,\mathrm{w},Q}^{\mathrm{PMMA}}(f,\mathrm{SSD})_{\mathrm{lab}}} \tag{84}$$

which, using the equivalent of Eq. (71) for the relationship between $N_{K,\mathrm{air},Q}$ and $N_{D,\mathrm{air},Q}$, becomes as follows:

$$k_{g,Q}^{\mathrm{PMMA}}(f,\mathrm{SSD})_{\mathrm{clin}} = \frac{N_{K,\mathrm{air},Q}^{\mathrm{PMMA}}(f,\mathrm{SSD})_{\mathrm{clin}}}{N_{K,\mathrm{air},Q}^{\mathrm{PMMA}}(f,\mathrm{SSD})_{\mathrm{lab}}} \times \frac{B_{\mathrm{w},Q}(f,\mathrm{SSD})_{\mathrm{clin}}}{B_{\mathrm{w},Q}(f,\mathrm{SSD})_{\mathrm{lab}}} \frac{p_{\mathrm{ch},Q}(f,\mathrm{SSD})_{\mathrm{clin}}}{p_{\mathrm{ch},Q}(f,\mathrm{SSD})_{\mathrm{lab}}} \tag{85}$$

where the ratio $\left[\mu_{\mathrm{en}}(Q)/\rho\right]_{\mathrm{w,air}}^{\mathrm{FIA}}$ is not included because of its independence of field size and distance.

As mentioned above, tables of $k_{g,Q}^{\mathrm{PMMA}}(f,\mathrm{SSD})_{\mathrm{clin}}$ values should ideally be provided by the calibrating laboratory (or be available from another source for the chamber type). Alternatively, the $N_{K,\mathrm{air},Q}^{\mathrm{PMMA}}$ values should be measured at the calibration laboratory for the chamber type; these depend on changes in f and SSD, so the ratio of the calibration coefficients in Eq. (85) needs to be provided by the laboratory. The $p_{\mathrm{ch},Q}$ factors are known only for some chambers and specific (f, SSD) conditions, so unless the geometry conditions are too different, the ratio of perturbation factors in Eq. (85) is assumed to cancel. The ratio of backscatter factors is chamber independent (by definition) but, as mentioned for the kerma in-air case, for a clinical beam in the range 30–100 kV, field diameters of 3–20 cm and SSDs of 30–100 cm, $B_{\mathrm{w}}(Q, f, \mathrm{SSD})$ may vary in the range 1–20% (the contribution of the variation with SSD is ~0.1–2%). The numerical value of the B_{w} ratio will thus depend on how different the terms $(f, \mathrm{SSD})_{\mathrm{clin}}$ and $(f, \mathrm{SSD})_{\mathrm{lab}}$ in Eq. (85) are.

I.4.2. Medium energy X rays

For medium energy X rays, several laboratories have developed standards for absorbed dose to water, which are disseminated in the form of $N_{D,\mathrm{w},Q}^{z=2}$ calibrations (measurements made at 2 cm depth in water). The development of a modified formalism closely follows that for low energy X rays, which is reproduced here with the relevant notation changes.

The clinical coefficients $N_{D,\mathrm{w},Q_{\mathrm{clin}}}^{z=2}$ are derived by interpolation from the $N_{D,\mathrm{w},Q_{\mathrm{lab}}}^{z=2}$ values supplied by the calibration laboratory, but it is emphasized that the clinical coefficients are exclusively applicable to the (f, SSD) conditions under which they were derived, that is, $(f, \mathrm{SSD})_{\mathrm{lab}}$.

To extend the formalism used in Eq. (78) for air kerma to absorbed dose to water, making it applicable to any $(f, \mathrm{SSD})_{\mathrm{clin}}$ condition, a geometry correction factor is introduced for a given chamber type and a clinical quality Q that will convert $N_{D,\mathrm{w},Q}^{z=2}$ from a condition $(f, \mathrm{SSD})_{\mathrm{lab}}$ to the general

condition $(f, \mathrm{SSD})_{\mathrm{clin}}$. Hence, the absorbed dose to water at 2 cm depth in water is determined using a modified formalism according to the following equation:

$$D_{\mathrm{w},Q}^{z=2}(f,\mathrm{SSD})_{\mathrm{clin}} = M_{Q}^{z=2}(f,\mathrm{SSD})_{\mathrm{clin}}\; N_{D,\mathrm{w},Q}^{z=2}(f,\mathrm{SSD})_{\mathrm{lab}}\; k_{\mathrm{g},Q}^{z=2}(f,\mathrm{SSD})_{\mathrm{clin}} \quad (86)$$

where Q corresponds to any of the Q_{clin} available, and tables of the geometry correction factor values $k_{\mathrm{g},Q}^{z=2}(f,\mathrm{SSD})$ should ideally be provided by the calibrating laboratory or be available from another source for the specific chamber type.

If one of the clinical qualities is selected as the reference value Q_{o}, the clinical beam quality factors are defined as follows:

$$k_{Q,Q_{\mathrm{o}}}^{z=2}(f,\mathrm{SSD})_{\mathrm{lab}} = \frac{N_{D,\mathrm{w},Q}^{z=2}(f,\mathrm{SSD})_{\mathrm{lab}}}{N_{D,\mathrm{w},Q_{\mathrm{o}}}^{z=2}(f,\mathrm{SSD})_{\mathrm{lab}}} \quad (87)$$

where Q corresponds to any of the Q_{clin} values available, and the explicit $(f, \mathrm{SSD})_{\mathrm{lab}}$ dependence has been included. Equation (86) then becomes the following:

$$\begin{aligned} D_{\mathrm{w},Q}^{z=2}(f,\mathrm{SSD})_{\mathrm{clin}} = {} & M_{Q}^{z=2}(f,\mathrm{SSD})_{\mathrm{clin}}\; N_{\mathrm{D,w},Q_{\mathrm{o}}}^{z=2}(f,\mathrm{SSD})_{\mathrm{lab}} \\ & \times k_{Q,Q_{\mathrm{o}}}^{z=2}(f,\mathrm{SSD})_{\mathrm{lab}}\; k_{\mathrm{g},Q}^{z=2}(f,\mathrm{SSD})_{\mathrm{clin}} \end{aligned} \quad (88)$$

I.4.2.1. The geometry factor

For medium energy X rays the geometry corction factor entering in Eqs (86, 88) is defined as follows:

$$k_{\mathrm{g},Q}^{z=2}(f,\mathrm{SSD})_{\mathrm{clin}} = \frac{N_{D,\mathrm{w},Q}^{z=2}(f,\mathrm{SSD})_{\mathrm{clin}}}{N_{D,\mathrm{w},Q}^{z=2}(f,\mathrm{SSD})_{\mathrm{lab}}} \quad (89)$$

Using the equivalent of Eq. (77) for the relationship between $N_{D,\mathrm{w},Q}^{z=2}$ and $N_{K,\mathrm{air},Q}^{\mathrm{FIA}}$, Eq. (89) becomes as follows:

$$k_{\mathrm{g},Q}^{z=2}(f,\mathrm{SSD})_{\mathrm{clin}} = \frac{N_{K,\mathrm{air},Q}^{\mathrm{FIA}}(f,\mathrm{SSD})_{\mathrm{clin}}}{N_{K,\mathrm{air},Q}^{\mathrm{FIA}}(f,\mathrm{SSD})_{\mathrm{lab}}} \frac{\left[\dfrac{\mu_{\mathrm{en}}(Q,f,\mathrm{SSD})_{\mathrm{clin}}}{\rho}\right]_{\mathrm{w,air}}^{z=2}}{\left[\dfrac{\mu_{\mathrm{en}}(Q,f,\mathrm{SSD})_{\mathrm{lab}}}{\rho}\right]_{\mathrm{w,air}}^{z=2}} \frac{p_{\mathrm{ch},Q}(f,\mathrm{SSD})_{\mathrm{clin}}}{p_{\mathrm{ch},Q}(f,\mathrm{SSD})_{\mathrm{lab}}} \quad (90)$$

As mentioned above, tables of $k_{\mathrm{g},Q}^{z=2}(f,\mathrm{SSD})_{\mathrm{clin}}$ values should ideally be provided by the calibrating laboratory (or be available from another source for the chamber type). Alternatively, the $N_{K,\mathrm{air}}^{\mathrm{FIA}}$ values should be measured by the

calibrating laboratory (or interpolated for clinical qualities) for the chamber type; however, as they have a reduced dependence on changes in f and SSD, the ratio of calibration coefficients in Eq. (90) can be assumed to cancel. The $p_{\mathrm{ch},Q}$ factors are only known for some chambers and specific (f,SSD) conditions, so that unless the geometry conditions are too different, their ratio is assumed to cancel. The only remaining ratio is $\left[\mu_{\mathrm{en}}(Q,f,\mathrm{SSD})_{\mathrm{clin}}/\rho\right]^{z=2}_{\mathrm{w,air}} \Big/ \left[\mu_{\mathrm{en}}(Q,f,\mathrm{SSD})_{\mathrm{lab}}/\rho\right]^{z=2}_{\mathrm{w,air}}$ which is chamber independent (by definition). For a clinical beam in the range 120–280 kV, field diameters of 3–20 cm and SSDs of 30–100 cm, $\left[\mu_{\mathrm{en}}(Q,f,\mathrm{SSD})_{\mathrm{clin}}/\rho\right]^{z=2}_{\mathrm{w,air}}$ varies only by up to ~1% (the contribution of the variation with SSD is practically negligible, i.e. ≤0.1%). The numerical value of the μ_{en} ratio will thus depend on how different the terms (f, SSD)$_{\mathrm{clin}}$ and (f, SSD)$_{\mathrm{lab}}$ in Eq. (90) are, but in most cases the ratio will cancel. This means that, to a first approximation, $k^{z=2}_{\mathrm{g},Q}(f,\mathrm{SSD})_{\mathrm{clin}}$ will be close to 1, except when the geometry conditions in the clinic are very different from those in the calibrating laboratory.

Appendix II

DETERMINATION OF k_{Q,Q_o} AND ITS UNCERTAINTY

II.1. GENERAL

The beam quality correction factor k_{Q,Q_o} (see Eq. (3)), is defined as the ratio of the calibration coefficients in terms of absorbed dose to water of an ionization chamber at the qualities Q and Q_o. This international code of practice recommends that values for k_{Q,Q_o} measured for a particular chamber should be used when available. However, in most cases, such data will not be available and calculated values have to be used.

In the first edition of this international code of practice, for conditions where the Bragg–Gray cavity theory is applicable [56, 246], values of k_{Q,Q_o} were calculated using the following expression:

$$k_{Q,Q_o} = \frac{\left(s_{w,air}\right)_Q}{\left(s_{w,air}\right)_{Q_o}} \frac{\left(W_{air}\right)_Q}{\left(W_{air}\right)_{Q_o}} \frac{p_{ch,Q}}{p_{ch,Q_o}} \tag{91}$$

where water to air electron stopping power ratios for photon and electron beams were calculated using data from Ref. [48], stopping power ratios for proton beams were based on those in Ref. [49] and the values for W_{air} were 33.97 eV for photon and electron beams, 34.23 eV for protons and 34.50 eV for heavier ions. This general expression for k_{Q,Q_o} was derived by comparing Eq. (3) with the $N_{D,air}$ formalism used in Refs [9, 10] and other dosimetry protocols. It is valid for all types of high energy beam and includes ratios, at the qualities Q and Q_o, of Spencer–Attix water to air stopping power ratios, $s_{w,air}$, of the mean energy expended in air per ion pair formed, W_{air}[65], and of the ionization chamber perturbation factors $p_{ch,Q}$.

The overall perturbation factors $p_{ch,Q}$ and p_{ch,Q_o} include all departures from the ideal Bragg–Gray detector conditions, namely p_{wall}, p_{cav}, p_{cel} and p_{dis} (see Section 1.8). Owing to the lack of consistent data for the different components of the chamber perturbation correction factors entering $p_{ch,Q}$, some values are derived from experiments and others by Monte Carlo or other calculations, and in some cases they are taken to be unity.

---

[65] It should be noted that W_{air}, as well as $s_{w,air}$, should be averaged over the entire spectra of particles present. This is an important limitation in the case of heavy charged particles, where the determination of all possible particle spectra involves a considerable undertaking.

In therapeutic electron and photon beams, the general assumption[66] of $(W_{air})_Q = (W_{air})_{Q_o}$ yields the following simpler equation for

$$k_{Q,Q_o} \approx \frac{(s_{w,air})_Q}{(s_{w,air})_{Q_o}} \frac{p_{ch,Q}}{p_{ch,Q_o}} \tag{92}$$

which depends solely on quotients of water to air stopping power ratios and perturbation factors at the beam qualities Q and Q_o. The only chamber specific factors involved are the perturbation correction factors $p_{ch,Q}$ and p_{ch,Q_o}.

Values of the product $(s_{w,air})_{Q_o} p_{ch,Q_o}$ in the denominator of Eq. (92) when the reference quality Q_o is ^{60}Co gamma radiation are given in Table 44 for the cylindrical and plane parallel ionization chambers discussed in this publication. These values were used in the calculation of all k_{Q,Q_o} factors provided in this international code of practice when they are normalized to ^{60}Co; the symbol k_Q is used in those cases. Bragg–Gray conditions do not apply in the case of low and medium energy kilovoltage X ray beams and therefore Eq. (92) cannot be used. In addition, the chamber to chamber variation in response is usually large (see Sections 8 and 9). For these radiation qualities, the formalism is based exclusively on the use of directly measured $N_{D,w,Q}$, N_K or k_{Q,Q_o} factors for individual user chambers.

In recent decades, advanced Monte Carlo techniques have been developed that enable the detailed simulation of ionization chambers and radiation sources (^{60}Co γ ray units and accelerators) with great efficiency. Instead of calculating $s_{w,air}$ and chamber perturbation factor components independently for a given beam quality and ionization chamber, Sempau et al. [247] proposed computing the following factor:

$$f_{ch}(Q) = \left[\frac{D_w(P)}{\bar{D}_{ch-air}} \right]_Q \tag{93}$$

directly within the Monte Carlo simulation, where $\bar{D}_{ch-air}$ and $D_w(P)$ are the Monte Carlo calculated mean absorbed dose in the chamber cavity and the dose to a point in water (in practice, a very small volume), respectively. Note that no specific components of the chamber perturbation correction factors are explicitly included in this factor, and the constraint of small and independent components in p_{ch} is no longer needed. Equation (93) provides a global $f_{ch}(Q)$ that includes $s_{w,air}$ and all possible chamber perturbation components, irrespective of their size or interrelation (i.e. they do not need to be small and independent), and has become the currently accepted Monte Carlo calculation approach. It differs from that used by other authors

[66] This is the same assumption as for the independence of $N_{D,air}$ from the quality of the beam (see Ref. [10]).

(e.g. Refs [248, 249]), where instead of the dose to a point, $D_w(P)$, the dose to water is calculated in a volume identical to that of the chamber, $D_w(\text{vol})$.

From Eq. (93), the beam quality correction factor is defined as follows:

$$k_{Q,Q_o} = \frac{f_{ch}(Q)}{f_{ch}(Q_o)} \tag{94}$$

More generally, when accounting for beams with different values of the mean energy needed to create an ion pair in air, W_{air}, the following definition is used:

$$k_{Q,Q_o} = \frac{f_{ch}(Q)}{f_{ch}(Q_o)} \frac{(W_{air})_Q}{(W_{air})_{Q_o}} \tag{95}$$

Using ^{60}Co γ rays as the reference quality Q_o, Eq. (95) becomes as follows:

$$k_Q = \frac{f_{ch}(Q)}{f_{ch}(^{60}\text{Co})} \frac{(W_{air})_Q}{(W_{air})_{^{60}\text{Co}}} \tag{96}$$

Computing $f_{ch}(Q) \approx (s_{w,air}\, p_{ch})_Q$ as a single quantity in a Monte Carlo simulation has important advantages over obtaining the $s_{w,air}$ and p_{ch} values separately. In addition to being independent of the intrinsic approximations involved in cavity theory, the main advantage of a Monte Carlo calculation of $f_{ch}(Q)$ is that its uncertainty is considerably smaller than that resulting from combining the uncertainties of $s_{w,air}$ and p_{ch}, where the values and their uncertainties are derived indirectly and independently.

Most of the k_Q values provided in this publication are based on the key data given in Ref. [32], which have also been endorsed by CCRI [53].

II.2. DETERMINATION OF k_Q AND DATA ANALYSIS

General aspects of the different calculations and measurements for the determination of beam quality correction factors for different beam and ionization chamber types are discussed in this section. In most cases, the data were obtained by different research groups, yielding a robust set of updated data. For high energy photon and electron beams, $f_{ch}(Q)$ and k_Q values were determined by Monte Carlo calculations according to Eq. (96) and by measurements at standards laboratories, respectively. For protons and heavier ion beams, k_Q values were derived from Monte Carlo calculated and experimental data, or analytically using Eq. (91) when such data were not available. All cases require data for ^{60}Co γ ray beams, which are discussed first.

II.2.1. ^{60}Co gamma radiation

All k_Q values reported in this publication are based on the reference quality of ^{60}Co γ rays. The quantity $f_{ch}(^{60}Co)$ (see Eq. (93)) was determined in Ref. [100] for each chamber type using Monte Carlo data supplied by different research groups; in practically all cases the Monte Carlo systems used were EGSnrc [250] and PENELOPE [45, 46]. The most common radiation source was the ^{60}Co spectrum of therapy or laboratory units, although in some cases specific phase space files were used for particular units. Values of this quantity are given in Table 44 for different chamber types, for which a common standard uncertainty estimate of 0.4% was obtained (strictly, the uncertainty varied between chamber types). The new $f_{ch}(^{60}Co)$ values replace those for $(s_{w,air}p_{ch})_{^{60}Co}$ given in table 37 of the first edition of this international code of practice.

For the analytical calculations of k_Q for protons and heavier ions using Eq. (91), the value $(W_{air})_{^{60}Co} = 33.97\,eV$, with a standard uncertainty of 0.35% [32], is used in the denominator, together with chamber specific Monte Carlo calculated values of $f_{ch}(^{60}Co)$.

TABLE 44. MONTE CARLO DERIVED $f_{ch}(^{60}Co)$ CHAMBER SPECIFIC FACTORS[a], APPROXIMATELY EQUAL TO THE PRODUCT $s_{w,air}p_{ch}$ IN ^{60}Co BEAMS *(adapted from Ref. [100])*

Cylindrical chambers	$f_{ch}(^{60}Co)$	Plane parallel chambers	$f_{ch}(^{60}Co)$
Capintec PR-06C Farmer	1.1045	Exradin A10	1.1137
Exradin A1SL Miniature	1.1036	Exradin A11	1.1115
Exradin A12 Farmer	1.1064	Exradin A11TW	1.0994
Exradin A12S Short Farmer	1.1046	IBA NACP-02	1.1526
Exradin A18	1.1023	IBA PPC05	1.1394
Exradin A19 Classic Farmer	1.1074	IBA PPC40	1.1405
Exradin A28	1.1095	PTW 34045 Adv. Markus	1.1439
IBA CC13	1.1098	PTW 23343 Markus	1.1407
IBA CC25	1.1039	PTW 34001 Roos	1.1414

TABLE 44. MONTE CARLO DERIVED $f_{ch}(^{60}Co)$ CHAMBER SPECIFIC FACTORS[a], APPROXIMATELY EQUAL TO THE PRODUCT $s_{w,air}p_{ch}$ IN ^{60}Co BEAMS *(adapted from Ref. [100])* (cont.)

Cylindrical chambers	$f_{ch}(^{60}Co)$	Plane parallel chambers	$f_{ch}(^{60}Co)$
IBA FC23-C Short Farmer	1.1077		
IBA FC65-G Farmer	1.1078		
IBA FC65-P Farmer	1.1135		
NE 2561/2611A (NPL 2611A) Secondary standard	1.1062		
NE 2571 Farmer	1.1083		
PTW 30010 Farmer	1.1072		
PTW 30011 Farmer	1.1129		
PTW 30012 Farmer	1.1000		
PTW 30013 Farmer	1.1082		
PTW 31010 Semiflex	1.1074		
PTW 31013 Semiflex	1.1110		
PTW 31016 PinPoint 3D	1.1260		
PTW 31021 Semiflex 3D	1.0951		
PTW 31022 PinPoint 3D[b]	1.1002		
Sun Nuclear SNC125c	1.1137		
Sun Nuclear SNC600c Farmer	1.1159		

[a] The $f_{ch}(^{60}Co)$ values were obtained by averaging the contribution from different Monte Carlo studies, yielding a common standard uncertainty estimate of 0.4%.

[b] Mean value from Ref. [251]; see footnote d in Table 45.

As emphasized in Section II.1, computing $f_{ch}\left({}^{60}\mathrm{Co}\right) \approx \left(s_{w,air} p_{ch}\right)_{{}^{60}\mathrm{Co}}$ as a single quantity in a Monte Carlo simulation, instead of obtaining the $s_{w,air}$ and p_{ch} values separately, has the advantage of a smaller uncertainty than that resulting from combining the uncertainties of $s_{w,air}$ and p_{ch}. Therefore, whereas the use of specific $s_{w,air}$ and p_{ch} values is acceptable for proton and heavier ions owing to the lack of chamber specific Monte Carlo derived $f_{ch}(Q)$ values, for the ^{60}Co data in the denominator of k_Q, the use of $f_{ch}(^{60}\mathrm{Co})$ is preferred.

II.3. High energy photon beams

For the Monte Carlo calculated and experimental megavoltage photon data, values of $f_{ch}(Q)$ and of $N_{D,w,Q}$ were determined for a large number of chamber types and beam qualities. This radiation modality had by far the largest number of datasets, consistent with its therapeutic use worldwide. Table 45 [100] shows the chamber types and number of Monte Carlo derived and experimental k_Q determinations.

TABLE 45. CHAMBER TYPES AND NUMBER OF MONTE CARLO DERIVED AND EXPERIMENTAL k_Q DETERMINATIONS FOR HIGH ENERGY PHOTON BEAMS OF DIFFERENT QUALITIES *(adapted from Ref. [100])*

Ionization chamber type	Number of data points		Chamber type specific parameters[a]	
	Monte Carlo	Experimental	*a*	*b*
Capintec PR-06C Farmer	10	3	1.06833	−0.08262
Exradin A1SL Miniature	14	6	1.21633	−0.13351
Exradin A12 Farmer	35	6	1.09783	−0.09544
Exradin A12S Short Farmer	16	3	1.11499	−0.10057
Exradin A18	10	3	1.10487	−0.09670
Exradin A19 Classic Farmer	29	6	1.12024	−0.10493
Exradin A26	10	3	1.09587	−0.09383
Exradin A28	19	3	1.12453	−0.10278

TABLE 45. CHAMBER TYPES AND NUMBER OF MONTE CARLO DERIVED AND EXPERIMENTAL k_Q DETERMINATIONS FOR HIGH ENERGY PHOTON BEAMS OF DIFFERENT QUALITIES *(adapted from Ref. [100])* (cont.)

Ionization chamber type	Number of data points		Chamber type specific parameters[a]	
	Monte Carlo	Experimental	*a*	*b*
IBA CC13	42	6	1.11441	−0.10260
IBA CC25	10	3	1.08981	−0.09254
IBA FC23-C Short Farmer	19	3	1.09189	−0.09346
IBA FC65-G Farmer	64	20	1.09752	−0.09642
IBA FC65-P Farmer	42	3	1.12374	−0.10784
NE 2561/2611A (NPL 2611A) Secondary standard	20	19	1.07699	−0.08732
NE 2571 Farmer	126	28	1.08918	−0.09222
PTW 30010 Farmer	25	3	1.12594	−0.10740
PTW 30011 Farmer	15	—[b]	1.10850	−0.10107
PTW 30012 Farmer	25	13	1.12442	−0.10415
PTW 30013 Farmer	65	23	1.18273	−0.13256
PTW 31010 Semiflex	29	6	1.23755	−0.15295
PTW 31013 Semiflex	48	6	1.19297	−0.13366
PTW 31016 PinPoint 3D	15	—[b]	1.11650	−0.10841
PTW 31021 Semiflex 3D	37	13	1.29612	−0.16514
PTW 31022 PinPoint 3D[c]	25	6	1.14435	−0.11130
Sun Nuclear SNC125c[d]	25	—[b]	1.09700	−0.09749
Sun Nuclear SNC600c Farmer[d]	25	5	1.06800	−0.08485

TABLE 45. CHAMBER TYPES AND NUMBER OF MONTE CARLO DERIVED AND EXPERIMENTAL k_Q DETERMINATIONS FOR HIGH ENERGY PHOTON BEAMS OF DIFFERENT QUALITIES *(adapted from Ref. [100])* (cont.)

Ionization chamber type	Number of data points		Chamber type specific parameters[a]	
	Monte Carlo	Experimental	*a*	*b*
Total number of determinations	800	190		

[a] Values of the chamber type specific parameters *a* and *b* obtained from the different fits using Eq. (97). The number of decimal places does not imply uncertainties of the same order. They are given to permit smooth interpolation of the data.

[b] —: data not available.

[c] Values from a PTW project comprising 6 PTB measured and 25 Monte Carlo calculated data points [251].

[d] Data from Ref. [252].

The k_Q data were supplied by different contributors and standards laboratories. Many of the k_Q measurements and some of the Monte Carlo simulations were carried out within the European Association of National Metrology Institutes (EURAMET) 16NRM03 RTNORM project [253]; other significant data were the comprehensive experimental set of McEwen [98] and updated Monte Carlo data from the National Research Council Canada (NRCC) group [254–256]. In practically all cases, the Monte Carlo codes for these calculations were EGSnrc [250] and PENELOPE [45, 46], mostly using phase space files for different WFF and FFF linacs, although in some cases the radiation sources were published spectra for several linacs [257–260]. Equation (94) was used to derive Monte Carlo calculated values of k_Q for different ionization chamber types irradiated by high energy photon beams, for which $(W_{\text{air}})_Q = (W_{\text{air}})_{^{60}\text{Co}}$. Experimental k_Q values for some chambers were measured in standards laboratories, by water or graphite calorimetry, with uncertainties of the order of 0.3–0.5%. The resulting two sets of beam quality factors for each chamber were combined to obtain statistically based consensus k_Q mean values and their uncertainty estimates, with the latter referring to the relative standard uncertainty ($k = 1$) expressed as a percentage.

The calculations to derive k_Q values carried out by different groups used different Monte Carlo systems and radiation sources, together with detailed ionization chamber type geometries provided by the respective manufacturers.

In all cases, the studies obtained k_Q values with type A standard uncertainties of the order of 0.1% or lower. To verify the homogeneity of the calculations, all the groups conducting Monte Carlo studies were requested to carry out a specific simulation of an NE-2571 ionization chamber in megavoltage photon beams of different quality. The goal was to establish the degree of variation of the k_Q values due to the implementation of the chamber geometry and the Monte Carlo transport parameters used by each group. The results obtained are shown in Fig. 26, which also includes experimental data measured at PSDLs for this chamber type. The complete dataset was fitted with the following functional form:

$$k_Q\left(\mathrm{TPR}_{20,10}\right)=\frac{1+\exp\left(\frac{a-0.57}{b}\right)}{1+\exp\left(\frac{a-\mathrm{TPR}_{20,10}}{b}\right)} \tag{97}$$

where a and b are specific parameters for each chamber type, and the value 0.57 is taken to be the mean $\mathrm{TPR}_{20,10}$ value of ^{60}Co γ ray units (assuming k_Q = 1 for this reference quality). The latter is included in Fig. 26[67] along with the 95% prediction limits of the fit, which yielded a root mean square difference of the data about the fit of 0.2%. It can be seen that most results agree within about ±0.5%, showing consistency in the different determinations. Values of the chamber type specific parameters a and b obtained from the fit using Eq. (97) for different chamber types are included in Table 45.

It should be mentioned that as the beam quality specifier Q ($\mathrm{TPR}_{20,10}$) does not take the beam profile around the point of measurement in the phantom into account, it could be possible to have two beams with identical Q values (e.g. WFF and FFF) and different beam profiles in the vicinity of the point of measurement. Because k_Q is taken to be a function of only Q (which does not consider the beam profile), different k_Q values for the identical Q of the two beams could be expected for a given chamber. However, in both Monte Carlo and experimental determinations, the differences in k_Q between WFF and FFF beams, and also in the use of phase space files or photon spectra, were found not to be significantly different [153, 261].

Examples of k_Q data and fits for two other ionization chamber types commonly used are presented in Fig. 27. It is emphasized that the k_Q values provided in this international code of practice do not distinguish chamber to chamber variations for a given chamber type, and their use necessarily

[67] It should be noted that considering the $\mathrm{TPR}_{20,10}$ values of ^{60}Co γ ray beams in parallel with values for megavoltage photon beams is not strictly consistent, as the photon spectra from a radionuclide and from bremsstrahlung are substantially different.

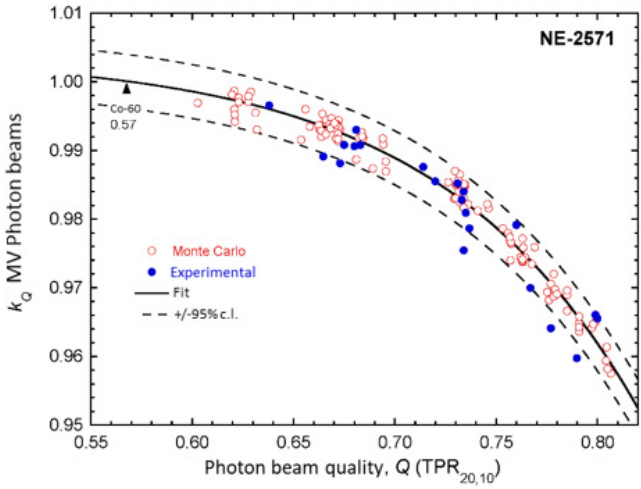

FIG. 26. Values of k_Q *for megavoltage (MV) photon beams obtained from Monte Carlo calculations by different groups (open circles) and measured at PSDLs (filled circles) for an NE-2571 ionization chamber. The solid line is a fit to the data using Eq. (97) and the dashed lines are the 95% prediction limits of the fit. Adapted from Ref. [100] (© Institute of Physics and Engineering in Medicine. Reproduced by permission of IOP Publishing Ltd). c.l.: confidence limit.*

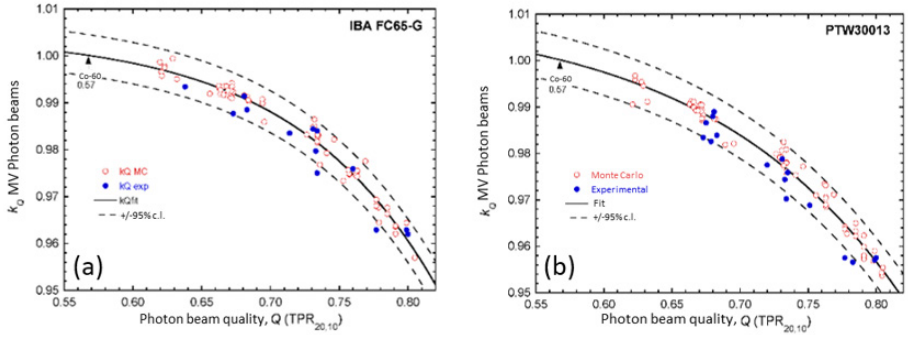

FIG. 27. Values of k_Q *for megavoltage (MV) photon beams obtained from Monte Carlo (MC) calculations by different groups (open circles) and measured at PSDLs (filled circles) for the ionization chamber types IBA FC65-G and PTW 30013. The solid lines are fits to the data using Eq. (97) and the dashed lines are the 95% prediction limits of the fit. Adapted from Ref. [100] (© Institute of Physics and Engineering in Medicine. Reproduced by permission of IOP Publishing Ltd). c.l.: confidence limit.*

involves larger uncertainties than when the values are measured at the standards laboratory for a specific user chamber.

The statistical analysis of the k_Q data for different ionization chamber types is similar to the procedure used in Ref. [12]; it included all the available datasets determined in the various Monte Carlo and experimental studies. For each chamber type, an initial fit was made using Eq. (97); data points outside the 99.73% (k = 3) prediction limits of the fit were filtered out and the fit was repeated. Considering that most determinations stated similar relative standard uncertainties and that these were of different types (type A or combined, for Monte Carlo calculated or measured data, respectively), the various input datasets were not weighted statistically. Regarding the estimation of uncertainties (see Ref. [100] for details), the following apply:

— The Monte Carlo calculations do not include estimates of type B uncertainties[68], and the calculated k_Q data provided by the different groups are expected to have correlated uncertainties that do not appear as scatter in their values (which were obtained with the same or similar Monte Carlo systems).
— In contrast, the experimental data for k_Q provided by different laboratories are largely uncorrelated and a fit to these data alone results in a more robust uncertainty estimate. For each chamber type, the relative deviation of the fit to the experimental data increased slightly with $TPR_{20,10}$, but the change was small enough to justify adopting an overall quality independent uncertainty. Regressions were made for the different chamber types, yielding on average a standard uncertainty component of ~0.5%; an additional contribution of ~0.3% was added for the experimental uncertainty.
— Finally, the uncertainty of assigning k_Q values to a given photon beam quality was estimated to be 0.2%. This includes an uncertainty for the use of phase space data files or photon spectra in the Monte Carlo calculations and for the measurement of $TPR_{20,10}$ by research groups and the end user for both WFF and FFF beams.

The different components are summarized in Table 46, yielding a combined standard uncertainty for the k_Q values of high energy photons of ~0.6%.

[68] It should be noted that the estimation of type B uncertainties in Monte Carlo calculations involves considerable difficulty. Although some authors have estimated type B uncertainties of 0.2–0.4% for megavoltage photon beams [262], their analysis did not account for components due to the single and multiple electron scattering theories and their implementation in the Monte Carlo system used, which for years have been considered a major constraint for the Monte Carlo simulation of ionization chambers (see e.g. Refs [108, 263]).

TABLE 46. ESTIMATED RELATIVE STANDARD UNCERTAINTY OF k_Q VALUES FOR HIGH ENERGY PHOTON BEAMS *(from Ref. 100])*

Component	u_c (%)
Prediction uncertainty from fit using Eq. (97)	0.51
Net experimental uncertainty	0.28
Assignment of k_Q to $TPR_{20,10}$	0.20
Combined standard uncertainty in k_Q	0.62

II.4. ELECTRON BEAMS

In contrast to the situation for photons, limited data are available for electron beams from which consensus values for k_Q can be selected. This is the case for both experimental values determined from comparison with primary standards of absorbed dose to water and Monte Carlo simulations that follow the same formalism as for other beam modalities. This lack of data reflects: (a) the smaller number of PSDLs that have developed primary standards and of currently active academic research groups and (b) the relatively low usage of megaelectronvolt electron beams in clinical radiotherapy. The expectation at the start of the project to revise the first edition of this international code of practice was that significant new data would be forthcoming and some kind of average (weighted or otherwise) could be determined for each chamber type from multiple determinations. However, for some chamber types there is no more than one dataset of each type — experimental and simulated — and the resolution and uncertainty are often significantly different for the two types.

Therefore, the approach taken in this publication was to base the consensus k_Q and $k_{Q,Q_{int}}$ values for electron beams on the Monte Carlo simulations of Muir and Rogers [167], the most extensive single dataset available, and use other determinations for validation and to provide an estimation of the uncertainty. The primary advantage of this approach is that there is consistency between chamber types, in terms of both the calculational method and the presentation of results. Experimental data were reviewed to not only validate the calculations but also provide direct evidence of the performance of chambers as reference class instruments, and therefore answer the question as to whether they are appropriate for use in this international code of practice.

Experimental data (k_Q, $k_{Q,Q_{\text{int}}}$, chamber characterization) from Refs [163, 174, 264–269] and calculated k_Q and $k_{Q,Q_{\text{int}}}$ data from Refs [167, 247, 270–273] were considered in the analysis. The tolerance value for comparing different datasets was chosen to be 0.5% for k_Q and 0.3% for $k_{Q,Q_{\text{int}}}$, according to a review of the uncertainties in the reported calculations and measurements. One of the challenges when reviewing experimental $N_{D,\text{w},Q}$ calibration coefficients is the lack of available comparisons between PSDLs. There is no BIPM coordinated comparison for megaelectronvolt electron beams, in contrast to kilovolt X ray, ^{60}Co and megavolt photon beams. Any difference in the primary standards will therefore lead to a difference in k_Q. In addition, not all experimental determinations include a determination of the $N_{D,\text{w}}$ calibration coefficient in a ^{60}Co beam. A different problem was encountered when comparing Monte Carlo simulations. With the exception of Ref. [247], all the data were obtained using the EGSnrc system. The level of agreement between such datasets is therefore reduced because of correlations.

Because of the sparsity of the datasets being used in the validation process, no modification was made to the calculations of the Ref. [167], except to apply the correct point of measurement, as defined in this international code of practice. This reduced the review to a simpler yes/no decision for each chamber type, with the guiding principle being to include only k_Q data with both the experimental and the Monte Carlo values available and for which those values agreed within the tolerances given above. As a final check, the new data were compared with those given in the first edition of this international code of practice; this showed that for the majority of chamber types with data in the previous version, changes in k_Q were <1%.

This analysis resulted in only a small number of chambers for which k_Q values could be confidently asserted — two plane parallel types and five cylindrical types. The data available indicated that PTW Roos and IBA NACP-02 could be calibrated in a ^{60}Co beam, but for all other plane parallel types direct calibration in a megaelectronvolt electron beam or cross-calibration against one of these seven chamber types are the only recommended options. For cylindrical chamber types, the choice is restricted to Farmer type (0.6 cm^3) chambers, as these have been investigated by more than one research group. Only k_Q data are given for these chambers, as they are all recommended for use in ^{60}Co beams. Recommending only a small number of chamber types for megaelectronvolt electron beams is consistent with other codes of practice, for example Ref. [106].

As for the data for megavolt photon beams, the k_Q and $k_{Q,Q_{\text{int}}}$ values given in this publication are based on fits of the following form:

$$k_{Q,\text{pp}} = a + be^{-\frac{R_{50,D}}{c}} \tag{98}$$

$$k_{Q,\text{cyl}} = a + bR_{50,D}^{-c} \tag{99}$$

for plane parallel and cylindrical chambers, respectively. For chambers for which only $k_{Q,Q_{\text{int}}}$ values are given, these are obtained from the k_Q calculations, by dividing by the value of $k_{Q_{\text{int}},Q_{\text{o}}}$. The fitting parameters *a*, *b* and *c* are given in Tables 47 and 48.

TABLE 47. FITTING PARAMETERS FOR k_Q FOR ELECTRON BEAMS FOR VARIOUS CHAMBER TYPES CALIBRATED IN ^{60}Co GAMMA RADIATION

Ionization chamber type[a]	*a*	*b*	*c*
Plane parallel chambers			
PTW 34001 Roos	0.884	0.120	3.511
IBA NACP-02	0.879	0.120	3.398
Cylindrical chambers			
NE 2571	0.892	0.103	0.920
IBA FC65-G	0.884	0.103	0.680
Exradin A12	0.880	0.108	0.607
Exradin A19	0.870	0.108	0.505
PTW 30013	0.888	0.101	0.816
PTW 30012	0.889	0.111	0.728

[a] Note that the equations used to calculate k_Q are different for plane parallel and cylindrical chambers (see Eqs (98, 99)).

TABLE 48. FITTING PARAMETERS FOR $k_{Q,Q_{int}}$ FOR ELECTRON BEAMS FOR VARIOUS CHAMBER TYPES CALIBRATED IN HIGH ENERGY ELECTRON BEAMS

Ionization chamber type[a]	*a*	*b*	*c*
Plane parallel chambers			
PTW 34001 Roos	0.984	0.134	3.511
IBA NACP-02	0.985	0.135	3.398
PTW 34045 Advanced Markus	0.986	0.135	3.349
PTW 23343 Markus	0.984	0.112	3.826
IBA PPC40	0.984	0.130	3.510
IBA PPC05	0.982	0.104	4.248
Exradin A10	0.991	0.112	2.927
Exradin A11	0.992	0.114	2.864
Exradin P11	0.989	0.177	2.687
Sun Nuclear SNC350p	0.984	0.134	3.511
Cylindrical chambers			
NE 2571	0.982	0.113	0.920
IBA FC65-G	0.971	0.113	0.680
Exradin A12	0.965	0.119	0.607
Exradin A19	0.957	0.119	0.505
PTW 30013	0.978	0.112	0.816
PTW 30012	0.972	0.121	0.728

[a] Note that the equations used to calculate k_Q are different for plane parallel and cylindrical chambers (see Eqs (98, 99)).

Andreo et al. [100] carried out an extensive uncertainty analysis of k_Q data for megavoltage photon beams using multiple datasets and arrived at a robust assessment of the overall uncertainty in k_Q values of ~0.6%. As it is not straightforward to repeat this analysis for electron beam k_Q data, the photon beam uncertainty is taken as a starting point for this discussion. The uncertainty in Monte Carlo calculations for electron beams should not be significantly different, as the underlying algorithms and interaction modelling are similar, and Refs [271, 272] report uncertainties consistent with this value. Experimental results state standard uncertainties for the determination of $N_{D,w,Q}$ in the range 0.4–1%, with lower uncertainties obtained for higher energies (greater than ~12 MeV). However, agreement between measured and calculated k_Q factors for the chambers in Table 47 is better than 0.4% in all cases, so this value is taken for the net uncertainty contributing to the uncertainty in k_Q for electron beams with $R_{50,D} \geq 2$ g/cm^2. For lower energy electron beams, the experimental uncertainty component is estimated to be 0.6%. As for the photon beam case, an additional uncertainty component is included to account for potential differences between the electron beams used to obtain k_Q values and those where the dose is to be measured. The corresponding values are given in Table 49.

The uncertainty in $k_{Q,Q_{\text{int}}}$ is somewhat lower, owing to the correlations in experimental data and the calculations. On the basis of the comparison of data for PTW Roos and IBA NACP-02, the only two chambers with multiple experimental determinations, a combined standard uncertainty in $k_{Q,Q_{\text{int}}}$ of 0.35% is obtained for $R_{50,D} \geq 2$ g/cm^2. For electron energies below this value, there is a divergence in the data based on different standards, and an increase in the uncertainty to 0.6% is justified.

TABLE 49. ESTIMATED RELATIVE STANDARD UNCERTAINTY OF k_Q VALUES FOR HIGH ENERGY ELECTRON BEAMS FOR $R_{50,D} \geq 2$ g/cm^2

Component	u_c (%)
Prediction uncertainty from fit	0.51
Net experimental uncertainty	0.40[a]
Assignment of k_Q to $R_{50,D}$	0.20
Combined standard uncertainty in k_Q	0.68[b]

[a] For $R_{50,D} < 2$ g/cm^2, this component is estimated to be 0.6%.
[b] For $R_{50,D} < 2$ g/cm^2, the combined uncertainty is estimated to be 0.81%.

It should be restated that the provision of such k_Q and $k_{Q,Q_{int}}$ data is not the preferred choice for obtaining the $N_{D,w,Q}$ calibration coefficient in a megaelectronvolt electron beam. As outlined in Section 1.4, a direct calibration in a beam that is as similar to the user beam as possible should result in the lowest uncertainty. However, it is still recommended to limit the choice of chamber to those listed in Tables 47 and 48, as these have been assessed to meet the requirements of a reference class instrument.

II.5. PROTON BEAMS

The availability of new k_Q values for proton beams, either Monte Carlo calculated [242, 274–279] or experimental [280–288], is limited to a reduced set of cylindrical and plane parallel ionization chambers (see Table 50). For this reason, the k_Q data recommended in this publication for proton beams have been obtained using the approximate analytical Eqs (91, 96) with chamber wall material dependent generic perturbation correction factors derived from the Monte Carlo calculations. In all cases, the stopping powers are those from Ref. [32], the reference beam quality is ^{60}Co, and account is taken of the different W_{air} values for protons and for ^{60}Co. It is worth noting that for most of the chamber types analysed, the perturbation correction factors have been confirmed by the various calculations to be different from unity; this represents a significant change compared with the first edition of this international code of practice, which was based on the approximation $p_Q \equiv 1$.

TABLE 50. CHAMBER TYPES AND NUMBER OF DATA POINTS DERIVED BY MONTE CARLO AND EXPERIMENTAL k_Q DETERMINATIONS IN PROTON BEAMS

Ionization chamber type	Number of data points Monte Carlo	Experimental (direct)	Experimental (cross-calibration)
Cylindrical chambers			
Capintec PR-06 Farmer	—[a]	2	—[a]
Exradin A1SL Miniature	4	—[a]	—[a]
Exradin A12 Farmer	5	—[a]	—[a]
Exradin A19 Classic Farmer	5	—[a]	—[a]

TABLE 50. CHAMBER TYPES AND NUMBER OF DATA POINTS DERIVED BY MONTE CARLO AND EXPERIMENTAL k_Q DETERMINATIONS IN PROTON BEAMS (cont.)

Ionization chamber type	Number of data points Monte Carlo	Experimental (direct)	Experimental (cross-calibration)
IBA FC65-G Farmer	14	4	3
IBA FC65-P Farmer	10	—[a]	3
NE 2571 Farmer	27	4	—[a]
PTW 30013 Farmer	14	—[a]	—[a]
PTW 30001 Farmer	—[a]	2	3
PTW 30006 Farmer	—[a]	—[a]	3
PTW 31021 Semiflex 3D	5	—[a]	—[a]
Plane parallel chambers			
Exradin A10	13	—[a]	—[a]
Exradin A11	13	—[a]	—[a]
Exradin A11 TW	13	—[a]	—[a]
IBA NACP-02	35	2	4
IBA PPC05	21	—[a]	—[a]
IBA PPC40	21	—[a]	—[a]
PTW 34045 Adv. Markus	25	—[a]	2
PTW 23343 Markus	25	2	—[a]
PTW 34001 Roos	29	—[a]	4
Total number of data points	279	14	22

[a] —: data not available.

For the analytical calculations using Eqs (91, 96), the following data were used:

(a) Monte Carlo derived water–air stopping power ratios for monoenergetic proton beams, given by the following empirical relation:

$$\left(s_{\mathrm{w,air}}\right)_{R_{\mathrm{res}}} = a + bR_{\mathrm{res}} + \frac{c}{R_{\mathrm{res}}} \tag{100}$$

where $a = 1.131$, $b = -2.327 \times 10^{-5}$ and $c = 2.046 \times 10^{-3}$. The coefficients were obtained from a fit to the stopping power ratios calculated using the Monte Carlo code PETRA [289, 290] for incident monoenergetic proton beams, as in the first edition of this international code of practice, but the key proton and secondary electron stopping powers are now taken from Ref. [32]. The PETRA calculations include the transport of secondary electrons, as well as nuclear inelastic processes for which Ref. [32] does not provide key data. PETRA calculates stopping power ratios 'in-line' — that is, during the transport of the particles — following the Spencer–Attix cavity theory. In-line calculations have the advantage of scoring the track ends accurately; in addition, any possible influence on the resulting number and size of the energy scoring bins in the fluence calculation is avoided. Compared with the stopping power ratios in the first edition of this international code of practice, these values are approximately 0.5% lower and the estimated uncertainty of $s_{\mathrm{w,air}}$ at the reference depth in a clinical beam remains 1%. Figure 28 shows $s_{\mathrm{w,air}}$ as a function of R_{res}. No correlation with electron stopping powers is assumed when evaluating the uncertainty of k_Q. The uncertainty of assigning stopping power ratios to a given proton beam quality is estimated to be 0.3%; this includes an uncertainty for the difference between the spectrum for a single energy layer field and for a SOBP proton beam with the same residual range.

(b) Ionization chamber perturbation correction factors obtained in a comprehensive analysis made by Palmans et al. [220] using Monte Carlo and experimental data. Most Monte Carlo k_Q data were calculated with the Monte Carlo codes Geant4 [291], PENH [292] or a combination of the two. The data are generally available for single layer scanned beams, except those from Ref. [242], which also included data for an SOBP beam. Most experimental determinations were made with water or graphite calorimetry. The goal of Ref. [220] was to extract $(p_{\mathrm{ch}})_Q$ values or, for reasons that will become apparent below, $(p_{\mathrm{ch}}/p_{\mathrm{dis}})_Q$ ratios, where p_{dis} is the chamber

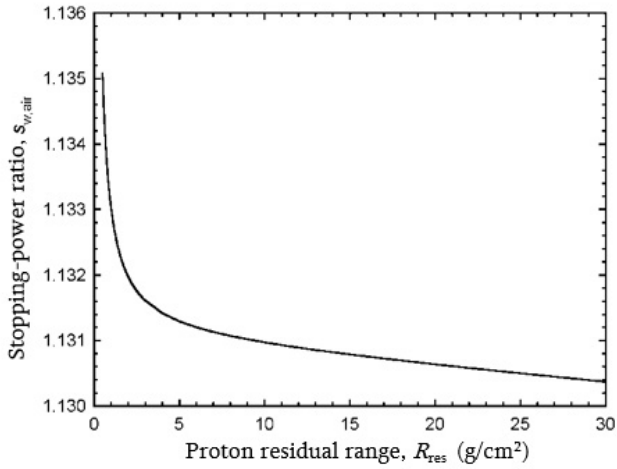

FIG. 28. Spencer–Attix (Δ = 10 keV) water to air stopping power ratios for clinical proton beams as a function of the beam quality index R_{res}. *The curve is a fit to stopping power ratios calculated using the Monte Carlo code PETRA [290] for incident monoenergetic proton beams. The data include the transport of secondary electrons and nuclear inelastic processes, and the key stopping powers are taken from Ref. [32].*

displacement correction factor. They were calculated using the following equations:

$$p_{\mathrm{ch},Q} = \frac{f_{\mathrm{ch}}(Q)}{\left(s_{\mathrm{w,air}}\right)_Q} \qquad \text{for plane parallel ionization chambers}$$

$$\left(\frac{p_{\mathrm{ch}}}{p_{\mathrm{dis}}}\right)_Q = \frac{f_{\mathrm{ch}}(Q)}{\left(s_{\mathrm{w,air}}\right)_Q p_{\mathrm{dis},Q}} \qquad \text{for cylindrical ionization chambers} \tag{101}$$

where $f_{\mathrm{ch}}(Q)$ is derived by solving Eq. (96) if only k_Q is provided in a given publication, $(s_{\mathrm{w,air}})_Q$ is calculated using Eq. (100) and p_{dis} values are taken from Ref. [218]. For cylindrical chamber types at low R_{res} values, there is a substantial difference between $(p_{\mathrm{ch}})_Q$ data for single layer or unmodulated beams and modulated beams because of the large depth dose gradients in the latter. Removing this gradient component from the perturbation correction factor by considering the ratio $(p_{\mathrm{ch}}/p_{\mathrm{dis}})_Q$ results in a spread of the data that is practically independent of R_{res} and of the beam type (single layer, unmodulated or modulated); the standard deviations of all data vary typically between 0.3% and 0.5%, with 0.4% a frequent value. For plane parallel chambers, the $(p_{\mathrm{ch}})_Q$ data are also independent of R_{res} and of the beam type.

The measured data generally confirm the results from the Monte Carlo simulations within the experimental uncertainties. Based on these findings, chambers were subsequently grouped according to the material composition of the chamber wall, and $(p_{ch})_Q$ and $(p_{ch}/p_{dis})_Q$ values for the chambers not listed in Table 50 were taken to be the average values of chamber types with the same wall materials. For the chambers in Table 50, average values for the specific chamber types were used. Final $f_{ch}(Q)$ values were computed according to the following equations:

$$
\begin{aligned}
f_{ch}(Q) &= \left(s_{w,air}\right)_Q p_{ch,Q} && \text{for plane parallel ionization chambers} \\
f_{ch}(Q) &= \left(s_{w,air}\right)_Q \left(\frac{p_{ch}}{p_{dis}}\right)_Q p_{dis,Q} && \text{for cylindrical ionization chambers, single layer fields} \\
f_{ch}(Q) &= \left(s_{w,air}\right)_Q \left(\frac{p_{ch}}{p_{dis}}\right)_Q && \text{for cylindrical ionization chambers, modulated beams (SOBPs)}
\end{aligned}
\qquad (102)
$$

Additionally, for cylindrical chambers a single optimized dataset was calculated with values differing by less than 0.4% from those obtained directly with the latter two formulas. The process of deriving $(p_{ch})_Q$ for plane parallel chambers and $(p_{ch}/p_{dis})_Q$ for cylindrical chambers demonstrates that, apart from the beam quality dependence of $s_{w,air}$, and of p_{dis} for non-modulated beams, no other $(p_{ch})_Q$ component or contributing factors in $f_{ch}(Q)$ depend on beam quality. Given the sparsity of the data available, this process also yields consistent and smooth datasets of $f_{ch}(Q)$ for all chamber types.

(c) The recommended [32] value $(W_{air})_Q = 34.44$ eV with a standard uncertainty of 0.4%, which is based on estimating [293] the relative change of $(W_{air})_Q$ for proton beams by comparing calorimetry with ionometry using different air kerma and absorbed dose to water codes or practice. This value, combined with the estimate for $\left(W_{air}\right)_{^{60}Co}$, yields 0.53% for the uncertainty of the $\left(W_{air}\right)_Q \Big/ \left(W_{air}\right)_{^{60}Co}$ ratio.

(d) The $f_{ch}(Q_o)$ values given in Table 44 for the reference quality of ^{60}Co γ ray beams.

Table 51 summarizes the relative uncertainty estimates of the different components, yielding a combined standard uncertainty in k_Q for proton beams of 1.4%. Note that the uncertainty component due to the different nuclear interaction data in the Monte Carlo codes has not been considered; even if some k_Q data at the highest energies show a scatter of up to 2%, the differences have not been analysed in a way that allows an unambiguous assignment to different nuclear cross-sections.

TABLE 51. ESTIMATED RELATIVE STANDARD UNCERTAINTY OF k_Q FOR PROTON BEAMS

Component	u_c (%)
$(s_{w,air})_Q$	1.0
$(p_{ch})_Q$	0.6
$\left(f_{ch}\right)_{^{60}Co}$	0.4
$\left(W_{air}\right)_Q / \left(W_{air}\right)_{^{60}Co}$ ratio	0.5
Assignment of values to beam quality	0.3
Combined standard uncertainty in k_Q	1.4

II.6. LIGHT ION BEAMS

There are no Monte Carlo calculations of k_Q for light ion beams available, and experimental k_Q values have been determined only for carbon ions for a very limited number of chambers either by direct measurements or by cross-calibration [95, 243, 244]. However, because only one ionization chamber of each type was used during the experimental determinations, the recommended k_Q data for light ions continue to be calculated based on Eq. (91). For light ion beams, the calculated beam quality correction factors given in this publication are based on a chamber calibration in ^{60}Co. The values to be used for the denominator of Eq. (91) are discussed in Section II.2.1.

The $s_{w,air}$ value should be obtained by averaging over the complete spectrum of primary particles and fragmented nuclei at the reference depth, as follows:

$$s_{w,air} = \frac{\sum_i \int_0^\infty \Phi_{E,i} \left(S_i(E)/\rho\right)_w \, dE}{\sum_i \int_0^\infty \Phi_{E,i} \left(S_i(E)/\rho\right)_{air} \, dE} \tag{103}$$

where $(S_i(E)/\rho)_m$ is the mass stopping power at energy E for particle i in medium m and Φ_E is the particle fluence differential in energy. However, in view of the lack of knowledge of the fluence spectra Φ_E, substantial simplifications were

made in the first edition of this international code of practice, whereas today detailed Monte Carlo simulations are available [241].

The first edition of this international code of practice suggested a constant value of $s_{w,air}$ = 1.13. This was based on computational results from Refs [49, 294, 295] for ions with Z = 1–18 that showed that all values lay in the range 1.12–1.14. The recent update of key data for dosimetry in Ref. [32] affects $s_{w,air}$ via changes in the mean excitation energy of water (I_w = 78.0 eV) and changes in the computation of stopping powers. The relative change in $s_{w,air}$ for light ions was estimated in Ref. [32] as –0.4%. A recalculation of $s_{w,air}$ for carbon beams [241] showed that an adopted constant value of 1.126 is compatible with a wide range of conditions used for beam calibration. $s_{w,air}$ values for carbon ions as a function of residual range energy, calculated using Geant4 with the updated stopping power data from Ref. [32] are shown in Fig. 29.

The uncertainty of $s_{w,air}$ in light ion beams is larger than that in proton beams because of its dependence on energy and particle type. Uncertainties in the basic stopping powers also have to be included and are estimated conservatively to be 1.5% [241]. In addition, the assignment of a value to a given beam quality increases the uncertainty estimate by 0.3%.

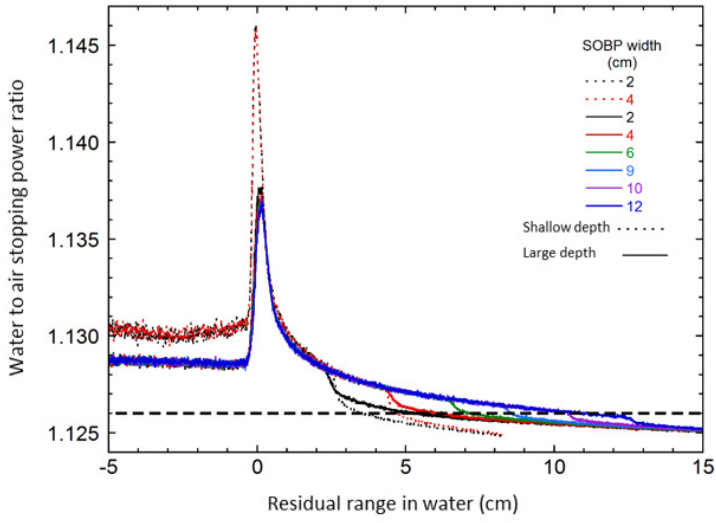

FIG. 29. Water to air stopping power ratio for carbon ions as a function of the residual range in water, calculated using Geant4 [241] with updated stopping power data from Ref. [32]. Computations were performed for spread-out Bragg peaks (SOBPs) with widths of 2–12 cm and two depths of the distal edge (8 and 30 cm) to cover a wide range of beam qualities. All values for $s_{w,air}$ at depths relevant for reference dosimetry (1–2 cm or mid-SOBP) fall within 0.2% around the recommended constant value of 1.126.

As discussed above for $s_{w,air}$, W_{air} should ideally be obtained by averaging over the complete spectrum of primary particles and fragmented nuclei at the reference depth, as follows:

$$\frac{\bar{w}}{e} = \frac{\sum_i \int_0^\infty \Phi_{E,i} \left(S_i(E)/\rho\right)_{air} \mathrm{d}E}{\sum_i \int_0^\infty \frac{\Phi_{E,i} \left(S_i(E)/\rho\right)_{air}}{w_i(E)/e} \mathrm{d}E} \tag{104}$$

where $w_i(E)$ is the differential value of W_{air} at energy E for particle i, and e is the elementary charge. The fluence differential in energy, Φ_E, should cover a wide energy spectrum and include all primary and secondary particles.

There are very few experimental investigations of W_{air} for high energy light ions. Using the same analysis procedure as applied for the proton beams, the updated key dosimetric data in Ref. [32] result in a relative change of +0.6% for W_{air}. Thus, a W_{air} value of 34.71 eV for carbon ions with a standard uncertainty of 0.52 eV or 1.5% [32] is used in this international code of practice. More recent experimental data by Osinga-Blättermann et al. [95] and Holm et al. [244] are in agreement with this value, while studies by Sakama et al. [296] and Rossomme et al. [297] indicate values higher by approximately 3%.

At present, no experimental information is available on perturbation factors in light ion beams and all components are taken to be unity. An overall uncertainty of 1.0% is assumed on the basis of the evaluation of Hartmann et al. [227].

Table 52 summarizes the uncertainty estimates and shows a combined relative standard uncertainty in k_Q of 2.4% in light ion beams for both cylindrical and plane parallel chambers. This arises largely from the uncertainty of the stopping power ratio $s_{w,air}$ and W_{air}. The experimental determination of k_Q in carbon beams for two Farmer type ionization chambers (FG65-G and TM3013) using water calorimetry yielded a considerably smaller uncertainty of 0.7% and 0.8%, respectively [95, 244], and a cross-calibration procedure determined standard measurement uncertainties of 1.1% for eight additional cylindrical ionization chambers (NE 2571, IBA FC65-P, IBA FC23-C, IBA CC25, IBA CC23, PTW 30010, PTW 30011 and PTW 30012) [243].

TABLE 52. ESTIMATED RELATIVE STANDARD UNCERTAINTY OF CALCULATED k_Q VALUES FOR LIGHT IONS

Component	Cylindrical and plane parallel chambers u_c (%)	
	Light ion beams	^{60}Co and light ion beams[a]
$s_{w,air}$	1.5	1.5
W_{air}	1.5	1.5
p (combined)	1.0	1.0
Assignment of k_Q to the beam quality	0.3	0.3
Combined standard uncertainty in k_Q	—[b]	2.4

[a] Includes the standard uncertainty for f_{ch} in ^{60}Co beams of 0.4%.
[b] —: data not available.

Appendix III

BEAM QUALITY SPECIFICATION

III.1. GENERAL

The values of mass stopping power ratios, mass energy absorption coefficient ratios, mean energy expended in air per ion pair formed, perturbation factors, etc., and thus also the values of the correction factor k_{Q,Q_o}, depend on the characteristics of the radiation field at the point of measurement. Of particular interest in this context is the spectral fluence distribution of primary and secondary particles, which is used as a weighting function for the determination of spectral averaged quantities.[69]

The spectral fluence of primary and secondary particles at the point of measurement depends on different parameters, such as the characteristics of the radiation source (i.e. the properties of the radiation beam impinging on a phantom), the phantom material, the field size, the depth in the phantom, the lateral distance from the beam axis, and the dosimeter detector (ionization chamber) itself. To reduce the number of parameters required for practical dosimetry, reference conditions have been defined for all parameters except the properties of the incident beam. For absorbed dose measurements complying with these reference conditions, the spectral fluence at the point of measurement depends on the properties of the incident beam. However, the experimental determination of either the spectral fluence at the point of measurement or the spectral and angular distribution of the incident beam is difficult to obtain or not feasible at all. Therefore, other parameters are used for the characterization of the properties of the incident beam and the spectral particle fluence at the point of measurement under reference conditions. Such parameters, which have to be closely correlated with the relevant properties of the corresponding spectral distribution and should be easily accessible by measurements, are called beam quality specifiers and are generally denoted by the symbol Q.

---

[69] In some cases the spectral fluence of only the primary or only the secondary particles is considered for the calculation of spectral averaged quantities, especially if the contribution of one class of particles (primary or secondary) to the signal generation in an ionization chamber can be neglected. An example is the Bragg–Gray (or Spencer–Attix) cavity theory, according to which the response of an ionization chamber in high energy photon beams (under certain conditions) is determined only by the spectral fluence of secondary (and higher order) electrons. Modern Monte Carlo methods usually do not rely on such approximations and take into account the spectral fluences of all types of particle for the calculation of k_{Q,Q_o} values.

By following this approach, the beam quality correction factor k_{Q,Q_o} under reference conditions can be expressed as a function of a suitable beam quality specifier, allowing an easy determination of its value in routine dose measurements. It has to be stressed that there is not one beam quality specifier that is appropriate for all types of radiation and all beam energies; instead, different parameters are used to characterize different beam types and beam energies. Furthermore, because there is no unique way of deriving beam quality specifiers, different beam quality specifiers may be in common use for the same type of radiation, each having its advantages and disadvantages.

For the dosimetry of external beam radiotherapy, parameters obtained from attenuation or range measurements are mainly used as beam quality specifiers. In some cases, a set of parameter values is used to characterize the beam properties. The following sections describe common beam quality specifiers for the different types of radiation and beam energies.

III.2. BEAM QUALITY SPECIFIER FOR KILOVOLTAGE X RAY BEAMS

For low and medium energy kilovoltage X ray beams, the spectral fluence of the useful radiation impinging on the phantom depends on the following:

(a) The value and time variation (ripple) of the generating potential;
(b) The material of the anode;
(c) The roughness of the anode;
(d) The age and usage of the anode;
(e) The angle of incidence of the electrons;
(f) The material, purity and thickness of the filters;
(g) The set-up of the diaphragms.

Therefore, the quality of X ray beams cannot be specified by the generating potential alone. Typical parameters used to further characterize the spectral properties of the beam are the total filtration, the first HVL and the homogeneity coefficient (i.e. the ratio between the first and second HVLs). The total filtration includes the inherent filtration of the X ray tube and the filtration of any monitor ionization chamber, together with the additional filtration. A low inherent filtration is required for an X ray tube to be used effectively down to the lowest generating potential. The first HVL is the thickness of an absorber that reduces the air kerma rate of a narrow unidirectional X ray beam at a point distant from the absorbing layer to 50% compared with the non-attenuated beam; the second HVL is the additional absorber thickness needed to reduce the air kerma rate to 25%.

It is often not possible to match all these parameters (generating potential, total filtration, first and second HVLs) simultaneously for X ray beams of different laboratories (e.g. clinical X ray beams and beams at standards laboratories). This is due to incomplete knowledge or uncertainties in the specification of the X ray facility (e.g. generating potential, inherent filtration, roughness of anode) or to uncertainties in the determination of the HVLs (e.g. purity of absorbers, finite size of beam, change of response of dosimeter). Therefore, traditionally the first HVL has been used as the primary beam quality specifier to describe the change of the response of ionization chambers with beam energy and to select beam quality correction factors.

The first HVL, together with the generating potential, is used in this international code of practice as the beam quality specifier for low and medium energy kilovoltage X ray beams.[70] In addition to the kilovoltage, k_{Q,Q_o} factors are given in terms of the first HVL in aluminium or copper. Aluminium is used for X rays with generating potential up to 100 kV and copper is used above 100 kV. As an example, the low and medium energy X ray qualities used at BIPM to calibrate radiotherapy dosimeters are given in Table 53.

It should be noted that the concept of the HVL is based on the response of a dosimeter to air kerma. So far, a generally accepted specification of the beam quality of low and medium energy kilovoltage X rays based solely on the absorbed dose to water has not been developed.

III.3. BEAM QUALITY SPECIFIER FOR ^{60}CO GAMMA RAY BEAMS

Gamma ray spectra from ^{60}Co therapy sources used at hospitals or SSDLs have a substantial component of low energy scattered photons, originated in the source capsule itself and in the collimator. However, ionization chamber measurements are not expected to be influenced by ^{60}Co spectral differences by more than a few tenths of one per cent [58], which may be neglected for routine measurements. For this reason, ^{60}Co gamma ray beams for radiotherapy dosimetry do not require a beam quality specifier other than the specification of the radionuclide.

[70] The specification of the total filtration is useful additional information.

TABLE 53. KILIVOLTAGE X RAY BEAM QUALITIES USED FOR DOSIMETER CALIBRATIONS AT BIPM

Generating potential (kV)	Total filtration		First half-value layer	
	Aluminium (mm)	Copper (mm)	Aluminium (mm)	Copper (mm)
10	0	—[a]	0.037	—[a]
30	0.21	—[a]	0.17	—[a]
25	0.37	—[a]	0.24	—[a]
50[b]	1.0	—[a]	1.0	—[a]
50[c]	4.0	—[a]	2.3	—[a]
100	3.4	—[a]	4.0	0.15
135	2.2	0.23	—[a]	0.50
180	2.2	0.49	—[a]	1.0
250	2.2	1.6	—[a]	2.5

[a] —: not applicable.
[b] Referred to as the 50 kVb quality [298].
[c] Referred to as the 50 kVa quality [298].

III.4. BEAM QUALITY SPECIFIER FOR HIGH ENERGY PHOTON BEAMS

The spectral fluence distribution of high energy photon radiation produced by modern clinical linear accelerators (linacs) is not only determined by the maximum energy and the spectrum of the electrons hitting the target, but also by the material and thickness of the target, the material and geometry of the filters, the material and construction of the collimator, the diaphragms, etc. As an additional complication, the photon beam exiting the linac includes some (unwanted but unavoidable) contaminating electrons whose spectral fluence depends on the constructional details of the linac head (i.e. target, filter and collimator).

The specification of the quality of high energy photon beams has been the subject of numerous studies because of its relevance in radiation dosimetry. Two of the most widely used beam quality specifiers are the tissue–phantom ratio, $TPR_{20,10}$, and the PDD at 10 cm depth, $\%dd(10)_x$ [85, 99]. Other beam quality specifiers have also been proposed for photon beam dosimetry [146, 299, 300], but they are used less frequently for reference dosimetry.

$TPR_{20,10}$ is defined as the ratio of water absorbed doses on the beam axis at the depths of 20 cm and 10 cm in a water phantom, obtained with a constant SDD of 100 cm and a 10 cm × 10 cm field size at the position of the detector. $\%dd(10)_x$ is the PDD at 10 cm depth in a water phantom that is solely due to photons (i.e. excluding electron contamination, which requires the use of an additional 1 mm lead filter) for a field size of 10 cm × 10 cm at the phantom surface and an SSD of 100 cm.

There has been controversy in the literature about the preferred method for specifying the beam quality of high energy photon beams [88, 301, 302]; a summary of the arguments and the advantages and limitations of the different photon beam quality specifiers can be found in appendix III of the previous edition of this international code of practice. The general conclusion is that no beam quality specifier satisfies the requirements of being unique for the entire range of photon energies used in radiotherapy and for all types of accelerators used in hospitals and standard laboratories, as well as being easy to measure. Nevertheless, it is now generally agreed that both $TPR_{20,10}$ and $\%dd(10)_x$ are adequate beam quality specifiers for high energy photon beams produced by conventional linear accelerators used in radiotherapy [303–305]. It has been shown that the impact on clinical photon beam dosimetry resulting from the use of either $TPR_{20,10}$ or $\%dd(10)_x$ as a beam quality specifier to select k_Q values is of the order of 0.2% [306, 307], which is smaller than the typical uncertainty of current primary standards for absorbed dose to water in high energy photon beams [308].

Owing to the different spectral photon fluence produced by WFF and FFF accelerators (unflattened beams have a larger spectral spread with a considerable low energy component), a larger impact on dosimetry was expected (up to 0.6%) from the use of $TPR_{20,10}$ or $\%dd(10)_x$ as a beam quality specifier for FFF beams [154]. However, investigations by Lye et al. [147] showed that for FFF beams with nominal accelerating voltages of up to 10 MV the difference in absorbed dose due to the use of $TPR_{20,10}$ or $\%dd(10)_x$ is less than 0.2%. The result was explained by the presence of backscatter plates and buildup filters in modern clinical FFF linacs, which, even in the absence of a flattening filter, harden the beam and produce a similar spectrum to that produced by a conventional WFF linac.

For a user in a hospital or clinic, there is strictly no advantage of one photon beam specifier over the other, as both lead to rather similar k_Q values and hence

yield the same absorbed dose to water in the user's beam within the uncertainty of the method. Most modern dosimetry protocols or codes of practice based on the calibration of ionization chambers in terms of absorbed dose to water use $TPR_{20,10}$ as the beam quality specifier for high energy photon beams [83, 84, 159, 309]; an exception is the AAPM TG-51 protocol [85, 99], which uses $\%dd(10)_x$ as the beam quality specifier. In this international code of practice, $TPR_{20,10}$ is used as the beam quality specifier for high energy photon beams.

III.5. BEAM QUALITY SPECIFIER FOR HIGH ENERGY ELECTRON BEAMS

High energy electron beams for external beam radiotherapy are usually produced by a linear accelerator. When the electron beam exits the accelerator tube through a thin metal vacuum window, it has a very narrow spectral fluence distribution, being nearly monoenergetic. Because of energy losses in the vacuum window, the scattering foils used to widen the beam and the air, and scattering in the diaphragms and applicator walls, the spectral electron fluence distribution is widened and shifted to lower energies. In addition, bremsstrahlung is generated by electron interactions in the treatment head and the applicator. The bremsstrahlung contamination of the electron beam is minimized by appropriate construction of the treatment head (e.g. use of lower atomic number materials in the vacuum exit window and scattering foils); however, it cannot be completely avoided.

While in principle the electron spectrum can be measured directly (e.g. by magnetic spectrometers [310]) or reconstructed (e.g. from depth dose measurements [311]), these methods are too complicated for routine use in the clinic.[71] A simpler alternative is the determination of some characteristic parameters of the electron spectrum, which can be obtained from measured depth dose distributions in water. These parameters are the mean electron energy at the phantom surface, $\bar{E}_0$, and the most probable electron energy at the phantom surface, $E_{p,0}$, which are related to the half-value depth in water, R_{50}, and the practical range of the electrons in water, R_p. Equations for the conversion of R_{50} and R_p to $\bar{E}_0$ and $E_{p,0}$, respectively, are given in Ref. [19]. These equations have been reanalysed using Monte Carlo simulations and experiments under idealized conditions (broad, parallel, monoenergetic beams), and it has been found that they are not applicable with the same accuracy for all clinical accelerators, mainly owing to differences in the number of lower energy scattered electrons and contaminating bremsstrahlung photons for accelerators of different designs [312].

[71] Other methods for determining the electron energy are described in Ref. [19], section 3.3.2.

Because the additional step of converting depth dose parameters into energies brings no benefit in characterizing an electron beam, the parameters R_{50} and R_p may be used directly to specify the quality of electron beams. It has been shown by Burns et al. [173] that the stopping power ratios $s_{w,air}$ for different accelerator types can be expressed as a unique function of R_{50} if the reference conditions are chosen appropriately. Therefore, in this international code of practice, the quality of electron beams is specified by the half-value depth of the absorbed dose distribution in water R_{50} under well specified reference conditions (see Table 18).

III.6. BEAM QUALITY SPECIFIER FOR PROTON BEAMS

In previous proton dosimetry protocols and recommendations [212, 312–314] the beam quality was specified by the effective energy, which is defined as the energy of a monoenergetic proton beam having a continuous slowing down approximation range equal to the residual range R_{res} of the clinical proton beam (see definition below). This choice was justified by the small energy dependence of water to air stopping power ratios and by the fact that the effective energy is close to the maximum energy of the proton energy spectrum at the reference depth (see Table 34).

In this international code of practice, the residual range R_{res} is chosen as the proton beam quality index because it is easily measurable. Although this choice slightly underestimates the stopping power ratios in the middle of the SOBP, the effect is unlikely to exceed 0.3% [212, 213].

The residual range R_{res} at a measurement depth z is defined as follows:

$$R_{res} = R_p - z \tag{105}$$

where z is the depth of measurement and R_p is the practical range, which is defined [212] as the depth at which the absorbed dose beyond the Bragg peak or the SOBP falls to 10% of its maximum value.

Unlike the beam quality specifiers for other types of radiation covered in this publication, the beam quality specifier for protons is not unique for a particular beam impinging on a phantom, as it is also determined by the depth z selected for the measurement.

III.7. BEAM QUALITY SPECIFIER FOR LIGHT ION BEAMS

The calculation of beam quality correction factors k_{Q,Q_o} for light ion beams is complex, since it involves the spectra of primary particles and all fragmented nuclei at the point of measurement. Knowledge on the projectile and target fragments and their spectral fluence distribution as a function of the type and energy of the primary particles and the depth in a phantom relies on Monte Carlo calculations using different codes [232–235, 237, 238, 241], each using different data for the modelling of nuclear fragmentation [236].

In the previous edition of this international code of practice, light ion beams were characterized by specifying the atomic number, the mass number and the energy of the incident ion, together with the width of the SOBP and the range in water. Lühr et al. [232] showed that the water to air stopping power ratio at a depth z in a phantom is mostly determined by the mean energy of the primary ions at that depth, rather than by their initial energy or their atomic number. Further, it was found that for depths smaller than the practical range R_p, the water to air stopping power ratio is dominated by that of the primary ion species, which renders a detailed knowledge of the fragments unnecessary. As the mean energy of the primary ions is closely related to the residual range R_{res} at depth z, defined as in Eq. (105), a beam characterization based on the residual range R_{res} could be used, as for proton beams. However, the definition of the practical range R_p for light ion beams is less straightforward than for proton beams owing to the pronounced dose tail beyond the Bragg peak caused by nuclear fragments [30].

The current estimated uncertainty for light ion dosimetry is, however, still larger than the influence of a beam quality specifier. In consequence, the residual range is not used as a beam quality specifier for ion beams heavier than protons in this international code of practice. k_Q values independent of beam quality are provided for carbon ion beams in Table 42, which shows constant values for each chamber type, as in the previous edition of this international code of practice.

Appendix IV

EXPRESSION OF UNCERTAINTIES

IV.1. INTRODUCTION

The evaluation of uncertainties in this international code of practice follows the guidance given by ISO [61]. In 1986, the ISO was given the task of developing detailed guidelines for the evaluation of uncertainties based on the new unified approach outlined in BIPM Recommendation INC-1. These recommendations were approved by CIPM [315]. This effort resulted in the ISO document entitled Guide to the Expression of Uncertainty in Measurement [61]. This appendix provides a practical implementation of the ISO recommendations, based on the summaries provided in Refs [9, 62].

IV.2. GENERAL CONSIDERATIONS ON ERRORS AND UNCERTAINTIES

In contrast to earlier practice, where the terms ‘error’ and ‘uncertainty’ were used interchangeably, the modern approach, initiated by CIPM [180], distinguishes between these two concepts. Traditionally an error has been viewed as having two components, namely a random component and a systematic component. According to current definitions, an error is the difference between a measured value and the true value; if errors are known exactly, the true value can be determined. In reality, errors are estimated in the best possible way and corrections are made for them. Therefore, after application of all known corrections, errors do not need any further consideration (their expectation value being zero) and the quantities of interest are uncertainties. An error has both a numerical value and a sign. In contrast, the uncertainty associated with a measurement is a parameter that characterizes the dispersion of the values “that could reasonably be attributed to the measurand” [61]. This parameter is normally an estimated standard deviation. An uncertainty, therefore, has no known sign and is usually assumed to be symmetrical. It is a measure of our lack of exact knowledge, after all recognized systematic effects have been eliminated by applying appropriate corrections.

Uncertainties of measurements are expressed as relative standard uncertainties and the evaluation of standard uncertainties is classified into type A and type B. Type A standard uncertainties are evaluated by statistical analysis

of a series of observations, whereas type B standard uncertainties are evaluated based on means other than statistical analysis of a series of observations.

In the traditional categorization of uncertainties, it was usual to distinguish between random and systematic contributions. This is undesirable because classifying the components instead of the method of evaluation is prone to ambiguities. For example, a random component of uncertainty in one measurement may become a systematic component of uncertainty in another measurement in which the result of the first measurement is used as an input datum.

IV.3. TYPE A STANDARD UNCERTAINTIES

In a series of n measurements, with observed values x_i, the best estimate of quantity x is usually given by the arithmetic mean value as follows:

$$\bar{x} = \frac{1}{n}\sum_{i=1}^{n} x_i \tag{106}$$

The scatter of the n measured values x_i around their mean $\bar{x}$ can be characterized by the standard deviation as follows:

$$s(x_i) = \sqrt{\frac{1}{n-1}\sum_{i=1}^{n}(x_i - \bar{x})^2} \tag{107}$$

and the quantity $s^2(x_i)$ is called the sample variance.

We are often interested in the standard deviation of the mean value, written as $s(\bar{x})$, for which the following general relation applies:

$$s(\bar{x}) = \frac{1}{\sqrt{n}} s(x_i) \tag{108}$$

An alternative way to estimate $s(\bar{x})$ is based on the outcome of several groups of measurements. If they are all of the same size, the formulas given above can still be used, provided that x_i is now taken as the mean of group i and $\bar{x}$ is the overall mean (or mean of the means) of the n groups. For groups of different size, statistical weights have to be used. This second approach may often be preferable, but it usually requires a larger number of measurements. A discussion of how much the two results of $s(\bar{x})$ may differ from each other is beyond the scope of this elementary presentation.

The standard uncertainty of type A, denoted here by u_A, is the standard deviation of the mean value, as follows:

$$u_A = s(\bar{x}) \tag{109}$$

Obviously, an empirical determination of an uncertainty cannot be expected to give its true value; it is by definition only an estimate. This is so for both type A and type B uncertainties. It will be noted from Eq. (108) that a type A uncertainty in the measurement of a quantity can, in principle, always be reduced by increasing the number n of individual readings. If several measurement techniques are available, the preference will be for the one that gives the least scatter of the results — that is, has the smallest standard deviation $s(x_i)$ — but in practice the possibilities for reduction are often limited.

In the past, uncertainties due to random effects have often been evaluated in the form of confidence limits, commonly at the 95% confidence level. This approach is not used now because there is no statistical basis for combining confidence limits. The theory of the propagation of uncertainties requires combination in terms of variances.

IV.4. TYPE B STANDARD UNCERTAINTIES

There are many sources of measurement uncertainty that cannot be estimated by repeated measurements. They are called type B uncertainties. These include not only unknown, although suspected, influences on the measurement process, but also little known effects of influence quantities (e.g. pressure, temperature), application of correction factors or physical data taken from the literature, etc.

Type B uncertainties have to be estimated so that they correspond to standard deviations; these are called type B standard uncertainties. Some experimenters claim that they can estimate this type of uncertainty directly, while others prefer to use some type of limit as an intermediate step. It is often helpful to assume that these uncertainties have a probability distribution that corresponds to some easily recognizable shape.

It is sometimes assumed, mainly for the sake of simplicity, that type B uncertainties can be described by a rectangular probability density, that is, that they have equal probability anywhere within the given maximum limits $-M$ and

$+M$. It can be shown that with this assumption, the type B standard uncertainty u_B is given by the following equation:

$$u_B = \frac{M}{\sqrt{3}} \tag{110}$$

Alternatively, if the assumed distribution is triangular (with the same limits), we are led to the following relation:

$$u_B = \frac{M}{\sqrt{6}} \tag{111}$$

Another assumption is that type B uncertainties have a distribution that is approximately Gaussian (normal). On this assumption, the type B standard uncertainty can be derived by first estimating some limits $\pm L$ and then dividing those limits by a suitable number. If, for example, the experimenter is fairly sure of the limit L, it can be considered to correspond approximately to a 95% confidence limit, whereas if the experimenter is almost certain, it may be taken to correspond approximately to a 99% confidence limit. Thus, the type B standard uncertainty u_B can be obtained from the following equation:

$$u_B = \frac{L}{k} \tag{112}$$

where $k = 2$ if the experimenters are fairly sure and $k = 3$ if the experimenters are almost certain of their estimated limits $\pm L$. These relations correspond to the properties of a Gaussian distribution. It is usually not worthwhile to apply divisors other than 2 or 3, because of the approximate nature of the estimation.

There are therefore no rigid rules for estimating type B standard uncertainties. Experimenters should use their best knowledge and experience and, whichever method is applied, provide estimates that can be used as if they were standard deviations. There is hardly ever any meaning in estimating type B uncertainties to more than one significant figure and certainly never to more than two.

IV.5. COMBINED AND EXPANDED UNCERTAINTIES

Because type A and type B uncertainties are both estimated standard deviations, they are combined using the statistical rules for combining variances (which are squares of standard deviations). If u_A and u_B are the type A and

type B standard uncertainties of a quantity, respectively, the combined standard uncertainty of that quantity is as follows:

$$u_c = \sqrt{u_A^2 + u_B^2} \tag{113}$$

The combined standard uncertainty thus still has the character of a standard deviation. If, in addition, it is believed to have a Gaussian probability density, then the standard deviation corresponds to a confidence limit of ~68%. Therefore, it is often felt to be desirable to multiply the combined standard uncertainty by a suitable factor, called the coverage factor, k, to yield an expanded uncertainty. Values of the coverage factor of $k = 2$ or 3 correspond to confidence limits of ~95% or ~99%. The approximate nature of uncertainty estimates, in particular for type B, makes it doubtful that more than one significant figure is ever justified in choosing the coverage factor. In any case, the numerical value taken for the coverage factor should be clearly indicated.

REFERENCES

[1] INTERNATIONAL COMMISSION ON RADIATION UNITS AND MEASUREMENTS, Determination of Absorbed Dose in a Patient Irradiated by Beams of X or Gamma Rays in Radiotherapy Procedures, ICRU Report 24, ICRU, Bethesda, MD (1976).

[2] BRAHME, A., et al., Accuracy requirements and quality assurance of external beam therapy with photons and electrons, Acta Oncol. Suppl. 1988 (1988).

[3] MIJNHEER, B.J., BATTERMANN, J.J., WAMBERSIE, A., What degree of accuracy is required and can be achieved in photon and neutron therapy? Radiother. Oncol. **8** (1987) 237–252, https://doi.org/10.1016/S0167-8140(87)80247-5

[4] MIJNHEER, B.J., BATTERMANN, J.J., WAMBERSIE, A., Reply to: Precision and accuracy in radiotherapy (by DJ Brenner), Radiother. Oncol. **14** 2 (1989) 163–167, https://doi.org/10.1016/0167-8140(89)90061-3

[5] INTERNATIONAL ATOMIC ENERGY AGENCY, "What accuracy is needed in dosimetry", Radiation Dose in Radiotherapy from Prescription to Delivery (Proceedings of an Interregional Seminar for Europe, the Middle East and Africa, Leuven, 16–20 September 1991), IAEA-TECDOC-734, IAEA, Vienna (1994) 11–35.

[6] WAMBERSIE, A., What accuracy is required and can be achieved in radiation therapy (review of radiobiological and clinical data), Radiochim. Acta **89** (2001) 255–264, https://doi.org/10.1524/ract.2001.89.4-5.255

[7] INTERNATIONAL ATOMIC ENERGY AGENCY, Accuracy Requirements and Uncertainties in Radiotherapy, IAEA Human Health Series No. 31, IAEA, Vienna (2016).

[8] INTERNATIONAL ATOMIC ENERGY AGENCY, Absorbed Dose Determination in Photon and Electron Beams: An International Code of Practice, Technical Reports Series No. 277, IAEA, Vienna (1987).

[9] INTERNATIONAL ATOMIC ENERGY AGENCY, Absorbed Dose Determination in Photon and Electron Beams: An International Code of Practice, Technical Reports Series No. 277, IAEA, Vienna (1997).

[10] INTERNATIONAL ATOMIC ENERGY AGENCY, Review of Data and Methods Recommended in the International Code of Practice for Dosimetry, IAEA Technical Reports Series No. 381, The Use of Plane Parallel Ionization Chambers in High Energy Electron and Photon Beams, IAEA-TECDOC-1173, IAEA, Vienna (2000).

[11] INTERNATIONAL ATOMIC ENERGY AGENCY, Calibration of Reference Dosimeters for External Beam Radiotherapy, Technical Reports Series No. 469, IAEA, Vienna (2009).

[12] INTERNATIONAL ATOMIC ENERGY AGENCY, Dosimetry of Small Static Fields Used in External Beam Radiotherapy: An International Code of Practice for Reference and Relative Dose Determination, Technical Reports Series No. 483, IAEA, Vienna (2017).

[13] ANDREO, P., Uncertainties in dosimetric data and beam calibration, Int. J. Radiat. Oncol. Biol. Phys. **19** (1990) 1233–1247, https://doi.org/10.1016/0360-3016(90)90237-E

[14] THWAITES, D.I., “Uncertainties at the end point of the basic dosimetry chain”, Measurement Assurance in Dosimetry, International symposium on measurement assurance in dosimetry, IAEA-SM-330/18, IAEA, Vienna (1994) 239–255.
[15] INTERNATIONAL ORGANIZATION FOR STANDARDIZATION, Quantities and units — Part 0: General Principles, ISO International Standard 31-0, ISO, Geneva (1992).
[16] NORDIC ASSOCIATION OF CLINICAL PHYSICS, Procedures in external radiation therapy dosimetry with electron and photon beams with maximum energies between 1 and 50 MeV, Acta Radiol. Oncol. **19** (1980) 55–79, https://doi.org/10.3109/02841868009130136
[17] HOSPITAL PHYSICISTS’ ASSOCIATION, Revised Code of Practice for the dosimetry of 2 to 25 MV x-ray, and of caesium-137 and cobalt-60 gamma-ray beams, Phys. Med. Biol. **28** (1983) 1097–1104, https://doi.org/10.1088/0031-9155/28/10/001
[18] AMERICAN ASSOCIATION OF PHYSICISTS IN MEDICINE – TASK GROUP 21 RADIATION THERAPY COMMITTEE, A protocol for the determination of absorbed dose from high-energy photon and electron beams, Med. Phys. **10** (1983) 741–771, https://doi.org/10.1118/1.595446
[19] INTERNATIONAL COMMISSION ON RADIATION UNITS AND MEASUREMENTS, Radiation Dosimetry: Electron Beams with Energies Between 1 and 50 MeV, ICRU Report 35, ICRU, Bethesda, MD (1984).
[20] SOCIEDAD ESPAÑOLA DE FÍSICA MÉDICA, Procedimientos Recomendados para la Dosimetría de Fotones y Electrones de Energías Comprendidas Entre 1 MeV y 50 MeV en Radioterapia de Haces Externos, Report SEFM 84-1, SEFM, Madrid (1984).
[21] SWISS SOCIETY OF RADIATION BIOLOGY AND RADIATION PHYSICS, Dosimetry of high energy photon and electron beams, Recomm. SGSMP No. 4, SGSMP, Zurich (1986).
[22] NEDERLANDSE COMMISSIE VOOR STRALINGSDOSIMETRIE, Code of Practice for the Dosimetry of High-Energy Photon Beams, Report NCS-2, NCS, Delft (1986).
[23] COMITÉ FRANÇAIS MESURE DES RAYONNEMENTS IONISANTS, Recommandations pour la Mesure de la Dose Absorbée en Radiothérapie dans les Faisceaux de Photons et d’Électrons d’Énergie Comprise entre 1 MeV et 50 MeV, Rapport CFMRI No. 2, CFMRI, Chiron (1987).
[24] SOCIEDAD ESPAÑOLA DE FÍSICA MÉDICA, Suplemento al Documento 84-1: Procedimientos Recomendados para la Dosimetría de Fotones y Electrones de Energías Comprendidas entre 1 MeV y 50 MeV en Radioterapia de Haces Externos, Report SEFM 87-1, SEFM, Madrid (1987).
[25] ASSOCIAZIONE ITALIANA DI FISICA BIOMEDICA, Protocollo per la Dosimetria di base nella Radioterapia con Fasci di Fotoni ed Elettroni con E_{max} fra 1 e 40 MeV, Fisica Biomedica, AIFM, Milan (1988).
[26] NEDERLANDSE COMMISSIE VOOR STRALINGSDOSIMETRIE, Code of Practice for the Dosimetry of High-Energy Electron Beams, Report NCS-5, NCS, Delft (1989).
[27] REICH, H., Choice of the measuring quantity for therapy-level dosemeters, Phys. Med. Biol. **24** (1979) 895–900, https://doi.org/10.1088/0031-9155/24/5/002

[28] COMITÉ CONSULTATIF DES LES ETALONS DE MESURE DES RAYONNEMENTS IONISANTS (SECTION I), Report to the Comité International des Poids et Mesures (Hargrave, N.J., Rapporteur), 9th Meeting CCEMRI(I), BIPM, Sèvres (1988).
[29] WAMBERSIE, A., DELUCA, P.M., ANDREO, P., HENDRY, J.H., 'Light' or 'heavy' ions: a debate of terminology? Radiother. Oncol. **73** Suppl. 2 (2004) iii, https://doi.org/10.1016/S0167-8140(04)80003-3
[30] INTERNATIONAL COMMISSION ON RADIATION UNITS AND MEASUREMENTS, Prescribing, Recording and Reporting Light Ion Beam Therapy, ICRU Report 93, ICRU, Bethesda, MD (2019).
[31] INTERNATIONAL COMMISSION ON RADIATION UNITS AND MEASUREMENTS, Clinical Neutron Dosimetry, Part I: Determination of Absorbed Dose in a Patient Treated by External Beams of Fast Neutrons, ICRU Report 45, ICRU, Bethesda, MD (1989).
[32] INTERNATIONAL COMMISSION ON RADIATION UNITS AND MEASUREMENTS, Key Data for Ionizing Radiation Dosimetry: Measurement Standards and Applications, ICRU Report 90, ICRU, Bethesda, MD (2016).
[33] BÜERMANN, L., et al., Measurement of the x-ray mass energy-absorption coefficient of air using 3 keV to 10 keV synchrotron radiation, Phys. Med. Biol. **51** (2006) 5125–5150, https://doi.org/10.1088/0031-9155/51/20/004
[34] BUHR, H., BÜERMANN, L., GERLACH, M., KRUMREY, M., RABUS, H., Measurement of the mass energy-absorption coefficient of air for x-rays in the range from 3 to 60 keV, Phys. Med. Biol. **57** (2012), https://doi.org/10.1088/0031-9155/57/24/8231
[35] HUBBELL, J.H., Photon mass attenuation and energy-absorption coefficients from 1 keV to 20 MeV, Int. J. Appl. Radiat. Isot. **33** (1982) 1269–1290, https://doi.org/10.1016/0020-708X(82)90248-4
[36] SCOFIELD, J.H., Theoretical photoionization cross sections from 1 to 1500 keV, Report UCRL-51326, Lawrence Livermore Laboratory, Livermore, CA (1973), https://doi.org/10.2172/4545040
[37] HUBBELL, J.H., SELTZER, S.M., Tables of X-Ray Mass Attenuation Coefficients and Mass Energy-Absorption Coefficients From 1 keV to 20 MeV for Elements $Z = 1$ to 92 and 48 Additional Substances of Dosimetric Interest, Report NISTIR-5632, NIST, Bethesda, MD (1996), https://doi.org/10.6028/NIST.IR.5632
[38] BERGER, M.J., HUBBELL, J.H., XCOM: Photon Cross Sections on a Personal Computer, Report NBSIR 87-3597, National Bureau of Standards, Gaithersburg, MD (1987), https://doi.org/10.2172/6016002
[39] SELTZER, S.M., Calculation of photon mass energy-transfer and mass energy-absorption coefficients, Radiat. Res. **136** (1993) 147–170, https://doi.org/10.2307/3578607
[40] CULLEN, D.E., Program RELAX — A Code Designed to Calculate Atomic Relaxation Spectra of X-rays and Electrons, Report UCRL-ID-110438, Lawrence Livermore Laboratory, Livermore, CA (1992), https://doi.org/10.2172/5360235

[41] KATO, M., et al., Photon W-value of dry air determined using a cryogenic radiometer combined with a multi-electrode ion chamber for soft X-rays, Radiat. Phys. Chem. **79** (2010) 397–404, https://doi.org/10.1016/j.radphyschem.2009.12.009
[42] WALLER, I., HARTREE, D.R., On the intensity of total scattering of X-rays, Proc. Math. Phys. Eng. Sci. **124** (1929) 119–142, https://doi.org/10.1098/rspa.1929.0101
[43] HUBBELL, J.H., et al., Atomic form factors, incoherent scattering functions, and photon scattering cross sections, J. Phys. Chem. Ref. Data **4** (1975) 471–538; erratum **6** (1977) 615–616, https://doi.org/10.1063/1.555523
[44] HUBBELL, J.H., et al., Atomic form factors, incoherent scattering functions, and photon scattering cross sections, J. Phys. Chem. Ref. Data **4** (1975) 471–538, https://doi.org/10.1063/1.555523
[45] SALVAT, F., PENELOPE-2014: A Code System for Monte Carlo Simulation of Electron and Photon Transport, Report NEA/NSC/DOC(2015)3, NEA, Issy-les-Moulineaux (2015).
[46] SALVAT, F., The PENELOPE code system. Specific features and recent improvements, Ann. Nucl. Energy **82** (2015) 98–109, https://doi.org/10.1016/j.anucene.2014.08.007
[47] RIBBERFORS, R., Relationship of the relativistic Compton cross section to the momentum distribution of bound electron states, Phys. Rev. B **12** (1975) 2067–2074, https://doi.org/10.1103/PhysRevB.12.2067
[48] INTERNATIONAL COMMISSION ON RADIATION UNITS AND MEASUREMENTS, Stopping Powers for Electrons and Positrons, ICRU Report 37, ICRU, Bethesda, MD (1984).
[49] INTERNATIONAL COMMISSION ON RADIATION UNITS AND MEASUREMENTS, Stopping Powers and Ranges for Protons and Alpha Particles, ICRU Report 49, ICRU, Bethesda, MD (1993).
[50] INTERNATIONAL COMMISSION ON RADIATION UNITS AND MEASUREMENTS, Stopping of Ions Heavier than Helium, ICRU Report 73, ICRU, Bethesda, MD (2005).
[51] SIGMUND, P., SCHINNER, A., PAUL, H., Errata and addenda for ICRU Report 73, stopping of ions heavier than helium, J. ICRU **5** 1 (2009) 1–10, https://doi.org/10.1093/jicru_ndi001
[52] SABBATUCCI, L., SALVAT, F., Theory and calculation of the atomic photoeffect, Radiat. Prot. Dosim. **121** (2016) 122–140, https://doi.org/10.1016/j.radphyschem.2015.10.021
[53] McEWEN, M., et al., Report to CCRI(I) on the Recommendations of ICRU Report 90, Report CCRI(I)/17-07, BIPM, Sèvres (2017).
[54] ANDREO, P., Data for the dosimetry of low- and medium-energy kV x rays, Phys. Med. Biol. **64** (2019) 20, https://doi.org/10.1088/1361-6560/ab421d
[55] HOHLFELD, K., The standard DIN 6800: procedures for absorbed dose determination in radiology by the ionization method (IAEA-SM-298/31), IAEA, Vienna (1988) 13–22.
[56] ANDREO, P., Absorbed dose beam quality factors for the dosimetry of high energy photon beams, Phys. Med. Biol. **37** (1992) 2189–2211, https://doi.org/10.1088/0031-9155/37/12/003

[57] ROGERS, D.W.O., The advantages of absorbed-dose calibration factors, Med. Phys. **19** (1992) 1227–1239, https://doi.org/10.1118/1.596921
[58] INTERNATIONAL COMMISSION ON RADIATION UNITS AND MEASUREMENTS, Dosimetry of High Energy Photon Beams based on Standards of Absorbed Dose to Water, ICRU Report 64, ICRU, Bethesda, MD (2000).
[59] BOUTILLON, M., PERROCHE, A.M., Determination of calibration factors in terms of air kerma and absorbed dose to water in the Co-60 gamma rays, IAEA SSDL Newsletter **32** (1993) 3–13.
[60] BIELAJEW, A.F., ROGERS, D.W.O., Implications of new correction factors on primary air kerma standards in Co-60 beams, Phys. Med. Biol. **37** (1992) 1283–1291, https://doi.org/10.1088/0031-9155/37/6/006
[61] JOINT COMMITTEE FOR GUIDES IN METROLOGY, Guide to the Expression of Uncertainty in Measurement, 2nd edn, JCGM 100:2008, BIPM, Sèvres (2008).
[62] INTERNATIONAL ATOMIC ENERGY AGENCY, Calibration of Dosimeters used in Radiotherapy, Technical Reports Series No. 374, IAEA, Vienna (1994).
[63] INTERNATIONAL COMMITTEE OF WEIGHTS AND MEASURES, Mutual Recognition of National Measurement Standards and of Calibration and Measurement Certificates Issued by National Metrology Institutes, CIPM, Paris (1999).
[64] BUREAU INTERNATIONAL DES POIDS ET MESURES, Key Comparison Database (KCDB) (2021), https://www.bipm.org/kcdb/
[65] BUREAU INTERNATIONAL DES POIDS ET MESURES (BIPM), Calibration and Measurement Capabilities (CMCs), https://www.bipm.org/kcdb/cmc/advanced-search
[66] ORGANISATION INTERNATIONALE DE METROLOGIE LEGALE, Secondary Standard Dosimetry Laboratories for the Calibration of Dosimeters Used in Radiotherapy, Document OIML D-21, OIML, Paris (1990).
[67] INTERNATIONAL ATOMIC ENERGY AGENCY, SSDL Network Charter — The IAEA/WHO Network of Secondary Standard Dosimetry Laboratories, IAEA/WHO/SSDL/99, IAEA, Vienna (2018).
[68] INTERNATIONAL ATOMIC ENERGY AGENCY, SSDL Network (2021), https://ssdl.iaea.org/Home/Members
[69] DOMEN, S.R., LAMPERTI, P.J., Heat-loss-compensated calorimeter — theory, design, and performance, J. Res. Natl Bur. Stand. A **78** (1974) 595–610, https://doi.org/10.6028/jres.078A.037
[70] RENAUD, J., PALMANS, H., SARFEHNIA, A., SEUNTJENS, J., Absorbed dose calorimetry, Phys. Med. Biol. **65** (2020) 05TR02, https://doi.org/10.1088/1361-6560/ab4f29
[71] PRUITT, J.S., DOMEN, S.R., LOEVINGER, R., The graphite calorimeter as a standard of absorbed dose for Co-60 gamma-radiation, J. Res. Natl Bur. Stand. **86** (1981) 495–502, https://doi.org/10.6028/jres.086.021
[72] GUERRA, A.S., LAITANO, R.F., PIMPINELLA, M., Characteristics of the absorbed dose to water standard at ENEA, Phys. Med. Biol. **41** (1996) 657–674, https://doi.org/10.1088/0031-9155/41/4/006

[73] NUTBROWN, R.F., DUANE, S., SHIPLEY, D.R., THOMAS, R.A.S., Evaluation of factors to convert absorbed dose calibrations from graphite to water for the NPL high-energy photon calibration service, Phys. Med. Biol. **47** (2002) 441–454, https://doi.org/10.1088/0031-9155/47/3/306

[74] LYE, J.E., et al., Direct MC conversion of absorbed dose to graphite to absorbed dose to water for ^{60}Co radiation, Rad. Prot. Dos. **155** (2013) 100–109, https://doi.org/10.1093/rpd/ncs276

[75] DOMEN, S.R., A sealed water calorimeter for measuring absorbed dose, J. Res. Natl Inst. Stan. **99** (1994) 121–141, https://doi.org/10.6028/jres.099.012

[76] KLASSEN, N.V., ROSS, C.K., Water calorimetry: the heat defect, J. Res. Natl Inst. Stan. **102** (1997) 63–74, https://doi.org/10.6028/jres.102.006

[77] FEIST, H., Determination of the absorbed dose to water for high-energy photons and electrons by total absorption of electrons in ferrous sulfate solution, Phys. Med. Biol. **27** (1982) 1435–1447, https://doi.org/10.1088/0031-9155/27/12/002

[78] BOUTILLON, M., PERROCHE, A.M., Ionometric determination of absorbed dose to water for Co-60 gamma-rays, Phys. Med. Biol. **38** (1993) 439–454, https://doi.org/10.1088/0031-9155/38/3/010

[79] BOHM, J., HOHLFELD, K., REICH, H., "A primary standard for determination of absorbed dose in water for X rays generated at potentials of 7.5 to 30 kV", National and International Standardization of Radiation Dosimetry (Proc. Symp. Atlanta, 1977), Vienna (1978).

[80] BÜERMANN, L., et al., First international comparison of primary absorbed dose to water standards in the medium-energy X-ray range, Metrologia **53** (2016) 06007, https://doi.org/10.1088/0026-1394/53/1A/06007

[81] ROGER, P., BURNS, D.T., KESSLER, C., Progress Report on New Facility for Medium-Energy X-rays, Report CCRI(I)/2021-13, BIPM, Sèvres (2021), https://www.bipm.org/documents/20126/56106449/13+Progress+report+on+new+facility+for+medium-energy+x-rays.pdf/fbf061f1-7190-f494-1810-f7c2bf3282bb

[82] PICARD, S., BURNS, D.T., ROGER, P., Construction of an Absorbed-Dose Graphite Calorimeter, Report BIPM-09/01, BIPM, Sèvres (2009).

[83] INSTITUTE OF PHYSICAL SCIENCES IN MEDICINE, Code of Practice for high-energy photon therapy dosimetry based on the NPL absorbed dose calibration service, Phys. Med. Biol. **35** (1990) 1355–1360, https://doi.org/10.1088/0031-9155/35/10/301

[84] DEUTSCHES INSTITUT FÜR NORMUNG, Dosismessverfahren nach der Sondenmethode für Photonen- und Elektronenstrahlung – Teil 2: Dosimetrie Hochenergetischer Photonen- und Elektronenstrahlung mit Ionisationskammern, DIN 6800-2, Deutsches Institut für Normung, Berlin (2018).

[85] ALMOND, P.R., et al., AAPM's TG-51 protocol for clinical reference dosimetry of high-energy photon and electron beams, Med. Phys. **26** (1999) 1847–1870, https://doi.org/10.1118/1.598691

[86] JOINT COMMITTEE FOR GUIDES IN METROLOGY, International Vocabulary of Metrology — Basic and General Concepts and Associated Terms (VIM), JCGM 200:2012, BIPM, Sèvres (2012).

[87] ANDREO, P., The status of high-energy photon and electron beam dosimetry five years after the implementation of the IAEA Code of Practice in the Nordic countries, Acta Oncol. **32** (1993) 483–500, https://doi.org/10.3109/02841869309096107
[88] ANDREO, P., On the beam quality specification of high-energy photons for radiotherapy dosimetry, Med. Phys. **27** (2000) 434–440, https://doi.org/10.1118/1.598892
[89] BURNS, J.E., Absorbed-dose calibrations in high-energy photon beams at the National Physical Laboratory: Conversion procedure, Phys. Med. Biol. **39** (1994) 1555–1575, https://doi.org/10.1088/0031-9155/39/10/004
[90] BOUTILLON, M., COURSEY, B.M., HOHLFELD, K., OWEN, B., ROGERS, D. W.O., "Comparison of primary water absorbed dose standards", Measurement Assurance in Dosimetry, International symposium on measurement assurance in dosimetry, IAEA-SM-330/18, IAEA, Vienna (1994) 95–111.
[91] ROGERS, D.W.O., ROSS, C.K., SHORTT, K.R., KLASSEN, N.V., BIELAJEW, A.F., "Towards a dosimetry system based on absorbed dose standards", ibid., 565–580.
[92] ROOS, M., HOHLFELD, K., "Status of the primary standard of water absorbed dose for high energy photon and electron radiation at the PTB", ibid., 25–33.
[93] ROSSER, K.E., et al., "The NPL absorbed dose to water calibration service for high energy photons", ibid., 73–81.
[94] THOMAS, R., LOURENCO, B., PALMANS, H., "Design, development and operation of a primary standard graphite calorimeter for proton beam dosimetry", International Symposium on Standards, Applications and Quality Assurance in Medical Radiation Dosimetry (IDOS 2019), IAEA, Vienna (2019) 71–76.
[95] OSINGA-BLÄTTERMANN, J.M., BRONS, S., GREILICH, S., JAKEL, O., KRAUSS, A., Direct determination of k_Q for Farmer-type ionization chambers in a clinical scanned carbon ion beam using water calorimetry, Phys. Med. Biol. **62** (2017) 2033–2054, https://doi.org/10.1088/1361-6560/aa5bac
[96] INTERNATIONAL ELECTROTECHNICAL COMMISSION, Medical Electrical Equipment — Dosimeters with Ionization Chambers as Used in Radiotherapy, IEC 60731, Edition 3.1, IEC, Geneva (2016).
[97] SHARPE, P., Progress Report on Radiation Dosimetry at NPL, Report CCRI(I)/1999-20, BIPM, Sèvres (1999).
[98] McEWEN, M.R., Measurement of ionization chamber absorbed dose k_Q factors in megavoltage photon beams, Med. Phys. **37** (2010) 2179–2193, https://doi.org/10.1118/1.3375895
[99] McEWEN, M., et al., Addendum to the AAPM's TG-51 protocol for clinical reference dosimetry of high-energy photon beams, Med. Phys. **41** (2014) 041501–041520, https://doi.org/10.1118/1.4866223
[100] ANDREO, P., et al., Determination of consensus k_Q values for megavoltage photon beams for the update of IAEA TRS-398, Phys. Med. Biol. **65** (2020) 095011, https://doi.org/10.1088/1361-6560/ab807b
[101] MIJNHEER, B.J., Variations in response to radiation of a nylon-walled ionization chamber induced by humidity changes, Med. Phys. **12** (1985) 625–626, https://doi.org/10.1118/1.595683

[102] KRANZER, R., et al., Ion collection efficiency of ionization chambers in ultra-high dose-per-pulse electron beams, Med Phys **48** (2021) 819–830, https://doi.org/10.1002/mp.14620
[103] INTERNATIONAL COMMISSION ON RADIATION UNITS AND MEASUREMENTS, Tissue Substitutes in Radiation Dosimetry and Measurement, ICRU Report 44, ICRU, Bethesda, MD (1989).
[104] AGOSTINELLI, A.G., SMOLEN, S.D., NATH, R., A new water-equivalent plastic for dosimetry calibration, Med. Phys. **19** (1992) 774.
[105] TELLO, V.M., TAILOR, R.C., HANSON, W.F., How water equivalent are water-equivalent solid materials for output calibration of photon and electron beams? Med. Phys. **22** (1995) 1177–1189, https://doi.org/10.1118/1.597613
[106] THWAITES, D.I., et al., The IPEM code of practice for electron dosimetry for radiotherapy beams of initial energy from 4 to 25 MeV based on an absorbed dose to water calibration, Phys. Med. Biol. **48** (2003) 2929–2970, https://doi.org/10.1088/0031-9155/48/18/301
[107] BUTSON, M.J., CHEUNG, T., YU, P.K., Solid water phantom heat conduction: Heating and cooling rates, J. Med. Phys. **33** (2008) 24–28, https://doi.org/10.4103/0971-6203.39421
[108] ANDREO, P., BURNS, D.T., NAHUM, A.E., SEUNTJENS, J., ATTIX, F.H., Fundamentals of Ionizing Radiation Dosimetry, Wiley-VCH, Weinheim (2017).
[109] TESSIER, F., KAWRAKOW, I., Effective point of measurement of thimble ion chambers in megavoltage photon beams, Med. Phys. **37** (2010) 96–107, https://doi.org/10.1118/1.3266750
[110] ZINK, K., WULFF, J., Positioning of a plane-parallel ionization chamber in clinical electron beams and the impact on perturbation factors, Phys. Med. Biol. **54** (2009) 2421–2435, https://doi.org/10.1088/0031-9155/54/8/011
[111] MCCAFFREY, J.P., DOWNTON, B., SHEN, H., NIVEN, D., McEWEN, M., Pre-irradiation effects on ionization chambers used in radiation therapy, Phys. Med. Biol. **50** (2005) N121–N133, https://doi.org/10.1088/0031-9155/50/13/N01
[112] COMITÉ CONSULTATIF DES LES ETALONS DE MESURE DES RAYONNEMENTS IONISANTS (SECTION I), Correction d'Humidité, CCEMRI(I) R(I)-30, BIPM, Sèvres (1977).
[113] NISBET, A., THWAITES, D.I., Polarity and ion recombination correction factors for ionization chambers employed in electron beam dosimetry, Phys. Med. Biol. **43** (1998) 435–443, https://doi.org/10.1088/0031-9155/43/2/016
[114] BOAG, J.W., Ionization measurements at very high intensities. I. Pulsed radiation beams, Brit. J. Radiol. **23** (1950) 601–611, https://doi.org/10.1259/0007-1285-23-274-601
[115] INTERNATIONAL ATOMIC ENERGY AGENCY, Manual of Dosimetry in Radiotherapy, Technical Reports Series No. 110, IAEA, Vienna (1970).
[116] BOAG, J.W., CURRANT, J., Current collection and ionic recombination in small cylindrical ionization chambers exposed to pulsed radiation, Brit. J. Radiol. **53** (1980) 471–478, https://doi.org/10.1259/0007-1285-53-629-471

[117] WEINHOUS, M.S., MELI, J.A., Determining Pion, the correction factor for recombination losses in an ionization chamber, Med. Phys. **11** (1984) 846–849, https://doi.org/10.1118/1.595574
[118] BURNS, D.T., McEWEN, M.R., Ion recombination corrections for the NACP parallel-plate chamber in a pulsed electron beam, Phys. Med. Biol. **43** (1998) 2033–2045, https://doi.org/10.1088/0031-9155/43/8/003
[119] DERIKUM, K., ROOS, M., Measurement of saturation correction factors of thimble-type ionization chambers in pulsed photon beams, Phys. Med. Biol. **38** (1993) 755–763, https://doi.org/10.1088/0031-9155/38/6/009
[120] DE ALMEIDA, C.E., NIATEL, M.T., Comparison Between IRD and BIPM Exposure and Air Kerma Standards for Cobalt Gamma Rays, Report BIPM-1986/12, BIPM, Sèvres (1986).
[121] BOUTILLON, M., Volume recombination parameter in ionization chambers, Phys. Med. Biol. **43** (1998) 2061–2072, https://doi.org/10.1088/0031-9155/43/8/005
[122] PICARD, S., BURNS, D.T., Determination of the recombination correction for the BIPM parallel-plate ionization chamber type in a pulsed photon beam, Report BIPM-2011/06, BIPM, Sèvres (2011).
[123] BRAHME, A., Correction of a measured distribution for the finite extension of the detector, Strahlentherapie **157** (1981) 258–259, https://doi.org/10.1007/978-3-662-00618-4_32
[124] SIBATA, C.H., MOTA, H.C., BEDDAR, A.S., HIGGINS, P.D., SHIN, K.H., Influence of detector size in photon-beam profile measurements, Phys. Med. Biol. **36** (1991) 621–631, https://doi.org/10.1088/0031-9155/36/5/005
[125] HIGGINS, P.D., SIBATA, C.H., SISKIND, L., SOHN, J.W., Deconvolution of detector size effect for small-field measurement, Med. Phys. **22** (1995) 1663–1666, https://doi.org/10.1118/1.597427
[126] GARCIA-VICENTE, F., BEJAR, M.J., PEREZ, L., TORRES, J.J., Clinical impact of the detector size effect in 3D-CRT, Radiother. Oncol. **74** (2005) 315–322, https://doi.org/10.1016/j.radonc.2004.10.012
[127] GARCIA-VICENTE, F., DELGADO, J.M., PERAZA, C., Experimental determination of the convolution kernel for the study of the spatial response of a detector, Med. Phys. **25** (1998) 202–207, https://doi.org/10.1118/1.598182
[128] GARCIA-VICENTE, F., DELGADO, J.M., RODRIGUEZ, C., Exact analytical solution of the convolution integral equation for a general profile fitting function and Gaussian detector kernel, Phys. Med. Biol. **45** (2000) 645–650, https://doi.org/10.1088/0031-9155/45/3/306
[129] LAUB, W.U., WONG, T., The volume effect of detectors in the dosimetry of small fields used in IMRT, Med. Phys. **30** (2003) 341–347, https://doi.org/10.1118/1.1544678
[130] PAPPAS, E., et al., Experimental determination of the effect of detector size on profile measurements in narrow photon beams, Med. Phys. **33** (2006) 3700–3710, https://doi.org/10.1118/1.2349691
[131] SAHOO, N., KAZI, A.M., HOFFMAN, M., Semi-empirical procedures for correcting detector size effect on clinical MV x-ray beam profiles, Med. Phys. **35** (2008) 5124–5133, https://doi.org/10.1118/1.2989089

[132] LOOE, H.K., et al., The dose response functions of ionization chambers in photon dosimetry — Gaussian or non-Gaussian? Z. Med. Phys. **23** (2013) 129–143, https://doi.org/10.1016/j.zemedi.2012.12.010
[133] KETELHUT, S., KAPSCH, R.P., Measurement of spatial response functions of dosimetric detectors, Phys. Med. Biol. **60** (2015) 6177–6194, https://doi.org/10.1088/0031-9155/60/16/6177
[134] BUTLER, D.J., et al., High spatial resolution dosimetric response maps for radiotherapy ionization chambers measured using kilovoltage synchrotron radiation, Phys. Med. Biol. **60** (2015) 8625–8641, https://doi.org/10.1088/0031-9155/60/22/8625
[135] LOOE, H.K., HARDER, D., POPPE, B., Understanding the lateral dose response functions of high-resolution photon detectors by reverse Monte Carlo and deconvolution analysis, Phys. Med. Biol. **60** (2015) 6585–6607, https://doi.org/10.1088/0031-9155/60/16/6585
[136] POPPINGA, D., et al., Experimental determination of the lateral dose response functions of detectors to be applied in the measurement of narrow photon-beam dose profiles, Phys. Med. Biol. **60** (2015) 9421–9436, https://doi.org/10.1088/0031-9155/60/24/9421
[137] TANTOT, L., SEUNTJENS, J., Modelling ionization chamber response to nonstandard beam configurations, J. Phys. Conf. Ser. **102** (2008) 0102023, https://doi.org/10.1088/1742-6596/102/1/012023
[138] EUROPEAN SOCIETY FOR THERAPEUTIC RADIOLOGY AND ONCOLOGY, Monitor Unit Calculation for High Energy Photon Beams, ESTRO, Brussels (1997).
[139] ANDREO, P., BRAHME, A., Stopping power data for high-energy photon beams, Phys. Med. Biol. **31** (1986) 839–858, https://doi.org/10.1088/0031-9155/31/8/002
[140] KAPSCH, R.-P., et al., Experimental determination of p_{Co} perturbation factors for plane-parallel chambers, Phys. Med. Biol. **52** (2007) 7167–7181, https://doi.org/10.1088/0031-9155/52/23/026
[141] MUIR, B.R., McEWEN, M.R., ROGERS, D.W.O., Beam quality conversion factors for parallel-plate ionization chambers in MV photon beams, Med. Phys. **39** (2012) 1618–1631, https://doi.org/10.1118/1.3687864
[142] McEWEN, M.R., DUANE, S., THOMAS, R.A.S., "Absorbed dose calibration factors for parallel-plate chambers in high energy photon beams", Standards and Codes of Practice in Medical Radiation Dosimetry, Proceedings Series — International Atomic Energy Agency, IAEA, Vienna (2003) 335–341.
[143] KAPSCH, R.-P., GOMOLA, I., "Beam quality correction factors for plane-parallel chambers in photon beams", Standards, Applications and Quality Assurance in Medical Radiation Dosimetry (IDOS), Proceedings Series — International Atomic Energy Agency, IAEA, Vienna (2012) 297–308.
[144] FOLLOWILL, D.S., TAILOR, R.C., TELLO, V.M., HANSON, W.F., An empirical relationship for determining photon beam quality in TG-21 from a ratio of percent depth doses, Med. Phys. **25** (1998) 1202–1205, https://doi.org/10.1118/1.598396
[145] ANDREO, P., NAHUM, A., BRAHME, A., Chamber-dependent wall correction factors in dosimetry, Phys. Med. Biol. **31** (1986) 1189–1199, https://doi.org/10.1088/0031-9155/31/11/001

[146] BRITISH INSTITUTE OF RADIOLOGY, Central axis depth dose data for use in radiotherapy, Brit. J. Radiol. Suppl. **25** (1996).
[147] LYE, J.E., et al., Comparison between the TRS-398 code of practice and the TG-51 dosimetry protocol for flattening filter free beams, Phys. Med. Biol. **61** (2016) N362–372, https://doi.org/10.1088/0031-9155/61/14/N362
[148] BRAHME, A., SVENSSON, H., Radiation beam characteristics of a 22 MeV microtron, Acta Radiol. Oncol. Radiat. Phys. Biol. **18** (1979) 244–272, https://doi.org/10.3109/02841867909128212
[149] GREENING, J.R., Fundamentals of Radiation Dosimetry, Adam Hilger, Bristol (1981).
[150] BRAHME, A., ANDREO, P., Dosimetry and quality specification of high energy photon beams, Acta Radiol. Oncol. **25** (1986) 213–223, https://doi.org/10.3109/02841868609136408
[151] BUDGELL, G., et al., IPEM topical report 1: Guidance on implementing flattening filter free (FFF) radiotherapy, Phys. Med. Biol. **61** (2016) 8360–8394, https://doi.org/10.1088/0031-9155/61/23/8360
[152] CZARNECKI, D., POPPE, B., ZINK, K., Monte Carlo-based investigations on the impact of removing the flattening filter on beam quality specifiers for photon beam dosimetry, Med. Phys. **44** (2017) 2569–2580, https://doi.org/10.1002/mp.12252
[153] DE PREZ, L., DE POOTER, J., JANSEN, B., PERIK, T., WITTKAMPER, F., Comparison of k_Q factors measured with a water calorimeter in flattening filter free (FFF) and conventional flattening filter (cFF) photon beams, Phys. Med. Biol. **63** (2018) 045023, https://doi.org/10.1088/1361-6560/aaaa93
[154] XIONG, G., ROGERS, D.W., Relationship between $\%dd(10)_x$ and stopping-power ratios for flattening filter free accelerators: A Monte Carlo study, Med. Phys. **35** (2008) 2104–2109, https://doi.org/10.1118/1.2905028
[155] CEBERG, C., JOHNSSON, S., LIND, M., KNOOS, T., Prediction of stopping-power ratios in flattening-filter free beams, Med. Phys. **37** (2010) 1164–1168, https://doi.org/10.1118/1.3314074
[156] DALARYD, M., KNOOS, T., CEBERG, C., Combining tissue-phantom ratios to provide a beam-quality specifier for flattening filter free photon beams, Med. Phys. **41** (2014) 111716, https://doi.org/10.1118/1.4898325
[157] SIMPSON, E., GAJEWSKI, R., FLOWER, E., STENSMYR, R., Experimental validation of the dual parameter beam quality specifier for reference dosimetry in flattening-filter-free (FFF) photon beams, Phys. Med. Biol. **60** (2015) N271–281, https://doi.org/10.1088/0031-9155/60/14/N271
[158] BURNS, J.E., DALE, J.W.G., Conversion of Absorbed Dose Calibration from Graphite into Water, NPL Report, National Physical Laboratory, Teddington (1990).
[159] NEDERLANDSE COMMISSIE VOOR STRALINGSDOSIMETRIE, Code of Practice for the Absorbed Dose Determination in High-Energy Photon and Electron Beams, Report NCS-18, NCS, Amsterdam (2012).
[160] BRITISH INSTITUTE OF RADIOLOGY, Central axis depth dose data for use in radiotherapy, Brit. J. Radiol. Suppl. **17** (1983).
[161] SHORTT, K.R., et al., A comparison of absorbed dose standards for high-energy x-rays, Phys. Med. Biol. **38** (1993) 1937–1955, https://doi.org/10.1088/0031-9155/38/12/016

[162] JOHNS, H.E., CUNNINGHAM, J.R., The Physics of Radiology, Thomas, Springfield, IL (1983).
[163] MUIR, B.R., McEWEN, M.R., Technical Note: On the use of cylindrical ionization chambers for electron beam reference dosimetry, Med. Phys. **44** (2017) 6641–6646, https://doi.org/10.1002/mp.12582
[164] McEWEN, M.R., KAWRAKOW, I., ROSS, C.K., The effective point of measurement of ionization chambers and the build-up anomaly in MV x-ray beams, Med. Phys. **35** (2008) 950–958, https://doi.org/10.1118/1.2839329
[165] LOOE, H.K., HARDER, D., POPPE, B., Experimental determination of the effective point of measurement for various detectors used in photon and electron beam dosimetry, Phys. Med. Biol. **56** (2011) 4267–4290, https://doi.org/10.1088/0031-9155/56/14/005
[166] HUANG, Y., WILLOMITZER, C., ZAKARIA, G.A., HARTMANN, G.H., Experimental determination of the effective point of measurement of cylindrical ionization chambers for high-energy photon and electron beams, Phys. Med. **26** (2010) 126–131, https://doi.org/10.1016/j.ejmp.2009.10.001
[167] MUIR, B.R., ROGERS, D.W.O., Monte Carlo calculations of electron beam quality conversion factors for several ion chamber types, Med. Phys. **41** (2014) 111701, https://doi.org/10.1118/1.4893915
[168] DING, G.X., ROGERS, D.W., MACKIE, T.R., Calculation of stopping-power ratios using realistic clinical electron beams, Med. Phys. **22** (1995) 489–501, https://doi.org/10.1118/1.597581
[169] BUCKLEY, L.A., ROGERS, D.W., Wall correction factors, P_{wall}, for parallel-plate ionization chambers, Med. Phys. **33** (2006) 1788–1796, https://doi.org/10.1118/1.2199988
[170] LACROIX, F., et al., Extraction of depth-dependent perturbation factors for parallel-plate chambers in electron beams using a plastic scintillation detector, Med. Phys. **37** (2010) 4331–4342, https://doi.org/10.1118/1.3463383
[171] ZINK, K., CZARNECKI, D., LOOE, H.K., VON VOIGTS-RHETZ, P., HARDER, D., Monte Carlo study of the depth-dependent fluence perturbation in parallel-plate ionization chambers in electron beams, Med. Phys. **41** (2014) 111707, https://doi.org/10.1118/1.4897389
[172] BAILEY, M., SHIPLEY, D.R., MANNING, J.W., Roos and NACP-02 ion chamber perturbations and water–air stopping-power ratios for clinical electron beams for energies from 4 to 22 MeV, Phys. Med. Biol. **60** (2015) 1087–1095, https://doi.org/10.1088/0031-9155/60/3/1087
[173] BURNS, D.T., DING, G.X., ROGERS, D.W., R_{50} as a beam quality specifier for selecting stopping-power ratios and reference depths for electron dosimetry, Med. Phys. **23** (1996) 383–388, https://doi.org/10.1118/1.597893
[174] MUIR, B.R., COJOCARU, C.D., McEWEN, M.R., ROSS, C.K., Electron beam water calorimetry measurements to obtain beam quality conversion factors, Med. Phys. **44** (2017) 5433–5444, https://doi.org/10.1002/mp.12463
[175] OLIVARES, M., DEBLOIS, F., PODGORSAK, E.B., SEUNTJENS, J.P., Electron fluence correction factors for various materials in clinical electron beams, Med. Phys. **28** (2001) 1727–1734, https://doi.org/10.1118/1.1388536

[176] McEWEN, M.R., DUSAUTOY, A.R., Characterization of the water-equivalent material WTe for use in electron beam dosimetry, Phys. Med. Biol. **48** (2003) 1885–1893, https://doi.org/10.1088/0031-9155/48/13/302
[177] McEWEN, M.R., NIVEN, D., Characterization of the phantom material Virtual Water™ in high-energy photon and electron beams, Med. Phys. **33** (2006) 876–887, https://doi.org/10.1118/1.2174186
[178] MARRALE, M., et al., Dosimetry for electron intra-operative radio therapy: comparison of output factors obtained through alanine/EPR pellets, ionization chamber and Monte Carlo-GEANT4 simulations for IORT mobile dedicate accelerator, Nucl. Instrum. Methods B **358** (2015) 52–58, https://doi.org/10.1016/j.nimb.2015.05.022
[179] SCALCHI, P., et al., Use of parallel-plate ionization chambers in reference dosimetry of NOVAC and LIAC (R) mobile electron linear accelerators for intraoperative radiotherapy: a multi-center survey, Med. Phys. **44** (2017) 321–332, https://doi.org/10.1002/mp.12020
[180] PIMPINELLA, M., et al., Output factor measurement in high dose-per-pulse IORT electron beams, Phys Med **61** (2019) 94–102, https://doi.org/10.1016/j.ejmp.2019.04.021
[181] LAW, J., FOSTER, C.J., Calibration of radiotherapy dosemeters against secondary standard dosemeters: An anomalous result, Phys. Med. Biol. **32** (1987) 1039–1043, https://doi.org/10.1088/0031-9155/32/8/007
[182] INTERNATIONAL COMMISSION ON RADIATION UNITS AND MEASUREMENTS, Physical Apects of Iradiation, ICRU Report 10b, ICRU, Bethesda, MD (1962).
[183] SEUNTJENS, J., THIERENS, H., VAN DER PLAETSEN, A., SEGAERT, O., Conversion factor f for X-ray beam qualities, specified by peak tube potential and HVL value, Phys. Med. Biol. **32** (1987) 595–603, https://doi.org/10.1088/0031-9155/32/5/005
[184] ROSSER, K.E., An alternative beam quality index for medium-energy x-ray dosimetry, Phys. Med. Biol. **43** (1998) 587–598, https://doi.org/10.1088/0031-9155/43/3/010
[185] MA, C.M., et al., AAPM protocol for 40-300 kV x-ray beam dosimetry in radiotherapy and radiobiology, Med. Phys. **28** (2001) 868–893, https://doi.org/10.1118/1.1374247
[186] ASPRADAKIS, M.M., ZUCCHETTI, P., Acceptance, commissioning and clinical use of the WOmed T-200 kilovoltage X-ray therapy unit, Brit. J. Radiol. **88** (2015) 1055, https://doi.org/10.1259/bjr.20150001
[187] HILL, R., et al., Australasian recommendations for quality assurance in kilovoltage radiation therapy from the Kilovoltage Dosimetry Working Group of the Australasian College of Physical Scientists and Engineers in Medicine, Australas. Phys. Eng. S **41** (2018) 781–808, https://doi.org/10.1007/s13246-018-0692-1
[188] KLEVENHAGEN, S.C., et al., The IPEMB code of practice for the determination of absorbed dose for x-rays below 300 kV generating potential (0.035 mm Al-4 mm Cu HVL; 10-300 kV generating potential). Institution of Physics and Engineering in Medicine and Biology, Phys. Med. Biol. **41** (1996) 2605–2625, https://doi.org/10.1088/0031-9155/41/12/002
[189] MAYLES, P., "Kilovoltage X-rays", Handbook of Radiotherapy Physics (MAYLES, P., NAHUM, A., ROSENWALD, J.C., Eds), Taylor & Francis, New York, London (2007), https://doi.org/10.1201/9781420012026

[190] DEUTSCHES INSTITUT FÜR NORMUNG, Clinical dosimetry — Part 4: X-ray Therapy with X-ray Tube Voltages Between 10 kV and 300 kV, DIN 6809-4, Deutsches Institut für Normung, Berlin (2020).
[191] HILL, R., et al., Advances in kilovoltage x-ray beam dosimetry, Phys. Med. Biol. **59** (2014) R183–231, https://doi.org/10.1088/0031-9155/59/6/R183
[192] BANCHERI, J., KETELHUT, S., BÜERMANN, L., SEUNTJENS, J., Monte Carlo and water calorimetric determination of kilovoltage beam radiotherapy ionization chamber correction factors, Phys. Med. Biol. **65** (2020) 105001, https://doi.org/10.1088/1361-6560/ab82e7
[193] HILL, R., MO, Z., HAQUE, M., BALDOCK, C., An evaluation of ionization chambers for the relative dosimetry of kilovoltage x-ray beams, Med. Phys. **36** (2009) 3971–3981, https://doi.org/10.1118/1.3183820
[194] HILL, R., HEALY, B., HOLLOWAY, L., BALDOCK, C., An investigation of surface dose changes for therapeutic kilovoltage X-ray beams with underlying lead shielding, Med. Phys. **32** (2005) 1991, https://doi.org/10.1118/1.1997862
[195] RAMASESHAN, R., KOHLI, K., CAO, F., HEATON, R.K., Dosimetric evaluation of plastic water diagnostic-therapy, J. Appl. Clin. Med. Phys. **9** (2008) 98–111, https://doi.org/10.1120/jacmp.v9i2.2761
[196] HILL, R., HOLLOWAY, L., BALDOCK, C., A dosimetric evaluation of water equivalent phantoms for kilovoltage x-ray beams, Phys. Med. Biol. **50** (2005) N331–N344, https://doi.org/10.1088/0031-9155/50/21/N06
[197] HAVERCROFT, J.M., KLEVENHAGEN, S.C., Ion recombination corrections for plane-parallel and thimble chambers in electron and photon radiation, Phys. Med. Biol. **38** (1993) 25–38, https://doi.org/10.1088/0031-9155/38/1/003
[198] CZARNECKI, D., et al., Monte Carlo calculation of quality correction factors based on air kerma and absorbed dose to water in medium energy x-ray beams, Phys. Med. Biol. **65** (2020) 245042, https://doi.org/10.1088/1361-6560/abc5c9
[199] SEUNTJENS, J., VERHAEGEN, F., Dependence of overall correction factor of a cylindrical ionization chamber on field size and depth in medium-energy x-ray beams, Med. Phys. **23** (1996) 1789–1796, https://doi.org/10.1118/1.597833
[200] AF ROSENSCHOLD, P.M., NILSSON, P., KNOOS, T., Kilovoltage x-ray dosimetry — an experimental comparison between different dosimetry protocols, Phys. Med. Biol. **53** (2008) 4431–4442, https://doi.org/10.1088/0031-9155/53/16/014
[201] LI, X.A., MA, C.M., SALHANI, D., Measurement of percentage depth dose and lateral beam profile for kilovoltage x-ray therapy beams, Phys. Med. Biol. **42** (1997) 2561–2568, https://doi.org/10.1088/0031-9155/42/12/019
[202] MA, C.M., LI, X.A., SEUNTJENS, J.P., Study of dosimetry consistency for kilovoltage x-ray beams, Med. Phys. **25** (1998) 2376–2384, https://doi.org/10.1118/1.598448
[203] KLEVENHAGEN, S.C., THWAITES, D.I., AUKETT, R.J., "Kilovoltage X rays", Radiotherapy Physics in Practice, 2nd edn, Oxford University Press, Oxford (1993) 99–117, https://doi.org/10.1093/oso/9780192628787.003.0006
[204] DAMODAR, J., ODGERS, D., POPE, D., HILL, R., A study on the suitability of the PTW microDiamond detector for kilovoltage x-ray beam dosimetry, Int. J. Appl. Radiat. Isot. **135** (2018) 104–109, https://doi.org/10.1016/j.apradiso.2018.01.025

[205] PRENTOU, E., LEKATOU, A., PANTELIS, E., KARAISKOS, P., PAPAGIANNIS, P., On the use of EBT3 film for relative dosimetry of kilovoltage X ray beams, Phys. Med. **74** (2020) 56–65, https://doi.org/10.1016/j.ejmp.2020.04.025
[206] FLETCHER, C.L., MILLS, J.A., An assessment of GafChromic film for measuring 50 kV and 100 kV percentage depth dose curves, Phys. Med. Biol. **53** (2008) N209–218, https://doi.org/10.1088/0031-9155/53/11/N02
[207] BURNS, D.T., KESSLER, C., BÜERMANN, L., KETELHUT, S., Key comparison BIPM.RI(I)-K9 of the absorbed dose to water standards of the PTB, Germany and the BIPM in medium-energy x-rays, Metrologia **55** (2018) 06006, https://doi.org/10.1088/0026-1394/55/1A/06006
[208] BJERKE, H., et al., Comparison of the air-kerma standards of the NRPA, the STUK, the SSM and the LNE-LNHB in low-energy and mammography x-ray ranges, Metrologia **55** (2018) 06008, https://doi.org/10.1088/0026-1394/55/1A/06008
[209] MOHAN, R., PAGANETTI, H., "Appendix: nomenclature and terminology in proton therapy", Principles and Practice of Proton Beam Therapy, AAPM Monograph No. 37, 2015 Summer School, AAPM, Madison, WI (2015) 819–828.
[210] INTERNATIONAL COMMISSION ON RADIATION UNITS AND MEASUREMENTS, Prescribing, Recording, and Reporting Proton Beam Therapy, ICRU Report 78, ICRU, Bethesda, MD (2007).
[211] LOURENCO, A., et al., Evaluation of the water-equivalence of plastic materials in low- and high-energy clinical proton beams, Phys. Med. Biol. **62** (2017) 3883–3901, https://doi.org/10.1088/1361-6560/aa67d4
[212] INTERNATIONAL COMMISSION ON RADIATION UNITS AND MEASUREMENTS, Clinical Proton Dosimetry, Part I: Beam Production, Beam Delivery and Measurement Of Absorbed Dose, ICRU Report 59, ICRU, Bethesda, MD (1999).
[213] PALMANS, H., VERHAEGEN, F., Monte Carlo study of fluence perturbation effects on cavity dose response in clinical proton beams, Phys. Med. Biol. **43** (1998) 65–89, https://doi.org/10.1088/0031-9155/43/1/005
[214] PALMANS, H., VYNCKIER, S., "Reference dosimetry for clinical proton beams", Recent Developments in Accurate Radiation Dosimetry, Medical Physics Publishing, Madison, WI (2002) 157–194.
[215] PALMANS, H., VATNITSKY, S.M., Beam monitor calibration in scanned light-ion beams, Med. Phys. **43** (2016) 5835–5847, https://doi.org/10.1118/1.4963808
[216] GOMA, C., LORENTINI, S., MEER, D., SAFAI, S., Proton beam monitor chamber calibration, Phys. Med. Biol. **59** (2014) 4961–4971, https://doi.org/10.1088/0031-9155/59/17/4961
[217] OSORIO, J., et al., Beam monitor calibration of a synchrotron-based scanned light-ion beam delivery system, Z. Med. Phys. **31** (2020) 03364–03367, https://doi.org/10.1016/j.zemedi.2020.06.005
[218] PALMANS, H., MEDIN, J., TRNKOVA, P., VATNITSKY, S., Gradient corrections for reference dosimetry using Farmer-type ionization chambers in single-layer scanned proton fields, Med Phys **47** (2020) 6531–6539, https://doi.org/10.1002/mp.14554

[219] INTERNATIONAL ELECTROTECHNICAL COMMISSION, Medical Electrical Equipment — Medical Light Ion Beam Equipment — Performance Characteristics, IEC 62667, IEC, Geneva (2017).
[220] PALMANS, H., LOURENCO, A., MEDIN, J., ANDREO, P., VATNITSKY, S., Current best estimates of beam quality correction factors for the reference dosimetry of clinical proton beams, Med. Phys. **67** (2022) 195012, https://doi.org/10.1088/1361-6560/ac9172
[221] VATNITSKY, S., MOYERS, M., VATNITSKY, A., "Parallel-plate and thimble ionization chamber calibrations in proton beams using the TRS 398 and ICRU 59 recommendations", Standards and Codes of Practice in Medical Radiation Dosimetry, Proceedings Series — International Atomic Energy Agency, IAEA, Vienna (2003) 327–336.
[222] ROSSOMME, S., et al., Response of synthetic diamond detectors in proton, carbon, and oxygen ion beams, Med. Phys. **44** (2017) 5445–5449, https://doi.org/10.1002/mp.12473
[223] MANDAPAKA, A.K., et al., Evaluation of the dosimetric properties of a synthetic single crystal diamond detector in high energy clinical proton beams, Med. Phys. **40** (2013) 121702, https://doi.org/10.1118/1.4828777
[224] KANAI, T., et al., Irradiation of mixed beam and design of spread-out Bragg peak for heavy-ion radiotherapy, Radiat. Res. **147** (1997) 78–85, https://doi.org/10.2307/3579446
[225] KANAI, T., et al., Biophysical characteristics of HIMAC clinical irradiation system for heavy-ion radiation therapy, Int. J. Radiat. Oncol. Biol. Phys. **44** (1999) 201–210, https://doi.org/10.1016/S0360-3016(98)00544-6
[226] BROERSE, J.J., LYMAN, J.T., ZOETELIEF, J., "Dosimetry of external beams of nuclear particles", The Dosimetry of Ionizing Radiation, Academic Press, New York (1987) 229–290, https://doi.org/10.1016/B978-0-12-400401-6.50009-7
[227] HARTMANN, G.H., JAKEL, O., HEEG, P., KARGER, C.P., KRIESSBACH, A., Determination of water absorbed dose in a carbon ion beam using thimble ionization chambers, Phys. Med. Biol. **44** (1999) 1193–1206, https://doi.org/10.1088/0031-9155/44/5/008
[228] FUKUMURA, A., et al., Carbon beam dosimetry intercomparison at HIMAC, Phys. Med. Biol. **43** (1998) 3459–3463, https://doi.org/10.1088/0031-9155/43/12/005
[229] HARTMANN, G.H., et al., "Results of a small scale dosimetry comparison with carbon-12 ions at GSI Darmstadt", Advances in Hadrontherapy, Proc. Int. Week Hadrontherapy and 2nd Int. Symp. on Hadrontherapy (ICS 1144), Elsevier, Amsterdam (1997) 346–350.
[230] MIZUNO, H., et al., External dosimetry audit for quality assurance of carbon-ion radiation therapy clinical trials, J. Appl. Clin. Medical Phys. **20** (2019) 31–36, https://doi.org/10.1002/acm2.12465
[231] JAKEL, O., HARTMANN, G.H., HEEG, P., SCHARDT, D., Effective point of measurement of cylindrical ionization chambers for heavy charged particles, Phys. Med. Biol. **45** (2000) 599–607, https://doi.org/10.1088/0031-9155/45/3/303
[232] LÜHR, A., et al., Fluence correction factors and stopping power ratios for clinical ion beams, Acta Oncol. **50** (2011) 797–805, https://doi.org/10.3109/0284186X.2011.581691

[233] HAETTNER, E., IWASE, H., KRAMER, M., KRAFT, G., SCHARDT, D., Experimental study of nuclear fragmentation of 200 and 400 MeV/u ^{12}C ions in water for applications in particle therapy, Phys. Med. Biol. **58** (2013) 8265–8279, https://doi.org/10.1088/0031-9155/58/23/8265

[234] HAETTNER, E., IWASE, H., SCHARDT, D., Experimental fragmentation studies with ^{12}C therapy beams, Radiat. Prot. Dosimetry **122** (2006) 485–487, https://doi.org/10.1093/rpd/ncl402

[235] HENKNER, K., BASSLER, N., SOBOLEVSKY, N., JAKEL, O., Monte Carlo simulations on the water-to-air stopping power ratio for carbon ion dosimetry, Med. Phys. **36** (2009) 1230–1235, https://doi.org/10.1118/1.3085877

[236] LUHR, A., et al., The impact of modeling nuclear fragmentation on delivered dose and radiobiology in ion therapy, Phys. Med. Biol. **57** (2012) 5169–5185, https://doi.org/10.1088/0031-9155/57/16/5169

[237] LUHR, A., HANSEN, D.C., JAKEL, O., SOBOLEVSKY, N., BASSLER, N., Analytical expressions for water-to-air stopping-power ratios relevant for accurate dosimetry in particle therapy, Phys. Med. Biol. **56** (2011) 2515–2533, https://doi.org/10.1088/0031-9155/56/8/012

[238] GUDOWSKA, I., SOBOLEVSKY, N., Simulation of secondary particle production and absorbed dose to tissue in light ion beams, Radiat. Prot. Dosimetry **116** (2005) 301–306, https://doi.org/10.1093/rpd/nci023

[239] ROSSOMME, S., et al., Ion recombination correction in carbon ion beams, Med. Phys. **43** (2016) 4198, https://doi.org/10.1118/1.4953637

[240] GEITHNER, O., ANDREO, P., SOBOLEVSKY, N., HARTMANN, G., JAKEL, O., Calculation of stopping power ratios for carbon ion dosimetry, Phys. Med. Biol. **51** (2006) 2279–2292, https://doi.org/10.1088/0031-9155/51/9/012

[241] BURIGO, L., GREILICH, S., Impact of new ICRU90 key data on stopping-power ratios and beam quality correction factors for carbon ion beams, Phys. Med. Biol. (2019) 195005, https://doi.org/10.1088/1361-6560/ab376e

[242] GOMA, C., ANDREO, P., SEMPAU, J., Monte Carlo calculation of beam quality correction factors in proton beams using detailed simulation of ionization chambers, Phys. Med. Biol. **61** (2016) 2389–2406, https://doi.org/10.1088/0031-9155/61/6/2389

[243] OSINGA-BLÄTTERMANN, J.M., KRAUSS, A., Determination of k_Q factors for cylindrical and plane-parallel ionization chambers in a scanned carbon ion beam by means of cross calibration, Phys. Med. Biol. **64** (2018) 015009, https://doi.org/10.1088/1361-6560/aaf5ac

[244] HOLM, K.M., JÄKEL, O., KRAUSS, A., Water calorimetry-based k_Q factors for Farmer-type ionization chambers in the SOBP of a carbon-ion beam, Phys. Med. Biol. **66** (2021) 145012, https://doi.org/10.1088/1361-6560/ac0d0d

[245] HOLM, K.M., JÄKEL, O., KRAUSS, A., Direct determination of kQ for Farmer-type ionization chambers in a clinical carbon-ion beam using water calorimetry, Phys. Med. Biol. **67** (2022) 049401, https://doi.org/10.1088/1361-6560/ac4fa0

[246] MEDIN, J., et al., Ionisation chamber dosimetry of proton beams using cylindrical and plane-parallel chambers. N_w versus N_K ion chamber calibrations, Phys. Med. Biol. **40** (1995) 1161–1176, https://doi.org/10.1088/0031-9155/40/7/002

[247] SEMPAU, J., ANDREO, P., ALDANA, J., MAZURIER, J., SALVAT, F., Electron beam quality correction factors for plane-parallel ionization chambers: Monte Carlo calculations using the PENELOPE system, Phys. Med. Biol. **49** (2004) 4427–4444, https://doi.org/10.1088/0031-9155/49/18/016

[248] CAPOTE, R., et al., An EGSnrc Monte Carlo study of the microionization chamber for reference dosimetry of narrow irregular IMRT beamlets, Med. Phys. **31** (2004) 2416–2422, https://doi.org/10.1118/1.1767691

[249] PASKALEV, K., SEUNTJENS, J., PODGORSAK, E.B., "Dosimetry of ultra small photon fields", Recent Developments in Accurate Radiation Dosimetry, Medical Physics Publishing, Madison, WI (2002) 298–318.

[250] KAWRAKOW, I., MAINEGRA-HING, E., ROGERS, D.W.O., TESSIER, F., WALTERS, B.R.B., The EGSnrc Code System: Monte Carlo Simulation of Electron and Photon Transport, NRCC Report PIRS-701, NRCC, Ottawa (2017).

[251] WÜRFEL, J.U., et al., Monte Carlo calculations and measurements of beam quality correction factors for the PTW PinPoint 3D chamber type 31022 in MV photon beams, Report PTW-024018, Physikalisch Technische Werkstätten, Freiburg (2021).

[252] ALISSA, M., ZINK, K., TESSIER, F., SCHOENFELD, A.A., CZARNECKI, D., Monte Carlo calculated beam quality correction factors for two cylindrical ionization chambers in photon beams, Phys. Med. **94** (2022) 17–23, https://doi.org/10.1016/j.ejmp.2021.12.012

[253] PINTO, M., k_Q factors in Modern External Beam Radiotherapy Applications to Update IAEA TRS-398, RTNORM Report 16NRM03, EURAMET, Braunschweig (2020).

[254] MAINEGRA-HING, E., MUIR, B.R., On the impact of ICRU Report 90 recommendations on k_Q factors for high-energy photon beams, Med. Phys. **45** (2018) 3904–3908, https://doi.org/10.1002/mp.13027

[255] MUIR, B.R., McEWEN, M.R., ROGERS, D.W.O., Measured and Monte Carlo calculated k_Q factors: accuracy and comparison, Med. Phys. **38** (2011) 4600–4609, https://doi.org/10.1118/1.3600697

[256] MUIR, B.R., ROGERS, D.W.O., Monte Carlo calculations of k_Q, the beam quality conversion factor, Med. Phys. **37** (2010) 5939–5950, https://doi.org/10.1118/1.3495537

[257] BRUALLA, L., RODRÍGUEZ, M., SEMPAU, J., ANDREO, P., PENELOPE/PRIMO-calculated photon and electron spectra from clinical accelerators, Radiat. Oncol. **14** (2019) 6, https://doi.org/10.1186/s13014-018-1186-8

[258] CAPOTE, R., et al., Phase-Space Database for External Beam Radiotherapy, IAEA Report INDC(NDS)-0484, IAEA, Vienna (2006).

[259] MOHAN, R., CHUI, C., LIDOFSKY, L., Energy and angular distributions of photons from medical linear accelerators, Med. Phys. **12** (1985) 592–597, https://doi.org/10.1118/1.595680

[260] SHEIKH-BAGHERI, D., ROGERS, D.W.O., Monte Carlo calculation of nine megavoltage photon beam spectra using the BEAM code, Med. Phys. **29** (2002) 391–402, https://doi.org/10.1118/1.1445413

[261] CZARNECKI, D., POPPE, B., ZINK, K., Impact of new ICRU Report 90 recommendations on calculated correction factors for reference dosimetry, Phys. Med. Biol. **63** (2018) 155015, https://doi.org/10.1088/1361-6560/aad148

[262] WULFF, J., HEVERHAGEN, J.T., ZINK, K., KAWRAKOW, I., Investigation of systematic uncertainties in Monte Carlo-calculated beam quality correction factors, Phys. Med. Biol. **55** (2010) 4481–4493, https://doi.org/10.1088/0031-9155/55/16/S04

[263] BERGER, M.J., WANG, R., "Multiple-scattering angular deflections and energy-loss straggling", Monte Carlo Transport of Electrons and Photons, Plenum Press, New York (1988) 21–56, https://doi.org/10.1007/978-1-4613-1059-4_2

[264] McEWEN, M.R., WILLIAMS, A.J., DUSAUTOY, A.R., Determination of absorbed dose calibration factors for therapy level electron beam ionization chambers, Phys. Med. Biol. **46** (2001) 741–755, https://doi.org/10.1088/0031-9155/46/3/310

[265] PEARCE, J., THOMAS, R., DUSAUTOY, A., The characterization of the Advanced Markus ionization chamber for use in reference electron dosimetry in the UK, Phys. Med. Biol. **51** (2006) 473–483, https://doi.org/10.1088/0031-9155/51/3/001

[266] STUCKI, G., VÖRÖS, S., "Experimental k_{Q,Q_0} electron beam quality correction factors for the types NACP02 and PTW34001 plane-parallel chambers", Proc. Absorbed Dose and Air Kerma Primary Standards Workshop, Paris, 2007, LNE-LNHB, Saclay (2007).

[267] COJOCARU, C.D., STUCKI, G., McEWEN, M.R., ROSS, C.K., "Determination of absorbed dose to water in megavoltage electron beams using a calorimeter-Fricke hybrid system", Standards, Applications and Quality Assurance in Medical Radiation Dosimetry (IDOS), Proceedings Series — International Atomic Energy Agency, IAEA, Vienna (2012) 99–109.

[268] RENAUD, J., et al., Direct measurement of electron beam quality conversion factors using water calorimetry, Med. Phys. **42** (2015) 6357–6368, https://doi.org/10.1118/1.4931970

[269] KRAUSS, A., KAPSCH, R.P., Direct determination of $k(Q)$ factors for cylindrical and plane-parallel ionization chambers in high-energy electron beams from 6 MeV to 20 MeV, Phys. Med. Biol. **63** (2018) 035041, https://doi.org/10.1088/1361-6560/aaa71e

[270] ARAKI, F., Monte Carlo calculations of correction factors for plane-parallel ionization chambers in clinical electron dosimetry, Med Phys **35** (2008) 4033–4040, https://doi.org/10.1118/1.2968102

[271] ZINK, K., WULFF, J., Beam quality corrections for parallel-plate ion chambers in electron reference dosimetry, Phys. Med. Biol. **57** (2012) 1831–1854, https://doi.org/10.1088/0031-9155/57/7/1831

[272] MUIR, B.R., ROGERS, D.W.O., Monte Carlo calculations for reference dosimetry of electron beams with the PTW Roos and NE2571 ion chambers, Med Phys **40** (2013) 121722, https://doi.org/10.1118/1.4829577

[273] ERAZO, F., BRUALLA, L., LALLENA, A.M., Electron beam quality k_{Q,Q_0} factors for various ionization chambers: a Monte Carlo investigation with PENELOPE, Phys. Med. Biol. **59** (2014) 6673–6691, https://doi.org/10.1088/0022-3727/59/21/6673

[274] WULFF, J., et al., TOPAS/Geant4 configuration for ionization chamber calculations in proton beams, Phys. Med. Biol. **63** (2018) 115013; corrigendum **64** (2019) 069501, https://doi.org/10.1088/1361-6560/ab0292

[275] LOURENCO, A., BOUCHARD, H., GALER, S., ROYLE, G., PALMANS, H., The influence of nuclear interactions on ionization chamber perturbation factors in proton beams: FLUKA simulations supported by a Fano test, Med. Phys. **46** (2019) 885–891, https://doi.org/10.1002/mp.13281

[276] GOMA, C., STERPIN, E., Monte Carlo calculation of beam quality correction factors in proton beams using PENH, Phys. Med. Biol. **64** (2019) 185009, https://doi.org/10.1088/1361-6560/ab3b94

[277] BAUMANN, K.-S., KAUPA, S., BACH, S., ENGENHART-CABILLIC, R., ZINK, K., Monte Carlo calculation of beam quality correction factors in proton beams using TOPAS/GEANT4, Phys. Med. Biol. **65** (2020) 055015, https://doi.org/10.1088/1361-6560/ab6e53

[278] KRETSCHMER, J., et al., Monte Carlo simulated beam quality and perturbation correction factors for ionization chambers in monoenergetic proton beams, Med. Phys. **47** (2020) 5890–5905; erratum **48** (2021) 3284–3284, https://doi.org/10.1002/mp.14499

[279] BAUMANN, K.-S., KAUPA, S., BACH, S., ENGENHART-CABILLIC, R., ZINK, K., Monte Carlo calculation of perturbation correction factors for air-filled ionization chambers in proton beams using TOPAS/GEANT4, Z. Med. Phys. **31** (2021) 175–191, https://doi.org/10.1016/j.zemedi.2020.08.004

[280] SEUNTJENS, J., et al., "Water calorimetry for clinical proton beams", Proc. NPL Workshop on Water Calorimetry, National Physical Laboratory, Teddington, 1994, National Physical Laboratory, Teddington (1995).

[281] VATNITSKY, S.M., SIEBERS, J.V., MILLER, D.W., k_Q factors for ionization chamber dosimetry in clinical proton beams, Med. Phys. **23** (1996) 25–31, https://doi.org/10.1118/1.597768

[282] PALMANS, H., VERHAEGEN, F., DENIS, J.-M., VYNCKIER, S., THIERENS, H., Experimental p_{wall} and p_{cel} correction factors for ionization chambers in low-energy clinical proton beams, Phys. Med. Biol. **46** (2001) 1187–1204, https://doi.org/10.1088/0031-9155/46/4/319

[283] PALMANS, H., VERHAEGEN, F., DENIS, J.-M., VYNCKIER, S., Dosimetry using plane-parallel ionization chambers in a 71 MeV clinical proton beam, Phys. Med. Biol. **47** (2002) 2895–2905, https://doi.org/10.1088/0031-9155/47/16/305

[284] PALMANS, H., et al., A small-body portable graphite calorimeter for dosimetry in low-energy clinical proton beams, Phys. Med. Biol. **49** (2004) 3737–3749, https://doi.org/10.1088/0031-9155/49/16/019

[285] MEDIN, J., et al., Experimental determination of beam quality factors, k_Q, for two types of Farmer chamber in a 10 MV photon and a 175 MeV proton beam, Phys. Med. Biol. **51** (2006) 1503–1521, https://doi.org/10.1088/0031-9155/51/6/010

[286] MEDIN, J., Implementation of water calorimetry in a 180 MeV scanned pulsed proton beam including an experimental determination of k_Q for a Farmer chamber, Phys. Med. Biol. **55** (2010) 3287–3298, https://doi.org/10.1088/0031-9155/55/12/002

[287] GOMÀ, C., HOFSTETTER-BOILLAT, B., SAFAI, S., VÖRÖS, S., Experimental validation of beam quality correction factors for proton beams, Phys. Med. Biol. **60** (2015) 3207–3216, https://doi.org/10.1088/0031-9155/60/8/3207

[288] MEDIN, J., ANDREO, P., PALMANS, H., Experimental determination of k_Q factors for two types of ionization chambers in scanned proton beams, Phys. Med. Biol. **67** (2022) 055001, https://doi.org/10.1088/1361-6560/ac4efa
[289] MEDIN, J., ANDREO, P., PETRA: A Monte Carlo Code for the Simulation of Proton and Electron Transport in Water, Report MSF 1997-1, Department of Medical Radiation Physics of Karolinska Institutet and Stockholm University, Stockholm (1997) 67 pp.
[290] MEDIN, J., ANDREO, P., Monte Carlo calculated stopping-power ratios water/air for clinical proton dosimetry (50–250 MeV), Phys. Med. Biol. **42** (1997) 89–105, https://doi.org/10.1088/0031-9155/42/1/006
[291] AGOSTINELLI, S., et al., GEANT4-a simulation toolkit, Nucl. Instrum. Methods A **506** (2003) 250–303, https://doi.org/10.1016/S0168-9002(03)01368-8
[292] SALVAT, F., A generic algorithm for Monte Carlo simulation of proton transport Nucl. Instrum. Methods B **316** (2013) 144–159, https://doi.org/10.1016/j.nimb.2013.08.035
[293] ANDREO, P., WULFF, J., BURNS, D.T., PALMANS, H., Consistency in reference radiotherapy dosimetry: resolution of an apparent conundrum when ^{60}Co is the reference quality for charged-particle and photon beams, Phys. Med. Biol. **58** (2013) 6593–6621, https://doi.org/10.1088/0031-9155/58/19/6593
[294] SALAMON, M.H., A range-energy program for relativistic heavy ions in the region $1 < E < 3000$ MeV/amu, LBL Report 10446, LBL, Berkeley, CA (1980), https://doi.org/10.2172/5611289
[295] HIRAOKA, T., BISCHEL, H., Stopping powers and ranges for heavy ions, Jpn J. Med. Phys. **15** (1995) 91–100.
[296] SAKAMA, M., KANAI, T., FUKUMURA, A., ABE, K., Evaluation of w values for carbon beams in air, using a graphite calorimeter, Phys. Med. Biol. **54** (2009) 1111–1130, https://doi.org/10.1088/0031-9155/54/5/002
[297] ROSSOMME, S., et al., Reference dosimetry for light-ion beams based on graphite calorimetry, Radiat. Prot. Dosim. **161** (2014) 92–95, https://doi.org/10.1093/rpd/nct299
[298] VILLEVALDE, A., BURNS, D.T., KESSLER, C., Beam Characterization for Low-Energy X-Rays and New Reference Qualities at 1 m, Rapport BIPM-2020/03, BIPM Sèvres (2020).
[299] JOHNSSON, S.A., CEBERG, C.P., KNOOS, T., NILSSON, P., On beam quality and stopping power ratios for high-energy x-rays, Phys. Med. Biol. **45** (2000) 2733–2745, https://doi.org/10.1088/0031-9155/45/10/301
[300] LARIVIERE, P.D., The quality of high-energy X-ray beams, Brit. J. Radiol. **62** (1989) 473–481, https://doi.org/10.1259/0007-1285-62-737-473
[301] ANDREO, P., A comparison between calculated and experimental k_Q photon beam quality correction factors, Phys. Med. Biol. **45** (2000) L25–38.
[302] ROGERS, D.W.O., Comment on "On the beam quality specification of high-energy photons for radiotherapy dosimetry" [Med. Phys. **27** (2000) 434–440], Med. Phys. **27** (2000) 441–444, https://doi.org/10.1118/1.598893
[303] KALACH, N.I., ROGERS, D.W., Which accelerator photon beams are 'clinic-like' for reference dosimetry purposes? Med. Phys. **30** (2003) 1546–1555, https://doi.org/10.1118/1.1573205

[304] HUQ, M.S., ANDREO, P., Advances in the determination of absorbed dose to water in clinical high-energy photon and electron beams using ionization chambers, Phys. Med. Biol. **49** (2004) R49–104, https://doi.org/10.1088/0031-9155/49/4/R01
[305] AMERICAN ASSOCIATION OF PHYSICISTS IN MEDICINE, Clinical Dosimetry Measurements in Radiotherapy, AAPM Monograph No. 34, 2009 AAPM Summer School, AAPM, Madison, WI (2011).
[306] HUQ, M.S., HOSSAIN, M., ANDREO, P., A comparison of the AAPM TG51 protocol and the IAEA absorbed-dose-to-water based Code of Practice for dosimetry calibration of high energy photon beams, Med. Phys. **26** (1999) 1153.
[307] STUCKI, G., Beam Quality Specification of High-Energy Photon Beams, Final Report on EURAMET Project 605, EURAMET, Bern-Wabern (2009), https://www.euramet.org/technical-committees/tc-projects/details/project/beam-quality-specification-of-high-energy-photon-beams
[308] PICARD, S., BURNS, D.T., LOS ARCOS, J.M., Establishment of degrees of equivalence of national primary standards for absorbed dose to water in accelerator photon beams, Metrologia **50** (2013) 06016, https://doi.org/10.1088/0026-1394/50/1A/06016
[309] SWISS SOCIETY OF RADIOBIOLOGY AND MEDICAL PHYSICS, Reference Dosimetry of High-energy Therapy Photon Beams with Ionization Chambers, Recomm. No. 8 Rev. 2018, SGSMP (2018), http://ssrpm.ch/wp-content/uploads/2018/04/SSRMP-recommendations-no8-rev2018-April-EN.pdf
[310] DEASY, J.O., ALMOND, P.R., McELLISTREM, M.T., ROSS, C.K., A simple magnetic spectrometer for radiotherapy electron beams, Med. Phys. **21** (1994) 170–1714, https://doi.org/10.1118/1.597271
[311] FADDEGON, B.A., BLEVIS, I., Electron spectra derived from depth dose distributions, Med. Phys. **27** (2000) 514–526, https://doi.org/10.1118/1.598919
[312] DING, G.X., ROGERS, D.W., Mean energy, energy-range relationships and depth-scaling factors for clinical electron beams, Med. Phys. **23** (1996) 361–376, https://doi.org/10.1118/1.597788
[313] VYNCKIER, S., BONNETT, D.E., JONES, D.T., Supplement to the code of practice for clinical proton dosimetry. ECHED (European Clinical Heavy Particle Dosimetry Group), Radiother. Oncol. **32** (1994) 174–179, https://doi.org/10.1016/0167-8140(94)90104-X
[314] VYNCKIER, S., BONNETT, D.E., JONES, D.T., Code of practice for clinical proton dosimetry, Radiother. Oncol. **20** (1991) 53–63, https://doi.org/10.1016/0167-8140(91)90112-T
[315] INTERNATIONAL COMMITTEE OF WEIGHTS AND MEASURES, Rapport du Groupe de Travail sur l'expression des incertitudes, CIPM Proces-Verbaux 49 A1-A12, BIPM, Sèvres (1981).

ABBREVIATIONS

BIPM	Bureau International des Poids et Mesures
CCRI	Comité Consultatif des Rayonnements Ionisants (Consultative Committee for Ionizing Radiation)
CIPM	Comité International des Poids et Mesures
FFF	flattening filter free
FIA	free in air
HVL	half-value layer
ICRU	International Commission on Radiation Units and Measurements
ISO	International Organization for Standardization
KCDB	key comparison database
MRA	mutual recognition arrangement
NIST	National Institute of Standards and Technology, USA
PBS	pencil beam scanning
PDD	percentage depth dose
PMMA	polymethyl methacrylate
PSDL	primary standards dosimetry laboratory
PTB	Physikalisch-Technische Bundesanstalt, Germany
RBE	relative biological effectiveness
SAD	source–axis distance
SCD	source–chamber distance
SDD	source–detector distance
SOBP	spread-out Bragg peak
SSD	source–surface distance
SSDL	secondary standards dosimetry laboratory
TMR	tissue–maximum ratio
TPR	tissue–phantom ratio
WFF	with flattening filter

CONTRIBUTORS TO DRAFTING AND REVIEW

Andreo, P.	Karolinska University Hospital and Karolinska Institutet, Sweden
Aspradakis, M.	European Society of Radiotherapy and Oncology, Belgium
Burns, D.	Bureau International des Poids et Mesures, France
Büermann, L.	Physikalisch-Technische Bundesanstalt, Germany
Carrara, M.	International Atomic Energy Agency
Christaki, K.	International Atomic Energy Agency
Healy, B.	Icon Group, Australia
Hill, R.	Chris O'Brien Lifehouse, Australia
Jäkel, O.	German Cancer Research Center, Germany
Kanematsu, N.	National Institute of Radiological Sciences, Japan
Kapsch, R.P.	Physikalisch-Technische Bundesanstalt, Germany
McEwen, M.	National Research Council Canada, Canada
Medin, J.	Skåne University Hospital, Sweden
Meghzifene, A.	International Atomic Energy Agency
Muir, B.	National Research Council Canada, Canada
Palmans, H.	National Physics Laboratory, United Kingdom, and MedAustron, Austria
Pinto, M.	National Institute of Ionizing Radiation Metrology, Italy
Vatnitsky, S.	MedAustron, Austria
Vynckier, S.	Université Catholique de Louvain, Belgium

Consultants Meetings

Vienna, Austria: 5–7 August 2015, 8–11 August 2016, 9–12 October 2017, 14–17 May 2018, 24–27 September 2018, 15–17 October 2019, 6–22 July 2021

IAEA
International Atomic Energy Agency

No. 26

ORDERING LOCALLY

IAEA priced publications may be purchased from the sources listed below or from major local booksellers.

Orders for unpriced publications should be made directly to the IAEA. The contact details are given at the end of this list.

NORTH AMERICA

Bernan / Rowman & Littlefield
15250 NBN Way, Blue Ridge Summit, PA 17214, USA
Telephone: +1 800 462 6420 • Fax: +1 800 338 4550
Email: orders@rowman.com • Web site: www.rowman.com/bernan

REST OF WORLD

Please contact your preferred local supplier, or our lead distributor:

Eurospan Group
Gray's Inn House
127 Clerkenwell Road
London EC1R 5DB
United Kingdom

Trade orders and enquiries:
Telephone: +44 (0)176 760 4972 • Fax: +44 (0)176 760 1640
Email: eurospan@turpin-distribution.com

Individual orders:
www.eurospanbookstore.com/iaea

For further information:
Telephone: +44 (0)207 240 0856 • Fax: +44 (0)207 379 0609
Email: info@eurospangroup.com • Web site: www.eurospangroup.com

Orders for both priced and unpriced publications may be addressed directly to:

Marketing and Sales Unit
International Atomic Energy Agency
Vienna International Centre, PO Box 100, 1400 Vienna, Austria
Telephone: +43 1 2600 22529 or 22530 • Fax: +43 1 26007 22529
Email: sales.publications@iaea.org • Web site: www.iaea.org/publications

This revised edition of the IAEA TRS-398 Code of Practice fulfils the need for a systematic and internationally unified approach to the calibration of ionization chambers in terms of absorbed dose to water and to the use of these detectors in determining the absorbed dose to water for the radiation beams used in radiotherapy. It is based on new key data for radiation dosimetry published by the International Commission on Radiation Units and Measurements (ICRU). It contains updated information on new commercially available ionization chambers and addresses the needs of professionals working with newer radiotherapy technologies.

INTERNATIONAL ATOMIC ENERGY AGENCY
VIENNA